Many-body systems draw ever more physicists' attention. Such an increase of interest often comes along with the development of new theoretical methods. In this thesis, a non-perturbative semiclassical approach is developed, which allows to analytically study many-body interference effects both in bosonic and fermionic Fock space and is expected to be applicable to many research areas in physics ranging from Quantum Optics and Ultracold Atoms to Solid State Theory and maybe even High Energy Physics.
After the derivation of the semiclassical approximation, which is valid in the limit of large total number of particles, first applications manifesting the presence of many-body interference effects are shown. Some of them are confirmed numerically thus verifying the semiclassical predictions. Among these results are coherent back-/forward-scattering in bosonic and fermionic Fock space as well as a many-body spin echo, to name only the two most important ones.

ISBN 978-3-86845-128-3
gefördert von:
Alumni der physikalischen Fakultät der Universität Regensburg e.V.

Universität Regensburg

Dissertationsreihe Physik - Band 47

Thomas Engl

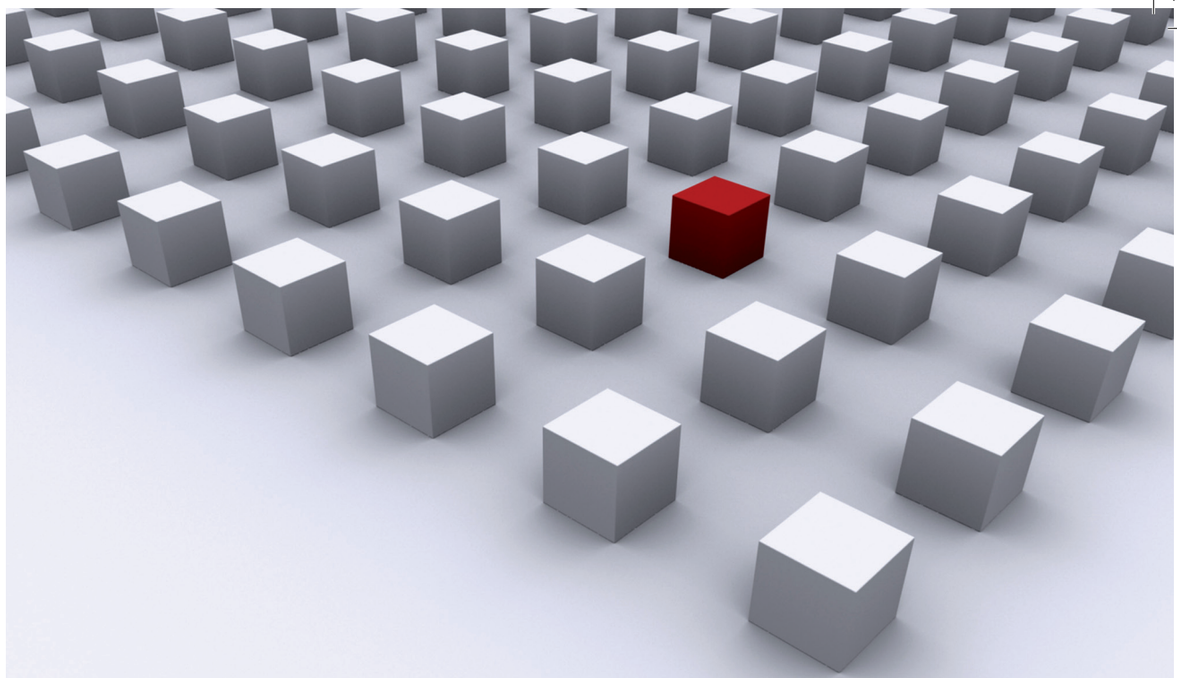

# Thomas Engl
# A Semiclassical Approach to Many-Body Interference in Fock-Space

Universitätsverlag Regensburg

47

Dissertationsreihe Physik

Thomas Engl

# A Semiclassical Approach to Many-Body Interference in Fock-Space

**A Semiclassical Approach to Many-Body Interference in Fock-Space**

Dissertation zur Erlangung des Doktorgrades der Naturwissenschaften (Dr. rer. nat.)
der naturwissenschaftlichen Fakultät II - Physik der Universität Regensburg
vorgelegt von

Thomas Engl

aus Roding
im Juni 2015

Promotionsgesuch eingereicht am: 10.06.2014
Die Arbeit wurde angeleitet von: Prof. Dr. Klaus Richter

Prüfungsausschuss: Vorsitzender: Prof. Dr. Rupert Huber
1. Gutachter: Prof. Dr. Klaus Richter
2. Gutachter: Prof. Dr. Milena Grifoni
weiterer Prüfer: Prof. Dr. Andreas Schäfer


**Dissertationsreihe der Fakultät für Physik der Universität Regensburg, Band 47**

Herausgegeben vom Präsidium des Alumnivereins der Physikalischen Fakultät:
Klaus Richter, Andreas Schäfer, Werner Wegscheider, Dieter Weiss

Thomas Engl

# A Semiclassical Approach to Many-Body Interference in Fock-Space

Universitätsverlag Regensburg

Bibliografische Informationen der Deutschen Bibliothek.
Die Deutsche Bibliothek verzeichnet diese Publikation
in der Deutschen Nationalbibliografie. Detailierte bibliografische Daten
sind im Internet über http://dnb.ddb.de abrufbar.

1. Auflage 2015

Leibnizstraße 13, 93055 Regensburg

Konzeption: Thomas Geiger
Umschlagentwurf: Franz Stadler, Designcooperative Nittenau eG
Layout: Thomas Engl
Druck: Docupoint, Magdeburg
ISBN: 978-3-86845-128-3



Weitere Informationen zum Verlagsprogramm erhalten Sie unter:
www.univerlag-regensburg.de

# A Semiclassical Approach to Many-Body Interference in Fock-Space


**DISSERTATION**
ZUR ERLANGUNG DES DOKTORGRADES
DER NATRUWISSENSCHAFTEN (DR. RER. NAT.)
DER FAKULTÄT FÜR PHYSIK

DER UNIVERSITÄT REGENSBURG

vorgelegt von

**Thomas Engl**

aus

Roding

im Jahr 2015

Promotionsgesuch eingereicht am: 10.06.2014
Die Arbeit wurde angeleitet von: Prof. Dr. Klaus Richter

| | | |
|---|---|---|
| Prüfungsausschuss: | Vorsitzender: | Prof. Dr. Rupert Huber |
| | 1. Gutachter: | Prof. Dr. Klaus Richter |
| | 2. Gutachter: | Prof. Dr. Milena Grifoni |
| | weiterer Prüfer: | Prof. Dr. Andreas Schäfer |

Dedicated to Martin C. Gutzwiller

# Contents

CHAPTER 1

# Introduction

## 1.1 Classical Mechanics gone Quantum

### *1.1.1 The first quantum revolution*

100 years ago, not only the first world war broke out, but also James Franck and Gustav Hertz showed in their experiment that the electrons in an atom can have only certain quantized energies [1]. The Franck-Hertz experiment was the first experimental proof of the quantum nature of atoms, and also resulted in a Nobel prize for Franck and Hertz in 1925. At that time, Bohr's heuristic atom model [2], which in a way could be considered as the first semiclassical model since it used quantized but otherwise classical orbits, was considered to be the correct theory to describe the inner structure of atoms.

The Bohr-Sommerfeld quantization rule actually yielded the correct energy levels for the hydrogen atom even including fine structure. However, although many physicists – among them Bohr, Born, Kramers, Landé , Sommerfeld and van Vleck – tried to compute it, the correct ground state energy of Helium could not be reproduced [3].

This failure to compute the energy levels of Helium marked the end of the "old quantum theory". Finally, in 1925, works by Louis de Broglie, Werner Heisenberg and Erwin Schrödinger culminated in the Schrödinger equation [4]. A test of the thus developed "new quantum theory" is the scattering of electrons on a Nickel cristal [5], which shows the same diffrac-

tion pattern as the scattering of X-rays on Nickel cristals – by the way a Nobel prize in 1914 for Max von Laue.

After the establishment of the new quantum theory, it became clear that the Bohr-Sommerfeld quantization rule follows from the semiclassical WKB or EBK approximation [6], respectively, such that denoting Bohr's atom model as a semiclassical description can actually be justified. However, WKB and EBK quantization is valid for classically integrable systems only, thus explaining the failure of the old quantum theory for Helium, which is a chaotic three-body system. On the other hand, within the new quantum theory, the WKB approximation was the first connection of a quantum object, namely the wave function, with classical trajectories and their actions. Such a connection was also established in 1928 by van Vleck, who made use of probabilistic arguments, in order to approximate the quantum mechanical propagator in configuration space in terms of classical trajectories starting and ending at the initial and final position, respectively, and their actions [7]. It is worth to notice that van Vleck's result coincides for short times with Pauli's short time approximation [8].

In 1948, Richard Feynman established another connection between the quantum mechanical propagator in configuration space and paths connecting the initial and final position [9]. However, in his path integral formalism, it is not just the classical trajectories, one has to sum over, but over all – classical and non-classical – paths, which ensures that also tunneling effects are included. The latter is important to notice, since classical trajectories do not tunnel, and therefore tunneling effects can not be resembled by semiclassical descriptions based on classical trajectories, unless they are incorporated artificially [10]. It was then Martin C. Gutzwiller [11], who unfortunatelly died one year ago, who applied a stationary phase approximation [12–14] to Feynman's path integral, in order to show that van Veck's result has to be modified by phases typically denoted as Maslov indexes, given by the number of focal points of the trajectory [6]. This propagator is nowadays referred to as van-Vleck-Gutzwiller propagator. The linearity and the consequential interference of the quantum theory is thereby resembled by the fact that the van-Vleck-Gutzwiller propagator is computed from *all* classical trajectories joining the initial and the final position.

In the very same publication [11], Gutzwiller also showed, how to perform the Laplace transfromation of the van-Vleck-Gutzwiller propagator from time to energy domain in order to arive at a semiclassical Green's function, which is then no longer given by classical trajectories with fixed time, but with fixed energy. From the Green's function, also the density of states of a quantum system can be computed [15], and Gutzwiller's approx-

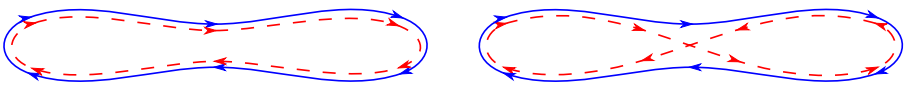

(a) Diagonal pair (b) Sieber-Richter pair

Figure 1.1: (a) A diagonal and (b) Sieber-Richter pair as those appearing in the computation of the spectral form factor.

imation provides a way to also connect this quantum mechanical quantity to classical trajectories. In fact, it was again Gutzwiller [16], who showed that semiclassically, the density of states can be decomposed into a smooth (Weyl) part [17] and an oscillatory part, where the latter is given by a sum over periodic orbits. This is Gutzwiller's famous trace formula, which is valid for classically chaotic systems like – guess what – the Helium atom.

In addition, latest with Berry's diagonal approximation [18], it became evident that semiclassics is a very powerful tool for studying universal quantum effects in single-particle systems. Among these effects are weak localization [19–21], weak anti-localization [22, 23], coherent backscattering [24], the decay of the Loschmidt Echo [25, 26] and the spectral form factor [18]. On the other hand, however, based on Bohiga's, Giannoni's and Schmidt's conjecture that systems with chaotic classical counterpart behave as if their hamiltonian would be a random matrix [27], many random matrix theory (RMT) results showed that the results obtained in diagonal approximation were often only leading order effects. It then took until the beginning of the new millenium to identify the next to leading order contributions for two dimensional systems [28], which are now often denoted as Sieber-Richter pairs (see Fig. 1.1(b) for a sketch of these pairs) or – more generally – loop contributions. Within their approach, Martin Sieber and Klaus Richter were also able to solve the problem of the missing normalization of the transmission probabilities for open chaotic systems, which appears, when sticking to the diagonal approximation [21].

The semiclassical approach has then been extended not only to include higher order contributions, but also higher dimensions [29–38], and has now for the spectral form factor been shown to be able to reproduce the full RMT result [39]. Again, the corrections to leading order results in single-particle systems have been studied extensively using this approach. For instance, the conductance of a chaotic conductor has been calculated to all orders in the inverse number of channels [34], as has been the density of states of Andreev Billiards [40, 41]. Within this approach, universal conductance fluctuations [20, 42–44] could also be described. Moreover, it

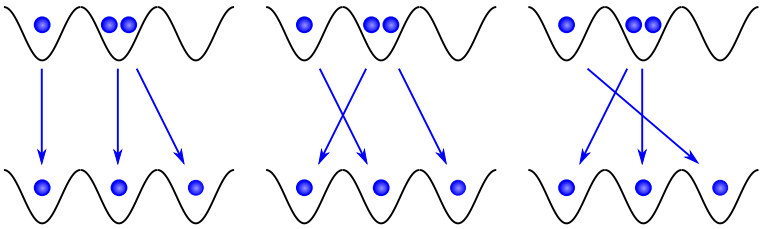

Figure 1.2: Three indistinguishable scattering processes, that give rise to many-body interference.

has been applied to the Loschmidt echo [45, 46], the conductance and thermopower of Andreev Billiards [47–49], transport of Bose-Einstein condensates through chaotic conductors [50], transport moments of chaotic conductors and Andreev Billiards [51–54]. Right now, even quantum graphs, which have eigenvalues given by the zeros of Riemann's Zeta Functions, are under investigation [55]. Furthermore, this semiclassical approach to quantum chaotic transport can reproduce Anderson localization [56–58].

This already pretty long, but surely not complete list of applications, shows that semiclassics is very successful in describing universal quantum effects of single-particle systems. However, the methods to describe universal quantum effects are not (or only with a huge effort) able to describe many-body effects, if the total number of particles is large [59]. This is due to the additional many-body interference depicted in Fig. 1.2 due to the indistuingishability of the particles and the necessary (anti-) symmetrization associated with it.

### *1.1.2 Second quantization*

Indistinguishability, and the fact that the symmetrization or antisymmetrization of wave functions becomes intractable for large particle number was the reason for the development of second quantization [60]. There, every operator is written as a combination of so called creation and annihilation operators, with coefficients which are determined by the corresponding single-particle system, only. For the creation and annihilation operators there are two possible interpretations. Either they create and annihilate, respectively, a particle in a certain single-particle state, or a certain excitation of the ground state. The first interpretation is commonly used in quantum field theories [61], while the second one is used for example for the description of the quantum harmonic oscillator [62]. Actually, these two

interpretations are equivalent, since any excitation can be interpreted as a quasi-particle [63]. When choosing the single-particle states in which the creation and annihilation operators create or annihilate particles or excitations as position states, the creation and annihilation operators are often denoted as field operators [64].

To the author's knowledge, the use of semiclassical methods in Fock space is rather limited. For Bosons, these approaches are mainly based on coherent states [65–69], initial value representations in terms of the Herman-Kluk propagator [70, 71] or WKB and EBK approximations [72–75]. While the latter is restricted to integrable systems, only, the first two approaches can be applied to any system, no matter whether it is integrable or not. If one wants to transfer the accomplishments in semiclassical methods for single-particle to many-body systems, they yield severe problems, though.

While an initial value representation may be very advantageous for numerical studies and integrable systems [71], it is not able to predict universal features analytically, since especially the loop contributions are not explicit in this case.

The coherent state propagator requires complex trajectories [65–69] with complex action. Therefore, unlike the usual van-Vleck-Gutzwiller propagator [11], for each trajectory the action not only contributes a phase, but also a real exponential factor, which makes the usual argumentation of strongly oscillating terms due to action differences of not correlated pairs of trajectories impossible. However, this kind of reasoning is necessary in order to be able to restrict the analysis to diagonal [18] and loop contributions [21, 28–37]. It is worth to notice that "it may happen that the complex trajectory is close enough to a real one [...]" (*cf.* [76]), such that one can use a real trajectory, in order to approximate the contribution of a complex one [67, 76, 77], "[...] if the latter is not too deep into the complex plane." (*cf.* [67]). However, as these statements already indicate, it is highly questionable, whether this approximation can be generally applied systematically, and the proponents of this approximation themselves recognized that it may give wrong or insufficient results [67, 76].

For fermions, the situation seems to be far worse. To the author's knowledge, rigorous semiclassical approaches in Fock space are so far restricted to spin-chains [65, 69], which describe essentially distinguishable particles, since each particle is fixed to one position. For systems with spin-orbit interactions, kind of hybrid systems have been introduced, where the orbital degrees of freedom are treated in configuration space, while for the spins coherent states are used [23, 78–84].

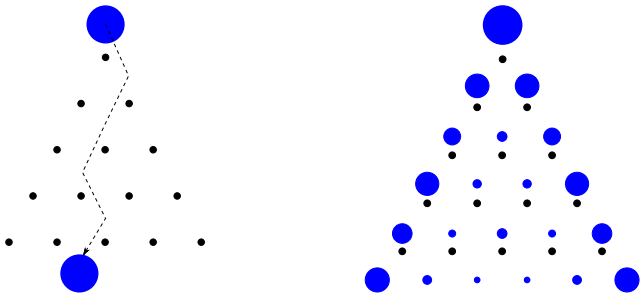


Figure 1.3: Classical (a) vs. quantum (b) discrete time random walk: While in the classical random walk, the particle goes either to the left or to the right at each step, in the quantum random walk the wave function splits up at each step and interferes.

The problem with a semiclassical approach in Fock space is that due to the antisymmetry of the fermions, coherent states are described by anti-commuting Grassmann variables [61, 64] and therefore a stationary phase approximation to the straight forward coherent state path integral for instance yields as classical limit Grassmann valued equations of motions and actions. This is probably the reason, why the theories closest to a semiclassical one in fermionic fock space are up to now quaiclassical approaches, where a heuristic classical Hamiltonian is imposed [85, 86].

The aim of this thesis is to address and – if possible – lift these issues of semiclassical approaches in Fock space for both, Bosons and Fermions. Once such semiclassical approaches are successfully derived, one may start to dream a little bit in which research areas they may be applied.

## 1.2 The Connection to Various Research Fields

### *1.2.1 Quantum Optics*

To start with non-interacting systems, one possible field of application could be quantum walks [87–91], which became of special importance in the context of quantum computation [92] and quantum search algorithms [93]. While "In classical random walks, a particle starting from an initial site on a lattice randomly choses a direction and then moves to a neighboring site accordingly" (cf. [91]), in a quantum random walk, the wave function of a

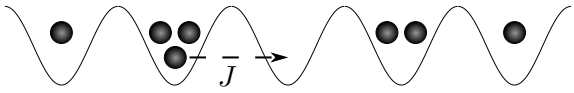


Figure 1.4: Schematic picture of seven ultra-cold atoms in an optical lattice consisting of five magneto-optical traps. The atoms can tunnel from one trap to a neighbouring one with a probability given by the hopping amplitude $J$.

particle splits at each site into two components, which finally will interfere again [94]. Such quantum walks are mainly performed using photons.

Quantum walks based on photons are usually classified as follows: In discrete time quantum walks, beam splitters are used, such that for discrete time steps, a photon can enter one of two wave guides [90, 95–97]. It is worth to mention the easiest case of a discrete time quantum walk having just one beam splitter, namely the well known Hong-Ou-Mandel effect [98]. In continuous time quantum walks, on the other hand, several waveguides are arranged periodically close to each other, such that a photon can tunnel from one wave guide to the other one [91, 99–101]. In both cases, time can due to the fixed speed of photons (namely the speed of light), be mapped to the position of the photon along a certain direction [102], which is often chosen to be the $z$-direction.

Interestingly, even disorder can be realized in these systems. For beam splitter this is by implying so called coin operators, which – classically speaking – change the probability to go to either side [97], while for waveguide arrays the refractive index can be adjusted for each wave guide separately [91]. The fact that, for waveguide arrays the system can be changed by changing the waveguides only, also allows for instance to study nonlinear effects [102, 103].

Since these experiments are usually done with one single [91, 95, 97, 99, 102, 103] or two photons [96, 100], these experiments can not be described using classical electrodynamics. However an approach based on a Hamiltonian given in terms of creation and annihilation operators as the one which will be considered in this thesis may be applied.

Finally, quantum walks are not only possible by using photons, but also with ultra-cold atoms and ions [104–108].

### *1.2.2 Ultra-cold Atoms in Optical Lattices*

These systems consist of several atoms, which are at very low temperatures (usually a few nK) trapped in a periodic potential built up by interfering laser beams, which are adjusted such that they form standing waves [109] and are generally described by Hubbard models [110]. An optical lattice consisting of five magneto-optical traps, which are often also denoted as sites, and seven particles is schematically shown in Fig. 1.4.

An advantage of these systems is their vast controllability [111]. By using Feshbach resonances [112–115] for instance, the scattering length, which in turn determines the interaction strength, can be adjusted and tuned within a wide range [116, 117].

Additionally, by increasing the intensities of the used laser beams, the tunneling probability, *i.e.* the probability for an atom to tunnel from one well of the optical lattice to another one, can be decreased, resulting in a relative increase of the interactions compared to the kinetic energy, which is often denoted as hopping amplitude. If the tunneling probability is increased so far that the hopping amplitude is much smaller than the interaction strength, the energy is dominated by the latter and tunneling from one well to an other is energetically suppressed or even forbidden. This regime is called the Mott insulating phase [118, 119] and for ultra-cold atoms it is accessible by the prescribed procedure. In fact, when increasing the laser intensity, bosonic ultra-cold atoms undergo a quantum phase transition from a superfluid to a Mott insulating phase [120, 121].

For Fermions the Mott insulating phase also appears when the hopping amplitude is not negligible but much smaller than the interaction strength for half filling and a phase transition from Mott insulating to superconducting can be achieved by hole doping, *i.e.* by removing particles [122–124]. For fermions, the Mott insulating ground state is also predicted to be antiferromagnetic [123].

The Mott insulating phase also allows a simple scheme for loading an optical lattice with atoms [125–127]. In the same way, it can be used, for fixing the atoms after time evolution and determine the number of atoms in each well by high resolution imaging techniques [128, 129].

Finally, the energy of each well of the periodic potential can also be adjusted individually, thus giving the possibility to create optical disorder [130] and, despite the fact that atoms have no electrical charge (therefore a magnetic field does not have any effect on their motion) time reversal invariance can be broken by artificial [131–134] and synthetic gauge fields [135].

These properties and especially the high controllability of the systems suggest that ultra-cold atoms can be used as simulators for condensed matter systems [111, 125] like for example graphene [136]. Since recently also spin-orbit interaction have been realized with ultra-cold atoms [137–139], one could also think of simulating spintronics in optical lattices.

### *1.2.3 Spintronics*

Spintronics is essentially the investigation of spin related effects, mainly solid state systems, and aims towards a spin-based, rather than the conventionally charge-based, information transport [140–142]. The punchlines there, are *e.g.* the generation of spin polarization, injection of spin polarized currents as well as possibilities to manipulate and measure them. Very often hetero-structures composed of ferromagnetic materials and semiconductors or ferromagnetic and insulating materials are used. In these systems, the ferromagnets serve as injectors or detectors of spin polarization. Very prominent effects in such hetero-structures are giant magnetoresistance (GMR) [143, 144] and tunneling magnetoresistance (TMR) [145]. For both, GMR and TMR, the (electrical) resistance is much larger if the magnetizations of the two ferromagnetic layers have opposite directions than if they are parallel. The difference in the setup between them is that for GMR a semiconductor is placed between two ferromagnets, while for TMR a so called magnetic tunnel junction is used, where an insulator (=tunneling barrier) is sandwiched by two ferromagnets. These two effects also made successfully their way to industrial applications and have been established in read heads in hard disk drives.

Another effect, which seems to be on its way to industrial applications in so called racetrack memory [142] are spin transfer torque effects [146]. In these effects, spin-polarized particles crossing a domain wall in a ferromagnetic material transfers its magnetic moment to the substrate and thus moves the domain wall.

Relativistic effects like Bychkov-Rashba [147] and Dresselhaus spin-orbit interactions [148] are also important in spintronics. For instance, they are the key elements of spin-hall [149, 150], quantum spin hall [151–154] and spin-based transistors [155]. While spin hall and quantum spin hall effect are both based on the fact that due to intrinsic spin-orbit interaction particles with spin up and spin down, respectively, moving in the same direction are dragged to opposite directions perpendicular to the overall direction of the current, in the spin field effect transistor [155] the

spin orbit interaction strength is determined by an external gate voltage. The spin-orbit coupling then leads to spin-precession of the crossing particle. The source and drain are magnetized, such that the electrons entering are also spin-polarized and can enter the drain only if the spin-precession is such that their spins are parallel to the magnetization in the drain.

So far, spintronics mainly focuses on single-particle effects [140–142, 156], for which using a Fock space approach of indistinguishable particles is not quite reasonable. However, for studying many-body effects in spintronics devices, the techniques developed in this thesis might be of particular help.

### *1.2.4 Many-Body effects in condensed matter physics*

More generally, it is important to study many-body effects in condensed matter systems. Well known amongst these are for instance the Coulomb blockade [157–163], inelastic and elastic co-tunneling [164–168] and the Kondo effect [168–170]. The Coulomb blockade arises due to the Coulomb repulsion of the electrons in a quantum dot coupled to leads via tunnel junctions. This repulsion implies a large energy cost in order to add a further electron which in turn results in peaks of the current-voltage characteristic only for specific voltages corresponding to the energy needed in order to add a electron to the quantum dot.

In quantum dots, cotunneling, where two electrons – one into the quantum dot and one out of the quantum dot – tunnel at the same time, and the Kondo effect are corrections to the Coulomb blockade at low temperatures. The Kondo effect originally refers to a minimum of the resistance as a function of temperature in a metal [170] due to scattering off magnetic impurities, where the impurity and the electron exchange their spin. Nowadays, the Kondo effect is mainly studied in quantum dots and carbon nanotubes [168, 171–188] and became a test case for many-body theories in condensed matter physics [189–196].

Due to their similarities, quantum dots are also regarded as artificial (two dimensional) atoms [177, 197, 198] and even the formation of artificial molecules [199–201] is possible using quantum dots.

### *1.2.5 Chemical Physics*

Real Atoms and Molecules, on the other hand, are the central objects in chemistry. In fact, the chemical physics community has made extensive use of semiclassical methods and played an important role in their development [70, 202–209].

Starting with Ref. [209] Miller and coworkers started the study of molecular collisions, which give rise to electronic transitions within the molecules and succeeded to describe resonance effects [210]. There, the electronic degrees of freedom have been treated semiclassically, while the nuclear motion was incorporated classically [209]. After that, in order to be able to derive electronic and nuclear motion on the same footing, they turned to deriving a classical theory of these collisions [85, 211–213]. These classical approaches are basically determined by a mapping of angular momenta, including spin, to classical action angle varibles [202, 214].

Motivated by this process, Miller and White tackled the problem of deriving a classical Hamiltonian for a second quantized fermionic Hamilonian already in 1986 [86]. By using similar techniques they managed to derive a Schwinger representation of the angular momentum [215]. Later on, it has been used heuristically in a semiclassical initial value representation including Langer substitutions [216].

The thus developed techniques have also been applied to electronic transport through a single quantum dot [217], two coupled quantum dots [218] and molecular junctions [219].

The problem with the Meyer-Miller-Stock-Thoss approach developed in [85, 86, 215, 216] is, however, that the Fock states, *i.e.* those states with well defined occupations of the single-particle states, are fixed points of the classical motion [220]. Moreover, it is based on heuristic mapping approaches, instead of a rigorous derivation by means of a path integral, where the classical Hamiltonian appears naturally. Finally, it does not yield any insight, what the effective Planck constant $\hbar_{\text{eff}}$, *i.e.* the small parameter in a stationary phase analysis of the path integral, actually is.

## 1.3 Outline of this thesis

During this thesis, an answer to this last question, what the effective Planck constant is, will be also given. This will be accomplished by first deriving an exact path integral both for Bosons and Fermions based on

complex variables, which will also determine the classical limit of the second quantized theory.

Before that, however, a brief introduction to the basic concepts used during this thesis will be given in the first part. This introduction contains a short review of the derivation of the path integral and the van-Vleck-Gutzwiller propagator in configuration space in Chapter 2, the basic concepts of second quantization as well as important states in Fock space and their properties in Chapter 3 for both, Bosons and Fermions.

The second part, finally, is dedicated to the construction of path integrals and semiclassical approximations for the propagator in Fock space based on complex variables for Bosons in Chapter 4 as well as for Fermions in Chapter 5. For the bosonic proapgator, it is also shown that the semiclassical approximation fulfills the semi-group property.

The thus derived bosonic propagator is applied in Part III to bosonic many-body systems, starting with non-interacting systems like quantum walks in photonic wave guide arrays in Chapter 6, and then turning to describing coherent backscattering in Fock space for interacting particles in Chapter 7, many-body transport of interacting Bosons in Chapter 8 and finally to the fidelity decay for interacting ultra-cold atoms in Chapter 9.

Similarly, in the fourth part of this thesis, fermionic many-body interference effects are considered by applying the approach derived in Chapter 5. These interference effects are enhanced and vanishing transition probabilities between Fock states, which are investigated in Chapter 10, as well as a many-body spin echo resulting from an intermediate manipulation of spins in Chapter 11 and a related quantity, which is here denoted as spin fidelity in Chapter 12.

Finally, concluding remarks as well as future perspectives are given in Chapter 13.

# Part I

# Basic concepts

CHAPTER 2

# Semiclassics for Single-Particle Systems

## 2.1 The Path Integral Representation of the Propagator

### *2.1.1 The quantum mechanical propagator*

Semiclassics as it is understood through out this thesis, is based on a stationary phase approximation to the quantum mechanical propagator (or time evolution operator), which is defined as the operator which connects the state $|\psi(t_i)\rangle$ at initial time $t_i$ with the one at final time $t_f$, $|\psi(t_f)\rangle$ by [221]

$$|\psi(t_f)\rangle = \hat{K}(t_f, t_i)\,|\psi(t_i)\rangle\,. \tag{2.1}$$

Since in quantum mechanics $|\psi(t)\rangle$ satisfies the time dependent Schrödinger equation

$$\mathrm{i}\hbar\frac{\partial}{\partial t}\,|\psi(t)\rangle = \hat{H}(t)\,|\psi(t)\rangle\,,$$

the propagator is the solution to the operator differential equation [13, 62]

$$\mathrm{i}\hbar\frac{\partial}{\partial t}\hat{K}(t, t_i) = \hat{H}(t)\hat{K}(t, t_i), \tag{2.2}$$

with initial condition

$$\hat{K}(t_f = t_i, t_i) = \hat{1}, \tag{2.3}$$

where $\hat{H}(t)$ is the (time-dependent) quantum mechanical Hamilton operator (or in short, quantum Hamiltonian), $\hat{1}$ is the unity operator, $t$ is the time, i is the imaginary unit and $\hbar$ is Planck's constant.

Formally, the solution of eqns. (2.2,2.3) can be written as [62, 221]

$$\hat{K}(t_f, t_i) = \hat{\mathcal{T}} \exp\left[-\frac{\mathrm{i}}{\hbar}\int_{t_i}^{t_f} \mathrm{d}t \hat{H}(t)\right], \tag{2.4}$$

where $\hat{\mathcal{T}}$ is the time ordering operator, which sorts the factors of the product right to it such that their time arguments decrease from left to right, *e.g.* for a product of two operators $\hat{A}_1(t)$ and $A_2(t)$ [13, 62],

$$\hat{\mathcal{T}}\hat{A}_1(t_1)\hat{A}_2(t_2) = \begin{cases} \hat{A}_1(t_1)\hat{A}_2(t_2) & \text{if } t_1 \geq t_2, \\ \hat{A}_2(t_2)\hat{A}_1(t_1) & \text{if } t_2 > t_1. \end{cases}$$

More generally, for $n$ operators $\hat{A}_1(t), \ldots, \hat{A}_n(t)$,

$$\hat{\mathcal{T}}\prod_{j=1}^{n}\hat{A}_j(t_j) = \sum_{\sigma\in S_n}\left(\prod_{j=1}^{n-1}\Theta\left(t_{\sigma(j)} - t_{\sigma(j+1)}\right)\right)\prod_{j=1}^{n}\hat{A}_{\sigma(j)}(t_{\sigma(j)}), \tag{2.5}$$

where the product $\prod_j$ is defined such that $j$ increases from left to write, and $S_n$ is the symmetric group of $n$, *i.e.* the group of all $n$-permutations, and

$$\Theta(x) = \begin{cases} 1 & \text{if } x \geq 0, \\ 0 & \text{if } x < 0. \end{cases}$$

is the Heaviside step function. A product of the form (2.5) is often also denoted as time-ordered product.

The combination $\hat{\mathcal{T}}\exp(\ldots)$, as it appears in (2.4) and is usually called time-ordered exponential, should be evaluated by first expanding the exponential using its Taylor series and after that applying the time ordering operator to each summand individually. Note that, although

$$\left[\hat{H}(t), \hat{H}(t)\right]_- = 0,$$

the Hamiltonian at time $t$ does in general not commute with the Hamiltonian at time $t'$,

$$\left[\hat{H}(t), \hat{H}(t')\right]_- \neq 0.$$

Here $\left[\hat{A},\hat{B}\right]_-$ denotes the commutator of the operators $\hat{A}$ and $\hat{B}$.

In order to further evaluate the propagator, one has to choose a certain basis. In principle, one could choose any basis, however since this part is meant for illustration of the basic methods used later on only the configuration space basis, given by the position eigenstates $|\mathbf{r}\rangle$ is used here.

Inserting a unit operator in terms of position eigenstates [221, 222],

$$\hat{1} = \int \mathrm{d}^D r \, |\mathbf{r}\rangle \langle \mathbf{r}| \,, \tag{2.6}$$

where $D$ is the spatial dimensionality of the systemm, in (2.1) and projecting it to the position eigenstate $|\mathbf{r}\rangle$ yields for the evolved wavefunction in configuration space [223]

$$\psi\left(\mathbf{r}, t_f\right) = \int \mathrm{d}^D r' K\left(\mathbf{r}, t_f; \mathbf{r}', t_i\right) \psi\left(\mathbf{r}', t_i\right),$$

where $\psi(\mathbf{r}, t) = \langle \mathbf{r}|\psi(t)\rangle$ and

$$K\left(\mathbf{r}, t_f; \mathbf{r}', t_i\right) = \left\langle \mathbf{r} \left| \hat{K}\left(t_f, t_i\right) \right| \mathbf{r}' \right\rangle \tag{2.7}$$

is the propagator in configuration space representation. The modulus square of this complex quantity then yields the probability that if a particle is at time $t_i$ at position $\mathbf{r}'$, it is found at time $t_f$ at position $\mathbf{r}$. Therefore, by choosing the initial state to be a Dirac delta in configuration space, $\psi(\mathbf{r}', t_i) = \delta\left(\mathbf{r}' - \mathbf{r}\right)$, due to the normalization of the wave function,

$$\int \mathrm{d}^D r' \left| K\left(\mathbf{r}', t_f; \mathbf{r}, t_i\right)\right|^2 = 1.$$

Moreover, the initial condition of the propagator (2.3) reads in configuration space

$$K\left(\mathbf{r}', t; \mathbf{r}, t\right) = \delta\left(\mathbf{r}' - \mathbf{r}\right).$$

Finally, the time evolution operator has to be unitary and satisfy [13]

$$\hat{K}(t_f, t)\hat{K}(t, t_i) = \hat{K}(t_f, t_i)$$

for any time $t$, *i.e.* propagating a state twice in time has to result in the same wave function as propagating it once over the whole duration. Moreover, it has to be unitary [13]. Thus, the propagator in configuration space has

to satisfy the semi-group properties

$$\int \mathrm{d}^D r'' K\left(\mathbf{r}', t_f; \mathbf{r}'', t\right) K\left(\mathbf{r}'', t; \mathbf{r}, t_i\right) = K\left(\mathbf{r}', t_f; \mathbf{r}, t_i\right), \tag{2.8a}$$

$$\int \mathrm{d}^D r'' K^*\left(\mathbf{r}'', t_f; \mathbf{r}', t\right) K\left(\mathbf{r}'', t; \mathbf{r}, t_i\right) = K\left(\mathbf{r}', t_f; \mathbf{r}, t_f\right), \tag{2.8b}$$

for any arbitrary time $t$.

### *2.1.2 The Path integral*

Despite all these nice properties, one still has to evaluate the time ordered product, in order to find the propagator in configuration space representation, a very difficult problem without general solution. However, Feynman found a way out of this problem by his famous path integral approach [9]. Here we follow mainly Refs. [12, 13].

First, Trotter's formula [224] is used, in order to split the time ordered exponential into an (infinite) product of exponentials with (infinitesimaly) small time steps [12, 13],

$$\hat{\mathcal{T}} \exp\left[\frac{\mathrm{i}}{\hbar} \int_{t_i}^{t_f} \mathrm{d}t \hat{H}(t)\right] = \lim_{M\to\infty} \prod_{m=1}^{M} \exp\left[-\frac{\mathrm{i}\tau}{\hbar} \hat{H}(t_f - m\tau)\right], \tag{2.9}$$

where $\tau = (t_f - t_i)/M$. Recall that the product is defined such that the value of $m$ increases from left to right.

Using (2.9) in (2.7), inserting a unit operator in position representation (2.6) between ever two exponentials and finally a unit operator in momentum representation [222],

$$\hat{1} = \int \mathrm{d}^D p \, |\mathbf{p}\rangle \langle \mathbf{p}| ,$$

left to every exponential, yields the path integral representation of the propagator in position space,

$$K\left(\mathbf{r}, t_f; \mathbf{r}', t_i\right) = \lim_{M\to\infty} \int \mathrm{d}^D p_0 \int \mathrm{d}^D r_1 \int \mathrm{d}^D p_1 \ldots \int \mathrm{d}^D r_M \int \mathrm{d}^D p_M \prod_{m=0}^{M} \langle \mathbf{r}_{m+1} \,|\, \mathbf{p}_m \rangle \left\langle \mathbf{p}_m \left| \exp\left[-\frac{\mathrm{i}\tau}{\hbar} \hat{H}\left(t_i + m\tau\right)\right] \right| \mathbf{r}_m \right\rangle,$$

where $\mathbf{r}_0 = \mathbf{r}'$ and $\mathbf{r}_{M+1} = \mathbf{r}$. The matrix elements can then be evaluated by making use of the fact that the quantum Hamiltonian has the form

$$\hat{H} = \frac{1}{2\mu}\hat{\mathbf{p}}^2 + V(\hat{\mathbf{r}}),$$

where $\mu$ is the mass of the particle, $V(\mathbf{r})$ the potential and $\hat{\mathbf{p}}$ and $\hat{\mathbf{r}}$ the momentum and position operator, respectively. Using the Baker-Campbell-Hausdorff formula [13], in the limit $M \to \infty$, each exponential can be split into two exponentials, where the first one consists of the momentum and the second one depends on the position operator, only. Note that this does not apply in the presence of magnetic field, however one can show that the final form of the path integral is the same up to replacing the momentum $\mathbf{p}$ by $\mathbf{p} - \frac{q}{c}\mathbf{A}(\mathbf{r})$ with $q$, $c$ and $\mathbf{A}$ being the charge of the particle, the speed of light and the vector potential, respectively [12]. Then, one can let act every momentum operator to the left and every position operator to the right, finally yielding [12, 13]

$$\begin{aligned} K\left(\mathbf{r}, t_f; \mathbf{r}', t_i\right) = \\ \lim_{M\to\infty} \int \frac{\mathrm{d}^D p_0}{(2\pi\hbar)^D} \int \mathrm{d}^D r_1 \int \frac{\mathrm{d}^D p_1}{(2\pi\hbar)^D} \cdots \int \mathrm{d}^D r_M \int \frac{\mathrm{d}^D p_M}{(2\pi\hbar)^D} \\ \exp\left\{ \frac{\mathrm{i}}{\hbar} \sum_{m=0}^{M} \left[\mathbf{p}_m \cdot (\mathbf{r}_{m+1} - \mathbf{r}_m) - \tau H\left(\mathbf{p}_m, \mathbf{r}_m; t_i + m\tau\right)\right] \right\}, \end{aligned} \tag{2.10}$$

with the classical Hamiltonian resulting from the quantum one by replacing the momenum and position operator by real numbers, which are the momentum and position, respectively,

$$H\left(\mathbf{p}, \mathbf{r}\right) = \frac{\mathbf{p}^2}{2\mu} + V\left(\mathbf{r}\right). \tag{2.11}$$

Eq. (2.10) is often written in the short-hand notation [13]

$$K\left(\mathbf{r}, t_f; \mathbf{r}', t_i\right) = \int_{\mathbf{r}'}^{\mathbf{r}} \mathcal{D}\left[\mathbf{p}(t), \mathbf{r}(t)\right] \exp\left(\frac{\mathrm{i}}{\hbar} R\left[\mathbf{p}(t), \mathbf{r}(t)\right]\right),$$

where the limits of the integral indicate that the initial and final positions are fixed to $\mathbf{r}'$ and $\mathbf{r}$, respectively and

$$R\left[\mathbf{p}(t), \mathbf{r}(t)\right] = \int_{t_i}^{t_f} \mathrm{d}t \left[\mathbf{p} \cdot \dot{\mathbf{r}} - H\left(\mathbf{p}(t), \mathbf{r}(t); t\right)\right]$$

is the action of the path $(\mathbf{p}(t), \mathbf{r}(t))$.

The name "path integral" comes from the fact that the integral

$$\int \mathcal{D}\left[\mathbf{p}(t), \mathbf{r}(t)\right] \ldots$$

runs over all paths in phase space. These paths, which are schematically depicted in Fig. 2.1(a), are neither restricted to the (classically) allowed regions nor do they need to be smooth.

Finally, making use of the form (2.11) of the classical Hamiltonian the integrals over the intermediate momenta can be carried out [12, 13],

$$K\left(\mathbf{r}, t_f; \mathbf{r}', t_i\right) = \lim_{M\to\infty} \int \mathrm{d}^D r_1 \ldots \int \mathrm{d}^D r_M \frac{\exp\left\{\frac{\mathrm{i}\tau}{\hbar} \sum\limits_{m=0}^{M} \left[\frac{\mu}{2\tau}\left(\mathbf{r}_{m+1} - \mathbf{r}_m\right)^2 - \tau V\left(\mathbf{r}_m\right)\right]\right\}}{\left(2\pi\mathrm{i}\hbar\tau/\mu\right)^{\frac{D(M+1)}{2}}}, \tag{2.12}$$

which finally connects the propagator with the Lagrange function of the system by [13, 94]

$$K\left(\mathbf{r}, t_f; \mathbf{r}', t_i\right) = \int\limits_{\mathbf{r}'}^{\mathbf{r}} \mathcal{D}\left[\mathbf{r}(t)\right] \exp\left(\frac{\mathrm{i}}{\hbar} R\left[\dot{\mathbf{r}}(t), \mathbf{r}(t)\right]\right), \tag{2.13}$$

with the action of the path $(\dot{\mathbf{r}}(t), \mathbf{r}(t))$

$$R\left[\dot{\mathbf{r}}(t), \mathbf{r}(t)\right] = \int\limits_{t_i}^{t_f} \mathrm{d}t \mathcal{L}\left(\dot{\mathbf{r}}(t), \mathbf{r}(t); t\right) = \int\limits_{t_i}^{t_f} \mathrm{d}t \left(\frac{\mu}{2}\dot{\mathbf{r}}^2(t) - V(\mathbf{r}(t))\right).$$

It is important to notice that the path integral runs over paths that are not necessarily restricted to the classically allowed region.

The huge advantage of the path integral representation is that one clearly sees the origin of interference: There are essentially an infinite number of possible paths a particle can take. However, during its evolution it will pick up a phase, which is given by the action of this path, and therefore every path yields a different phase. Finally, all paths add up and therefore interference occurs.

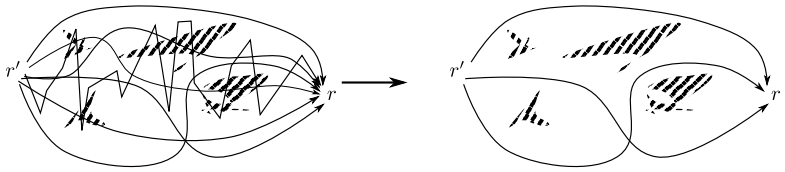


(a) Possible paths summed over in the path integral

(b) Classical paths among the quantum ones shown in (a) selected by the stationarity condition

Figure 2.1: Selection of classical paths due to the stationary phase condition. The shaded areas mark classically forbidden regions. While the quantum paths can be non-smooth and cross these regions the classical ones can not

## 2.2 The Semiclassical Approximation

The path integral (2.12) is also the starting point for the semiclassical approximation to the propagator. It is based on the observation that in many relevant cases, the actions are much largher than $\hbar$. Then the integrals in (2.12) can be evaluated using the stationary phase approximation [11].

### *2.2.1 Stationary phase approximation*

The stationary phase approximation is a method to evaluate integrals of the form

$$I = \int_{-\infty}^{\infty} \mathrm{d}x g(x) \exp\left[\mathrm{i}\lambda f(x)\right],$$

where $\lambda \gg 1$ is a large parameter and $g(x)$ a smooth function. As illustrated for the case of the integral representation for the Bessel function in Fig. 2.2, the integrand oscillates very fast as a function of $x$ except for those values of $x$ close to the stationary points $x_1, \ldots, x_n$ of $f$, for which

$$\left.\frac{\partial}{\partial x} f(x)\right|_{x=x_j} = 0. \tag{2.14}$$

Therefore, one first splits the integral into $n$ integrals, where the $j$-th integral runs over an interval containing the $j$-th stationary point and the

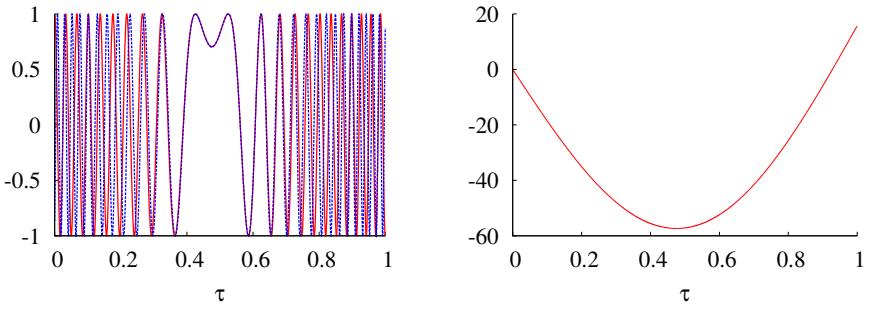


(a) Comparison between the exact (red) integrand and the one in the stationary phase approximation (blue) for the integral representation of the fifth Bessel function at $x = 65$.

(b) Argument of the integrand for the integral representation of the fifth Bessel function at $x = 65$.

Figure 2.2: The integrand of the integral-representation of the $n$-th Bessel function, $J_n(x) = \int_0^\pi \tau \cos\left[n\tau\pi - x\sin\left(\tau\pi\right)\right]$, strongly oscillates except in the region around $x \approx 0.47549$ ((a), where the argument of the cosine is stationary (b). Therefore, the main contribution to the integral stems from this region.

exponential is expanded up to second order around the stationary point. Dropping the higher order contributions of $f(x)$ yields an error of the order of $1/\lambda$ [12]. Since the main contributions to $I$ stem from regions close to the stationary points – more precisely from the interval $[x - 1/\sqrt{\lambda}, x + 1/\sqrt{\lambda}]$ [12] – each integral can be extended to the whole real axes,

$$I \approx \sum_{j=1}^{n} \int_{-\infty}^{\infty} \mathrm{d}x g(x + x_j) \exp\left[\frac{\mathrm{i}}{\hbar}\left(f(x_j) + \frac{1}{2}f''(x_j)x^2\right)\right],$$

with $f''$ denoting the second derivative of $f$. Fig. 2.2(a) shows for the case of the Bessel function how this approximation indeed resembles the exact integral, within the region where it varies slowly, very well. Expanding $g(x - x_j)$ around zero then allows to compute the integrals term by term, where the contributions from the $x$-dependent terms of $g$ again lead to contributions of the order $1/\lambda$, whereas the leading order contribution is of the order of $1/\sqrt{\lambda}$ [12]. Thus, finally $I$ is within the stationary phase

approximation given by [12, 13]

$$\begin{aligned} I &\approx \sum_{j=1}^{n} g(x_j) \sqrt{\frac{2\pi \mathrm{i}}{\lambda f''(x_j)}} \exp\left[\mathrm{i}\lambda f(x_j)\right] \\ &= \sum_{j=1}^{n} g(x_j) \sqrt{\frac{2\pi}{\lambda \left|f''(x_j)\right|}} \exp\left[\mathrm{i}\lambda f(x_j) + \mathrm{i}\frac{\pi}{4}\mathrm{sign}\left(f''(x_j)\right)\right]. \end{aligned} \tag{2.15}$$

with an error of the order $1/\lambda$.

For higher dimensional system, the same steps can be performed and yields for scalar functions $g(\mathbf{x})$ and $f(\mathbf{x})$ [14]

$$\begin{aligned} \int \mathrm{d}^D x g(\mathbf{x}) \exp\left[\mathrm{i}\lambda f(\mathbf{x})\right] &\approx \sum_{j=1}^{n} g(\mathbf{x}_j) \sqrt{\frac{(2\pi \mathrm{i})^D}{\lambda^D \det \frac{\partial^2 f}{\partial \mathbf{x}^2}(\mathbf{x}_j)}} \exp\left[\mathrm{i}\lambda f(\mathbf{x}_j)\right] \\ &= \sum_{j=1}^{n} g(\mathbf{x}_j) \sqrt{\frac{(2\pi)^D}{\lambda^D \left|\det \frac{\partial^2 f}{\partial \mathbf{x}^2}(\mathbf{x}_j)\right|}} \exp\left[\mathrm{i}\lambda f(\mathbf{x}_j) + \mathrm{i}\beta\left(\mathbf{x}_j\right)\frac{\pi}{4}\right] \\ &= \sum_{j=1}^{n} g(\mathbf{x}_j) \sqrt{\frac{(2\pi \mathrm{i})^D}{\lambda^D \left|\det \frac{\partial^2 f}{\partial \mathbf{x}^2}(\mathbf{x}_j)\right|}} \exp\left[\mathrm{i}\lambda f(\mathbf{x}_j) - \mathrm{i}\nu\left(\mathbf{x}_j\right)\frac{\pi}{2}\right], \end{aligned} \tag{2.16}$$

where

$$\beta\left(\mathbf{x}\right) = D - 2\nu\left(\mathbf{x}\right),$$

and $\nu(\mathbf{x}_j)$ is the number of negative eigenvalues of the matrix of second derivatives of $f$. Thus, $\beta(\mathbf{x})$ is the difference in the number of positive and negative eigenvalues of $\partial^2 f/\partial x^2$.

Note that since in semiclassics this approximation is used frequently, it is also called the semiclassical approximation. Moreover, since the stationary phase approximation requires a large parameter in the phase, which is in semiclassics usually $1/\hbar$, the inverse of the large parameter, *i.e.* in this section $1/\lambda$ is called the effective Planck's constant $\hbar_{\mathrm{eff}}$

### *2.2.2 The van-Vleck-Gutzwiller Propagator*

It was Martin C. Gutzwiller [11], who first applied the stationary phase approximation (2.16) to Feynman's path integral (2.12). In terms of functional derivatives the stationarity condition (2.14) for the propagator reads

$$\frac{\delta}{\delta \mathbf{r}(t)} R\left[\dot{\mathbf{r}}(t), \mathbf{r}(t)\right] = \frac{\mathrm{d}}{\mathrm{d}t}\frac{\partial \mathcal{L}}{\partial \dot{\mathbf{r}}(t)} - \frac{\partial \mathcal{L}}{\partial \mathbf{r}(t)} = 0, \tag{2.17}$$

still with fixed boundary conditions $\mathbf{r}(t_i) = \mathbf{r}'$ and $\mathbf{r}(t_f) = \mathbf{r}$. Eq. (2.17) is exactly Hamilton's principle of the least action and leads to the Euler-Lagrange equations. Thus, the stationary phase approximation selects from all paths only the classical trajectories starting at intitial position $\mathbf{r}'$ and ending at the final one $\mathbf{r}$ (see Fig. 2.1 for a schematic example). Note that, in general, there might be several classical trajectories joining the two end points and thus following Eqns. (2.15,2.16) the semiclassical propagator will be a sum over classical trajectories, rather than just one term.

The semiclassical propagator in configuration space has thus the form

$$K^{(sc)}\left(\mathbf{r}, t_f; \mathbf{r}', t_i\right) = \sum_{\gamma:\mathbf{r}'\to\mathbf{r}} \mathcal{A}_\gamma\left(\mathbf{r}, t_f; \mathbf{r}', t_i\right) \exp\left[\frac{\mathrm{i}}{\hbar} R_\gamma\left(\mathbf{r}, t_f; \mathbf{r}', t_i\right) + \mathrm{i}\nu_\gamma\left(\mathbf{r}, t_f; \mathbf{r}', t_i\right)\frac{\pi}{2}\right],$$

where the sum runs over all trajectories of the corresponding classical system joining the inital and final points $\mathbf{r}'$ and $\mathbf{r}$,

$$A_\gamma\left(\mathbf{r}, t_f; \mathbf{r}', t_i\right) = \lim_{M\to\infty}\left(\frac{\mu}{2\pi\mathrm{i}\hbar\tau}\right)^{\frac{D}{2}} \left|\det \frac{\tau}{\mu}\delta^2 R_M\right|^{-\frac{1}{2}} \tag{2.18}$$

is the semiclassical amplitude and $\nu_\gamma\left(\mathbf{r}, t_f; \mathbf{r}', t_i\right)$ is the number of negative eigenvalues of

$$\delta^2 R_M = \frac{\partial^2}{\partial\left(\mathbf{r}_1, \ldots, \mathbf{r}_M\right)^2} \sum_{m=0}^{M}\left[\frac{\mu}{2\tau}\left(\mathbf{r}_{m+1} - \mathbf{r}_m\right)^2 - \tau V\left(\mathbf{r}_m\right)\right],$$

which is the matrix of the second derivatives of the (discrete) action. Both, the semiclassical amplitude $\mathcal{A}_\gamma$ and the phase $\nu_\gamma$ have to be evaluated in the limit $M \to \infty$ and along the classical trajectory $\gamma$.

Connecting $\mathcal{A}_\gamma$ and $\nu_\gamma$ with classical quantities is the actual achievement of Gutzwiller's work [11]. He recognized that Morse's theory [225, 226] identifies $\nu_\gamma$ with the number of conjugate points of the trajectory $\gamma$. Therefore, $\nu_\gamma$ is also called Morse index. A conjugate, or sometimes also called focal point, of a trajectory is the position, at which the derivative $\partial\mathbf{r}(t)/\partial\mathbf{p}(t_i)$ vanishes, *i.e.* all trajectories, starting at the same initial position $\mathbf{r}'$, but with slightly different momenta within the interval $[\mathbf{p}(t_i) - \delta\mathbf{p}/2, \mathbf{p}(t_i) + \delta\mathbf{p}/2]$ will cross each other at time $t$ in the conjugate point $\mathbf{r}(t)$ [6] (see Fig. 2.3).

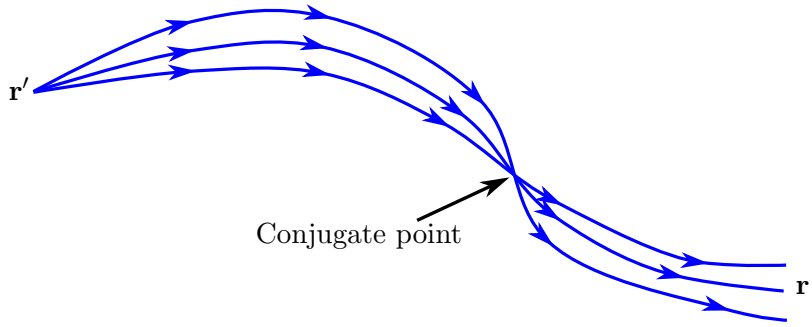


Figure 2.3: Points in configuration space, at which trajectories with slightly different initial momenta but same initial position coincide are called conjugate points.

The connection of $\det \delta^2 R_M$ with a classical quantity can be found following *e.g.* [14]. First, one notices that the matrix $\delta^2 R_M$ is block-tridiagonal,

$$\delta^2 R_M = \frac{\mu}{\tau} \begin{pmatrix} d_1 & -\mathbb{I}_D & 0 & \dots & & & 0 \\ -\mathbb{I}_D & d_2 & -\mathbb{I}_D & 0 & \dots & & 0 \\ & & & \ddots & & & \\ 0 & & \dots & 0 & -\mathbb{I}_D & d_{M-1} & -\mathbb{I}_D \\ 0 & & & \dots & 0 & -\mathbb{I}_D & d_M \end{pmatrix},$$

where $d_j = 2\mathbb{I}_D - \frac{\tau^2}{\mu} \frac{\partial V}{\partial \mathbf{r}^2} (\mathbf{r}_j)$ and $\mathbb{I}_D$ is the $D \times D$ unit matrix. Since the off-diagonal entries are unit matrices and therefore commute with the diagonal ones, one can formally expand the determinant $G_M = \det \frac{\tau}{\mu} \delta^2 R_M$ along the last row, which yields the recursion relation

$$G_M = \det (d_M)\, G_{M-1} - G_{M-2},$$

with the initial conditions $G_1 = \det d_1$ and $G_0 = 1$.

On the other hand, from the stationarity condition for $\mathbf{r}_{M-1}$, one finds

$$\mathbf{r}_M = 2\mathbf{r}_{M-1} - \frac{\tau^2}{\mu} \frac{\partial V}{\partial \mathbf{r}} (\mathbf{r}_{M-1}) - \mathbf{r}_{M-2},$$

which after taking the derivative with repsect to $\mathbf{r}_1$ and taking the determinant turns into

$$\begin{aligned} \det \frac{\partial \mathbf{r}_M}{\partial \mathbf{r}_1} &= \det \left[ \left( 2\mathbb{I}_D - \frac{\tau^2}{\mu} \frac{\partial^2 V}{\partial \mathbf{r}^2} (\mathbf{r}_{M-1}) \right) \frac{\partial \mathbf{r}_{M-1}}{\partial \mathbf{r}_1} \right] - \det \frac{\partial \mathbf{r}_{M-2}}{\partial \mathbf{r}_1} \\ &= \det (d_{M-1}) \det \frac{\partial \mathbf{r}_{M-1}}{\partial \mathbf{r}_1} - \det \frac{\partial \mathbf{r}_{M-2}}{\partial \mathbf{r}_1}. \end{aligned}$$

The initial conditions for this determinant are given by

$$\det \frac{\partial \mathbf{r}_1}{\partial \mathbf{r}_1} = 1$$
$$\det \frac{\partial \mathbf{r}_2}{\partial \mathbf{r}_1} = \det d_1.$$

Therefore $G_M$ can be identified to be

$$G_M = \det \frac{\partial \mathbf{r}_{M+1}}{\partial \mathbf{r}_1} = \det \frac{\mu}{\tau} \frac{\partial \mathbf{r}_{M+1}}{\partial \mathbf{p}_0},$$

where in last equality, $\mathbf{r}_1 = \mathbf{r}_0 + \frac{\tau}{\mu}\mathbf{p}_0$, with $\mathbf{p}_0$ being the initial momentum, has been used. Thus, using $\mathbf{p}_0 = -\frac{\partial R_\gamma(\mathbf{r}, t_f; \mathbf{r}', t_i)}{\partial \mathbf{r}'}$, (2.18) finally becomes

$$A_\gamma\left(\mathbf{r}, t_f; \mathbf{r}', t_i\right) = \frac{1}{(2\pi \mathrm{i}\hbar)^{\frac{D}{2}}} \left| \det \frac{\partial^2 R_\gamma\left(\mathbf{r}, t_f; \mathbf{r}', t_i\right)}{\partial \mathbf{r} \partial \mathbf{r}'} \right|^{\frac{1}{2}}$$

and therefore the semiclassical propagator in configuration space is finally given by the van-Vleck-Gutzwiller propagator

$$K^{(sc)}\left(\mathbf{r}, t_f; \mathbf{r}', t_i\right) = \sum_{\gamma: \mathbf{r}' \to \mathbf{r}} \frac{1}{(2\pi \mathrm{i}\hbar)^{\frac{D}{2}}} \sqrt{\left| \det \frac{\partial^2 R_\gamma}{\partial \mathbf{r} \partial \mathbf{r}'} \right|} \exp\left( \frac{\mathrm{i}}{\hbar} R_\gamma + \mathrm{i} \frac{\pi}{2} \nu_\gamma \right). \tag{2.19}$$

Previous to Gutzwiller, van-Vleck already derived (2.19) from statistical arguments [7], however missed the phase given by the Morse index. Therefore, in order to get the correct phases, the semiclassical propagator should always be computed using the stationary phase approximation.

Moreover, for small propagation times, in (2.19) only one classical trajectory contributes, and thus the van-Vleck-Gutzwiller propagator turns into the short time propagator found by Pauli [8]. This equality shows that for times smaller than a certain time scale, called Ehrenfest time $t_E$, the quantum evolution follows the classical one.

Finally, it should be noted that the stationary phase approximation becomes exact if $g(x) = const.$ and $f(x)$ is a quadratic polynomial. Therefore, if the quantum Hamiltonian is quadratic in $\hat{\mathbf{p}}$ and $\hat{\mathbf{q}}$, like for the free particle or the harmonic oscillator, the semiclassical van-Vleck-Gutzwiller propagator (2.19) is exact.

## 2.3 Semiclassical Perturbation Theory

One important and frequently used tool in semiclassics is the semiclassical perturbation theory. In conventional semiclassics it is mainly used in order to include a weak magnetic field.

Although, it is widely used, there does not seem to be any reference for the derivation of the semiclassical perturbation theory on the level of the propagator, so it will be presented here.

Suppose, the quantum Hamiltonian can be decomposed into a non-perturbed one, for which for simplicity here momentum and position operators are assumed to be separated, plus some small perturbation,

$$\hat{H} = \hat{H}_0 + \epsilon \hat{V}_1 = \frac{\hat{\mathbf{p}}^2}{2\mu} + V_0\left(\hat{\mathbf{r}}\right) + \epsilon V_1\left(\hat{\mathbf{p}}, \hat{\mathbf{r}}\right),$$

where $\epsilon$ is a measure of the strength of the perturbation.

When pluggin in this hamiltonian into the discrete path integral (2.10) and expanding the exponential in powers of $\epsilon$, one finds

$$\begin{aligned} K\left(\mathbf{r}, t_f; \mathbf{r}', t_i\right) = & \\ & \lim_{M\to\infty} \int \frac{\mathrm{d}^D p_0}{(2\pi\hbar)^D} \int \mathrm{d}^D r_1 \int \frac{\mathrm{d}^D p_1}{(2\pi\hbar)^D} \cdots \int \mathrm{d}^D r_M \int \frac{\mathrm{d}^D p_M}{(2\pi\hbar)^D} \\ & \exp\left\{ \frac{\mathrm{i}}{\hbar} \sum_{m=0}^{M} \left[ \mathbf{p}_m \cdot \left(\mathbf{r}_{m+1} - \mathbf{r}_m\right) - \tau H_0\left(\mathbf{p}_m, \mathbf{r}_m; t_i + m\tau\right) \right] \right\} \\ & \times \sum_{k=0}^{\infty} \frac{(-\mathrm{i}\tau\epsilon)^k}{\hbar^k k!} \left[ \sum_{m=0}^{M} V_1\left(\mathbf{p}_m, \mathbf{r}_m\right) \right]^k . \end{aligned} \tag{2.20}$$

Note that this formula also represents an expansion in terms of Feynman diagrams, where the $k$-th term in the sum yields those diagrams where the system is evolved under the unperturbed Hamiltonian $k+1$ times with one scattering event due to the perturbation occurs between each evolution.

On the other hand, the semiclassical perturbation theory is achieved by evaluating the integrals in (2.20) in a stationary phase approximation. Since the stationary points are determined by the exponent only, the perturbation has no effect on the classical trajectory, *i.e.* the sum will still be over the unperturbed trajectories.

After taking the limit $M \to \infty$, one obtains the van-Vleck-Gutzwiller

propagator in semiclassical perturbation theory,

$$K^{(sc)}\left(\mathbf{r},t_f;\mathbf{r}',t_i\right)=\sum_{\gamma_0:\mathbf{r}'\to\mathbf{r}}\frac{1}{(2\pi\mathrm{i}\hbar)^{\frac{D}{2}}}\sqrt{\left|\det\frac{\partial^2 R_{\gamma_0}}{\partial\mathbf{r}\partial\mathbf{r}'}\right|}\exp\left(\frac{\mathrm{i}}{\hbar}R_{\gamma_0}+\mathrm{i}\frac{\pi}{2}\nu_{\gamma_0}\right)\\ \times\sum_{k=0}^{\infty}\frac{1}{k!}\left(\frac{-\mathrm{i}\epsilon}{\hbar}\int_{t_i}^{t_f}\mathrm{d}tV_1\left(\mu\dot{\mathbf{r}}_{\gamma_0}(t),\mathbf{r}_{\gamma_0}(t)\right)\right)^k.$$

Note that for a classical trajectory the relation $\mathbf{p}=\mu\dot{\mathbf{r}}$ holds, such that the perturbation is evaluated at the classical momentum and position and is finally integrated over time.

Finally, the expansion in powers of $\epsilon$ can be undone, such that the semiclassical perturbation theory is finally given by

$$K^{(sc)}\left(\mathbf{r},t_f;\mathbf{r}',t_i\right)=\sum_{\gamma_0:\mathbf{r}'\to\mathbf{r}}\frac{1}{(2\pi\mathrm{i}\hbar)^{\frac{D}{2}}}\sqrt{\left|\det\frac{\partial^2 R_{\gamma_0}}{\partial\mathbf{r}\partial\mathbf{r}'}\right|}\exp\left(\frac{\mathrm{i}}{\hbar}R_{\gamma_0}+\mathrm{i}\frac{\pi}{2}\nu_{\gamma_0}\right)\\ \times\exp\left(-\frac{\mathrm{i}\epsilon}{\hbar}\int_{t_i}^{t_f}\mathrm{d}tV_1\left(\mathbf{p}_{\gamma_0}(t),\mathbf{r}_{\gamma_0}(t)\right)\right),\tag{2.21}$$

where the subscript 0 at the trajectory $\gamma_0$ indicates that it is the trajectory of the unperturbed classical system. Moreover, $R_{\gamma_0}$ is the action of the unperturbed trajectory for $\epsilon=0$.

Within the semiclassical perturbation theory the classical trajectories are kept unchanged, while each term of the propagator is multiplied by an additional phase, which is given by the perturbation evaluated along the classical trajectory. Note that classically the momentum $\mathbf{p}$ and the time derivative of the position $\dot{\mathbf{r}}$ are related by $\mathbf{p}=\mu\dot{\mathbf{r}}$ and therefore the perturbation is evaluated at the momentum and position of the classical trajectory.

Now consider for a moment the derivative of the action of an exact classical trajectory of the perturbed system. This derivative can be computed

as

$$\frac{\partial}{\partial\epsilon}R_{\gamma_\epsilon} = \frac{\partial}{\partial\epsilon}\int_{t_i}^{t_f} \mathrm{d}t \left[\mathbf{p}_{\gamma_\epsilon}\cdot\dot{\mathbf{r}}_{\gamma_\epsilon} - H_\epsilon\left(\mathbf{p}_{\gamma_\epsilon},\mathbf{r}_{\gamma_\epsilon}\right)\right] =$$

$$\int_{t_i}^{t_f}\mathrm{d}t\left\{\frac{\partial\mathbf{p}_{\gamma_\epsilon}}{\partial\epsilon}\cdot\dot{\mathbf{r}}_{\gamma_\epsilon} + \mathbf{p}_{\gamma_\epsilon}\cdot\frac{\partial\dot{\mathbf{r}}_{\gamma_\epsilon}}{\partial\epsilon} - \frac{\partial H_\epsilon}{\partial\mathbf{r}_{\gamma_\epsilon}}\frac{\partial\mathbf{r}_{\gamma_\epsilon}}{\partial\epsilon} - \frac{\partial H_\epsilon}{\partial\mathbf{p}_{\gamma_\epsilon}}\frac{\partial\mathbf{p}_{\gamma_\epsilon}}{\partial\epsilon} - V_1\left(\mathbf{p}_{\gamma_\epsilon},\mathbf{r}_{\gamma_\epsilon}\right)\right\}.$$

Using Hamilton's equations of motion, the two terms containing the derivative of the momentum with respect to $\epsilon$ cancel, such that after a partial integration of the term $\mathbf{p}\cdot\partial\dot{\mathbf{r}}/\partial\epsilon$, one gets

$$\begin{aligned}\frac{\partial}{\partial\epsilon}R_{\gamma_\epsilon} &= \left[\mathbf{p}_{\gamma_\epsilon}\cdot\frac{\partial\mathbf{r}_{\gamma_\epsilon}}{\partial\epsilon}\right]_{t_i}^{t_f} - \int_{t_i}^{t_f}\mathrm{d}t\left[\dot{\mathbf{p}}_{\gamma_\epsilon}\cdot\frac{\partial\mathbf{r}_{\gamma_\epsilon}}{\partial\epsilon} + \frac{\partial H_\epsilon}{\partial\mathbf{r}_{\gamma_\epsilon}}\frac{\partial\mathbf{r}_{\gamma_\epsilon}}{\partial\epsilon}\right] - \int_{t_i}^{t_f}\mathrm{d}tV_1\left(\mathbf{p}_{\gamma_\epsilon},\mathbf{r}_{\gamma_\epsilon}\right)\\ &= -\int_{t_i}^{t_f}\mathrm{d}tV_1\left(\mathbf{p}_{\gamma_\epsilon},\mathbf{r}_{\gamma_\epsilon}\right),\end{aligned}$$

where in the last step again Hamilton's equations of motion have been used as well as the fact that the intial and final positions are fixed and therefore independent of $\epsilon$.

If the perturbation is small enough the trajectories are only slightly deformed by the perturbation, such that there is a one-to-one corresponding between perturbed and unperturbed trajectories. Therefore, the phase in (2.21) is the expansion of the classical action up to linear order in $\epsilon$, while in the prefactor, only the constant term in the expansion in $\epsilon$ is kept.

CHAPTER 3

# From Single- to Many-Body Physics: Second quantization and many-body states

## 3.1 Second Quantization and Fock states

In this section the basic concepts of second quantization will be reviewed very briefly, while a more detailed description can be found *e.g.* in [227].

The basic idea of second quantization is to describe a system of many identical and indistinguishable particles by utilizing the solutions of the corresponding single-particle system. This is possible by noticing that the many-body Hilbert space can only be constructed from single-particle states.

It turns out to be useful to introduce the occupation number $n_l$, which is the number of particles, occupying the (normalized) single-particle state $l$. For Bosons, these numbers can be any integer from zero to infinity, while for Fermions – due to the Pauli principle – they are either 0 or 1. Here it should be noted that the spatial single-particle state and the spin state together form the single-particle state, such that a spin up and spin down particle in the same spatial (or orbital) single-particle state are regarded as particles occupying two *different* single-particle states (see Fig. 3.2). With

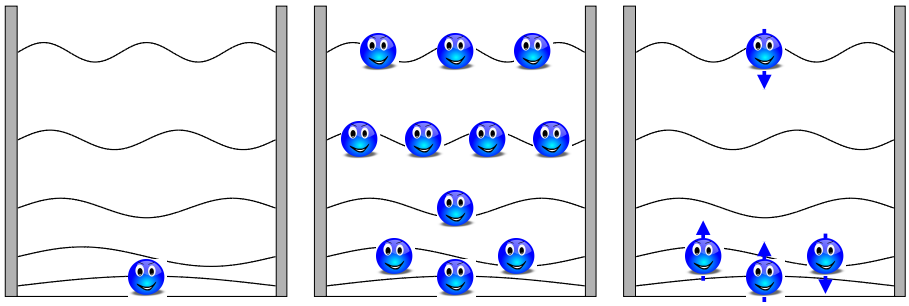

(a) $|1,0,0,0,0\rangle$ (b) $|1,2,1,4,3\rangle$ (c) $|1,0,1,1,0,0,0,0,0,1\rangle$

Figure 3.1: Illustration of the definitions of Fock states for a quantum well with five bound states for (a) one spin-less particle, (b) eleven spin-less particles and (c) four spin-1/2 particles.

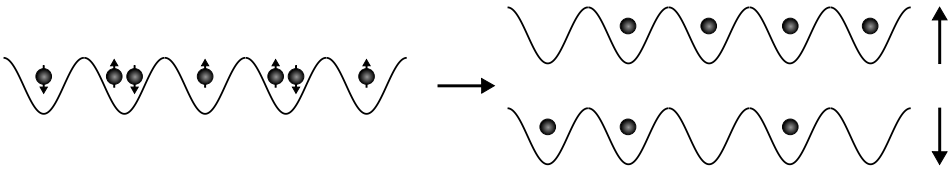

Figure 3.2: A spin-up and spin-down particle in the same spatial (or orbital) single-particle state are regarded as particles occupying two *different* single-particle states.

these occupation numbers, each many-body state with given symmetry under exchange of particles (symmetric for Bosons and antisymmetric for Fermions), can be represented by a Fock state (see also Fig. 3.1)

$$|\mathbf{n}\rangle = |n_1, n_2, \ldots\rangle\,.$$

Fock states are orthonormal,

$$\langle \mathbf{n} \,|\, \mathbf{n}' \rangle = \prod_l \delta_{n_l,n_l'} = \delta_{\mathbf{n},\mathbf{n}'}$$

and complete,

$$\sum_{\mathbf{n}} |\mathbf{n}\rangle \langle \mathbf{n}| = \mathbb{I}.$$

The space spanned by these Fock states (including the so called vacuum state $|0\rangle = |0,0\ldots\rangle$), is called Fock space.

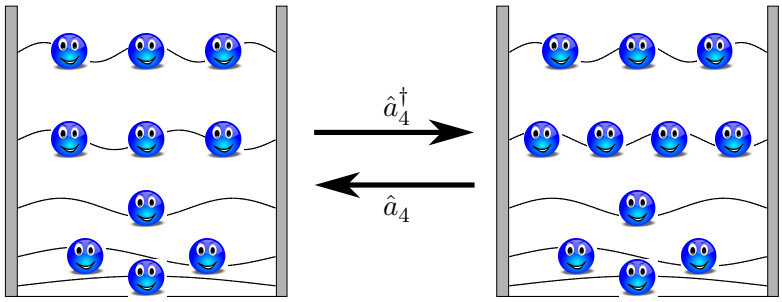


(a) $|1,2,1,3,3\rangle$ (b) $|1,2,1,4,3\rangle$

Figure 3.3: Applying the creation operator $\hat{a}_4^\dagger$ to the bosonic state in (a) results in the state shown in (b), while with the help of the annihilation operator $\hat{a}_4$, one can go from left to right.

Since $n_l$ is the number of particles in state $l$, one can easily find the subspace of fixed total number of particles $N$. This is the space spanned by all Fock states $|\mathbf{n}\rangle$ which satisfy

$$\sum_l n_l = N.$$

Within the procedure of second quantization, one also defines creation and annihilation operators. Since their properties and actions on the Fock states depends on whether the described particles are Bosons or Fermions, from now on these two cases are discussed separately.

### *3.1.1 Bosonic creation and annihilation operators*

The bosonic creation and annihilation operators will be denoted by $\hat{a}_l^\dagger$ and $\hat{a}_l$, respectively, throughout the entire thesis. The creation operator $\hat{a}_l^\dagger$ increases the number of particles in the single-particle state $l$ by one (see Fig. 3.3),

$$\hat{a}_l^\dagger |n_1, \ldots, n_l, \ldots\rangle = \sqrt{n_l + 1}\, |n_1, \ldots, n_l + 1, \ldots\rangle .$$

Analoguously, the annihilation operator $\hat{a}_l$ is defined as the operator decreasing the number of particles in the single-particle state $l$,

$$\hat{a}_l |n_1, \ldots, n_l, \ldots\rangle = \sqrt{n_l}\, |n_1, \ldots, n_l - 1, \ldots\rangle .$$

This definition of the annihilation operators also implies that applying $\hat{a}_l$ to a Fock states with $n_l = 0$ yields zero,

$$\hat{a}_l \left|n_1, \ldots, n_{l-1}, 0, n_{l+1}, \ldots\right\rangle = 0.$$

These definitions also require that the commutation relations for creation and annihilation operators to read

$$\left[\hat{a}_l^\dagger, \hat{a}_{l'}^\dagger\right]_- = 0 \tag{3.1a}$$

$$\left[\hat{a}_l, \hat{a}_{l'}\right]_- = 0 \tag{3.1b}$$

$$\left[\hat{a}_l, \hat{a}_{l'}^\dagger\right]_- = \delta_{l,l'}, \tag{3.1c}$$

where

$$\left[\hat{A}, \hat{B}\right]_- = \hat{A}\hat{B} - \hat{B}\hat{A}$$

is the commutator of the operators $\hat{A}$ and $\hat{B}$.

It is important to notice that any Fock state $|\mathbf{n}\rangle = |n_1, n_2, \ldots\rangle$ can be derived by applying the creation operator $\hat{a}_1^\dagger$ $n_1$ times, $n_2$ times the creation operator $\hat{a}_2^\dagger$, etc., to the vacuum,

$$\left|n_1, n_2, \ldots\right\rangle = \frac{1}{\sqrt{n_1!\, n_2! \cdots}} \left(\hat{a}_1^\dagger\right)^{n_1} \left(\hat{a}_2^\dagger\right)^{n_2} \cdots \left|0\right\rangle.$$

From the definitions of the creation and annihilation operators, it is easy to see that a Fock state is an eigenstate to the number operator $\hat{n}_l = \hat{a}_l^\dagger \hat{a}_l$ with eigenvalue $n_l$,

$$\hat{n}_l \left|n_1, \ldots, n_l, \ldots\right\rangle = n_l \left|n_1, \ldots, n_l, \ldots\right\rangle.$$

Since the eigenvalue of $\hat{n}_l$ is the occupation number of the $l$-th single-particle eigenstate, $\hat{n}_l$ is refered to as the $l$-th number operator. Moreover, this allows to define the total number operator

$$\hat{N} = \sum_l \hat{n}_l.$$

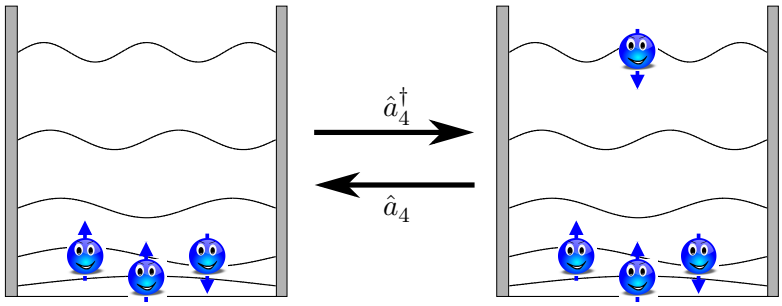


(a) $|1,0,1,1,0,0,0,0,0,0\rangle$ (b) $|1,0,1,1,0,0,0,0,0,1\rangle$

Figure 3.4: Applying the creation operator $\hat{c}_{5\downarrow}^\dagger$ to the fermionic state in (a) results in the state shown in (b), while with the help of the annihilation operator $\hat{a}_{5\downarrow}$, one can go from left to right.

In the following chapters, the shorthand notations

$$\hat{\mathbf{a}}^\dagger = \left(\hat{a}_1^\dagger, \hat{a}_2^\dagger, \ldots\right) \tag{3.2a}$$

$$\hat{\mathbf{a}} = \begin{pmatrix} \hat{a}_1 \\ \hat{a}_2 \\ \vdots \end{pmatrix} \tag{3.2b}$$

$$\hat{\mathbf{n}} = \begin{pmatrix} \hat{n}_1 \\ \hat{n}_2 \\ \vdots \end{pmatrix} \tag{3.2c}$$

will also be used.

### *3.1.2 Fermionic creation and annihilation operators*

The fermionic creation and annihilation operators $\hat{c}_l^\dagger$ and $\hat{c}_l$ are defined similarly as the bosonic ones. However, one has to keep in mind that due to the Pauli principle, a particle can not be created in a state, which is already occupied, such that

$$\hat{c}_l^\dagger \, |n_1, \ldots, n_{l-1}, 0, n_{l+1}, \ldots\rangle = (-1)^{\sum_{l'=1}^{l-1} n_{l'}} \, |n_1, \ldots, n_{l-1}, 1, n_{l+1}, \ldots\rangle \tag{3.3a}$$

$$\hat{c}_l^\dagger \, |n_1, \ldots, n_{l-1}, 1, n_{l+1}, \ldots\rangle = 0 \tag{3.3b}$$

as well as

$$\hat{c}_l \left|n_1, \ldots, n_{l-1}, 0, n_{l+1}, \ldots\right\rangle = 0, \tag{3.4a}$$

$$\hat{c}_l \left|n_1, \ldots, n_{l-1}, 1, n_{l+1}, \ldots\right\rangle = (-1)^{\sum_{l'=1}^{l-1} n_{l'}} \left|n_1, \ldots, n_{l-1}, 0, n_{l+1}, \ldots\right\rangle, \tag{3.4b}$$

where the additional signs in (3.3a) and (3.4b) account for the antisymmetry of Fermions under exchange of particles.

Accordingly, the fermionic creation and annihilation operators obey certain *anti*commutation relations, rather than commutatoin relations. These are

$$\begin{aligned} \left[\hat{c}_l^\dagger, \hat{c}_{l'}^\dagger\right]_+ &= 0, \\ \left[\hat{c}_l, \hat{c}_{l'}\right]_+ &= 0, \\ \left[\hat{c}_l, \hat{c}_{l'}^\dagger\right]_+ &= \delta_{l,l'}, \end{aligned}$$

with the anticommutator of two operators $\hat{A}$ and $\hat{B}$ given by

$$\left[\hat{A}, \hat{B}\right]_+ = \hat{A}\hat{B} + \hat{B}\hat{A}.$$

The connection between a fermionic Fock state and the vacuum state therefore reads

$$\left|n_1, n_2, \ldots\right\rangle = \cdots \left(\hat{c}_2^\dagger\right)^{n_2} \left(\hat{c}_1^\dagger\right)^{n_1} \left|0\right\rangle, \tag{3.5}$$

where now it is crucial to apply the creation operators in the correct order, since exchanging two creation operators gives an additional minus sign. This additional minus sign is also the reason, why there has to be an additional sign in equations (3.3a) and (3.4b).

In the same way as for Bosons, a number operator can be defined for Fermions too,

$$\hat{n}_l = \hat{c}_l^\dagger \hat{c}_l.$$

The number operator has eigenvalues 0 and 1, with the eigenvectors beeing the Fock states,

$$\hat{n}_l \left|n_1, \ldots, n_l, \ldots\right\rangle = n_l \left|n_1, \ldots, n_l, \ldots\right\rangle,$$

and allows to define the total number operator

$$\hat{N} = \sum_l \hat{n}_l.$$

For the fermionic operators the shorthand notations

$$\hat{\mathbf{c}}^\dagger = \left(\hat{c}_1^\dagger, \hat{c}_2^\dagger, \dots\right)$$
$$\hat{\mathbf{c}} = \begin{pmatrix} \hat{c}_1 \\ \hat{c}_2 \\ \vdots \end{pmatrix}$$
$$\hat{\mathbf{n}} = \begin{pmatrix} \hat{n}_1 \\ \hat{n}_2 \\ \vdots \end{pmatrix}$$

will also be used in the following chapters.

### *3.1.3 Hamiltonian and observables in second quantization*

The whole theory of second quantization would be worthless, if many-body Hamiltonians and observables could not be expressed in terms of creation and annihilation operators. Here, general observables will be considered since the Hamiltonian is just a special kind of observable, namely the energy of the system.

In many-body systems, operators are classified by the number of particles they couple. A $n$-body operator in second quantization is an operator of the form

$$\hat{O}_n = \sum_{i_1,\dots,i_n,j_1,\dots,j_n} O_{i_1,\dots,i_n,j_1,\dots,j_n} \hat{a}_{i_1}^\dagger \cdots \hat{a}_{i_n}^\dagger \hat{a}_{j_1} \cdots \hat{a}_{j_n}, \tag{3.6}$$

where in this section, $\hat{a}_j^\dagger$ and $\hat{a}_j$ denote either fermionic or bosonic creation and annihilation operators for the $j$-th single-particle states. Here, the tensor elements $O_{i_1,\dots,i_n,j_1,\dots,j_n}$ are given by

$$O_{i_1,\dots,i_n,j_1,\dots,j_n} = \left\langle i_n \middle| \cdots \left\langle i_1 \middle| \hat{O} \middle| j_1 \right\rangle \cdots \middle| j_n \right\rangle. \tag{3.7}$$

Eq. (3.6) can be interpreted as removing $n$ particles – each one from the single-particle states $j_1, \dots, j_n$ – and put it to $i_1, \dots, j_n$ with an amplitude given by (3.7). Finally, one has to sum over all possible of such processes.

An $n$-body observable is then a linear hermitian combination of such $n$-body operators and in general an observable may be given by the linear combination of $n$-body observables with different values of $n$, *e.g.* a very important Hamiltonian especially in the theory of ultra-cold atoms, is the Hamiltonian for a 1-dimensional Bose-Hubbard chain with nearest neighbor hopping and two-body on-site interactions,

$$\hat{H} = \sum_{l=1}^{L} \epsilon_l \hat{a}_l^\dagger \hat{a}_l - \sum_{l=1}^{L-1} \left( \kappa \hat{a}_l^\dagger \hat{a}_{l+1} + \kappa^* \hat{a}_{l+1}^\dagger \hat{a}_l \right) + \frac{U}{2} \sum_{l=1}^{L} \hat{a}_l^\dagger \hat{a}_l^\dagger \hat{a}_l \hat{a}_l. \tag{3.8}$$

This Hamiltonian models for instance atoms in a chain of $L$ magneto-optical traps, where the energy of the $l$-th trap is $\epsilon_l$, the particles tunnel from one trap to the adjacent one with probability $\kappa$ and the two body interaction stems from $s$-wave scattering among particles within the same trap. In order to arive at the Hamiltonian (3.8), the chosen basis for the single-particle state are the Wannier functions of the individual traps.

One should also notice that for a non-interacting many-body system, the many-body Hamiltonian in the eigenbasis of the single-particle Hamiltonian is given by

$$\hat{H} = \sum_j E_j \hat{a}_j^\dagger \hat{a}_j = \sum_j E_j \hat{n}_j.$$

Moreover, in second quantization, the total number of particles is no longer an extrinsic parameter, but an observable

$$\hat{N} = \sum_j \hat{n}_j,$$

which is conserved for closed systems.

## 3.2 Bosonic Many-Body States

Due to the fact that bosonic operators for different single-particle states commute it is enough to consider only single-state systems in this section.

### *3.2.1 Quadrature States*

In this section, we follow to some extend the consideration of quadrature eigenstates given in section 3.3.3 of [228].

The quadrature states are defined as the eigenstates of the quadrature operator,

$$\hat{x}(\varphi)\ |x\rangle_\varphi = x(\varphi)\,|x\rangle_\varphi$$
$$\hat{x}(\varphi) = b\left[\hat{a}\exp(\mathrm{i}\varphi) + \hat{a}^\dagger\exp(-\mathrm{i}\varphi)\right],$$

where $b$ and $\varphi$ are for now arbitrary, but real parameters.

This definition can also be used, in order to express the annihilation and creation operators in terms of quadrature operators,

$$\hat{a}_j = \frac{\exp(-\mathrm{i}\varphi)}{2b}\left[\hat{x}(\varphi) + \mathrm{i}\hat{x}\left(\varphi - \frac{\pi}{2}\right)\right] \tag{3.9a}$$
$$\hat{a}_j^\dagger = \frac{\exp(\mathrm{i}\varphi)}{2b}\left[\hat{x}(\varphi) - \mathrm{i}\hat{x}\left(\varphi - \frac{\pi}{2}\right)\right]. \tag{3.9b}$$

Moreover, it is straight forward to compute the commutation relation of the quadrature operators,

$$\left[\hat{x}(\varphi), \hat{x}\left(\varphi'\right)\right] = 2\mathrm{i}b^2\sin\left(\varphi - \varphi'\right). \tag{3.10}$$

Since the quadrature operators are obviously hermitian, the eigenvalues $x$ are real. For the sake of generality, a dependence of the eigenvalue on the quadrature phase $\varphi$ has been included. However, by making use of the commutation relations (3.1) it can be shown that for an arbitrary quadrature phase $\varphi$, the quadrature operator is related to the one with $\varphi = 0$ by

$$\hat{x}(\varphi) = \exp\left(-\mathrm{i}\varphi\hat{a}^\dagger\hat{a}\right)\hat{x}(0)\exp\left(\mathrm{i}\varphi\hat{a}^\dagger\hat{a}\right).$$

which plugged into the eigenvalue equation for $\varphi = 0$ yields

$$x\,|x\rangle_{\varphi=0} = \hat{x}(0)\,x\,|x\rangle_{\varphi=0} = \exp\left(\mathrm{i}\varphi\hat{a}^\dagger\hat{a}\right)\hat{x}(\varphi)\exp\left(-\mathrm{i}\varphi\hat{a}^\dagger\hat{a}\right)\ |x\rangle_{\varphi=0}$$

and therefore

$$\hat{x}(\varphi)\exp\left(-\mathrm{i}\varphi\hat{a}^\dagger\hat{a}\right)\ |x\rangle_{\varphi=0} = x\exp\left(-\mathrm{i}\varphi\hat{a}^\dagger\hat{a}\right)\ |x\rangle_{\varphi=0},$$

which shows that the eigenvalue $x(\varphi) = x$ does not depend on the quadrature phase, and the quadrature eigenstate for non-zero phase is connected to the one with $\varphi = 0$ by

$$|x\rangle_\varphi = \exp\left(-\mathrm{i}\varphi\hat{a}^\dagger\hat{a}\right)\ |x\rangle_{\varphi=0}. \tag{3.11}$$

This observation allows to compute properties for non-zero quadrature phases easily out of the quadrature eigenstates for $\varphi = 0$.

In order to shorten the notation, from now on the quadrature operators with zero quadrature phase will be denoted by $\hat{q}$, the corresponding eigenstates by $|q\rangle$, as well as their eigenvalues by $q$. Likewise, the quadrature operators for $\varphi = -\pi/2$ will be denoted by $\hat{p}$ as well as their eigenstates by $|p\rangle$ and their eigenvalues by $p$.

The expansion of the quadrature eigenstates $|q\rangle$ in Fock states can be found by considering

$$\frac{q}{b}\langle n \,|\, q\rangle = \frac{1}{b}\langle n|\,\hat{q}\,|q\rangle = \sqrt{n+1}\,\langle n+1 \,|\, q\rangle + \sqrt{n}\,\langle n-1 \,|\, q\rangle\,.$$

The normlized solution to this recurrence relation is given by [229]

$$\langle n \,|\, q\rangle = \frac{\exp\left(-\frac{q^2}{4b^2}\right)}{\sqrt{2^n n!\,\sqrt{2\pi}b}} H_n\left(\frac{q}{\sqrt{2}b}\right),$$

where $H_n$ denotes the $n$-th Hermite polynomial.

Using (3.11), one immediately sees that for arbitrary $\varphi$,

$$\langle n \,|\, x\rangle_\varphi = \frac{\exp\left(-\frac{x^2}{4b^2} - \mathrm{i}n\varphi\right)}{\sqrt{2^n n!\,\sqrt{2\pi}b}} H_n\left(\frac{x}{\sqrt{2}b}\right) \tag{3.12}$$

In the semiclassical treatment of the propagator, we will have to evaluate integrals involving the overlap between quadrature and Fock states, which are very hard to compute. If the occupation number $n$ is large, however, one may use the asymptotic form of this overlap, which is - for $\varphi = 0$ - given by the WKB-approximation [6],

$$\langle n \,|\, q\rangle \approx \sqrt{\frac{2}{\pi\sqrt{4b^2\left(n+\frac{1}{2}\right) - q^2}}}\cos\left[F\left(q,n\right) + \frac{\pi}{4}\right], \tag{3.13}$$

where $F(q,n)$ is the generating function for the canonical transformation from $(q,p)$ to $(n,\theta)$ with $q = 2b\sqrt{n+\frac{1}{2}}\cos\theta$ and $p = 2b\sqrt{n+\frac{1}{2}}\sin\theta$ and is given by

$$F\left(q,n\right) = \frac{q}{4b^2}\sqrt{4b^2\left(n+\frac{1}{2}\right) - q^2} - \left(n+\frac{1}{2}\right)\arccos\left(\frac{q}{2b\sqrt{n+\frac{1}{2}}}\right).$$

It is worth to notice that the generating function can also be written as an integral along a classical path,

$$F(q,n) = \frac{1}{b}\int_{q_0}^{q} \mathrm{d}x \sqrt{n+\frac{1}{2}-\frac{x^2}{4b^2}},$$

where $q_0 = 2b\sqrt{n+1/2}$. As a generating function of a canonical transformation, the derivatives of $F(q,n)$ satisfy

$$\frac{\partial F(q,n)}{\partial q} = \frac{1}{b}\sqrt{n+\frac{1}{2}-\frac{q^2}{4b^2}} = \frac{|p|}{2b^2}$$
$$\frac{\partial F(q,n)}{\partial n} = -\arccos\left(\frac{q}{2b\sqrt{n+\frac{1}{2}}}\right) = -\theta$$

Note that, by this definition of $\theta$, the phase is only defined between 0 and $\pi$, and therefore $|p| = p$.

Having found the overlap (3.12) and using the properties of the Hermite polynomials, one can also find the overlap between two quadrature eigenstates as well as the resolution of unity,

$${}_{\varphi}\langle x \,|\, x' \rangle_{\varphi'} = \frac{\exp\left[\mathrm{i}\frac{2xx' - \left(x^2+x'^2\right)\cos(\varphi-\varphi')}{4b^2\sin(\varphi-\varphi')}\right]}{b\sqrt{2\pi\left(1-\exp\left[2\mathrm{i}\left(\varphi-\varphi'\right)\right]\right)}} \quad \text{for } \varphi \neq \varphi', \tag{3.14a}$$

$${}_{\varphi}\langle x \,|\, x' \rangle_{\varphi} = \delta\left(x-x'\right), \tag{3.14b}$$

$$\int_{-\infty}^{\infty} \mathrm{d}x \, |x\rangle_{\varphi}\, {}_{\varphi}\langle x| = 1, \tag{3.14c}$$

and in particular for $\varphi' = \varphi - \pi/2$,

$${}_{\varphi}\langle x \,|\, x' \rangle_{\varphi-\frac{\pi}{2}} = \frac{1}{\sqrt{4b^2\pi}} \exp\left(\frac{\mathrm{i}}{2b^2}xx'\right). \tag{3.15}$$

Thus, for fixed $\varphi$, the quadrature eigenstates $|x\rangle_{\varphi}$ form a continuous, but complete and orthogonal basis of the Fock space.

In the following chapters,

$${}_{\varphi-\frac{\pi}{2}}\langle x \,|\, \hat{a} \,|\, x' \rangle_{\varphi} = \frac{1}{4b^2\sqrt{\pi}}\left(x' + \mathrm{i}x\right)\exp\left(-\frac{\mathrm{i}}{2b^2}xx'\right), \tag{3.16a}$$

$${}_{\varphi-\frac{\pi}{2}}\left\langle x \,\middle|\, \hat{a}^{\dagger} \,\middle|\, x' \right\rangle_{\varphi} = \frac{1}{4b^2\sqrt{\pi}}\left(x' - \mathrm{i}x\right)\exp\left(-\frac{\mathrm{i}}{2b^2}xx'\right), \tag{3.16b}$$

will also be used. Eq. (3.16) follows immediately from the representation of the creation and annihilation operators in terms of quadrature operators, Eq. (3.9).

Using the resolution of unity, Eq. (3.14c), as well as Eq. (3.16), it is straight forward to compute,

$$ {}_{\varphi}\langle x \,|\, \hat{a} \,|\, x' \rangle_{\varphi} = \left( \frac{1}{2b} x - b \frac{\partial}{\partial x} \right) \delta\left(x - x'\right) \tag{3.17a} $$

$$ {}_{\varphi}\left\langle x \,\middle|\, \hat{a}^{\dagger} \,\middle|\, x' \right\rangle_{\varphi} = \left( \frac{1}{2b} x - b \frac{\partial}{\partial x'} \right) \delta\left(x - x'\right) \tag{3.17b} $$

### *3.2.2 Coherent States*

Coherent states are defined as the eigenstates of the anihilation operator,

$$ \hat{a} \,|\phi\rangle = \phi \,|\phi\rangle \,. $$

Since the annihilation operators are non-hermitian, the eigenvalues $\phi$ are in general complex. One can show that these states are given by

$$ |\phi\rangle = \exp\left( -\frac{1}{2} |\phi|^2 + \hat{a}^{\dagger} \phi \right) |0\rangle \,. $$

where $|0\rangle$ is the bosonic vacuum state. With this definition it is easy to see that the overlap of a coherent state with a Fock state is given by

$$ \langle n \,|\, \phi \rangle = \exp\left( -\frac{1}{2} |\phi|^2 \right) \frac{\phi^n}{\sqrt{n!}}. $$

Note that the coherent states are defined such that they are normalized to one,

$$ \langle \phi \,|\, \phi \rangle = 1. $$

However, coherent states are not orthogonal

$$ \left\langle \phi \,\middle|\, \phi' \right\rangle = \exp\left[ -\frac{1}{2} |\phi|^2 - \frac{1}{2} \left|\phi'\right|^2 + \phi^* \phi' \right] $$

but they satisfy the closure relation

$$ \frac{1}{\pi} \int_{-\infty}^{\infty} \mathrm{d}\Re\phi \int_{-\infty}^{\infty} \mathrm{d}\Im\phi \,|\phi\rangle \,\langle\phi| = 1. \tag{3.18} $$

Therefore, the coherent states form an overcomplete set.

Applying a creation operator to a coherent state yields

$$\hat{a}^\dagger \left|\phi\right\rangle = \left(\frac{\partial}{\partial\phi} + \frac{\phi^*}{2}\right)\left|\phi\right\rangle .$$

Finally, the overlap of a coherent state with a quadrature eigenstate is given by

$$\left\langle\phi \,|\, x\right\rangle_\varphi = \frac{1}{\sqrt{b\sqrt{2\pi}}} \exp\left[-\frac{1}{2}\left|\phi\right|^2 - \left(\frac{1}{2b}x - \phi^* \mathrm{e}^{-\mathrm{i}\varphi}\right)^2 + \frac{1}{2}\left(\phi^* \mathrm{e}^{-\mathrm{i}\varphi}\right)^2\right]. \tag{3.19}$$

## 3.3 Fermionic Many-Body States

Since Fermionic operators do not commute, the vector notation for the fermionic many-body states will be readopted.

### *3.3.1 Coherent States*

In the same way as for bosons, one can define coherent states for Fermions [64, 230],

$$\hat{c}_l \left|\boldsymbol{\zeta}\right\rangle = \zeta_l \left|\boldsymbol{\zeta}\right\rangle .$$

However, since the occupation numbers for fermions are only zero or one, the $\zeta$'s cannot be ordinary complex numbers. In fact, they must be (complex) Grassmann variables, which are anticommuting numbers,

$$\zeta\zeta' = -\zeta'\zeta.$$

This anticommutativity has some drastic consequences. For one, multiplying a Grassmann number with itself gives zero, and therefore the Taylor series of each function truncates after the first order,

$$f(\zeta) = f(0) + f'(0)\zeta,$$

where $f'$ denotes the first derivative of $f$. The derivative with respect to a Grassmann variable yields then just the first Taylor coefficient,

$$\frac{\partial}{\partial\zeta} f(\zeta) = f'(0)$$

and integration is the same as differentiation,

$$\int \mathrm{d}\zeta = 0,$$

$$\int \mathrm{d}\zeta\zeta = -1.$$

It is important to notice that $\zeta$ and $\zeta^*$ are independent variables, such that $\zeta\zeta^* \neq 0$ and

$$\begin{aligned} \int \mathrm{d}\zeta\mathrm{d}\zeta^* &= 0, \\ \int \mathrm{d}\zeta\mathrm{d}\zeta^*\zeta &= 0, \\ \int \mathrm{d}\zeta\mathrm{d}\zeta^*\zeta^* &= 0, \\ \int \mathrm{d}\zeta\mathrm{d}\zeta^*\zeta^*\zeta &= 1. \end{aligned} \tag{3.20}$$

With this, the discussion of Fermionic coherent states can be continued. First of all, one can check that the definition of the coherent states as eigenstates of the annihilation operators is fulfilled by

$$|\boldsymbol{\zeta}\rangle = \exp\left(-\frac{1}{2}\sum_{l=1}^{L}\zeta_l^*\zeta_l\right)\left[\prod_{l=0}^{L-1}\left(1-\zeta_{L-l}\hat{c}_{L-l}^\dagger\right)\right]|0\rangle\,,$$

with $|0\rangle$ being the Fermionic vacuum state and $L$ the number of single-particle states. Note that the order of the product is the same as in the definition of the Germionic Fock states, (3.5). Again, the coherent states have been chosen such that they are normalized to one,

$$\langle\boldsymbol{\zeta}\,|\,\boldsymbol{\zeta}\rangle = 1.$$

Many properties of the Fermionic coherent states can be written formally in the same way as those of the bosonic ones. However, one always has to take care of the correct ordering of Grassmann variables, since exchanging two of them yields an additional minus sign.

One of the important properties is the overlap between two coherent states and the overlap of a coherent state with a Fock state,

$$\langle \boldsymbol{\zeta} \,|\, \boldsymbol{\zeta}' \rangle = \exp\left( -\frac{1}{2}\boldsymbol{\zeta}^* \cdot \boldsymbol{\zeta} - \frac{1}{2}\boldsymbol{\zeta}'^* \cdot \boldsymbol{\zeta}' + \boldsymbol{\zeta}^* \cdot \boldsymbol{\zeta}' \right).$$

$$\langle \mathbf{n} \,|\, \boldsymbol{\zeta} \rangle = \exp\left( -\frac{1}{2}\boldsymbol{\zeta}^* \cdot \boldsymbol{\zeta} \right) \prod_{l=0}^{L-1} \zeta_{L-l}^{n_{L-l}}.$$

Moreover, the resolution of unity is given by

$$\int \mathrm{d}^{2L}\zeta \, |\boldsymbol{\zeta}\rangle \, \langle \boldsymbol{\zeta}| = 1. \tag{3.21}$$

where $\int \mathrm{d}^{2L}\zeta = \mathrm{d}\zeta_1 \mathrm{d}\zeta_1^* \cdots \int \mathrm{d}\zeta_L \mathrm{d}\zeta_L^*$.

For the sake of completeness, we also state the action of a creation operator on a coherent state:

$$\hat{c}_l^\dagger \, |\boldsymbol{\zeta}\rangle = \left( \frac{\partial}{\partial \zeta_l} + \frac{1}{2}\zeta_l^* \right) |\boldsymbol{\zeta}\rangle \,.$$

### *3.3.2 Klauder coherent states*

In [231], Klauder introduced a different kind of fermionic coherent states (we will call them Klauder coherent states), which are described by complex numbers rather than Grassmann variables. However, these states are no eigenstates of the annihilation operator. Generalizing them to many single-particle states, they are defined as

$$|\mathbf{b}\rangle = \left[ \prod_{l=0}^{L-1} \left( \sqrt{1 - |b_{L-l}|^2} + b_{L-l} \hat{c}_{L-l}^\dagger \right) \right] |0\rangle \,.$$

It follows that the Klauder coherent states satisfy the closure relation

$$\left( \frac{2}{\pi} \right)^L \int_{-\infty}^{\infty} \mathrm{d}^L \Re b \int_{-\infty}^{\infty} \mathrm{d}^L \Im b \left[ \prod_{l=1}^{L} \Theta\left(1 - |b_l|\right) \right] |\mathbf{b}\rangle \, \langle \mathbf{b}| = 1, \tag{3.22}$$

where $\Theta(x)$ is Heaviside's step function

$$\Theta(x) = \begin{cases} 0 & \text{if} \quad x < 0 \\ 1 & \text{if} \quad x \geq 0 \end{cases}.$$

Moreover, if $|b_l - b'_l|$ is very small for every $l \in \{1, \ldots, L\}$, the overlap between the two coherent states $|\mathbf{b}\rangle$ and $|\mathbf{b}'\rangle$ is up to linear order in the differences

$$\langle \mathbf{b} \,|\, \mathbf{b}' \rangle = \exp\left\{ -\frac{1}{2} \left[ \mathbf{b}^* \cdot (\mathbf{b} - \mathbf{b}') - (\mathbf{b}^* - \mathbf{b}'^*) \cdot \mathbf{b}' \right] \right\} + \mathcal{O}\left( (\mathbf{b} - \mathbf{b}')^2 \right). \tag{3.23}$$

The overlap of a Klauder coherent state with a Fock state is given by

$$\langle \mathbf{n} \,|\, \mathbf{b} \rangle = \prod_{l=1}^{L} \sqrt{1 - |b_l|^2}^{1-n_l} b_l^{n_l}.$$

Since these states are no eigenstates of the annihilation operator, for the later derivation of the path integral, one needs to compute expressions like $\langle \mathbf{b}| \, \hat{n}_l \, |\mathbf{b}'\rangle$, $\langle \mathbf{b}| \, \hat{a}^\dagger_{l_1} \hat{a}_{l_2} \, |\mathbf{b}'\rangle$ and $\langle \mathbf{b}| \, \hat{a}^\dagger_{l_1} \hat{a}^\dagger_{l_2} \hat{a}_{l_3} \hat{a}_{l_4} \, |\mathbf{b}'\rangle$. Assuming that only continuous paths contribute significantly to the path integral, one can restrict oneself to those matrix elements where the difference of $\mathbf{b}$ and $\mathbf{b}'$ is very small. For $l_1 = l_4$ and $l_2 = l_3$ but $l_1 \neq l_2$ these are to leading order in $\mathbf{b} - \mathbf{b}'$ given by

$$\langle \mathbf{b}| \, \hat{n}_l \, |\mathbf{b}'\rangle = b_l^* b'_l \, \langle \mathbf{b} \,|\, \mathbf{b} \rangle' \,, \tag{3.24a}$$

$$\begin{aligned} \langle \mathbf{b}| \, \hat{a}^\dagger_{l_1} \hat{a}_{l_2} \, |\mathbf{b}'\rangle = {} & b^*_{l_1} b'_{l_2} \, \langle \mathbf{b} \,|\, \mathbf{b} \rangle' \sqrt{1 - \left| b_{l_1} \right|^2} \sqrt{1 - \left| b'_{l_2} \right|^2} \\ & \times \prod_{l=\min(l_1,l_2)+1}^{\max(l_1,l_2)-1} \left( 1 - 2 {b_l}^* b'_l \right), \end{aligned} \tag{3.24b}$$

$$\langle \mathbf{b}| \, \hat{a}^\dagger_{l_1} \hat{a}^\dagger_{l_2} \hat{a}_{l_2} \hat{a}_{l_1} \, |\mathbf{b}'\rangle = b^*_{l_1} b^*_{l_2} b'_{l_2} b'_{l_1} \, \langle \mathbf{b} \,|\, \mathbf{b}' \rangle \,. \tag{3.24c}$$

These results will be of particular importance in section 5.1.

# Part II

# The Many-Body van-Vleck-Gutzwiller-Propagator in Fock Space

CHAPTER 4

# Bosons

## 4.1 The semiclassical coherent state propagator

Using coherent states one can easily derive a path integral representation of the propagator for a system given by a second quantized Hamiltonian. A stationary phase approximation to this path integral then yields the semiclassical approximation. One should notice that the semiclassical limit in this case is achieved by $N \to \infty$, where $N$ is the total number of particles in the system, rather than $\hbar \to 0$. In other words, the effective $\hbar$ is given by $\hbar_{\text{eff}} = 1/N$.

These steps have been performed *e.g.* in [66] and provide a semiclassical propagator in coherent state representation given by

$$\begin{aligned} K\left(\boldsymbol{\phi}^{(f)}, \boldsymbol{\phi}^{(i)}; t_f, t_i\right) &= \langle \boldsymbol{\phi}^{(f)} | \, \hat{\mathcal{T}} \exp\left( -\frac{\mathrm{i}}{\hbar} \int_{t_i}^{t_f} \mathrm{d}t \hat{H}(t) \right) | \boldsymbol{\phi}^{(i)} \rangle \\ &= \sum_{\gamma} \sqrt{ \frac{\mathrm{i}}{\hbar} \frac{\partial^2 R_\gamma \left( \boldsymbol{\phi}^{(f)*}, \boldsymbol{\phi}^{(i)} \right)}{\partial \boldsymbol{\phi}^{(i)} \partial \boldsymbol{\phi}^{(f)*}} } \exp\left\{ \frac{\mathrm{i}}{2\hbar} \int_{t_i}^{t_f} \mathrm{d}t \frac{\partial^2 H^{(\mathrm{cl})} \left( \overline{\boldsymbol{\psi}}(t), \boldsymbol{\psi}(t); t \right)}{\partial \boldsymbol{\phi}^{(i)} \partial \boldsymbol{\phi}^{(f)*}} \right\} \\ &\qquad \exp\left\{ \frac{\mathrm{i}}{\hbar} R_\gamma \left( \boldsymbol{\phi}^{(f)*}, \boldsymbol{\phi}^{(i)}; t_i, t_f \right) - \frac{1}{2} \left( \left| \boldsymbol{\phi}^{(f)} \right|^2 + \left| \boldsymbol{\phi}^{(i)} \right|^2 \right) \right\}, \end{aligned} \tag{4.1}$$

where the sum runs over all classical trajectories $\gamma$ given by the equations

of motion

$$\mathrm{i}\hbar\frac{\partial\boldsymbol{\psi}(t)}{\partial t} = \frac{\partial H^{(\mathrm{cl})}\left(\overline{\boldsymbol{\psi}}(t),\boldsymbol{\psi}(t);t\right)}{\partial\overline{\boldsymbol{\psi}}(t)}, \tag{4.2a}$$

$$-\mathrm{i}\hbar\frac{\partial\overline{\boldsymbol{\psi}}(t)}{\partial t} = \frac{\partial H^{(\mathrm{cl})}\left(\overline{\boldsymbol{\psi}}(t),\boldsymbol{\psi}(t);t\right)}{\partial\boldsymbol{\psi}(t)}, \tag{4.2b}$$

wit the boundary conditions $\boldsymbol{\psi}(t_i) = \boldsymbol{\phi}^{(i)}$ and $\overline{\psi}(t_f) = \boldsymbol{\phi}^{(f)^*}$. In order to fulfill these boundary conditions, $\boldsymbol{\psi}(t)$ and $\overline{\boldsymbol{\psi}}(t)$ have to be considered to be independent variables, such that, in general, they are not hermitian conjugate of each other.

The classical Hamiltonian $H^{(\mathrm{cl})}\left(\overline{\boldsymbol{\psi}}(t),\boldsymbol{\psi}(t);t\right)$ is given by the mean field Hamiltonian corresponding to the quantum one and is obtained by replacing each creation operator $\hat{a}_l^\dagger$ by $\overline{\psi}_l(t)$ and each annihilation operator $\hat{a}_l$ by $\psi_l(t)$. Moreover, the classical action is given by

$$\begin{aligned} R_\gamma\left(\boldsymbol{\phi}^{(f)^*},\boldsymbol{\phi}^{(i)};t_f,t_i\right) = \\ \int_{t_i}^{t_f}\mathrm{d}t\left\{\frac{\mathrm{i}\hbar}{2}\left[\frac{\partial\boldsymbol{\psi}(t)}{\partial t}\cdot\overline{\boldsymbol{\psi}}(t) - \frac{\partial\overline{\boldsymbol{\psi}}(t)}{\partial t}\cdot\boldsymbol{\psi}(t)\right] - H^{(\mathrm{cl})}\left(\overline{\boldsymbol{\psi}}(t),\boldsymbol{\psi}(t);t\right)\right\} \\ -\frac{\mathrm{i}\hbar}{2}\left[\boldsymbol{\psi}(t_f)\cdot\overline{\boldsymbol{\psi}}(t_f) + \boldsymbol{\psi}(t_i)\cdot\overline{\boldsymbol{\psi}}(t_i)\right]. \end{aligned} \tag{4.3}$$

The fact that one has to let go of $\overline{\boldsymbol{\psi}}(t) = \boldsymbol{\psi}(t)^\dagger$, is called the complexification of the classical limit. Having complex trajectories in turn means that the action $R_\gamma$ itself becomes complex. However, in order to apply the standard approximations in semiclassics like diagonal approximation [18], Sieber-Richter pairs [28] as well as the higher order loops [30–38], which allow for analytical and intuitive predictions and descriptions of universal quantum interference effects like coherent backscattering [232], weak localization [233] or Anderson localization [58], it is important to have real actions thus allowing that an ensemble average leads to large oscillations due to the phase given by the action difference of pairs of trajectories.

At this point it should be noted that there have also been attempts to approximate the complex trajectories in the semiclassical coherent state propagator by real ones [67, 76, 77]. Moreover, the power of the coherent state representation lies in the initial value representation, given by the Herman-Kluk propagator [70], which allows to propagate initial wave packets semiclassically.

On the other hand, a van-Vleck-Gutzwiller like propagator with a *real* action would allow to use the now well established methods of quantum chaos to predict and explain universal interference effects now in the many-body domain. Moreover, since coherent states are superpositions of number eigenstates with different numbers of particles, they cannot be prepared in an experiment [234]. Therefore it would be of paramount importance for the semiclassical program, to have a semiclassical propagator in Fock state representation. To my knowledge, up to now, nobody succeeded in performing a basis transformation of the semiclassical propagator from coherent state to Fock state representation.

## 4.2 The Quadrature Path Integral Representation

A direct computation of a semiclassical propagator in Fock state representation is not possible, since for a path integral representation, one has to be able to find a *continuous* eigenbasis for some operator, in which the hamiltonian can be expressed. Noticing that the complexification of the trajectories in the coherent state representation is neccessary, since the coherent states themselves are complex, one may want to use a eigenbasis of a hermitian combination of creation and annihilation operators, such that there eigenvalues are real. Such a combination are for instance the quadrature operators introduced in section 3.2.1.

In quadrature representation, the exact quantum mechanical propagator is given by the matrix element

$$K\left(\mathbf{q}^{(f)},\mathbf{q}^{(i)};t_f,t_i\right)=\langle\mathbf{q}^{(f)}|\,\hat{K}\left(t_f,t_i\right)|\mathbf{q}^{(i)}\rangle\,, \tag{4.4}$$

with $|\mathbf{q}^{(i/f)}\rangle$ beeing quadrature eigenstates with $\varphi=0$ and

$$\hat{K}\left(t_f,t_i\right)=\hat{\mathcal{T}}\exp\left(-\frac{\mathrm{i}}{\hbar}\int\limits_{t_i}^{t_f}\mathrm{d}t\hat{H}(t)\right) \tag{4.5}$$

is the quantum mechanical evolution operator for a many-body Hamiltonian of the type (3.8). In the following, the exact form of the Hamiltonian will not be an issue.

Next, we follow the steps in section 2.1 to derive a path integral representation of the many-body propagator in terms of quadratures. However,

here, instead of position and momentum eigenstates, one has to use quadrature eigenstates with with two different phases $\varphi$ and $\varphi'$, respectively, to express the inserted unit operators. For the sake of simplicity, only the case where $\varphi = 0$ and $\varphi' = -\pi/2$ will be considered. To keep the analogy with the path integral representation in configuration space, the quadrature eigenstates with the phase equal to zero will be denoted by $q$'s, while the latter ones will be denoted by $p$'s.

In order to evaluate the resulting matrix elements at intermediate times, one has to take care of the ordering of the operators, appearing in the Hamiltonian. In case of normal ordering (all creation operators left to the annihilation operators) it may be helpful to first introduce unit operators in terms of coherent states, which are integrated out again after evaluating the matrix elements and overlaps. It is also possible, to express all creation and annihilation operators by a linear combination of quadrature operators $\hat{q} = \hat{x}(0)$ and $\hat{p} = \hat{x}(-\pi/2)$ and then commute all operators $\hat{q}$ to the left of all operators $\hat{p}$. This intermediate insertion of coherent states or commutation of quadrature operators in the end leads to a renormalization of the single-particle Hamiltonian as well an additional phase, given by the zero point energy of the (empty) system.

Eventually, one arrives at the path integral representation [12, 13]

$$K\left(\mathbf{q}^{(f)}, \mathbf{q}^{(i)}; t_f, t_i\right) = \lim_{M\to\infty} \frac{1}{\left(4\pi b^2\right)^{ML}} \int \mathrm{d}^L q^{(1)} \cdots \int \mathrm{d}^L q^{(M-1)} \int \mathrm{d}^L p^{(1)} \cdots \int \mathrm{d}^L p^{(M)} \exp\left\{ \mathrm{i} \sum_{m=1}^{M} \left[ \frac{\mathbf{p}^{(m)}}{2b^2} \left(\mathbf{q}^{(m)} - \mathbf{q}^{(m-1)}\right) - \frac{\tau}{\hbar} H^{(\mathrm{cl})}\left(\boldsymbol{\psi}^{(m)*}, \boldsymbol{\psi}^{(m)}; t_i + m\tau\right) \right] \right\}, \tag{4.6}$$

where $\tau = (t_f - t_i)/M$ and $\boldsymbol{\psi}^{(m)} = \left(\mathbf{q}^{(m-1)} + \mathrm{i}\mathbf{p}^{(m)}\right)/(2b)$.

Moreover the classical Hamiltonian is defined by

$$H^{(\mathrm{cl})}\left(\boldsymbol{\psi}^*, \boldsymbol{\psi}; t\right) = \lim_{\tau\to 0} \frac{\mathrm{i}\hbar}{\tau} \ln \frac{\left\langle \mathbf{p} \left| \exp\left[-\frac{\mathrm{i}\tau}{\hbar}\hat{H}(t)\right] \right| \mathbf{q} \right\rangle}{\langle \mathbf{p} \,|\, \mathbf{q} \rangle}, \tag{4.7}$$

which obviously depends only on $\boldsymbol{\psi}$ and $\boldsymbol{\psi}^*$, rather than separately on $\mathbf{q}$ and $\mathbf{p}$ due to Eq. (3.16). Consider for example a general Bose-Hubbard

Hamiltonian with two-body interactions,

$$\hat{H} = \sum_{l_1,l_2=1}^{L} H^{(0)}_{l_1 l_2} \hat{a}^\dagger_{l_1} \hat{a}_{l_2} + \frac{1}{2} \sum_{l_1,l_2,l_3,l_4=1}^{L} V_{l_1 l_2 l_3 l_4} \hat{a}^\dagger_{l_1} \hat{a}^\dagger_{l_2} \hat{a}_{l_3} \hat{a}_{l_4}, \tag{4.8}$$

where the coefficients must satisfy

$$\begin{aligned} H^{(0)}_{ll'} &= H^{(0)*}_{l'l} \\ V_{l_1 l_2 l_3 l_4} &= V^*_{l_4 l_3 l_2 l_1} \end{aligned}$$

in order for the Hamiltonian to be hermitian. Moreover, due to the commutation relations of the creation and annihilation operators, one is free to choose the interaction coefficients such that

$$V_{l_1 l_2 l_3 l_4} = V_{l_2 l_1 l_3 l_4} = V_{l_1 l_2 l_4 l_3} = V_{l_2 l_1 l_4 l_3}.$$

In the case of normal ordering, for such a Hamiltonian, one finds the classical limit in quadrature representation to be given by (see App. A.1 for details of the derivation)

$$\begin{aligned} H^{(\mathrm{cl})}(\boldsymbol{\psi}^*, \boldsymbol{\psi}) = & \\ & \sum_{l_1,l_2=1}^{L} H^{(0)}_{l_1 l_2} \left( \psi^*_{l_1} \psi_{l_2} - \frac{1}{2} \delta_{l_1 l_2} \right) \\ & + \frac{1}{2} \sum_{l_1,l_2,l_3 l_4=1}^{L} V_{l_1 l_3 l_2 l_4} \left( \psi^*_{l_1} \psi_{l_2} - \frac{1}{2} \delta_{l_1 l_2} \right) \left( \psi^*_{l_3} \psi_{l_4} - \frac{1}{2} \delta_{l_3 l_4} \right). \end{aligned} \tag{4.9}$$

This example specifically shows that the classical Hamiltonian is not determined by just replacing $\hat{a}_l \to \psi_l$ and $\hat{a}^\dagger_l \to \psi^*_l$. In fact, for the general Bose-Hubbard Hamiltonian, Eq. (4.8), the replacement rule would be

$$\hat{a}^\dagger_l \hat{a}_{l'} \to \psi^*_l \psi_{l'} - \frac{1}{2} \delta_{ll'}.$$

Moreover, note that the classical Hamiltonian also contain constant terms, which give rise to a constant phase in the propagator. Such phases have been found on the level of the semiclassical propagator, when using coherent states as the basis [65–67, 69, 235–238], where they have been denoted as the Solari-Kochetov extra-phase. It should also be noted that the classical Hamiltonian depends on the chosen ordering of the propagator. Finally,

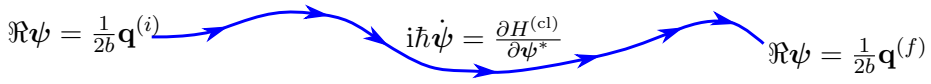


Figure 4.1: Graphical representation of a trajectory involved in the semiclassical propagator in quadrature representation.

the boundary conditions of the path integral are given by $\mathbf{q}^{(0)} = \mathbf{q}^{(i)}$ as well as $\mathbf{q}^{(M)} = \mathbf{q}^{(f)}$.

It is worth to note that for a Hamiltonian which can be written in terms of combinations $\hat{a}_l^\dagger \hat{a}_{l'}$ only, (4.6) is independent of the choice of the quadrature states, as long as the phase difference between the $q$'s and $p$'s is $-\pi/2$, *i.e.* when chosing $\hat{q} = \hat{x}(\varphi)$ and $\hat{p} = \hat{x}(\varphi - \pi/2)$, the resulting path integral representation is independent on the choice of $\varphi$. This can be seen from the expressions of the creation and annihilation operators in terms of quadrature operators, Eq. (3.9), as well as the commutation relations of the quadratures (3.10) and the overlap of quadrature eigenstates with phase difference $\pi/2$, (3.15). Therefore, the following results are valid for any phase $\varphi$ chosen for the quadrature eigenstates $\mathbf{q}$.

## 4.3 The Semiclassical Propagator in Quadrature Representation

### *4.3.1 Propagator between quadratures with the same phase*

Starting from equation (4.6), the semiclassical propagator in quadrature representation is derived, following the steps in section 2.2 by a stationary phase approximation to the path integral. This yields the many-body van-Vleck-Gutzwiller propagator in quadrature representation, given by

$$K\left(\mathbf{q}^{(f)}, \mathbf{q}^{(i)}; t_f, t_i\right) = \sum_{\gamma:\mathbf{q}^{(i)}\to\mathbf{q}^{(f)}} \sqrt{\det \frac{1}{(-2\pi\mathrm{i}\hbar)} \frac{\partial^2 R_\gamma\left(\mathbf{q}^{(f)}, \mathbf{q}^{(i)}; t_f, t_i\right)}{\partial \mathbf{q}^{(f)} \partial \mathbf{q}^{(i)}}} \times \exp\left[\frac{\mathrm{i}}{\hbar} R_\gamma\left(\mathbf{q}^{(f)}, \mathbf{q}^{(i)}; t_f, t_i\right)\right]. \tag{4.10}$$

The trajectories, which can graphically be represented as in Fig. 4.1 are

given by the equations of motion

$$\mathrm{i}\hbar\frac{\partial\boldsymbol{\psi}(t)}{\partial t}=\frac{\partial H^{(\mathrm{cl})}\left(\boldsymbol{\psi}^{*}(t),\boldsymbol{\psi}(t);t\right)}{\partial\boldsymbol{\psi}^{*}(t)}. \tag{4.11}$$

Furthermore, in (4.10), $\mathbf{q}(t)$ and $\mathbf{p}(t)$ are the real and imaginary parts of $\boldsymbol{\psi}(t)$, respectively, *i.e.* $\boldsymbol{\psi}(t)=\left(\mathbf{q}(t)+\mathrm{i}\mathbf{p}(t)\right)/(2b)$, where $\mathbf{q}(t)$ and $\mathbf{p}(t)$ are both real functions of time. Finally, the boundary conditions are

$$\begin{aligned}\Re\boldsymbol{\psi}\left(t_{i}\right)&=\frac{1}{2b}\mathbf{q}^{(i)},\\ \Re\boldsymbol{\psi}\left(t_{f}\right)&=\frac{1}{2b}\mathbf{q}^{(f)}.\end{aligned} \tag{4.12}$$

Since the boundary conditions in quadrature representation fix the real parts of $\boldsymbol{\psi}(t_i)$ and $\boldsymbol{\psi}(t_f)$ only, the overdetermination problem, which arises in the coherent state representation is solved. The trajectories don't have to be complexified, a key advantage of this formulation.

The action along the trajectory can be read from (4.6):

$$R_{\gamma}\left(\mathbf{q}^{(f)},\mathbf{q}^{(i)};t_{f},t_{i}\right)=\int_{t_{i}}^{t_{f}}\mathrm{d}t\left[\frac{\hbar}{2b^{2}}\mathbf{p}(t)\cdot\dot{\mathbf{q}}(t)-H^{(\mathrm{cl})}\left(\boldsymbol{\psi}^{*}(t),\boldsymbol{\psi}(t);t\right)\right]. \tag{4.13}$$

In the same way as for the single-particle case, the derivatives of the action with respect to the boundary conditions can be calculated by using the equations of motion and yield

$$\begin{aligned}\frac{\partial R_{\gamma}\left(\mathbf{q}^{(f)},\mathbf{q}^{(i)};t_{f},t_{i}\right)}{\partial q_{l}^{(i)}}&=-\frac{\hbar}{2b^{2}}p_{l}^{(\gamma)}\left(t_{i}\right),\\ \frac{\partial R_{\gamma}\left(\mathbf{q}^{(f)},\mathbf{q}^{(i)};t_{f},t_{i}\right)}{\partial q_{l}^{(f)}}&=\frac{\hbar}{2b^{2}}p_{l}^{(\gamma)}\left(t_{f}\right).\end{aligned} \tag{4.14}$$

Furthermore for a time-independent hamiltonian, the time derivative of the action is given by

$$\frac{\partial R_{\gamma}\left(\mathbf{q}^{(f)},\mathbf{q}^{(i)};t_{f},t_{i}\right)}{\partial t_{f}}=E_{\gamma},$$

where $E_{\gamma}=H^{(\mathrm{cl})}\left(\boldsymbol{\psi}^{*}(t_{i}),\boldsymbol{\psi}(t_{i})\right)$ is the energy of the trajectory.

### *4.3.2 Propagator between quadratures with different phases*

Having the propagator in quadrature representation, where the phases of the initial and final quadrature states are the same also allows to derive the semiclassical propagator in a mixed basis, for which the initial and final quadrature phases are different. However, since (4.10) is valid for any choice of the quadrature phase (provided, the final one is the same as the initial one), here only the case of a vanishing initial quadrature phase is considered.

The propagator between quadrature states with different phases can be related to the one between two quadrature states with the same phases by inserting a unity operator in terms of quadrature eigenstates,

$$K^{(\varphi)}\left(\mathbf{x}^{(f)},t_f;\mathbf{q}^{(i)},t_i\right) = {}_{\varphi}\left\langle \mathbf{x}^{(f)}\right| \hat{\mathcal{T}}\exp\left(-\frac{\mathrm{i}}{\hbar}\int\limits_{t_i}^{t_f}\mathrm{d}t\hat{H}\left(t\right)\right)\left|\mathbf{q}^{(i)}\right\rangle$$

$$= \int \mathrm{d}\mathbf{q}^{(f)}\, {}_{\varphi}\left\langle \mathbf{x}^{(f)}\right|\left.\mathbf{q}^{(f)}\right\rangle K\left(\mathbf{q}^{(f)},t_f;\mathbf{q}^{(i)},t_i\right).$$

Inserting the overlap of two quadrature eigenstates (3.14a) and the semiclassical propagator (4.10) allows to evaluate the integral in stationary phase approximation. The stationary phase condition reads

$$\frac{1}{\sin\varphi}\left[\mathbf{x}^{(f)}-\mathbf{q}^{(f)}\cos\varphi\right]+\mathbf{p}^{(\gamma)}\left(t_f\right)=0,$$

which selects those trajectories satisfying

$$\mathbf{x}^{(f)} = 2b\Re\left[\boldsymbol{\psi}^{(\gamma)}\left(t_f\right)\exp\left(\mathrm{i}\varphi\right)\right].$$

After expanding the exponential up to second order in $\mathbf{q}^{(f)}$ around this stationary point and computing this integral, the resulting semiclassical propagator between two quadratures with different phase is given by

$$K^{(\varphi)}\left(\mathbf{x}^{(f)},t_f;\mathbf{q}^{(i)},t_i\right) = \sum_{\tilde{\gamma}}\sqrt{\det\frac{1}{(-2\pi\mathrm{i}\hbar)}\frac{\partial^2 R_{\tilde{\gamma}}}{\partial\mathbf{q}^{(i)}\partial\mathbf{x}^{(f)}}}\exp\left(\frac{\mathrm{i}}{\hbar}R_{\tilde{\gamma}}-\frac{\mathrm{i}L\varphi}{2}\right), \tag{4.15}$$

where the sum runs over all classical trajectories satisfying the equations of motion (4.11) as well as the boundary conditions

$$\begin{aligned} \Re\boldsymbol{\psi}\left(t_i\right) &= \frac{1}{2b}\mathbf{q}^{(i)} \\ \Re\left[\boldsymbol{\psi}\left(t_f\right)\exp\left(\mathrm{i}\varphi\right)\right] &= \frac{1}{2b}\mathbf{x}^{(f)} \end{aligned} \tag{4.16}$$

with the classical action is given by

$$\begin{aligned} R_{\bar{\gamma}}\left(\mathbf{x}^{(f)},\mathbf{q}^{(i)};t_f,t_i\right) = \\ \hbar\frac{2\mathbf{x}^{(f)}\cdot\Re\boldsymbol{\psi}\left(t_f\right)-\left(\mathbf{x}^{(f)^2}+\left[\Re\boldsymbol{\psi}\left(t_f\right)\right]^2\right)\cos\left(\varphi\right)}{4b^2\sin\left(\varphi\right)} \\ +\int_{t_i}^{t_f}\mathrm{d}t\left[2\hbar\Im\boldsymbol{\psi}(t)\cdot\Re\dot{\boldsymbol{\psi}}(t)-H^{(\mathrm{cl})}\left(\boldsymbol{\psi}^*(t),\boldsymbol{\psi}(t);t\right)\right]. \end{aligned}$$

With this result, by transforming from the initial quadrature with zero phase to a quadrature state with phase $\varphi$, one could also check again that the result for the propagator between two quadrature states with the same phase is independent of $\varphi$. By evaluating the integration involoved in this transformation in stationary phase approximation, the boundary conditions for the resulting trajectories $\bar{\gamma}$ are found to be

$$\mathbf{x}^{(i/f)} = 2b\Re\left[\boldsymbol{\psi}\left(t_{i/f}\right)\exp\left(\mathrm{i}\varphi\right)\right],$$

while the action is given by

$$R_{\bar{\gamma}} = 2\hbar\int_{t_i}^{t_f}\mathrm{d}t\left\{\Im\left[\boldsymbol{\psi}\exp\left(\mathrm{i}\varphi\right)\right]\cdot\Re\left[\dot{\boldsymbol{\psi}}\exp\left(\mathrm{i}\varphi\right)\right]-H^{(\mathrm{cl})}\left(\boldsymbol{\psi}^*(t),\boldsymbol{\psi}(t);t\right)\right\}.$$

The general form is again the same as in (4.10) and also the equations of motion are not changed. Due to the invariance of the classical hamiltonian with respect to the transformation $\boldsymbol{\psi}\to\boldsymbol{\psi}\exp\left(\mathrm{i}\beta\right)$ for any $\beta$, one can also substitute $\boldsymbol{\psi}$ by $\boldsymbol{\phi}=\boldsymbol{\psi}\exp\left(\mathrm{i}\varphi\right)$ and recovers (4.10).

### *4.3.3 An initial value representation using quandratures*

The semiclassical propagator as a shooting problem, *i.e.* given by a sum over trajectories fixed by an initial and final conditions such as Eq. (4.12),

has proofed very successful to describe interference effects [19–25, 31, 32, 34–37, 39–41, 43, 47–54]. However, especially when considering a specific system without wanting to impose a disorder average, it is a very hard task, to find all these trajectories.

Although there are in principle methods to do this root search numerically [239–246] based on the Newton-Raphson root search method [246, 247], it might be advantageous to have an initial value representation of the propagator, *i.e.* a representation along the lines of Herman and Kluk [70], where the initial value of $\boldsymbol{\psi}(t)$ is completely fixed and then evolved under the classical equations of motion, which is finally iterated over different initial conditions.

To find such an initial value representation, consider an arbitrary initial state $|\psi_i\rangle$ which is evolved quantum mechanically in time, such that the final state is given by

$$\begin{aligned}|\psi\left(t_f\right)\rangle &= \hat{K}\left(t_f, t_i\right)|\psi_i\rangle \\ &= \int \mathrm{d}^L q^{(f)} \int \mathrm{d}^L q^{(i)} \left|\mathbf{q}^{(f)}\right\rangle \left\langle \mathbf{q}^{(f)} \left| \hat{K}\left(t_f, t_i\right) \right| \mathbf{q}^{(i)} \right\rangle \left\langle \mathbf{q}^{(i)} \left| \psi_i \right.\right\rangle .\end{aligned}$$

In the second line this final state has been written in a form, such that the semiclassical propagator in quadrature representation, Eq. (4.10), can be inserted directly. Using furthermore Eq. (4.14) in order to transform the semiclassical prefactor into a derivative of the initial imaginary part of the mean field wave function, $\mathbf{p}^{(\gamma)}\left(t_i\right)$ with respect to the final real part, $\mathbf{q}^{(f)}$, yields

$$\begin{aligned}|\psi\left(t_f\right)\rangle = \\ \int \mathrm{d}^L q^{(f)} \int \mathrm{d}^L q^{(i)} \left|\mathbf{q}^{(f)}\right\rangle \left\langle \mathbf{q}^{(i)} \left| \psi_i \right.\right\rangle \sum_{\gamma:\mathbf{q}^{(i)}\to\mathbf{q}^{(f)}} \sqrt{\det \frac{1}{4\mathrm{i}\pi b^2} \frac{\partial \mathbf{p}^{(\gamma)}\left(t_i\right)}{\partial \mathbf{q}^{(f)}}} \\ \times \exp\left[\frac{\mathrm{i}}{\hbar} R_\gamma\left(\mathbf{q}^{(f)}, \mathbf{q}^{(i)}; t_f, t_i\right)\right].\end{aligned}$$

Finally, the sum over classical trajectories can be transformed into an integral over the initial imaginary part according to

$$\sum_{\gamma:\mathbf{q}^{(i)}\to\mathbf{q}^{(f)}} = \int \mathrm{d}^L p^{(i)} \delta\left[\mathbf{q}\left(\mathbf{q}^{(i)}, \mathbf{p}^{(i)}; t_f\right) - \mathbf{q}^{(f)}\right] \left| \det \frac{\partial \mathbf{q}\left(\mathbf{q}^{(i)}, \mathbf{p}^{(i)}; t_f\right)}{\partial \mathbf{p}^{(i)}} \right|,$$

with $\mathbf{q}\left(\mathbf{q}^{(i)}, \mathbf{p}^{(i)}; t_f\right)$ being the real part of the classical time evolution of the initial state $\mathbf{q}^{(i)} + \mathrm{i}\mathbf{p}^{(i)}$. The integration over $\mathbf{q}^{(f)}$ can now be carried

out easily due to the Dirac delta and yields the initial value representation in quadrature representation,

$$|\psi(t_f)\rangle = \int \mathrm{d}^L q^{(i)} \int \mathrm{d}^L p^{(i)} \sqrt{\det \frac{1}{4\mathrm{i}\pi b^2} \frac{\partial \mathbf{q}(t_f)}{\partial \mathbf{p}^{(i)}}} \left\langle \mathbf{q}^{(i)} \middle| \psi_i \right\rangle |\mathbf{q}(t_f)\rangle \times \exp\left[\frac{\mathrm{i}}{\hbar} R\left(\mathbf{q}^{(i)}, \mathbf{q}^{(f)}; t_f, t_i\right)\right]. \tag{4.17}$$

The square root depends only on the derivative of the final real part of the mean field trajectory with respect to the initial imaginary part and is therefore much easier to compute than the determinant arising in the Herman-Kluk propagator [70]. However, to be honest, Eq. (4.17), has a numerical disadvantage when compared to the Herman-Kluk propagator. This lies in the fact that the integration over $\mathbf{p}^{(i)}$ runs over the whole $\mathbb{R}^L$, without any weight function, which prevent an efficient computation of the integral by monte carlo methods [247].

## 4.4 The Semiclassical Propagator in Fock State Representation

### *4.4.1 The propagator*

For ultra-cold atoms, the experimental preparation of a quadrature eigenstate is not possible, since these states are a superposition of all possible Fock states and therefore of states with different total particle numbers $N$ [234]. Therefore it is important to have a propagator in Fock state representation. A direct derivation of a path integral representation in Fock state representation, however is not possible, since at intermediate times, one would need a resolution of unity given by an integral, rather than a sum.

To avoid this problem, one can use the semiclassical propagator in quadrature representation and project it to Fock states via

$$\begin{aligned} K\left(\mathbf{n}^{(f)}, \mathbf{n}^{(i)}; t_f, t_i\right) &= \langle \mathbf{n}^{(f)} | \hat{K}(t_f, t_i) | \mathbf{n}^{(i)} \rangle \\ &= \int \mathrm{d}^L q^{(f)} \int \mathrm{d}^L q^{(i)} \left\langle \mathbf{n}^{(f)} \middle| \mathbf{q}^{(f)} \right\rangle K\left(\mathbf{q}^{(f)}, \mathbf{q}^{(i)}; t_f, t_i\right) \left\langle \mathbf{q}^{(i)} \middle| \mathbf{n}^{(i)} \right\rangle. \end{aligned}$$

The integrals can easily be evaluated within the stationary phase approximation, after the overlap of the quadrature eigenstates with Fock states is approximated by its asymptotic formula, (3.13). However, there is a subtle detail, which complicates the evaluation. This is due to the $U(1)$-gauge invariance, *i.e.* the fact that if $\boldsymbol{\psi}(t)$ solves the equations of motion, $\boldsymbol{\psi}(t)\mathrm{e}^{\mathrm{i}\theta}$ also does, implying that the global phase does not play any role, but only the phase differences of the components of $\boldsymbol{\psi}$ matter. This also reflects itself in the classical Hamiltonian, where the phases itself do not enter, but the phase differences do. Obviously, $\theta$ is a cyclic variable, implying an additional constant of motion. This constant of motion, on the other hand is obvious: the total number of particles $N$.

The presence of the gauge freedom implies that there is a continuous family of trajectories, for which $|\psi_l(t_i)|^2$ is the same, and since the stationary approximation breaks down in the presence of such continuous families of trajectories, the integral over the global phase $\theta$ has to be done exactly, leaving only $2L-1$ integrals to be done in stationary phase approximation. After evaluating these integrals (see appendix A.3 for details), the propagator in Fock state representation is found to be given by

$$K\left(\mathbf{n}^{(f)},\mathbf{n}^{(i)};t_f,t_i\right)=\sum_{\gamma:\mathbf{n}^{(i)}\to\mathbf{n}^{(f)}}\sqrt{\det{}'\frac{1}{(-2\pi\mathrm{i}\hbar)}\frac{\partial^2 R_\gamma\left(\mathbf{n}^{(f)},\mathbf{n}^{(i)};t_f,t_i\right)}{\partial\mathbf{n}^{(f)}\partial\mathbf{n}^{(i)}}}\times\exp\left[\frac{\mathrm{i}}{\hbar}R_\gamma\left(\mathbf{n}^{(f)},\mathbf{n}^{(i)};t_i,t_f\right)\right]\delta_{N^{(i)},N^{(f)}}, \tag{4.18}$$

where

$$N^{(i)}=\sum_{l=1}^{L}n_l^{(i)},$$
$$N^{(f)}=\sum_{l=1}^{L}n_l^{(f)}$$

is the total number of particles at initial and final time, respectively. The trajectories, which are schematically depicted in Fig. 4.2, here are determined by the equations of motion (4.11) as well as the boundary conditions

$$\begin{aligned}|\psi_l\left(t_i\right)|^2&=n_l^{(i)}+\frac{1}{2},\\ |\psi_l\left(t_f\right)|^2&=n_l^{(f)}+\frac{1}{2}\end{aligned} \tag{4.19}$$

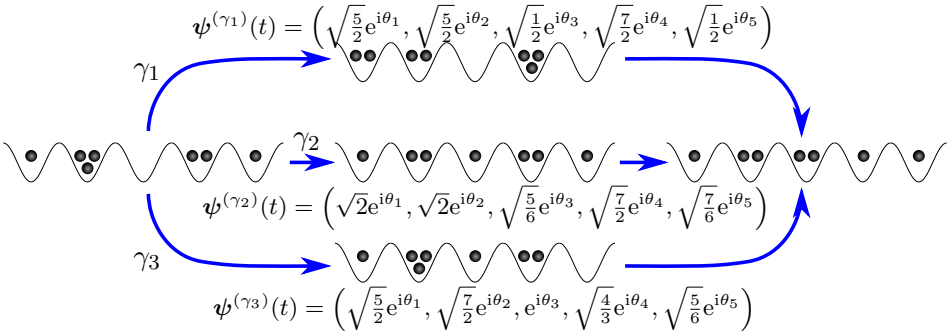


Figure 4.2: Illustration of the classical trajectories. While at initial and final time, the occupation number have to be integer, this needs not be true at intermediate times. The total number of particles $N = \sum_\alpha |\psi_\alpha(t)|^2$, however, stays constant along the classical trajectories.

where one of the initial phases, say the initial phase of the $i = 1$-component, of $\psi$ has to be fixed to a certain value. Due to the gauge invariance, the trajectories and the action do not depend on the value of this phase. Finally, the prime at the determinant in Eq. (4.18) indicates that the derivative has to be taken only with respect to the subspace resulting from skipping the component, for which the initial phase has been fixed. This is a consequence of the conservation of the total number of particles.

The action in (4.18) is given by

$$R\left(\mathbf{n}^{(f)}, \mathbf{n}^{(i)}; t_f, t_i\right) = \int_{t_i}^{t_f} \mathrm{d}t \left[\hbar\boldsymbol{\theta}(t) \cdot \dot{\mathbf{n}}(t) - H^{(\mathrm{cl})}\left(\boldsymbol{\psi}^*(t), \boldsymbol{\psi}(t)\right)\right], \qquad (4.20)$$

where $\theta_l(t)$ and $n_l(t)$ are the real variables given by the phase and the modulus of $\psi_l(t)$, *i.e.*

$$\psi_l(t) = \sqrt{n_l(t) + \frac{1}{2}} \exp\left(\mathrm{i}\theta_l(t)\right).$$

The integral has again to be calculated along the classical trajectory. Similar to the derivative of the action in quadrature representation with respect to $\mathbf{q}^{(i)}$ and $\mathbf{q}^{(f)}$, the derivatives of the action in Fock state representation

with respect to $\mathbf{n}^{(i)}$ and $\mathbf{n}^{(f)}$ are

$$\begin{aligned}\frac{\partial R_\gamma\left(\mathbf{n}^{(f)},\mathbf{n}^{(i)};t_i,t_f\right)}{\partial n_l^{(i)}} &= -\hbar\theta_l^{(\gamma)}\left(t_i\right),\\ \frac{\partial R_\gamma\left(\mathbf{n}^{(f)},\mathbf{n}^{(i)};t_i,t_f\right)}{\partial n_l^{(f)}} &= \hbar\theta_l^{(\gamma)}\left(t_f\right).\end{aligned} \tag{4.21}$$

### *4.4.2 The (approximate) semi-group property*

An important property of the propagator is the semi-group property, Eq. (2.8). It can be shown that the van-Vleck-Gutzwiller propagator satisfies it when integrals are evaluated in stationary phase approximation [15]. Therefore, one might expect that the semi-group property holds for the semiclassical Propagator in Fock basis as well, within a stationary phase approximation.

However, in Fock space, the right hand side of the semi-group property is given by a sum over Fock states, rather than an integral,

$$K\left(\mathbf{n}^{(f)},\mathbf{n}^{(i)};t_f,t_i\right)=\sum_{\mathbf{m}}{}^{(N)}K\left(\mathbf{n}^{(f)},\mathbf{m};t_f,t_0\right)K\left(\mathbf{m},\mathbf{n}^{(i)};t_0,t_i\right), \tag{4.22}$$

such that the stationary phase approximation is not directly applicable. Here, the superscript $(N)$ to the sum indicates that it runs only over those occupations with the total number of particles being equal to $N$. This restriction is possible, since the propagator is non-zero only if the initial and final total number of particles are the same.

In order to be able to apply a stationary phase approximation, one first of all has to transform the summation over the intermediate occupations $\mathbf{m}$ into an integration. This is usually done by Poisson summation. However, here the additional condition $\sum_\alpha m_\alpha = N$ does not allow a direct application of the Poisson sum formula. Instead, one can introduce an integration by hand, *e.g.* by replacing the sum over Fock states according to

$$\begin{aligned}&\sum_{\mathbf{m}\in\mathbb{N}^L}\delta_{N^{(f)},N_{\mathbf{m}}}\delta_{N_{\mathbf{m}},N^{(i)}}\ldots=\\ &\qquad\sum_{\mathbf{m}\in\mathbb{N}^{L-1}}\delta_{N^{(f)},N^{(i)}}\int_0^\infty \mathrm{d}^L k\prod_{l=2}^{L}\delta\left(m_l-k_l'\right)\delta\left(N_{\mathbf{k}}-N^{(i)}\right)\ldots\end{aligned}$$

The sum over occupations on the right hand side, is now restricted to the single-particle states $2, \ldots, L$. In the same way, $\mathbf{k}'$ is defined as the vector resulting from $\mathbf{k}$ by removing its first entry. Moreover,

$$N_{\mathbf{m}} = \sum_{l=1}^{L} m_l.$$

is the total number of particles of the Fock state $|\mathbf{m}\rangle$.

Still, the Dirac delta does not allow for a stationary phase approximation, and thus one has to get rid of it. This is possible by applying the Poisson summation,

$$\sum_{m=0}^{\infty} f(m) = \sum_{j=-\infty}^{\infty} \int_0^{\infty} \mathrm{d}m f(m) \exp\left(2\pi \mathrm{i} m j\right),$$

to the sum over occupations. The evaluation of the resulting integral over $\mathbf{m}$ is then straight forward and yields, after insertion of the semiclassical propagator, Eq. (4.18), for the right hand side of the semi-group property

$$\begin{aligned}
&\delta_{N^{(f)},N^{(i)}} \sum_{\mathbf{j}\in\mathbb{Z}^{L-1}} \int_0^{\infty} \mathrm{d}^L k \frac{\delta\left(N_{\mathbf{k}} - N^{(i)}\right)}{\left(2\pi\mathrm{i}\hbar\right)^{L-1}} \exp\left(2\pi\mathrm{i}\mathbf{j}\cdot\mathbf{k}'\right) \\
&\times \sum_{\substack{\gamma:\mathbf{n}^{(i)}\to\mathbf{k} \\ \gamma':\mathbf{k}\to\mathbf{n}^{(f)}}} \sqrt{\det{}' \frac{\partial^2 R_{\gamma'}}{\partial\mathbf{k}\partial\mathbf{n}^{(f)}} \det{}' \frac{\partial^2 R_{\gamma}}{\partial\mathbf{n}^{(i)}\partial\mathbf{k}}} \exp\left\{\frac{\mathrm{i}}{\hbar}\left[R_{\gamma'} + R_{\gamma}\right]\right\}.
\end{aligned}$$

The $k_1$-integration of course can be carried out exactly, while the remaining $L-1$ $k$-integrals will be evaluated in stationary phase approximation. Before doing so, it is convenient to replace the trajectory $\gamma'$ by $\gamma^*$ with the initial phase of the first component $\theta_{\gamma^*,1}(t_0) = \theta_{\gamma,1}(t_0)$, *i.e.* by a trajectory which initial phase of the first component is the same as the final one of $\gamma$. This replacement can be done by simply multiplying $\boldsymbol{\psi}_{\gamma'}(t)$ with a global and time-independent phase. The stationarity condition for the integration over $k_l$ with $l \in \{2, \ldots, L\}$ then reads

$$-\theta_{\gamma^*,l}(t_0) + \theta_{\gamma,l}(t_0) + 2\pi j_l = 0.$$

Here it is important to notice that $\theta_{\gamma^*,l}(t_0) \in [-\pi, \pi]$, while in principle $\theta_{\gamma,l}(t_0) \in \mathbb{R}$. Thus the term $2\pi j_l$ corrects the discrepancy between the final phase of the trajectory $\gamma$ and the initial one of the trajectory $\gamma^*$, *i.e.* if

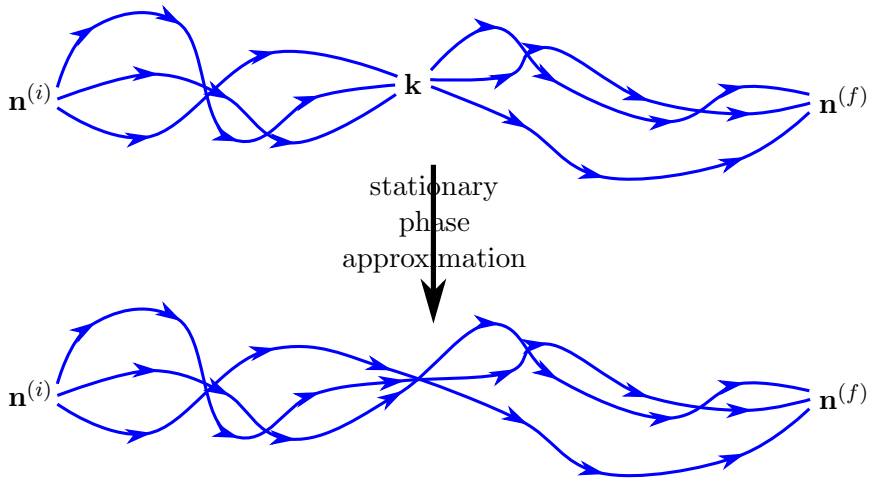


Figure 4.3: The stationary phase approximation selects those pairs of trajectories, which are analytical continuations of each other.

we would replace $\theta_{\gamma^*,l}(t_0)$ by $\theta_{\gamma^*,l}(t_0)+2\pi j_l$ the stationary phase condition would just say that the initial phase of the second trajectory has to be the same as the final phase of the first trajectory, such that the second one is just the analytic continuation of the first one (see Fig. 4.3). Moreover this replacement would change the action of the second trajectory by an additional term of $2\pi j_l(n_l^{(f)}-k_j)$, finally yielding for the sum of the actions at the stationary point

$$R_{\gamma^*}+R_\gamma+2\pi\mathbf{j}\cdot\mathbf{k}'=R_{\gamma+\gamma^*}+2\pi\mathbf{j}\cdot\mathbf{n}^{(f)\prime},$$

where the prime again indicates that the first entry of the vector is removed and $\gamma+\gamma^*$ is defined as the trajectory resulting from continuing $\gamma$ by $\gamma^*$.

The last term is now an integer multiple of $2\pi$ and therefore does not play any role for the propagator. Hence the stationary phase condition selects all those pairs of trajectories $\gamma$ and $\gamma^*$ which are match each other to form a trajectory with duration $t_f-t_i$ and connecting the initial to the final occupations. Together with the sum over all possible $\mathbf{j}$ the double sum over trajectories is therefore just a sum over the trajectories which start at $\mathbf{n}^{(i)}$ at time $t_i$ and end at $\mathbf{n}^{(f)}$ at time $t_f$ and the phase contributed by each trajectory is its action.

Thus, the only quantity, which still has to be determined, in order to

check the semi-group property is the functional determinant,

$$\frac{\det' \frac{\partial^2 R_{\gamma^*}}{\partial \mathbf{k} \partial \mathbf{n}^{(f)}} \det' \frac{\partial^2 R_\gamma}{\partial \mathbf{n}^{(i)} \partial \mathbf{k}}}{\det \frac{\partial^2 \left( R_{\gamma^*} + R_\gamma + 2\pi \mathbf{j} \cdot \mathbf{k}' \right)}{\partial \mathbf{k}'^2}}$$

To this end, consider the derivative of the stationary phase condition with respect to $n_l^{(i)}$ for $l \in \{2, \ldots, L\}$,

$$\begin{aligned} \frac{\mathrm{d} \left( -\boldsymbol{\theta}'_{\gamma^*}(t_0) + \boldsymbol{\theta}'_\gamma(t_0) + 2\pi \mathbf{j} \right)}{\mathrm{d} \mathbf{n}^{(i)\prime}} &= \frac{\partial \boldsymbol{\theta}'_\gamma(t_0)}{\partial \mathbf{n}^{(i)\prime}} + \frac{\partial \left[ -\boldsymbol{\theta}'_{\gamma^*}(t_0) + \boldsymbol{\theta}'_\gamma(t_0) \right]}{\partial \mathbf{k}'} \frac{\partial \mathbf{k}'}{\partial \mathbf{n}^{(i)\prime}} \\ &= 0. \end{aligned}$$

Therefore,

$$\frac{\det' \frac{\partial^2 R_{\gamma^*}}{\partial \mathbf{k} \partial \mathbf{n}^{(f)}} \det' \frac{\partial^2 R_\gamma}{\partial \mathbf{n}^{(i)} \partial \mathbf{k}}}{\det \frac{\partial^2 \left( R_{\gamma^*} + R_\gamma + 2\pi \mathbf{j} \cdot \mathbf{k}' \right)}{\partial \mathbf{k}'^2}} = -\frac{\det \frac{\partial \boldsymbol{\theta}'_{\gamma^*}(t_f)}{\partial \mathbf{k}'} \frac{\partial \boldsymbol{\theta}'_\gamma(t_0)}{\partial \mathbf{n}^{(i)\prime}}}{\det \frac{\partial \boldsymbol{\theta}'_\gamma(t_0)}{\partial \mathbf{n}^{(i)\prime}} \frac{\partial \mathbf{n}^{(i)\prime}}{\partial \mathbf{k}'}} = \frac{\partial \boldsymbol{\theta}'_{\gamma^*}(t_f)}{\partial \mathbf{n}^{(i)\prime}}.$$

Thus, also the functional determinant is the same as the one of the full semiclassical propagator, which finally proofs the validity of the semi-group property, Eq. (4.22), for the semiclassical propagator in Fock basis within a stationary phase approximation.

CHAPTER 5

# Fermions

As in the bosonic case, the quantity of interest in this chapter is first of all a semiclassical approximation to the propagator for Fermionic fields in Fock state representation,

$$K\left(\mathbf{n}^{(f)},\mathbf{n}^{(i)};t_f,t_i\right)=\langle\mathbf{n}^{(f)}|\,\hat{\mathcal{T}}\exp\left[-\frac{\mathrm{i}}{\hbar}\int_{t_i}^{t_f}\mathrm{d}t\hat{H}(t)\right]|\mathbf{n}^{(i)}\rangle\,,$$

where the entries of $\mathbf{n}^{(i/f)}$ are either zero or one. For later reference, we define $l_1^{(i)},\ldots,l_{N^{(i)}}^{(i)}$ to label those single-particle states which are initially occupied, and $l_1^{(f)},\ldots,l_{N^{(f)}}^{(f)}$ those single-particle states, which are finally occupied, *i.e.*

$$n_l^{(i)}=\begin{cases}1 & \text{if } l\in\left\{l_1^{(i)},\ldots,l_{N^{(i)}}^{(i)}\right\}\\ 0 & \text{else}\end{cases}\,,$$

$$n_l^{(f)}=\begin{cases}1 & \text{if } l\in\left\{l_1^{(f)},\ldots,l_{N^{(f)}}^{(f)}\right\}\\ 0 & \text{else}\end{cases}\,.$$

Note that here the $L$ single-particle states are defined to also include the spin component $\sigma\in\{\uparrow,\downarrow\}$. The definition of the labels $l_1^{(i/f)},\ldots,l_{N^{(i)}}^{(i/f)}$ is also illustrated graphically in Fig. 5.1

The main complication for Fermions is that quadrature eigenstates with real eigenvalues can not be defined, since the occupation numbers can only

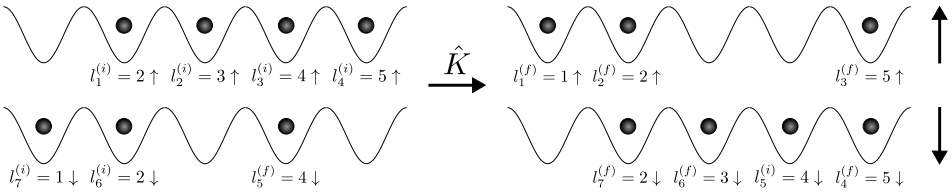


Figure 5.1: Definition of the labels $l_1^{(i/f)}, \ldots, l_{N^{(i)}}^{(i/f)}$ as the initially and finally occupied single-particle states. Note that here, the ordering of the single-particle states has been chosen such that the spin-up states come first with the spatial states in ascending order and after that the spin-down states in descending order.

be zero or one. Therefore, one needs to find a different approach compared to the bosonic case in order to find a semiclassical approximation to the propagator.

Finally, here for the sake of simplicity, only Hamiltonians of the form

$$\hat{H} = \sum_{l,l'=1}^{L} \left( h_{ll'} \hat{c}_l^\dagger \hat{c}_{l'} + U_{l,l'} \hat{c}_l^\dagger \hat{c}_{l'}^\dagger \hat{c}_{l'} \hat{c}_l \right).$$

will be considered.

## 5.1 The Propagator using Klauder's Coherent State Representation

### *5.1.1 The Path Integral*

Klauder's intention with his fermionic coherent state analogue, as reviewed in §3.3.2, was to determine a path integral for the fermionic propagator based on complex variables [231]. However, in his work he considered only one single-particle state and considered the propagator in the Klauder-coherent state basis, rather than the Fock basis.

This section aims to generalize his idea to $L$ single-particle states, and to perform a semiclassical approximation to the resulting path integral. However, as will be demonstrated later on, this semiclassical limit rises severe problems.

Being interested in the path integral representation of the propagator in Fock basis, one needs the representation of the initial and final Fock

state in Klauder coherent states,

$$|\mathbf{n}^{(i)}\rangle = \frac{1}{\pi^L} \int_0^1 \mathrm{d}^L J^{(i)} \int_0^{2\pi} \mathrm{d}^L \theta^{(i)} \left( \prod_{l=1}^{L} \left(1 - J_l^{(i)}\right)^{\frac{1-n_l^{(i)}}{2}} {b_l^{(i)}}^{n_l^{(i)}} \right) |\mathbf{b}^{(i)}\rangle$$

with $b_l^{(i)} = \sqrt{J_l^{(i)}} \exp\left(\mathrm{i}\theta_l^{(i)}\right)$. In view of the semiclassical approximation, and problems that would arise there otherwise, for the final Fock state the integration over the amplitudes of $\mathbf{b}^{(f)}$ will be performed exactly, such that the representation

$$\langle \mathbf{n}^{(f)}| = \left(\frac{1}{2\pi}\right)^L \int_0^{2\pi} \mathrm{d}^L \theta^{(f)} \exp\left( -\mathrm{i} \sum_{l=1}^{L} n_l^{(f)} \theta_l^{(f)} \right) \langle \mathbf{b}^{(f)}|$$

with $b_l^{(f)} = n_l^{(f)} \exp\left(\mathrm{i}\theta_l^{(f)}\right)$ will be used. This is because if the same representation is used for the final Fock state as for the initial one and all integrals would be performed in stationary phase approximation, the resulting semiclassical approximation diverges.

In a way, this mixed way of representing the initial and final Fock states, is in accordance with the derivation of the semiclassical propagator in configuration space, where there is one integration more over the momenta than over the positions.

With this, the propagator in fermionic Fock space can be written as

$$K\left(\mathbf{n}^{(f)}, \mathbf{n}^{(i)}; t_f, t_i\right) = \langle \mathbf{n}^{(f)}| \hat{\mathcal{T}} \exp\left( -\frac{\mathrm{i}}{\hbar} \int_{t_i}^{t_f} \mathrm{d}t \hat{H}(t) \right) |\mathbf{n}^{(i)}\rangle =$$

$$\int_0^{2\pi} \frac{\mathrm{d}^L \theta^{(f)}}{\pi^L} \int_0^1 \mathrm{d}^L J^{(i)} \int_0^{2\pi} \mathrm{d}^L \theta^{(i)} \langle \mathbf{b}^{(f)}| \hat{\mathcal{T}} \exp\left( -\frac{\mathrm{i}}{\hbar} \int_{t_i}^{t_f} \mathrm{d}t \hat{H}(t) \right) |\mathbf{b}^{(i)}\rangle$$

$$\times \prod_{l=1}^{L} \left(1 - J_l^{(i)}\right)^{\frac{1-n_l^{(i)}}{2}} {J_l^{(i)}}^{\frac{n_l^{(i)}}{2}} \exp\left[\mathrm{i}\left(n_l^{(i)}\theta_l^{(i)} - n_l^{(f)}\theta_l^{(f)}\right)\right].$$

In order to derive a path integral representation, one now follows the steps presented in section 2.1, but now the unit operators are inserted in terms of Klauder coherent states, Eq. (3.22). Here, in order to evaluating the resulting overlaps and matrix elements it is convenient to assume that the

paths contributing to the path integral are continuous [248], such that Eqns. (3.23) and (3.24) can be applied. This yields for the path integral

$$
\begin{aligned}
K\left(\mathbf{n}^{(f)},\mathbf{n}^{(i)};t_f,t_i\right) = \\
\lim_{M\to\infty}\frac{1}{2^L}\int_0^1 \mathrm{d}^L J^{(0)} \int_0^{2\pi}\frac{\mathrm{d}^L\theta^{(0)}}{\pi^L}\cdots\int_0^1 \mathrm{d}^L J^{(M)}\int_0^{2\pi}\frac{\mathrm{d}^L\theta^{(M)}}{\pi^L}\int_0^{2\pi}\frac{\mathrm{d}^L\theta^{(M+1)}}{\pi^L} \\
\exp\left\{\sum_{m=0}^{M}\frac{\left(\mathbf{b}^{(m+1)^*}-\mathbf{b}^{(m)^*}\right)\mathbf{b}^{(m)}-\mathbf{b}^{(m+1)^*}\left(\mathbf{b}^{(m+1)}-\mathbf{b}^{(m)}\right)}{2}\right\} \\
\times\left(\prod_{l=1}^{L}\left(1-J_l^{(0)}\right)^{\frac{1-n_l^{(i)}}{2}}\left(b_l^{(0)^*}\right)^{n_l^{(i)}}\exp\left(\mathrm{i}n_l^{(f)}\theta_l^{(M+1)}\right)\right) \\
\times\exp\left[-\frac{\mathrm{i}\tau}{\hbar}\sum_{m=0}^{M}H^{(\mathrm{cl})}\left(\mathbf{b}^{(m+1)^*},\mathbf{b}^{(m)};t_m\right)\right],
\end{aligned}
$$

with the boundary condition

$$b_l^{(M+1)} = J_l^{(M+1)}\exp(\mathrm{i}\theta_j^{(M+1)})$$

and the classical Hamiltonian

$$H^{(\mathrm{cl})}\left(\mathbf{b}^{(m+1)^*},\mathbf{b}^{(m)};t_m\right) = \langle\mathbf{b}^{(m+1)}|\,\hat{H}(t_m)\,|\mathbf{b}^{(m)}\rangle\,,$$

is evaluated using Eq. (3.24) neglecting the differences between $\mathbf{b}^{(m)}$ and $\mathbf{b}^{(m+1)}$.

By substituting $\theta_l^{(m)}\to\theta_l^{(m)}+\theta_1^{(0)}$, the initial phase of the first single-particle state can be integrated out exactly yielding a factor $2\pi\delta_{N^{(i)}N^{(f)}}$, while the remaining integrals can be performed in a stationary phase approximation.

### *5.1.2 Stationary phase approximation*

However, it turns out that the resulting semiclassical propagator obtained using Klauder's representation shows severe problems, which make it inapplicable. Therefore, here only the result of the stationary phase approximation will be presented, in order to discus the problems. Due to this inapplicability, the results will not be not discussed furthermore.

Readers interested in details of the stationary phase approximation are referred to section 5.2.2, where a semiclassical approximation, which is pretty similar to the one using Klauder's coherent states, will be discussed in detail.

First of all, the stationarity conditions in the continuous limit $\tau \to 0$ read

$$\mathrm{i}\hbar \frac{\partial \mathbf{b}(t)}{\partial t} = \frac{\partial H^{(\mathrm{cl})}\left(\mathbf{b}^\dagger(t), \mathbf{b}(t); t\right)}{\partial \mathbf{b}^\dagger(t)}$$

as well as

$$|b_l(t_i)|^2 = n_l^{(i)}.$$

Together with the boundary condition

$$|b_l(t_f)|^2 = n_l^{(f)}$$

already fixed by the path integral. The stationary phase condition selects mean then field trajectories connecting the initial to the final occupations.

Note that the additional factors

$$\left(1 - J_l^{(0)}\right)^{\frac{1-n_l^{(i)}}{2}} \left(J_l^{(0)}\right)^{\frac{n_l^{(i)}}{2}}$$

have not been included in the stationarity analysis and are equal to unity, when evaluated at the stationary point.

Here, we already observe a first severe problem: In order to derive the classical limit from the path integral, the off-diagonal terms of the classical Hamilontian are obtained by replacement

$$\hat{c}_l^\dagger \hat{c}_{l'} \to b_l^* b_{l'} \sqrt{\left(1 - \left|b_l\right|^2\right)\left(1 - \left|b_{l'}\right|^2\right)}.$$

Then, inserting the initial condition $|b_l| = n_l^{(i)}$ immediately shows that the off-diagonal terms vanish. Therefore, the resulting semiclassical propagator can in general not provide reasonable results, as the classical limit has the physical Fock states as fixed points.

Let us nevertheless assume that this problem can somehow be lifted, and continue with the semiclassical approximation. After a rather lengthy calculation, performing all limits one can perform, one ends up with the

semiclassical propagator

$$K\left(\mathbf{n}^{(f)},\mathbf{n}^{(i)};t_f,t_i\right) = \lim_{M\to\infty} 2^{(M+3/2)L} \sum_{\gamma:\mathbf{n}^{(i)}\to\mathbf{n}^{(f)}} \sqrt{\det \frac{1}{(-2\pi\mathrm{i}\hbar)} \frac{\partial^2 R_\gamma}{\partial\mathbf{n}^{(f)}\partial\mathbf{n}^{(i)}}} \exp\left(\frac{\mathrm{i}}{\hbar}R_\gamma\right) \times \exp\left(\frac{\mathrm{i}}{2}\sum_{l=1}^{L}\left[\theta_l(t_f)-\theta_l(t_i)\right] + \frac{\mathrm{i}}{2\hbar}\int_{t_i}^{t_f}\mathrm{d}t\mathrm{Tr}\frac{\partial^2 H^{(\mathrm{cl})}}{\partial\mathbf{b}^\dagger\partial\mathbf{b}}\right).$$

Here, we finally observe another severe problem, which is the factor

$$\lim_{M\to\infty} 2^{(M+3/2)L},$$

which actually is infinite. Thus, even if we could lift the above problem that the off-diagonal terms in this approach vanish, the final result would be infinite. This does have sence, however, since the sum over classical trajectories vanishes. Nevertheless, since the Fock states are fixed points of the classical motion, Klauder's coherent states seem not to be applicable for deriving a semiclassical propagator for Fermions in Fock state representation.

## 5.2 The Semiclassical Propagator in Fermionic Fock States

### *5.2.1 The complex Path Integral for the Propagator in Fock state Representation*

It seems then that there is no choice but to use coherent states in order to evaluate the propagator. The semiclassical approximation for the Grassmann path integral however, would lead to classical Grassmannian equations of motion, which would not be of great help. Therefore, one may want to somehow replace the integrals over Grassmann variables by ones over complex variables. The procedure introduced here may somehow remind to a supersymmetric approach, where the fermions are replaced by their bosonic supersymmetric partners.

To carry on this program after using Trotter's formula between two consecutive exponentials not only one unit operator but two are inserted

in terms of fermionic coherent states, Eq. (3.21),

$$K\left(\mathbf{n}^{(f)},\mathbf{n}^{(i)};t_f,t_i\right)=\langle\mathbf{n}^{(f)}|\,\hat{\mathcal{T}}\exp\left[-\frac{\mathrm{i}}{\hbar}\int_{t_i}^{t_f}\mathrm{d}t\hat{H}\left(t\right)\right]|\mathbf{n}^{(i)}\rangle=$$
$$\lim_{M\to\infty}\int\mathrm{d}^{2L}\zeta^{(0)}\int\mathrm{d}^{2L}\chi^{(0)}\cdots\int\mathrm{d}^{2L}\zeta^{(M)}\int\mathrm{d}^{2L}\chi^{(M)}\left\langle\mathbf{n}^{(f)}\,\middle|\,\boldsymbol{\chi}^{(M)}\right\rangle$$
$$\times\left\{\prod_{m=0}^{M-1}\left\langle\boldsymbol{\zeta}^{(m+1)}\,\middle|\,\exp\left[-\frac{\mathrm{i}\tau}{\hbar}\hat{H}^{(m)}\right]\,\middle|\,\boldsymbol{\chi}^{(m)}\right\rangle\left\langle\boldsymbol{\chi}^{(m)}\,\middle|\,\boldsymbol{\zeta}^{(m)}\right\rangle\right\}$$
$$\times\left\langle\boldsymbol{\chi}^{(M)}\,\middle|\,\boldsymbol{\zeta}^{(M)}\right\rangle\left\langle\boldsymbol{\zeta}^{(0)}\,\middle|\,\mathbf{n}^{(i)}\right\rangle. \tag{5.1}$$

Note that the overlap $\langle\boldsymbol{\chi}^{(m)}|\boldsymbol{\zeta}^{(m)}\rangle$ can be placed anywhere, since it contains only terms of even number of Grassmann numbers.

Here, the short hand notation $\mathrm{d}^2\zeta=\mathrm{d}\zeta\mathrm{d}\zeta^*$ as well as $\tau=(t_f-t_i)/M$ and $\hat{H}^{(m)}=\hat{H}\left(t_i+m\tau\right)$ have been introduced. Since

$$\left\langle\boldsymbol{\zeta}^{(m+1)}\,\middle|\,\exp\left[-\mathrm{i}\hat{H}^{(m)}/\hbar\right]\,\middle|\,\boldsymbol{\chi}^{(m)}\right\rangle\langle\boldsymbol{\chi}^{(m)}|\boldsymbol{\zeta}^{(m)}\rangle$$

always contains an even number of Grassmann variables, and therefore commutes with every other Grassmann variable, one does not have to pay attention of the ordering of the product in the second to last line.

As shown in Appendix B, it then turns out that since each function of Grassmann variables has a Taylor series truncating after linear order, the Grassmann integrals can be carried out exactly after inserting integrals of the form

$$\int_0^{2\pi}\mathrm{d}\theta\int\mathrm{d}^2\phi\exp\left(-\left|\phi\right|^2+\phi^*\mathrm{e}^{\mathrm{i}\theta}-\mathrm{i}j\theta\right)=2\pi^2\delta_{j,1}\qquad\text{and}$$
$$\int\mathrm{d}^2\phi\int\mathrm{d}^2\mu\exp\left(-\left|\phi\right|^2-\left|\mu\right|^2+\phi^*\mu\right)\phi^j\left(\mu^*\right)^{j'}=\pi^2 j!\,\delta_{j,j'}$$

for $j,j'\in\mathbb{N}_0$.

It is important to notice that there is a certain arbitrariness in the way these integrals are inserted. When demanding that the action appearing in the path integral has the same form as in the bosonic case (but of

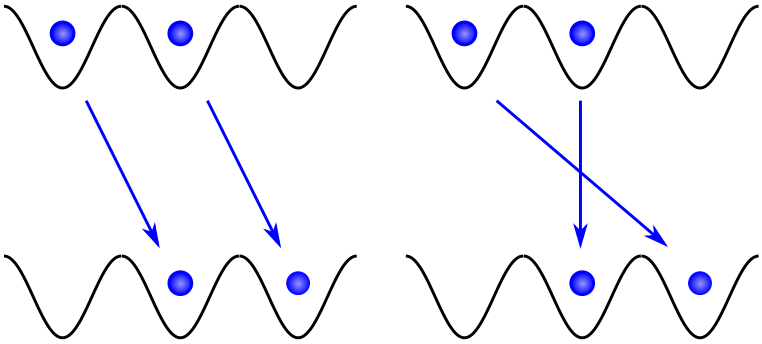

Figure 5.2: For indistinguishable particles, these two processes can not be told apart. However, the right one results from the left one by exchanging the two particles, which for fermions requires an additional minus sign

course with a different Hamiltonian), this arbitrariness affects the boundary terms and the classical Hamiltonian only. Here, the choice is such that the classical Hamiltonian reads

$$\begin{aligned} H^{(\mathrm{cl})}\left(\boldsymbol{\mu}^*, \boldsymbol{\phi}; t_k\right) = & \\ & \sum_{\alpha=1}^{L} h_{\alpha\alpha}^{(k)} \mu_\alpha^* \phi_\alpha + \sum_{\substack{\alpha,\beta=1 \\ \alpha\neq\beta}}^{L} U_{\alpha\beta}^{(k)} \mu_\alpha^* \mu_\beta^* \phi_\beta \phi_\alpha \\ & + \sum_{\substack{\alpha,\beta=1 \\ \alpha\neq\beta}}^{L} h_{\alpha\beta}^{(k)} \mu_\alpha^* \phi_\beta \exp\left(-\mu_\alpha^* \phi_\alpha - \mu_\beta^* \phi_\beta\right) \prod_{l=\min(\alpha,\beta)+1}^{\max(\alpha,\beta)-1} \left(1 - 2\mu_l^* \phi_l\right). \end{aligned} \tag{5.2}$$

In Eq. (5.2), the fermionic character is included in the last term, which discribes the hopping from one site $\alpha$ to another one $\beta \neq \alpha$,

$$h_{\alpha\beta}^{(k)} \mu_\alpha^* \phi_\beta \exp\left(-\mu_\alpha^* \phi_\alpha - \mu_\beta^* \phi_\beta\right) \prod_{l=\min(\alpha,\beta)+1}^{\max(\alpha,\beta)-1} \left(1 - 2\mu_l^* \phi_l\right).$$

Here, the last factor, which is a product over all sites between $\alpha$ and $\beta$, accounts for the anticommutativity, which yields an additional minus sign for each occupied state between the ones, for which the hopping occurs (see Fig. 5.2). This additional minus sign is exactly the one included in the definition of the creation (3.3) and annihilation operators (3.4). Moreover, the exponential factor suppresses those hopping events for which the final

occupation number is larger than one accounting effectively for the Pauli exclusion principle. Furthermore, in the classical limit occupations larger than one are not strictly forbidden. Instead, they are just penalized. However, in Eq. (5.1), only the physical Fock states with occupations 0 or 1 are used, and therefore, only those trajectories with physical initial and final occupations will matter, as will become more clearly, when the semiclassical limit is considered. Yet, at intermediate times, the occupations may still be larger than one.

The boundary conditions are chosen such that the path integral is given by

$$\begin{aligned} &K\left(\mathbf{n}^{(f)},\mathbf{n}^{(i)};t_f,t_i\right) = \\ &\lim_{M\to\infty}\int_0^{2\pi} \mathrm{d}^{N^{(i)}}\theta^{(i)} \int \mathrm{d}^{2L}\phi^{(1)}\cdots\int \mathrm{d}^{2L}\phi^{(M-1)} \int \mathrm{d}^{2N^{(f)}}\phi^{(M)} \left(\prod_{j=1}^{N^{(f)}} \phi^{(M)}_{l_j^{(f)}}\right) \\ &\exp\left\{\sum_{m=1}^{M}\left[\boldsymbol{\phi}^{(m)*}\cdot\left(\boldsymbol{\phi}^{(m-1)}-\boldsymbol{\phi}^{(m)}\right) - \frac{\mathrm{i}\tau}{\hbar}H^{(\mathrm{cl})}\left(\boldsymbol{\phi}^{(m)*},\boldsymbol{\phi}^{(m-1)};t_{m-1}\right)\right]\right\} \\ &\qquad\qquad \times\frac{1}{(2\pi)^{N^{(i)}}\,\pi^{N^{(f)}+(M-1)L}} \exp\left(-\mathrm{i}\sum_{j=1}^{N^{(i)}}\theta^{(i)}_{l_j^{(i)}}\right), \end{aligned} \tag{5.3}$$

with $\phi_l^{(0)} = n_l^{(i)}\exp\left(\mathrm{i}\theta_l^{(i)}\right)$. This path integral can also be written in a more common form as,

$$\begin{aligned} &K\left(\mathbf{n}^{(f)},\mathbf{n}^{(i)};t_f,t_i\right) = \\ &\qquad\int_0^{2\pi}\frac{\mathrm{d}^{N^{(i)}}\theta^{(i)}}{(2\pi)^{N^{(i)}}}\exp\left(-\mathrm{i}\sum_{j=1}^{N^{(i)}}\theta^{(i)}_{l_j^{(i)}}\right)\int\frac{\mathrm{d}^{2N^{(f)}}\phi^{(f)}}{\pi^{N^{(f)}}}\left(\prod_{j=1}^{N^{(f)}}\phi^{(f)}_{l_j^{(f)}}\right) \\ &\qquad\int\mathcal{D}\left[\boldsymbol{\phi}(t)\right]\exp\left\{-\frac{\mathrm{i}}{\hbar}\int_{t_i}^{t_f}\mathrm{d}t\left[\hbar\mathbf{J}(t)\cdot\dot{\boldsymbol{\theta}}(t)+H^{(\mathrm{cl})}\left(\boldsymbol{\phi}^*(t),\boldsymbol{\phi}(t);t\right)\right]\right\} \\ &\qquad\qquad\times\exp\left\{\frac{1}{2}\left(N^{(i)}-\left|\boldsymbol{\phi}^{(f)}\right|^2\right)\right\}, \end{aligned}$$

where we defined $\mathbf{J}(t)$ to be the vector containing the amplitudes of the field, $J_l(t) = \left|\phi_l(t)\right|^2$ and the path integral runs over all paths $\boldsymbol{\phi}(t)$ with

the boundary conditions

$$\phi_l(t_i) = n_l^{(i)} \exp\left(\mathrm{i}\theta_l^{(i)}\right)$$
$$\phi_l(t_i) = \phi_l^{(f)}$$

Note that (5.3) results from

$$K\left(\mathbf{n}^{(f)}, \mathbf{n}^{(i)}; t_f, t_i\right) = \int \mathrm{d}^{N^{(i)}}\phi^{(i)} \int \mathrm{d}^{2N^{(f)}}\phi^{(f)} \left(\prod_{j=1}^{N^{(f)}} \phi^{(f)}_{l_j^{(f)}}\right) \left(\prod_{j=1}^{N^{(i)}} \phi^{(f)*}_{l_j^{(i)}}\right) \frac{1}{\pi^{N^{(i)}+N^{(f)}}} \int \mathcal{D}\left[\boldsymbol{\phi}(t)\right] \exp\left\{\frac{\mathrm{i}}{\hbar}\int_{t_i}^{t_f} \mathrm{d}t \left[-\hbar\mathbf{J}(t)\cdot\dot{\boldsymbol{\theta}}(t) - H^{(\mathrm{cl})}\left(\boldsymbol{\phi}^*(t), \boldsymbol{\phi}(t); t\right)\right]\right\} \times \exp\left[-\frac{1}{2}\left(\left|\boldsymbol{\phi}^{(f)}\right|^2 + \left|\boldsymbol{\phi}^{(i)}\right|^1\right)\right],$$

by integrating out $|\phi^{(i)}_{l_j^{(i)}}|^2$ exactly. These mixed boundary conditions have been chosen such that for a diagonal non-interacting Hamiltonian, the semiclassical approximation coincides with the exact propagator and therefore can be understood as a choice for the regularization of the path integral. Including the integration over the amplitudes at initial time in the stationary point, would yield an additional factor given by Stirling's approximation to $1! \approx \sqrt{2\pi}/\mathrm{e}$, while performing the integrals over the final amplitudes also exactly would contribute the inverse of this factor.

### *5.2.2 Semiclassical Approximation*

For the evaluation of the integrals in (5.3) it seems to be best to substitute the real and imaginary part of $\phi_l^{(m)}$ by the square of its amplitude $J_l^{(m)}$ and its phase $\theta_l^{(m)}$ relative to $\theta_{l_1}^{(i)}$:

$$\phi_l^{(m)} = \sqrt{J_l^{(m)}} \exp\left[\mathrm{i}\left(\theta_l^{(m)} - \theta_{l_1}^{(i)}\right)\right].$$

This is so because after this substitution, the Hamiltonian is independent of $\theta^{(i)}_{l_1^{(i)}}$, such that we can integrate out this phase exactly, yielding a factor

$2\pi\delta_{N^{(i)},N^{(f)}}$, which accounts for the conservation of the total number of particles $N = N^{(i)} = N^{(f)}$. After this integration the value of $\theta^{(i)}_{l^{(i)}_1}$ has to be fixed, *e.g.* to zero. For simplicity, in the following we will also define

$$\theta^{(i)}_l = 0 \qquad \forall l \in \{1,\ldots,L\} \setminus \{l^{(i)}_2,\ldots,l^{(i)}_{N^{(i)}}\},$$
$$\theta^{(f)}_l = 0 \qquad \forall l \in \{1,\ldots,L\} \setminus \{l^{(f)}_1,\ldots,l^{(f)}_{N^{(i)}}\}.$$

The remaining details of the stationary phase approximation to the path integral will be left to Appendix C, while here we just discuss the resulting semiclassical propagator.

First of all, after performing the continuous limit, $M \to \infty \Leftrightarrow \tau \to 0$, the stationary phase conditions select the trajectories given by the equations of motion

$$\mathrm{i}\hbar\dot{\boldsymbol{\phi}} = \frac{\partial H^{(\mathrm{cl})}\left(\boldsymbol{\phi}^*,\boldsymbol{\phi};t\right)}{\partial\boldsymbol{\phi}^*}. \tag{5.4}$$

as well as the boundary conditions

$$\left|\phi_l\left(t_i\right)\right|^2 = n^{(i)}_l \tag{5.5}$$
$$\left|\phi_l\left(t_f\right)\right|^2 = n^{(f)}_l \tag{5.6}$$

and $\phi_{l^{(i)}_1}\left(t_i\right) = 1$. Therefore, the semiclassical propagator will again be given by a sum over Gross-Pitaevskii-like trajectories $\gamma$ joining the initial and final occupations. The phase of each contribution in this sum is given by the classical action along the trajectory $\gamma$

$$R_\gamma = \int_{t_i}^{t_f} \mathrm{d}t \left[\hbar\boldsymbol{\theta}(t)\cdot\dot{\mathbf{J}}(t) - H^{(\mathrm{cl})}\left(\boldsymbol{\phi}^*(t),\boldsymbol{\phi}(t);t\right)\right], \tag{5.7}$$

where $\phi_l(t) = \sqrt{J_l(t)}\exp\left(\mathrm{i}\theta_l(t)\right)$.

In the following, matrices, which will be denoted as $\mathcal{P}^{(i)}$, $\mathcal{P}^{(f)}$, $\mathcal{P}^{(i)}_0$, $\mathcal{P}^{(f)}_0$, $\bar{\mathcal{P}}^{(i)}$, $\bar{\mathcal{P}}^{(f)}$, $\bar{\mathcal{P}}^{(i)}_0$, $\bar{\mathcal{P}}^{(f)}_0$, $Q^{(i)}$ and $Q^{(f)}$ will be used. $\mathcal{P}^{(i)}$ and $\mathcal{P}^{(f)}$ are defined as the $N \times L$-matrices, which removes those entries of an $L$-dimensional vector $\mathbf{v}$, which correspond to initially and finally occupied single-particle state, respectively,

$$\mathcal{P}^{(i/f)}\mathbf{v} = \begin{pmatrix} v_{l^{(i/f)}_1} \\ v_{l^{(i/f)}_2} \\ \vdots \\ v_{l^{(i/f)}_N} \end{pmatrix}. \tag{5.8}$$

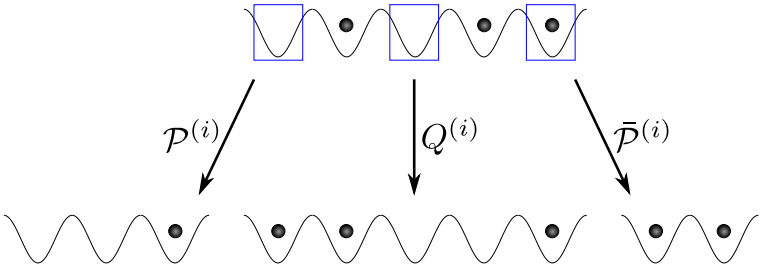


Figure 5.3: Illustration of the definitions of $\mathcal{P}^{(i)}$, $\bar{\mathcal{P}}^{(i)}$ and $Q^{(i)}$ in Eqns. (5.8), (5.9) and (5.10). The blue boxes mark the initially occupied single-particle states.

In particular, $\mathcal{P}^{(i)}$ and $\mathcal{P}^{(f)}$ map the vectors $\mathbf{n}^{(i)}$ of initial and $\mathbf{n}^{(f)}$ of final occupations, respectively, to the $N$-dimensional vector, which entries are all equal to one,

$$\mathcal{P}^{(i/f)}\mathbf{n}^{(i/f)} = \begin{pmatrix} 1 \\ \vdots \\ 1 \end{pmatrix},$$

while $\bar{\mathcal{P}}^{(i)}$ and $\bar{\mathcal{P}}^{(f)}$ are their complements defined by

$$\bar{\mathcal{P}}^{(i/f)}\mathbf{v} = \begin{pmatrix} v_1 \\ \vdots \\ v_{l_1^{(i/f)}-1} \\ \vdots \\ v_{l_N^{(i/f)}+1} \\ \vdots \\ v_L \end{pmatrix}, \tag{5.9}$$

*i.e.* the $(L-N)\times L$-matrices defined such that it selects from a vector $\mathbf{v}$ those entries, which correspond to initially and finally empty sites, respectively, which yields for the special cases $\mathbf{v} = \mathbf{n}^{(i)}$ and $\mathbf{v} = \mathbf{n}^{(f)}$

$$\bar{\mathcal{P}}^{(i/f)}\mathbf{n}^{(i/f)} = \left.\begin{pmatrix} 0 \\ \vdots \\ 0 \end{pmatrix}\right\} L-N.$$

Then, $\mathcal{P}_0^{(i)}$ results from $\mathcal{P}^{(i)}$ and $\mathcal{P}_0^{(f)}$ from $\mathcal{P}^{(f)}$ by removing the first line, while $\bar{\mathcal{P}}_0^{(i)}$ results from $\bar{\mathcal{P}}^{(i)}$ and $\bar{\mathcal{P}}_0^{(f)}$ from $\bar{\mathcal{P}}^{(f)}$ by adding the first line of

$\mathcal{P}^{(i)}$, respectively $\mathcal{P}^{(f)}$ to $\bar{\mathcal{P}}^{(i)}$, respectively $\bar{\mathcal{P}}^{(f)}$, and the $L \times L$-matrices $Q^{(i)}$ and $Q^{(f)}$ are given by

$$Q^{(i/f)} = \begin{pmatrix} \bar{\mathcal{P}}^{(i/f)} \\ \mathcal{P}^{(i/f)} \end{pmatrix} \tag{5.10}$$

That means, they are the (orthogonal) matrices, which move all entries of $\mathbf{n}^{(i/f)}$ equal to zero to the first $L - N$ positions and those, which are one to the last $N$ positions,

$$Q^{(i/f)}\mathbf{n}^{(i/f)} = \begin{pmatrix} 0 \\ \vdots \\ 0 \\ 1 \\ \vdots \\ 1 \end{pmatrix} \begin{matrix} \Big\} L-N \\ \\ \Big\} N \end{matrix} . \tag{5.11}$$

The definitions of $\mathcal{P}^{(i)}$, $\bar{\mathcal{P}}^{(i)}$ and $Q^{(i)}$ are also illustrated graphically in Fig. 5.3.

With these definitions, the semiclassical propagator is given by

$$K\left(\mathbf{n}^{(f)}, \mathbf{n}^{(i)}; t_f, t_i\right) = \sum_{\gamma:\mathbf{n}^{(i)}\to\mathbf{n}^{(f)}} \exp\left(\frac{\mathrm{i}}{\hbar} R_\gamma\right) K_{\mathrm{red}}^{(\gamma)},$$

where the amplitude $K_{\mathrm{red}}^{(\gamma)}$ can be shown to read (see Appendix C.1)

$$\begin{aligned} K_{\mathrm{red}}^{(\gamma)} = & \sqrt{\det\left\{\mathbb{I}_N + \exp\left[-2\mathrm{i}\mathrm{diag}\left(\mathcal{P}^{(f)}\boldsymbol{\theta}\left(t_f\right)\right)\right]\mathcal{P}^{(f)}X\left(t_f\right)\mathcal{P}^{(f)\mathrm{T}}\right\}}^{-1} \\ & \times \frac{1}{\sqrt{2\pi}^{N-1}} \exp\left\{\frac{\mathrm{i}}{2\hbar}\int_{t_i}^{t_f} \mathrm{d}t \mathrm{Tr}\left[\frac{\partial^2 H^{(\mathrm{cl})}\left(\boldsymbol{\phi}^*(t), \boldsymbol{\phi}(t); t\right)}{\partial\boldsymbol{\phi}(t)^2} X(t)\right]\right\}, \end{aligned} \tag{5.12}$$

where $X(t)$ satisfies

$$X(t_i) = Q^{(i)\mathrm{T}} \begin{pmatrix} 0 & \\ & \exp\left[2\mathrm{i}\mathrm{diag}\left(\mathcal{P}_0^{(i)}\boldsymbol{\theta}^{(i)}\right)\right] \end{pmatrix} Q^{(i)} \tag{5.13a}$$

$$\dot{X} = \frac{\mathrm{i}}{\hbar}\frac{\partial^2 H^{(\mathrm{cl})}}{\partial\boldsymbol{\phi}^{*2}} - \frac{\mathrm{i}}{\hbar}\frac{\partial^2 H^{(\mathrm{cl})}}{\partial\boldsymbol{\phi}^*\partial\boldsymbol{\phi}} X - \frac{\mathrm{i}}{\hbar} X\frac{\partial^2 H^{(\mathrm{cl})}}{\partial\boldsymbol{\phi}\partial\boldsymbol{\phi}^*} + \frac{\mathrm{i}}{\hbar} X\frac{\partial^2 H^{(\mathrm{cl})}}{\partial\boldsymbol{\phi}^2} X. \tag{5.13b}$$

To solve this differential equation for $X(t)$, consider a small perturbation of the trajectory $\gamma$ in an initial variable $W_l^{(i)}$ ($W_l^{(i)}$ can be *e.g.* $\theta_l^{(i)}$, $J_l^{(i)}$, $\phi_l^{(i)}$ or $\phi_l^{(i)^*}$). The perturbed trajectory $\gamma'$, described by $\boldsymbol{\phi}'$ and $\boldsymbol{\phi}'^*$, which must be considered as independent variables, can be expanded up to first order in the perturbation and is thus written as

$$\begin{aligned}\phi'_{l'}(t) =&\phi_{l'}(t) + \rho_{l'l}(t)W_l^{(i)}\\ {\phi_{l'}}^{*\prime}(t) =&{\phi_{l'}}^*(t) + \sigma_{l'l}(t)W_l^{(i)}\end{aligned}$$

The matrices $\rho(t)$ and $\sigma(t)$ then satisfy the linearized equations of motion

$$\begin{aligned}\dot\rho(t) =& -\frac{\mathrm{i}}{\hbar}\frac{\partial^2 H^{(\mathrm{cl})}}{\partial\boldsymbol{\phi}^{*2}}\sigma(t) - \frac{\mathrm{i}}{\hbar}\frac{\partial^2 H^{(\mathrm{cl})}}{\partial\boldsymbol{\phi}^*\partial\boldsymbol{\phi}}\rho(t)\\ \dot\sigma(t) =&\frac{\mathrm{i}}{\hbar}\frac{\partial^2 H^{(\mathrm{cl})}}{\partial\boldsymbol{\phi}^2}\rho(t) + \frac{\mathrm{i}}{\hbar}\frac{\partial^2 H^{(\mathrm{cl})}}{\partial\boldsymbol{\phi}\partial\boldsymbol{\phi}^*}\sigma(t).\end{aligned}$$

Therefore $-\rho(t)\sigma^{-1}(t)$ satisfies the same equation of motion as $X(t)$, which means that we only have to find the variables $W_l^{(i)}$ such that $\sigma(t_i)$ is invertible and at the same time $X(t_i) = -\rho(t_i)\sigma^{-1}(t_i)$. Since $\phi_l(t)$ and ${\phi_l}^*(t)$ are independent variables, this is obtained by the choice $W_{l_j^{(i)}} = \theta^{(i)}_{l_j^{(i)}}$ for $j = 2, \dots, N$ and $W_l = {\phi_l}^*(t_i)$ for $l \notin \{l_2^{(i)}, \dots l_N^{(i)}\}$, *i.e.*

$$\begin{aligned}X(t) = -{Q^{(i)}}^{\mathrm{T}} &\begin{pmatrix} \dfrac{\partial\left(\bar{\mathcal{P}}_0^{(i)}\boldsymbol{\phi}(t)\right)}{\partial\left(\bar{\mathcal{P}}_0^{(i)}{\boldsymbol{\phi}^{(i)}}^*\right)} & \dfrac{\partial\left(\bar{\mathcal{P}}_0^{(i)}\boldsymbol{\phi}(t)\right)}{\partial\left(\mathcal{P}_0^{(i)}\boldsymbol{\theta}^{(i)}\right)} \\ \dfrac{\partial\left(\mathcal{P}_0^{(i)}\boldsymbol{\phi}(t)\right)}{\partial\left(\bar{\mathcal{P}}_0^{(i)}\boldsymbol{\phi}^{(i)}\right)} & \dfrac{\partial\left(\mathcal{P}_0^{(i)}\boldsymbol{\phi}(t)\right)}{\partial\left(\mathcal{P}_0^{(i)}\boldsymbol{\theta}^{(i)}\right)} \end{pmatrix}\\ &\times \begin{pmatrix} \dfrac{\partial\left(\bar{\mathcal{P}}_0^{(i)}\boldsymbol{\phi}^*(t)\right)}{\partial\left(\bar{\mathcal{P}}_0^{(i)}{\boldsymbol{\phi}^{(i)}}^*\right)} & \dfrac{\partial\left(\bar{\mathcal{P}}_0^{(i)}\boldsymbol{\phi}^*(t)\right)}{\partial\left(\mathcal{P}_0^{(i)}\boldsymbol{\theta}^{(i)}\right)} \\ \dfrac{\partial\left(\mathcal{P}_0^{(i)}\boldsymbol{\phi}^*(t)\right)}{\partial\left(\bar{\mathcal{P}}_0^{(i)}\boldsymbol{\phi}^{(i)}\right)} & \dfrac{\partial\left(\mathcal{P}_0^{(i)}\boldsymbol{\phi}^*(t)\right)}{\partial\left(\mathcal{P}_0^{(i)}\boldsymbol{\theta}^{(i)}\right)} \end{pmatrix}^{-1} Q^{(i)}\end{aligned}$$

Finally, the reduced propagator can be further simplified (see Appendix C.2) and the propagator can be written as

$$K\left(\mathbf{n}^{(f)}, \mathbf{n}^{(i)}; t_f, t_i\right) = \sum_{\gamma:\mathbf{n}^{(i)}\to\mathbf{n}^{(f)}} \mathcal{A}_\gamma\mathcal{B}_\gamma \exp\left(\frac{\mathrm{i}}{\hbar}R_\gamma\right). \tag{5.14}$$

with

$$\mathcal{A}_\gamma = \sqrt{\det \frac{1}{-2\mathrm{i}\pi\hbar} \frac{\partial^2 R_\gamma}{\partial\left(\mathcal{P}_0^{(f)}\mathbf{n}^{(f)}\right)\partial\left(\mathcal{P}_0^{(i)}\mathbf{n}^{(i)}\right)}}.$$

and $\mathcal{B}_\gamma$ given by

$$\mathcal{B}_\gamma = \frac{\sqrt{\det Q^{(f)}Q^{(i)}}\exp\left[\frac{\mathrm{i}}{2\hbar}\int_{t_i}^{t_f}\mathrm{d}t\mathrm{Tr}\frac{\partial^2 H^{(\mathrm{cl})}}{\partial\boldsymbol{\phi}\partial\boldsymbol{\phi}^*} + \frac{\mathrm{i}}{2}\sum_{l=1}^{L}\left(\theta_l^{(f)} - \theta_l^{(i)}\right)\right]}{\sqrt{\det\left[\frac{\partial\left(\bar{\mathcal{P}}^{(f)}\boldsymbol{\phi}^*(t_f), J^{(f)}_{l_1^{(f)}}\right)}{\partial\left(\bar{\mathcal{P}}^{(i)}\boldsymbol{\phi}^*(t_i)\right)} - \frac{\partial\left(\bar{\mathcal{P}}^{(f)}\boldsymbol{\phi}^*(t_f), J^{(f)}_{l_1^{(f)}}\right)}{\partial\left(\mathcal{P}_0^{(i)}\boldsymbol{\theta}^{(i)}\right)}\left(\frac{\partial\left(\mathcal{P}_0^{(f)}\mathbf{J}^{(f)}\right)}{\partial\left(\mathcal{P}_0^{(i)}\boldsymbol{\theta}^{(i)}\right)}\right)^{-1}\frac{\partial\left(\mathcal{P}_0^{(f)}\mathbf{J}^{(f)}\right)}{\partial\left(\bar{\mathcal{P}}^{(i)}\boldsymbol{\phi}^*(t_i)\right)}\right]}}. \tag{5.15}$$

As usual, using the equations of motion, the derivatives of the action with respect to the initial and final occupation numbers can be shown to satisfy

$$\frac{\partial R_\gamma}{\partial \mathbf{n}^{(i)}} = -\hbar\boldsymbol{\theta}^{(i)}$$
$$\frac{\partial R_\gamma}{\partial \mathbf{n}^{(f)}} = \hbar\boldsymbol{\theta}^{(f)}.$$

This explains also the form of $\mathcal{A}_\gamma$. The typical form of the functional determinant would be the second derivative of the action with respect to *all* initial and final occupation numbers. However, here the derivatives are only with respect to the non-zero entries of $\mathbf{n}^{(i)}$ and $\mathbf{n}^{(f)}$. This is due to the fact that the integrals over the phases which belong to unoccupied sites, as well as the one over $\theta^{(i)}_{l_1^l}$ have been performed exactly. This exact integration is necessary, since these phases are arbitrary (but fixed) and therefore independent of the initial and final occupation numbers. This exact integration also is the origin of the additional factor $\mathcal{B}_\gamma$.

Apart from this the overall form of the semiclassical propagator is the same as in the Bosonic case, (4.18), namely it is given by a sum over classical trajectories, where each trajectory is weighted with the determinant of the second derivatives of the action and contributes a phase given by its the classical action. The classcial limit, however is obviously different in both cases, which is a consequence of the antisymmetry and the resulting Pauli principle for fermions. Moreover, the boundary conditions are slightly different: While for Fermions, they are given by the initial occupation numbers, for Bosons they have to be increased by 1/2.

# Part III

# Interference Effects in Bosonic Fock Space

CHAPTER 6

# Non-Interacting Systems

## 6.1 The Transition Probability for Quadratures

### *6.1.1 The exact propagator in quadrature representation*

For a non-interacting bosonic many-body system, the classical Hamiltonian in quadrature representation is quadratic,

$$H^{(\mathrm{cl})}\left(\boldsymbol{\psi}^{\dagger}, \boldsymbol{\psi}; t\right) = \sum_{l,l'=1}^{L} h_{ll'} {\psi_l}^* \psi_{l'}. \tag{6.1}$$

Therefore, the exponential in the path integral (4.6) is also quadratic. This in turn means that expanding the exponential up to second order in the variables which are integrated over, yields again an exact expression, and the stationary phase approximation is exact.

Hence, for the derivation of the exact propagator in quadrature representation, one can start from (4.15).

In this case, the equations of motion can be written as

$$\mathrm{i}\hbar\dot{\boldsymbol{\psi}} = H\boldsymbol{\psi},$$

where $H$ is the matrix which entries are given by $h_{l,l'}$. The solution of the equations of motion is given by the (unitary) classical time evolution operator

$$U\left(t, t'\right) = \exp\left(-\frac{\mathrm{i}}{\hbar} H\left(t - t'\right)\right)$$

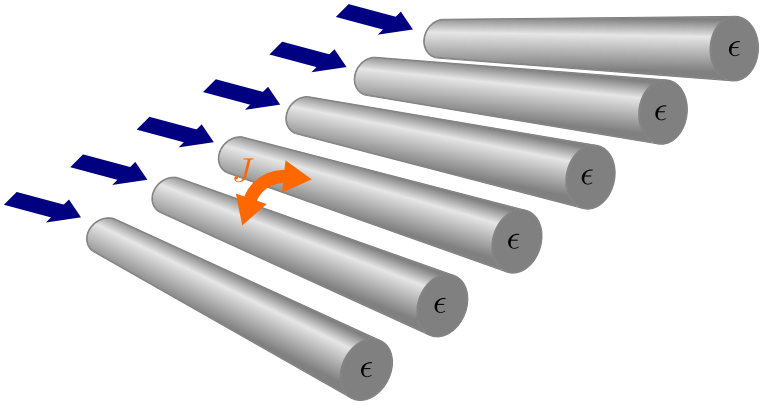


Figure 6.1: Schematic picture of a waveguide array consisting of six waveguides. The energy of a photon is the same in every waveguide as is the hopping amplitude between two neighboring waveguides. The blue arrows symbolize the entering photons.

applied to $\boldsymbol{\psi}(t_i)$, which has to be determined according to the boundary conditions (4.16) and is given by

$$\boldsymbol{\psi}(t_i) = \frac{1}{2b}\left\{\mathbf{q}^{(i)} - \mathrm{i}\left(\tilde{U}^{(I)}\right)^{-1}\left[\mathbf{x}^{(f)} - \tilde{U}^{(R)}\mathbf{q}^{(i)}\right]\right\},$$

where $\tilde{U}^{(R/I)}$ are the real/imaginary part of $\tilde{U} = U(t_f, t_i)\exp(\mathrm{i}\varphi)$. Within this chapter, $\tilde{U}$ will also be denoted the *effective* classical propagator.

After a lengthy but otherwise straightforward calculation, the action for this path is found to read

$$R = -\frac{\hbar}{4b^2}\begin{pmatrix}\mathbf{q}^{(i)}\\ \mathbf{x}^{(f)}\end{pmatrix}\begin{pmatrix}\left(\tilde{U}^{(I)}\right)^{-1}\tilde{U}^{(R)} & -\left(\tilde{U}^{(I)}\right)^{-1}\\ -\left[\left(\tilde{U}^{(I)}\right)^{\mathrm{T}}\right]^{-1} & \tilde{U}^{(R)}\left(\tilde{U}^{(I)}\right)^{-1}\end{pmatrix}\begin{pmatrix}\mathbf{q}^{(i)}\\ \mathbf{x}^{(f)}\end{pmatrix},$$

such that finally the exact propagator can be written as

$$K^{(\varphi)}\left(\mathbf{x}^{(f)},t_f;\mathbf{q}^{(i)};t_i\right)= \\ \frac{\exp\left\{-\frac{\mathrm{i}}{4b^2}\begin{pmatrix}\mathbf{q}^{(i)}\\ \mathbf{x}^{(f)}\end{pmatrix}\begin{pmatrix}\left(\tilde{U}^{(I)}\right)^{-1}\tilde{U}^{(R)} & -\left(\tilde{U}^{(I)}\right)^{-1}\\ -\left[\left(\tilde{U}^{(I)}\right)^{\mathrm{T}}\right]^{-1} & \tilde{U}^{(R)}\left(\tilde{U}^{(I)}\right)^{-1}\end{pmatrix}\begin{pmatrix}\mathbf{q}^{(i)}\\ \mathbf{x}^{(f)}\end{pmatrix}\right\}}{\sqrt{\det\left[-4\pi\mathrm{i}b^2U\left(\tilde{U}^{(I)}\right)^{\mathrm{T}}\right]}}. \tag{6.2}$$

Having the propagator in the simple form Eq. (6.2), immediately allows to obtain certain conclusions about the propagation of photons in an waveguide array as the one shown in Fig. 6.1, if the state of the electromagnetic field is both prepared and measured in a quadrature state.

### *6.1.2 Propagation between quadratures with the same phase*

The result Eq. (6.2) depends on the individual system only via the classical propagator $U(t)$, which can be computed most efficiently by diagonalizing the matrix $H$ corresponding to the classical Hamiltonian. Let us denote the unitary matrix, which diagonalizes $H$, by $\mathcal{O}$, such that

$$\mathcal{O}^\dagger H\mathcal{O}=\mathrm{diag}\left(\boldsymbol{\lambda}\right),$$

where $\boldsymbol{\lambda}$ is the vector with entries given by the eigenvalues of $H$, and $\mathrm{diag}\left(\mathbf{v}\right)$ is the diagonal matrix with entries given by those of the vector $\mathbf{v}$. Then the classical propagator can be written as

$$U(t)=\mathcal{O}\exp\left[-\frac{\mathrm{i}}{\hbar}\mathrm{diag}\left(\boldsymbol{\lambda}\right)t\right]\mathcal{O}^\dagger.$$

Here, for real $H$, *i.e.* for real hopping parameters $h_{l\neq l'}$ in Eq. (6.1), something important happens. For a real symmetric matrix, $\mathcal{O}$ is a real orthogonal matrix, which also implies that it diagonalizes not only $H$ and $U(t)$, but also the real and imaginary parts of the classical propagator individually,

$$\Re\left[U(t)\right]=\mathcal{O}\cos\left(\frac{\boldsymbol{\lambda}t}{\hbar}\right)\mathcal{O}^{\mathrm{T}} \tag{6.3}$$

$$\Im\left[U(t)\right]=\mathcal{O}\sin\left(\frac{\boldsymbol{\lambda}t}{\hbar}\right)\mathcal{O}^{\mathrm{T}}. \tag{6.4}$$

Since the determinant of an orthogonal matrix is always equal to $\pm 1$, one sees immediately from Eq. (6.4) that the determinant of $U^{(I)} = \Im[U]$ is zero for all times, if at least one eigenvalue of $H$ is zero, and therefore the propagator seems to diverge. But, the normalization of the propagator demands that it will actually become a Dirac delta. Indeed, in this case Eq. (6.2) can also be written in the form

$$K^{(\varphi)}\left(\mathbf{x}^{(f)}, t_f; \mathbf{q}^{(i)}; t_i\right) = \exp\left\{-\frac{\mathrm{i}}{4b^2}\left[\mathbf{q}^{(i)} - \left(\tilde{U}^{(R)}\right)^{-1}\mathbf{x}^{(f)}\right]\left(\tilde{U}^{(I)}\right)^{-1}\tilde{U}^{(R)}\left[\mathbf{q}^{(i)} - \left(\tilde{U}^{(R)}\right)^{-1}\mathbf{x}^{(f)}\right]\right\} \times\sqrt{\det\left[-4\pi\mathrm{i}b^2U\left(\tilde{U}^{(I)}\right)^{\mathrm{T}}\right]}^{-1}\exp\left[\frac{\mathrm{i}}{4b^2}\mathbf{x}^{(f)}\tilde{U}^{(I)}\left(\tilde{U}^{(R)}\right)^{-1}\mathbf{x}^{(f)}\right],$$

which in the case where the determinant of the imaginary part of the effective classical propagator vanishes yields

$$K^{(\varphi)}\left(\mathbf{x}^{(f)}, t_f; \mathbf{q}^{(i)}; t_i\right) \xrightarrow{\det\tilde{U}^{(I)}\to 0} \frac{1}{\det\tilde{U}^{(R)}}\delta\left[\mathbf{q}^{(i)} - \left(\tilde{U}^{(R)}\right)^{-1}\mathbf{x}^{(f)}\right].$$

For the case of a (linear) waveguide-array with constant nearest neighbor hopping and all the onsite-energies being equal to one another, *i.e.* for a classical Hamiltonian given by the matrix

$$H = \begin{pmatrix} \epsilon & -J & & & \\ -J & \epsilon & -J & & \\ & \ddots & \ddots & \ddots & \\ & & -J & \epsilon & -J \\ & & & -J & \epsilon \end{pmatrix}, \tag{6.5}$$

it is particularly easy to find the condition on the parameters $J$ and $\epsilon$, for which one of the eigenvalues vanishes. For such a matrix, the eigenvalues are given by

$$\lambda_k = \epsilon + 2J\cos\left(\frac{k\pi}{L+1}\right), \qquad k = 1, \ldots, L,$$

where $L$ is the number of waveguides. This gives the condition that the on-site energies are given by

$$\epsilon = -2J\cos\left(\frac{k\pi}{L+1}\right) \tag{6.6}$$

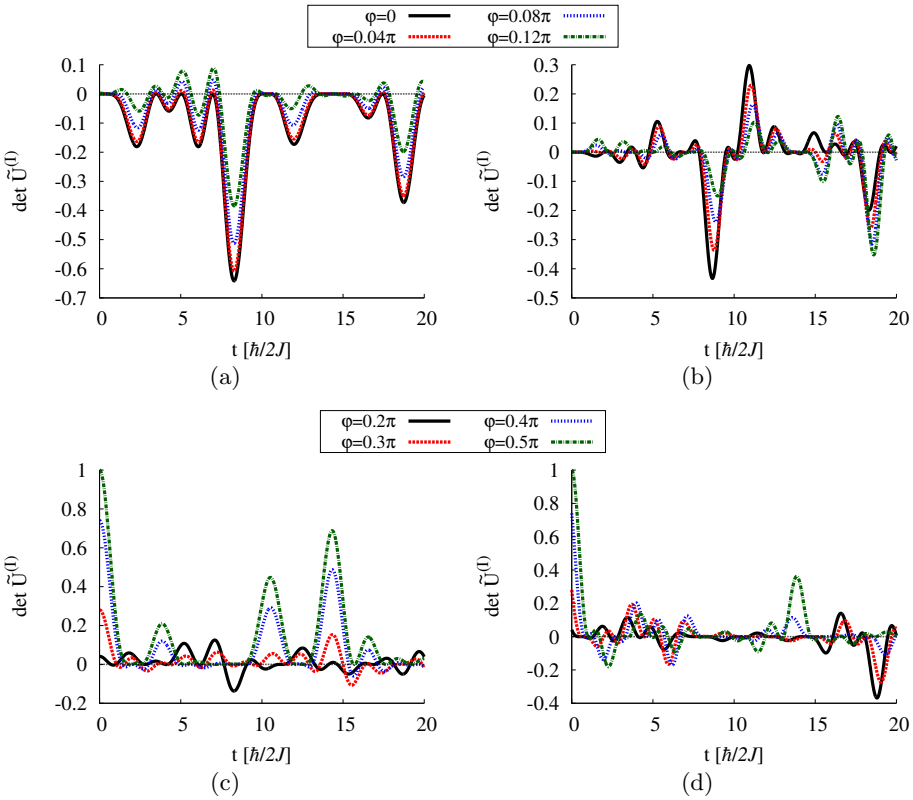


Figure 6.2: The determinant of the imaginary part of the effective classical propagator as a function of time for a linear chain of six wave guides with nearest neighbor hopping $J = 0.5$ and on-site energies (a), (c) $\epsilon = 0$ and (b), (d) $\epsilon = 0.7$ for different phase differences $\varphi$.

for a $k \in \{1, \ldots, L\}$. For an odd number of waveguides, one possible solution would be $\epsilon = 0$.

On the other hand, even if the condition Eq. (6.6) is not fulfilled, the determinant of the imaginary part of the classical propagator vanishes for certain times, which corresponds to the existence of caustics, and therefore again the propagator is given by a Dirac delta.

### *6.1.3 Propagation between quadratures with different phase*

The last observation still holds when the phase difference between the quadrature bases used to measure the initial and final state are different.

Considering again the classical Hamiltonian, Eq. (6.5), yields that

$$\det \tilde{U}^{(I)} = \prod_{l=1}^{L} \sin\left[\varphi - \frac{1}{\hbar}\left(\epsilon + 2J\cos\frac{l\pi}{L+1}\right)t\right], \tag{6.7}$$

which holds as the condition on the time for a caustic

$$t_{n,l} = \frac{(n\pi + \varphi)\,\hbar}{\epsilon + 2J\cos\frac{l\pi}{L+1}}$$

with $n \in \mathbb{N}$. Thus, the phase $\varphi$ shifts the times, at which the caustic happens. This can be seen, when looking at the zeros of $\det \tilde{U}^{(I)}$ in Fig. 6.2. It may also happen that for a certain value of $\varphi$ several of these zeros collapse as for example for $\epsilon = 0$ and $\varphi = 0$ as in Fig. 6.2(a).

For $\epsilon = 0$ it is straightforward to check that the determinant of the effective classical propagator is symmetric in $\varphi$ around $\pi$, which is also demonstrated in the left columns of Figs. 6.3, 6.4 and 6.5. This symmetry, however no longer holds for $\epsilon \neq 0$ (see right columns of Figs. 6.3, 6.4 and 6.5). However, when changing $\varphi$ to $\varphi + \pi$, the determinant, Eq. (6.7), clearly changes only by an additional sign given by $(-1)^L$.

The general dependence on $\varphi$ and $t$, however, is not so easy to summarize. Fig. 6.2 shows the dime dependence of the determinant for different values of $\varphi$ for a chain consisting of six wave guides with nearest neighbour coupling $J = 0.5$, only. As expected, it is a highly oscillatory function of time, where the height and position of each peak – especially for $\epsilon \neq 0$ – is strongly affected by $\varphi$. To get a better impression on how $\det \tilde{U}^{(I)}$ changes with $\varphi$, in Figs. 6.3, 6.4 and 6.5, the dependence on $\varphi$ is plotted for different propagation times.

Depending on the propagation time, in some cases $\det \tilde{U}^{(I)}$ as a function of $\varphi$ shows two peaks, which are more pronounced than the others, as in Figs. 6.3(a), 6.3(b), 6.3(c), 6.3(d), 6.4(e) and 6.4(f). In other cases, it shows several peaks of almost the same heights as in Figs. 6.3(e), 6.3(f), 6.5(c) and 6.5(d).

## 6.2 The Transition Probability in Coherent States

The exact propagator for a non-interacting system in coherent state representation can be found by relating it - by inserting unit operators in

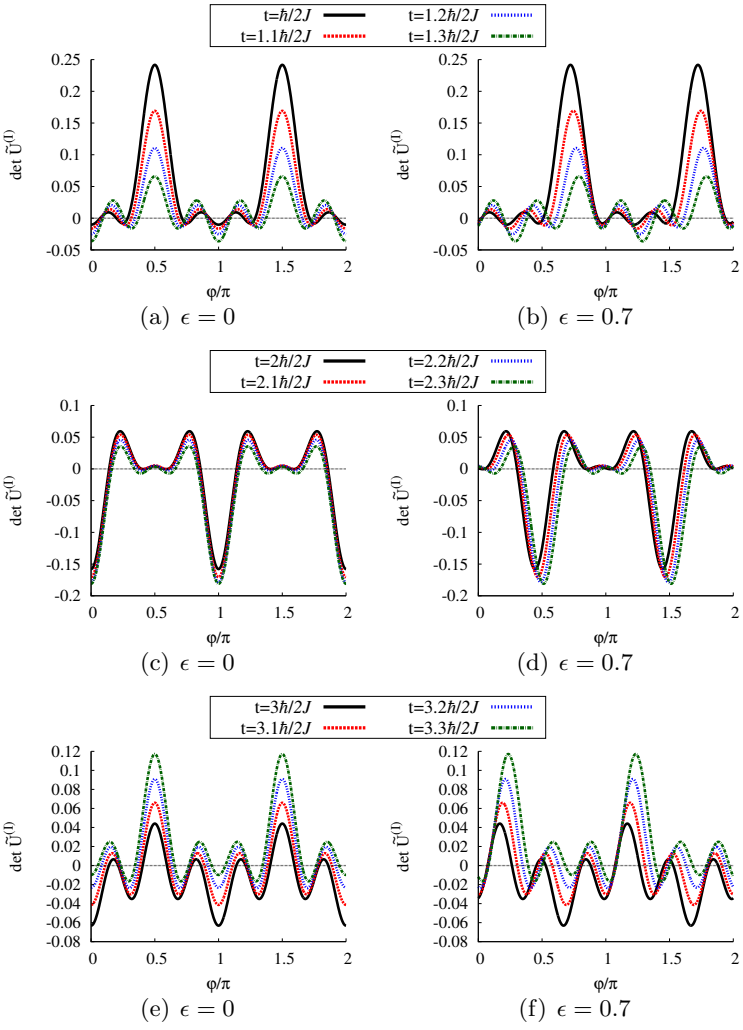


(a) $\epsilon = 0$ (b) $\epsilon = 0.7$

(c) $\epsilon = 0$ (d) $\epsilon = 0.7$

(e) $\epsilon = 0$ (f) $\epsilon = 0.7$

Figure 6.3: The determinant of the imaginary part of the effective classical propagator as a function of the phase difference $\varphi$ of the quadratures for a linear chain of six wave guides with nearest neighbor hopping $J = 0.5$ and on-site energies (a), (c), (e) $\epsilon = 0$ and (b), (d), (f) $\epsilon = 0.7$ for different propagation times $t$.

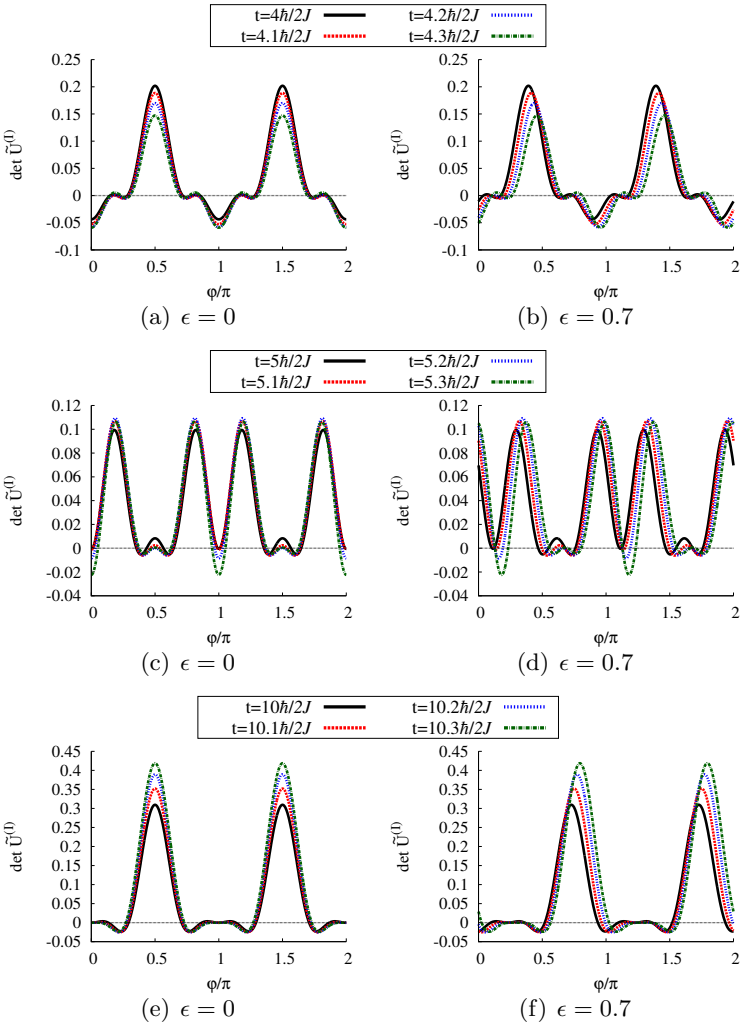


(a) $\epsilon = 0$ (b) $\epsilon = 0.7$

(c) $\epsilon = 0$ (d) $\epsilon = 0.7$

(e) $\epsilon = 0$ (f) $\epsilon = 0.7$

Figure 6.4: The determinant of the imaginary part of the effective classical propagator as a function of the phase difference $\varphi$ of the quadratures for a linear chain of six wave guides with nearest neighbor hopping $J = 0.5$ and on-site energies (a), (c), (e) $\epsilon = 0$ and (b), (d), (f) $\epsilon = 0.7$ for different propagation times $t$.

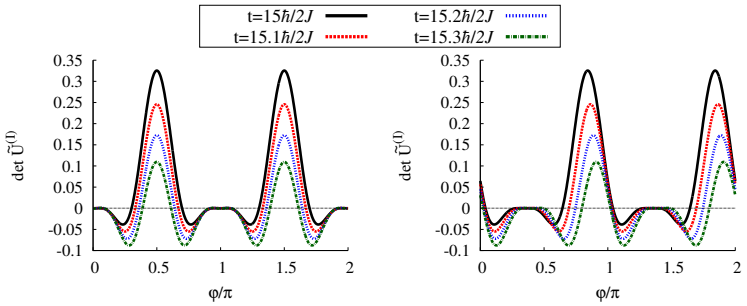


(a) $\epsilon = 0$ (b) $\epsilon = 0.7$

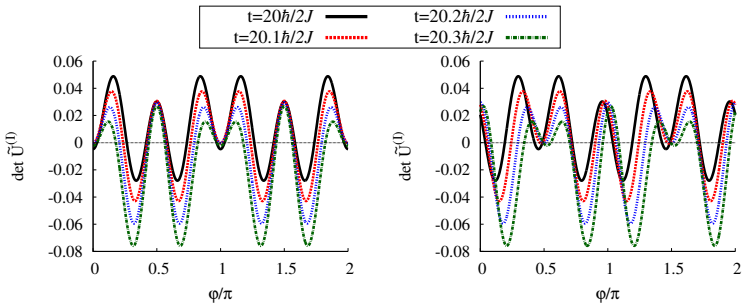


(c) $\epsilon = 0$ (d) $\epsilon = 0.7$

Figure 6.5: The determinant of the imaginary part of the effective classical propagator as a function of the phase difference $\varphi$ of the quadratures for a linear chain of six wave guides with nearest neighbor hopping $J = 0.5$ and on-site energies (a), (c) $\epsilon = 0$ and (b), (d) $\epsilon = 0.7$ for different propagation times $t$.

terms of quadratures - to the propagator in quadrature representation (6.2) for $\varphi = 0$. The resulting integral consists of gaussian integrals only and is therefore easily computed to find

$$K\left(\boldsymbol{\phi}^{(f)}, t_f; \boldsymbol{\phi}^{(i)}, t_i\right) = \exp\left(-\frac{1}{2}\left|\boldsymbol{\phi}^{(f)}\right|^2 - \frac{1}{2}\left|\boldsymbol{\phi}^{(i)}\right|^2 + \boldsymbol{\phi}^{(f)*} U\left(t_f, t_i\right) \boldsymbol{\phi}^{(i)}\right).$$

Computing the modulus square of the propagator now yields for the transition probability between two coherent states

$$\begin{aligned} P\left(\boldsymbol{\phi}^{(f)}, \boldsymbol{\phi}^{(i)}\right) &= \left|K\left(\boldsymbol{\phi}^{(f)}, t_f; \boldsymbol{\phi}^{(i)}, t_i\right)\right|^2 \\ &= \exp\left[-\left|\boldsymbol{\phi}^{(f)}\right|^2 - \left|\boldsymbol{\phi}^{(i)}\right|^2 + 2\Re\left(\boldsymbol{\phi}^{(f)*} U\left(t_f, t_i\right) \boldsymbol{\phi}^{(i)}\right)\right]. \end{aligned}$$

Obviously, in contrast to the transition probability between quadratures, the transition probability between coherent states is not constant but depends strongly on the chosen initial and final coherent state.

In particular, it is strongly enhanced when

$$\boldsymbol{\phi}^{(f)} = U\left(t_f, t_i\right) \boldsymbol{\phi}^{(i)},$$

namely at the classcial solution.

CHAPTER 7

# Many-Body Coherent Backscattering

## 7.1 Chaotic Regime

The object of interest in this section is the transition probability from an initial Fock state $\mathbf{n}^{(i)}$ to a final one $\mathbf{n}^{(f)}$,

$$P\left(\mathbf{n}^{(f)},t_f;\mathbf{n}^{(i)},t_i\right)=\left|\langle\mathbf{n}^{(f)}|\,\hat{K}\left(t_f,t_i\right)|\mathbf{n}^{(i)}\rangle\right|^2=\left|K\left(\mathbf{n}^{(f)},t_f;\mathbf{n}^{(i)},t_i\right)\right|^2,$$

*i.e.* the probability to measure the Fock state $\mathbf{n}^{(f)}$ at time $t_f$, if the system was prepared in the Fock state $\mathbf{n}^{(i)}$ at the initial time $t_i$. Here $\hat{K}\left(t_f,t_i\right)=\hat{\mathcal{T}}\exp\left[-\mathrm{i}\int_{t_i}^{t_f}\mathrm{d}t\hat{H}\left(t\right)/\hbar\right]$ is the quantum mechanical propagator.

Inserting the semiclassical propagator (4.18), yields for the transition probability a double sum over trajectories,

$$P\left(\mathbf{n}^{(f)},t_f;\mathbf{n}^{(i)},t_i\right)\approx \sum_{\gamma,\gamma':\mathbf{n}^{(i)}\to\mathbf{n}^{(f)}}\sqrt{\det{}'\frac{\partial^2 R_\gamma}{\partial\mathbf{n}^{(f)}\partial\mathbf{n}^{(i)}}}\sqrt{\det{}'\frac{\partial^2 R_{\gamma'}}{\partial\mathbf{n}^{(f)}\partial\mathbf{n}^{(i)}}}^{*}\frac{\exp\left[\frac{\mathrm{i}}{\hbar}\left(R_\gamma-R_{\gamma'}\right)\right]}{\left(2\pi\hbar\right)^{L-1}}. \quad (7.1)$$

In general, one can not say much about the contributions of the double sums. However, under disorder average, *i.e.* an average over the on-site energies $\epsilon_l=h_{ll}$, due to the scaling of the action with the total number

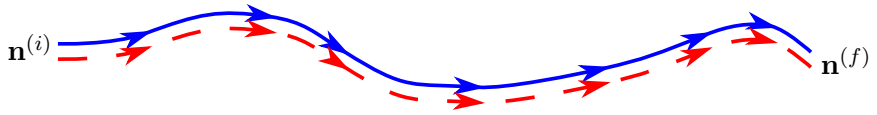


Figure 7.1: In the diagonal approximation, only identical pairs of trajectories are taken into account

of particles, the action difference in the exponential gives rise to strong oscillations. Most contributions to the double sum cancel out on disorder average, unless the two actions for trajectories $\gamma$ and $\gamma'$ are correlated.

### *7.1.1 Diagonal approximation*

The most obvious pairs of trajectories, which are correlated, are the identical ones, *i.e.* $\gamma = \gamma'$ (see Fig. 7.1). For those pairs, the action difference is obviously zero and the transition probability in diagonal approximation reduces to

$$P^{(\mathrm{da})}\left(\mathbf{n}^{(f)}, t_f; \mathbf{n}^{(i)}, t_i\right) = \frac{1}{(2\pi)^{L-1}} \sum_{\gamma} \left| \det{}' \frac{\partial \boldsymbol{\theta}\left(t_i\right)}{\partial \mathbf{n}^{(f)}} \right|,$$

where $\boldsymbol{\theta}\left(t_i\right)$ is the vector containing the initial phases for the trajectory $\gamma$.

By inserting an integration over the initial phases together with a Dirac delta, ensuring that only those phases contribute which match the ones given by the trajectories and using the properties of the delta function, one can prove the sum rule

$$\begin{aligned} \sum_{\gamma} \left| \det{}' \frac{\partial \boldsymbol{\theta}\left(t_i\right)}{\partial \mathbf{n}^{(f)}} \right| &= \int_0^{2\pi} \mathrm{d}^{L-1}\theta^{(i)} \prod_{l=2}^{L} \delta\left[ \left| \psi_l\left(\mathbf{n}^{(i)}; \boldsymbol{\theta}^{(i)}; t_f\right) \right|^2 - 1/2 - n_l^{(f)} \right] \\ &= (2\pi)^{L-1} P^{(\mathrm{cl})}\left(\mathbf{n}^{(f)}, t_f; \mathbf{n}^{(i)}, t_i\right), \end{aligned} \tag{7.2}$$

with $\boldsymbol{\psi}(\mathbf{n}^{(i)}; \boldsymbol{\theta}^{(i)}; t_f)$ being the classical time evolution of the initial state $\boldsymbol{\psi}^{(i)}$ with components

$$\psi_l^{(i)} = \sqrt{n_l^{(i)} + 1/2}\, \exp(\mathrm{i}\theta_l^{(i)}).$$

Therefore, the diagonal approximation yields the classical transition probability

$$P^{(\mathrm{da})}\left(\mathbf{n}^{(f)}, t_f; \mathbf{n}^{(i)}, t_i\right) = P^{(\mathrm{cl})}\left(\mathbf{n}^{(f)}, t_f; \mathbf{n}^{(i)}, t_i\right).$$

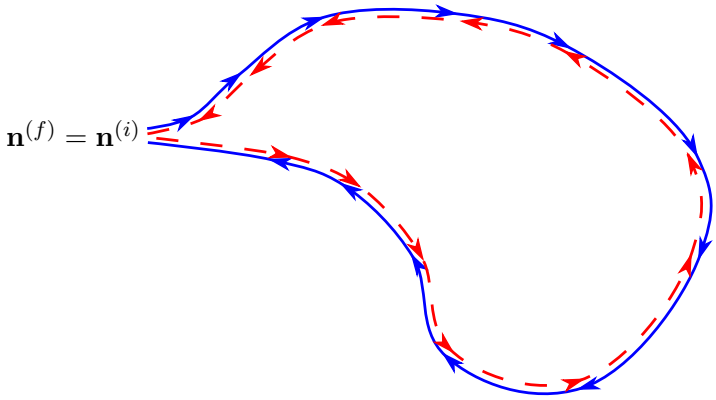


Figure 7.2: Trajectory pairs responsible for coherent backscattering

### *7.1.2 Coherent backscattering contribution*

An other class of correlated pairs of trajectories are those shown in Fig. 7.2, namely $\gamma' = \mathcal{T}\gamma$, where $\mathcal{T}$ denotes time reversal. For Bose-Hubbard systems, time reversal is achieved by complex conjugation, such that the time reversal of a solution $\boldsymbol{\phi}(t + t_i)$ of the equations of motion is $\boldsymbol{\phi}(t_f - t)^*$. Of course, these pairs exist only if the Hamiltonian itself is time reversal symmetric, which for a Bose-Hubbard system corresponds to a real Hamiltonian. It turns out that a Bose-Hubbard chain with nearest neighbor hopping only is always time reversal symmetric, since it can be transformed into a real one by multiplying each component of the wave function with a certain time-independent phase. In the same way, for certain combinations of the phases of the hopping parameter in a Bose-Hubbard ring, the Hamiltonian can be transformed into a real one.

Having identified the time reversed of a trajectory $\gamma$, it is straightforward to check that the actions of both trajectories are the same,

$$R_{\mathcal{T}\gamma} = R_\gamma.$$

However, in (7.1) pairing $\gamma$ with its time reversed is possible only, if $\mathbf{n}^{(f)} = \mathbf{n}^{(i)}$. Therefore, one first has to replace $\gamma$ and $\gamma'$ by nearby trajectories $\tilde{\gamma}$ and $\tilde{\gamma}'$, which both start and end at $\mathbf{n}^{(0)} = \left(\mathbf{n}^{(i)} + \mathbf{n}^{(f)}\right)/2$. In the course of this replacement, one also has to expand the actions in $\mathbf{n}^{(f)}$ and $\mathbf{n}^{(i)}$ up to linear order around $\mathbf{n}^{(0)}$,

$$\begin{aligned} R_\gamma - R_{\gamma'} \approx R_{\tilde{\gamma}} - R_{\tilde{\gamma}'} &+ \hbar\left(\boldsymbol{\theta}^{\tilde{\gamma}}(t_f) - \boldsymbol{\theta}^{\tilde{\gamma}'}(t_f)\right)\cdot\left(\mathbf{n}^{(f)} - \mathbf{n}^{(0)}\right) \\ &-\hbar\left(\boldsymbol{\theta}^{\tilde{\gamma}}(t_i) - \boldsymbol{\theta}^{\tilde{\gamma}'}(t_i)\right)\cdot\left(\mathbf{n}^{(i)} - \mathbf{n}^{(0)}\right). \end{aligned}$$

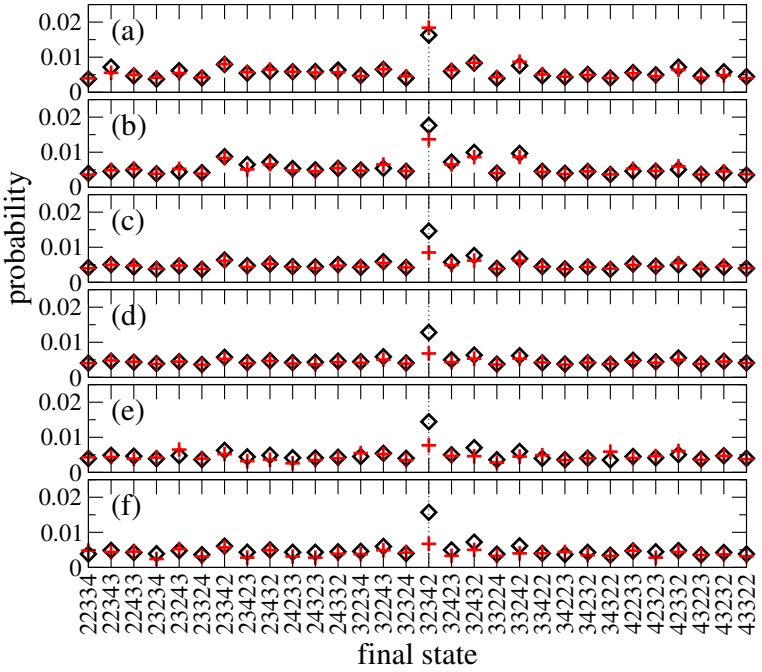


Figure 7.3: Emergence of the coherent backscattering for a Bose-Hubbard chain with five sites from numerical calculations. The initial occupation was chosen to be $(3, 2, 3, 4, 2)$. The red crosses are the classical transition probability, while the black diamonds are the quantum ones. The evolution times are (a) $t = 1.5\hbar/J$, (b) $t = 2.5\hbar/J$, (c) $t = 5\hbar/J$, (d) $t = 10\hbar/J$, (e) $t = 20\hbar/J$, (f) $t = 50\hbar/J$, where $J$ is the hopping parameter. Figure by courtesy of Julien Dujardin, Arturo Argüelles and Peter Schlagheck.

In the prefactor one can simply replace the second derivative of the action of the original trajectory by the corresponding one of the new trajectory.

If $\tilde{\gamma}'$ is the time reversed of $\tilde{\gamma}$, the initial and final phases of $\tilde{\gamma}'$ are related to those of $\tilde{\gamma}$ by

$$\begin{aligned} \boldsymbol{\theta}^{(\tilde{\gamma}')}(t_f) &= -\boldsymbol{\theta}^{(\tilde{\gamma})}(t_i) \\ \boldsymbol{\theta}^{(\tilde{\gamma}')}(t_i) &= -\boldsymbol{\theta}^{(\tilde{\gamma})}(t_f)\,, \end{aligned}$$

which, after applying the sum rule (7.2), yields for the coherent backscattering contribution to the transition probability

$$P^{(\mathrm{cbs})}\left(\mathbf{n}^{(f)},t_f;\mathbf{n}^{(i)},t_f\right)=$$
$$\frac{\delta_{TRI}}{(2\pi)^{L-1}}\int_0^{2\pi}\mathrm{d}^{L-1}\theta^{(i)}\exp\left\{\mathrm{i}\left[\boldsymbol{\theta}^{(i)}+\boldsymbol{\theta}\left(\mathbf{n}^{(i)},\boldsymbol{\theta}^{(i)};t_f\right)\right]\cdot\left(\mathbf{n}^{(f)}-\mathbf{n}^{(i)}\right)\right\}$$
$$\times\prod_{l=2}^{L}\delta\left[\left|\psi_l\left(\mathbf{n}^{(i)},\boldsymbol{\theta}^{(i)};t_f\right)\right|^2-\frac{1}{2}-\mathbf{n}^{(i)}\right],$$

where $\delta_{TRI}$ is one, if the system is time reversal invariant and zero otherwise.

For a classically chaotic system, within a disorder average one can replace the final phases $\boldsymbol{\theta}(\mathbf{n}^{(i)},\boldsymbol{\theta}^{(i)};t_f)$ by identically, independent, in $[0,2\pi]$ uniformly distributed random variables, such that for $P^{(cbs)}$ one can perform an average over the final phases yielding a factor $\delta_{\mathbf{n}^{(i)},\mathbf{n}^{(f)}}$. Thus, the averaged coherent backscattering contribution to the transition probability is given by

$$P^{(\mathrm{cbs})}\left(\mathbf{n}^{(f)},t_f;\mathbf{n}^{(i)},t_i\right)=\delta_{TRI}\delta_{\mathbf{n}^{(i)},\mathbf{n}^{(f)}}P^{(\mathrm{cl})}\left(\mathbf{n}^{(f)},t_f;\mathbf{n}^{(i)},t_i\right).$$

Here, the bar denotes an averaged quantity.

As long as time reversal symmetry is the only discrete symmetry of the system, pairing a trajectory with itself or its time reverse, are the only two generic possibilities to get a contribution with vanishing action difference. All further possible pairs of trajectories give contributions which are suppressed by a factor of $1/N$ compared to the two latter. In the semiclassical limit, the averaged transition probability is then given by

$$P\left(\mathbf{n}^{(f)},t_f;\mathbf{n}^{(i)},t_i\right)=\left(1+\delta_{TRI}\delta_{\mathbf{n}^{(f)},\mathbf{n}^{(i)}}\right)P^{(\mathrm{cl})}\left(\mathbf{n}^{(f)},t_f;\mathbf{n}^{(i)},t_i\right),\quad(7.3)$$

*i.e.* the quantum transition probability is enhanced for $\mathbf{n}^{(f)}=\mathbf{n}^{(i)}$ compared to the classical one by a factor of two due to the constructive interference between time-reversed paths.

However, only paths which are not self-retracing may contribute to the coherent backscattering peak, because the time reverse of a self-retracing path is again the path itself and therefore this pairing would already be included in the diagonal approximation. For short times, one can expect that all trajectories coming back to the initial occupations are all self-retracing and therefore a certain minimal time is required to observe coherent backscattering (see supplementary material of [249]). This behavior as well as the existence of coherent backscattering itself is shown in Fig. 7.3.

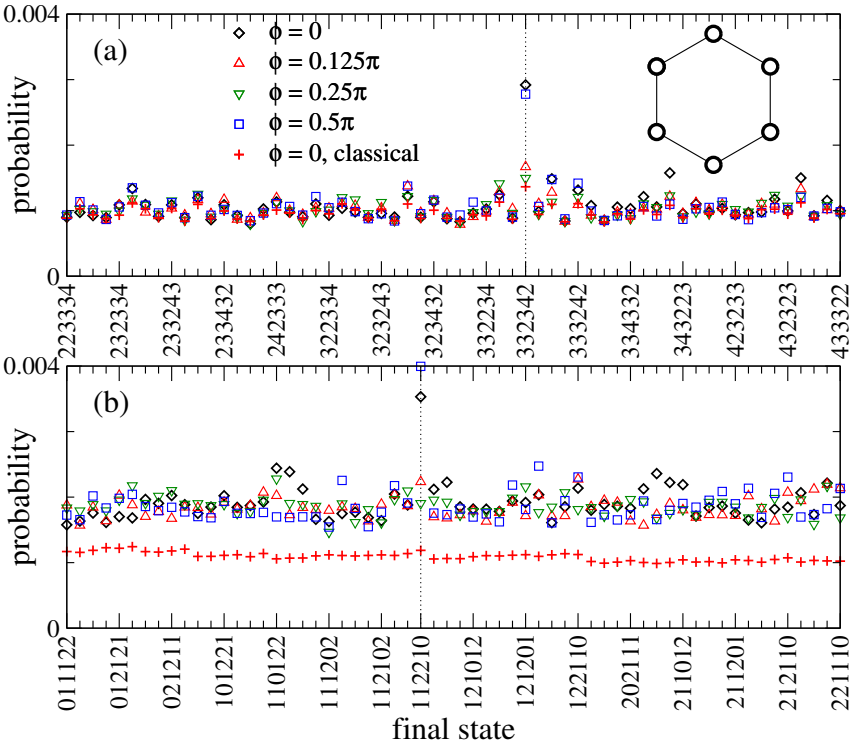


Figure 7.4: Dependence of the coherent backscattering peak on the phase $\phi$ of the hopping parameter $J$ for a Bose-Hubbard ring consisting of six sites (see inset of (a)). The initial occupations were chosen to be (a) $(3,3,2,3,4,2)$ and $(1,1,2,2,1,0)$. Figure by courtesy of Julien Dujardin, Arturo Argüelles and Peter Schlagheck.

Fig. 7.4 shows that the peak indeed vanishes, when time reversal invariance is broken, which clearly identifies the source of the peak to be coherent backscattering. The fact that for certain phases $\phi$ (apart from $2\pi$) of the hopping parameter the coherent backscattering peak reappears is due to the effective reestablishment of time reversal invariance (see [249]). Moreover, Fig. 7.4 shows that – although the semiclassical theory is strictly speaking valid for large occupations only, coherent backscattering can be observed already for very small particle number.

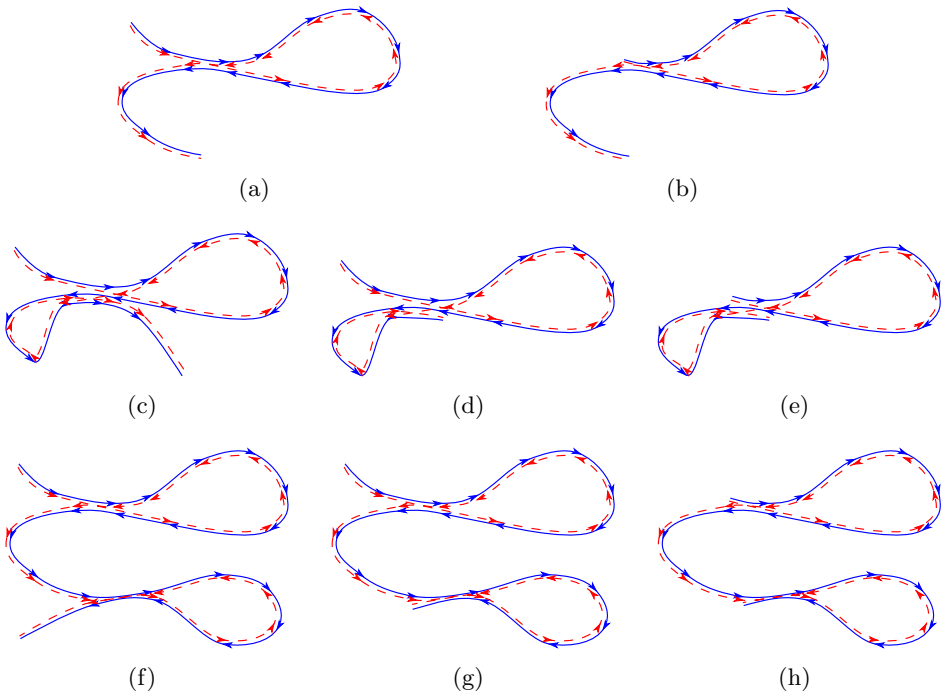


Figure 7.5: Loop diagrams arising in the calculation of the transition probability up to second order. For the one-leg-loops (Diagrams (b), (d), (g)) only one of the two possibilities to shift an end into the encounter is shown. Note that for the case of one 2-encounter, there is no no-leg-loop, since these are already included in the coherent backscattering.

### *7.1.3 Loop contributions*

The result above is expected to be just the leading order result of a semiclassical expansion in action differences. Typically, sub-leading contributions arise due to loop diagrams as those shown in Fig. 7.5, which essentially renormalize the background [21, 33–35, 37, 250, 251].

These loop diagrams consist of encounter regions, where the trajectories come close to themselves or their time-reverse, and so called links, which connect the encounter regions. Within these links, the two trajectories $\gamma$ and $\gamma'$ follow each other or the time-reverse of the other, while within the encounter region both trajectories connect *different* links. The action difference of the two trajectories then stems solely from the encounter region.

The loop diagrams can be divided into three classes, which are deter-

mined into three groups of loop contributions. The first of which are the two leg loops shown in Figs. 7.5(a), 7.5(c) and 7.5(f) for which both the starting and ending point of the trajectory lies *outside* the encounter regions. For one-leg-loop diagrams, such as Figs. 7.5(b), 7.5(d) and 7.5(g), either the starting or the ending point lies within an encounter region, while for no-leg-loops (see Figs. 7.5(e) and 7.5(h)) *both* the starting and ending point lies in the encounter region.

Two leg loops

According to Appendix F, the contribution from two leg loops, *i.e.* from those trajectories for which both the start and the end lie outside of the encounter regions, is given by

$$P^{(2\mathrm{ll})}\left(\mathbf{n}^{(f)},t_f;\mathbf{n}^{(i)},t_i\right)= \frac{1}{(2\pi)^{L-1}}\sum_{\gamma:\mathbf{n}^{(\mathbf{i})}\to\mathbf{n}^{(\mathbf{f})}}\left|\det{}'\frac{\partial^2 R_\gamma}{\partial\mathbf{n}^{(f)}\partial\mathbf{n}^{(i)}}\right|\sum_{\mathbf{v}}\mathcal{N}(\mathbf{v})\int_{-c}^{c}\mathrm{d}^{(L-2)(O-N_{enc})}s \int_{-c}^{c}\mathrm{d}^{(L-2)(O-N_{enc})}u\frac{\left[t_f-t_i-\sum_\alpha o_\alpha t_{enc}^{(\alpha)}(\mathbf{s},\mathbf{u})\right]^O}{O!\,\Omega_N^{O-N_{enc}}\prod_\alpha t_{enc}^{(\alpha)}}\exp\left(\mathrm{i}N\mathbf{s}\cdot\mathbf{u}\right), \tag{7.4}$$

where $\mathbf{v}$ is the vector which entries $v_o$ are the numbers of $o$-encounters and $\mathcal{N}(\mathbf{v})$ is the number of encounter structures with characteristic $\mathbf{v}$, *i.e.* with $v_o$ $o$-encounters. The total number of links between encounters for two leg loops, $O+1=\sum_o ov_o+1$, as well as the total number of encounters, $N_{enc}=\sum_o v_o$ are uniquely defined by this characteristic.

Moreover, the boundary $c$ of the integration over stable and unstable coordinates, $\mathbf{s}$ and $\mathbf{u}$, respectively, is an arbitrary classical bound large compared to $1/N$, but small enough to allow linearization of the partner trajectory $\gamma'$ around $\gamma$.

The reduced phase space volume $\Omega_N(E)$ for constant total number of particles $N$ and energy $E$ is defined as

$$\Omega_N(E)=\int\mathrm{d}^{2L}\psi\,\delta(\theta_1)\,\delta\left(N-\sum_{l=1}^{L}|\psi_l|^2+\frac{L}{2}\right)\delta\left[H(\boldsymbol{\psi}^*,\boldsymbol{\psi})-E\right].$$

In principle, in Eq. (7.4), the reduced phase space volume has to be evaluated at the energy of the trajectory $\gamma$. However, on disorder average,

the exact Dirac delta in the energy can be approximated by some broadened delta function with an averaged mean energy, such that the resulting reduced phase space volume can be assumed to be independent of the trajectory.

Finally, the encounter time $t_{enc}^{(\alpha)}$, which is the time the trajectory needs, in order to traverse the $\alpha$-th encounter once, is the sum of two contributions,

$$t_{enc}^{(\alpha)} = t_s^{(\alpha)} + t_u^{(\alpha)},$$

where $t_s$ and $t_u$ are given by

$$t_s^{(\alpha)} \sim \frac{1}{\lambda} \min \left( \ln \frac{c}{\left| \tilde{s}_k^{(\alpha,j)} \right|} \right),$$
$$t_u^{(\alpha)} \sim \frac{1}{\lambda} \min \left( \ln \frac{c}{\left| \tilde{u}_k^{(\alpha,j)} \right|} \right)$$

with $\lambda$ being the largest Lyapunov exponent. Just as in F, the minimum here and in the following runs for fixed $\alpha$ over both, the dimensional and sequential, indexes $k \in \{1, \ldots, L-2\}$ and $j \in \{2, \ldots, o_\alpha\}$.

It has been shown in [32], how to evaluate the integrals in Eq. (7.4) in general: Neglecting higher order as well as on average highly oscillatory terms, the only contributing term is found by using only the term in the expansion of the power in the numerator, which contains every $t_{enc}^{(\alpha)}$ exactly once.

Finally, after substituting

$$x_j = s_j u_j / c^2, \qquad \sigma_j = c/u_j$$

the integrals, which then run over the domains $-1 < x_j < 1$ and $1 < \sigma_j < 1/|x_j|$ yield after again identifying the sum over classical trajectories with the classical transition probability yields [32]

$$P^{(2\mathrm{ll})}\left(\mathbf{n}^{(f)}, t_f; \mathbf{n}^{(i)}, t_i\right) =$$
$$P^{(\mathrm{cl})} \sum_{\mathbf{v}} \mathcal{N}(\mathbf{v}) \frac{(t_f - t_i)^{O-N_{enc}}}{(O-N_{enc})\,!\,\Omega_N^{O-N_{enc}}} \left(\frac{2\pi}{N}\right)^{(L-2)(O-N_{enc})} \prod_{\alpha} (-o_\alpha)$$

One leg loop

The vanishing of one link, in this case does not require further links to vanish, such that also one leg loop contributions have to be taken into account [45, 252, 253]. Following F.2, the contributions of one leg loops can be calculated from

$$
\begin{aligned}
&P^{(1\mathrm{ll})}\left(\mathbf{n}^{(f)},t_f;\mathbf{n}^{(i)},t_i\right)= \\
&\quad\frac{1}{(2\pi)^{L-1}}\sum_{\gamma:\mathbf{n^{(i)}}\to\mathbf{n^{(f)}}}\left|\det{}'\frac{\partial^2 R_\gamma}{\partial\mathbf{n}^{(f)}\partial\mathbf{n}^{(i)}}\right|\sum_{\mathbf{v}}\sum_{o_1}v_{o_1}o_1\frac{\mathcal{N}(\mathbf{v})}{O} \\
&\quad\int_{-c}^{c}\mathrm{d}^{(L-2)(O-N_{enc})}s\int_{0}^{c}\mathrm{d}^{(L-2)(O-N_{enc})}u\int_{0}^{t_\gamma-\sum_\alpha o_\alpha t_{enc}^{(\alpha)}}\mathrm{d}t_O \\
&\qquad\int_{0}^{t_O}\mathrm{d}t_{O-1}\cdots\int_{0}^{t_3}\mathrm{d}t_2\int_{0}^{\min\frac{1}{\lambda}\ln\frac{c}{|\mathbf{s_j}|}}\mathrm{d}t'\frac{\exp\left(\mathrm{i}N\mathbf{s}\cdot\mathbf{u}\right)}{\Omega_N^{O-N_{enc}}\prod_\alpha t_{enc}^{(\alpha)}},
\end{aligned}
\tag{7.5}
$$

where now the encounter time is reduced and given by $t_{enc}^{(1)}=t'+t_u^{(1)}$. Note that, although strictly speaking Eq. (7.5) determines the contributions for those one leg loops, where the starting point lies inside an encounter, the contribution from trajectories with an ending point lying inside an encounter is exactly the same. Thus, when finally the higher order contributions to the transition probability are computed, $P^{(1ll)}$ has to be multiplied by a factor of two.

The integrations over the link times $t_2,\ldots,t_O$ as well as those over the stable and unstable coordinates of the $N_{enc}-1$ encounters, which do not contain the starting point, are exactly the same as above, such that

performing these integrals yields [253]:

$$P^{(1\mathrm{ll})}\left(\mathbf{n}^{(f)},t_f;\mathbf{n}^{(i)},t_i\right)=$$
$$2P^{(\mathrm{cl})}\sum_{\mathbf{v}}\sum_{o_1}v_{o_1}o_1\frac{\mathcal{N}(\mathbf{v})}{O}\left(\frac{2\pi}{N}\right)^{(L-2)(O-o_1-N_{enc}+1)}\int\limits_{-c}^{c}\mathrm{d}^{(L-2)(o_1-1)}s$$
$$\int\limits_{-c}^{c}\mathrm{d}^{(L-2)(o_1-1)}u\int\limits_{0}^{\min\frac{1}{\lambda}\ln\frac{c}{|\mathbf{s_j}|}}\mathrm{d}t'\frac{\left(t_f-t_i-o_1t_{enc}^{(1)}\right)^{O-N_{enc}}}{(O-N_{enc})\,!\,\Omega^{O-N_{enc}}t_{enc}^{(1)}}\cos\left(N\mathbf{s}\cdot\mathbf{u}\right)$$
$$\times\prod_{\alpha>1}(-o_\alpha). \tag{7.6}$$

Performing the integrals is somewhat simpler than in Refs. [45, 46, 252–254], since there are no additional exponentials containing the encounter time. In fact, the integrals in Eq. (7.6) are a special case of those in the mentioned work.

Redoing the steps in Ref. [253] – that is substituting $x_j=s_ju_j/c^2$, $\sigma_j=c/u_j$, $t_{enc}^{(1)}=t'+\ln\left(c/|u|\right)/\lambda$ with integration domains $-1<x_j<1$, $0<t_{enc}^{(1)}<\ln\min\left(1/|x_j|\right)/\lambda$, $1<\sigma_j<\exp\left(\lambda t_{enc}^{(1)}\right)$, replacing after integration over $\sigma$ $t_{enc}^{(1)}$ by $\frac{\partial}{\partial\alpha}\exp\left(\alpha t_{enc}^{(1)}\right)|_{\alpha=0}$ and neglecting terms oscillating under disorder average – determines the contribution of one leg loops with the starting point of the trajectory inside an encounter to read [253]

$$P^{(1\mathrm{ll})}\left(\mathbf{n}^{(f)},t_f;\mathbf{n}^{(i)},t_i\right)=$$
$$P^{(\mathrm{cl})}\sum_{\mathbf{v}}\sum_{o_1}v_{o_1}o_1\frac{\mathcal{N}(\mathbf{v})}{O}\left(\frac{2\pi}{N}\right)^{(L-2)(O-N_{enc})}\frac{\left(t_f-t_i\right)^{O-N_{enc}}\prod\limits_{\alpha>1}(-o_\alpha)}{(O-N_{enc})\,!\,\Omega^{O-N_{enc}}}.$$

Again, it should be stressed that the end point lying inside an encounter yields exactly the same contribution, and therefore this contribution has to be multiplied by a factor of two, when calculating the full transition probability.

It is easy to verify that when restricting oneself to the leading order loop contributions,*i.e.* to the case of only one 2-encounter, two-leg-loops and one-leg-loops cancel exactly. For higher order contributions, there is yet another possibility, which has to be taken into account, namely, the case that both, the ending and the starting point lie inside *different* encounters.

No leg loop

The calculation of these contributions, however is completely analogously to the one of one leg loops, only with the fact that now also $t_O$ has to be replaced by an integral over $t''$, which is the duration, the trajectory needs to get from the reduced Poincaré section of surface to the end point.

Redoing essentially the same steps as in the one leg loop case yields[253]

$$P^{(0\mathrm{ll})}\left(\mathbf{n}^{(f)},t_f;\mathbf{n}^{(i)},t_i\right)=P^{(\mathrm{cl})}\sum_{\mathbf{v}}\sum_{o_1,o_{N_{enc}}}\mathcal{N}_{o_1,o_{N_{enc}}}(\mathbf{v})\left(\frac{2\pi}{N}\right)^{(L-2)(O-N_{enc})} \times\frac{(t_f-t_i)^{O-N_{enc}}\prod_{\alpha=2}^{N_{enc}-1}(-o_\alpha)}{(O-N_{enc})!\,\Omega^{O-N_{enc}}},$$

where $\mathcal{N}_{o_1,o_{N_{enc}}}(\mathbf{v})$ is the number of structures with characteristic $\mathbf{v}$ starting with an $o_1$-encounter and ending with an $o_{N_{enc}}$-encounter.

Overall loop contribution

Summing up all these contributions yields

$$\begin{aligned}P^{(2\mathrm{ll})}+P^{(1\mathrm{ll})}+P^{(0\mathrm{ll})}=&\\ P^{(\mathrm{cl})}\sum_{\mathbf{v}}\left(\frac{2\pi}{N}\right)^{(L-2)(O-N_{enc})}&\frac{(t_f-t_i)^{O-N_{enc}}\prod_{\alpha}(-o_\alpha)}{(O-N_{enc})!\,\Omega^{O-N_{enc}}}\\ \times\left[\mathcal{N}(\mathbf{v})-2\frac{N_{enc}}{O}\mathcal{N}(\mathbf{v})+\sum_{o_1,o_{N_{enc}}}\right.&\left.\frac{\mathcal{N}_{o_1,o_{N_{enc}}}(\mathbf{v})}{o_1 o_{N_{enc}}}\right],\end{aligned}\tag{7.7}$$

where the factor $N_{enc}$ in the second term stems from the sum $\sum_{o_1} v_{o_1}$. It has been shown in [254] that this sum is identically zero. Yet, for the sake of completeness, this cancellation is demonstrated explicitely here.

The main task is to express the very last term in such a way that it also depends on $\mathcal{N}(\mathbf{v})$. Usually, a trajectory with certain encounter structure is obtained by considering it as arising from a periodic orbit by cutting one link. In this case, the link, which is cut has to connect an $o_{N_{enc}}$- to an $o_1$-encounter. On the other hand, a trajectory, which has its starting and ending point inside different encounters, can be considered to be generated by cutting a periodic orbit inside an $(o_1+o_{N_{enc}}-1)$-encounter. The latter periodic orbit, in turn, can be obtained by merging the $o_1$- and the $o_{N_{enc}}$-encounter of the original one. This way, the characteristic

$\mathbf{v}^{[o_1,o_{N_{enc}}\to o_1+o_{N_{enc}}-1]}$ of the new periodic orbit is determined from the original one by reducing $v_{o_1}$ and $v_{o_{N_{enc}}}$ by one, while increasing $v_{o_1+o_{N_{enc}}-1}$ by one. Furthermore, obviously the total number of links for the new periodic orbit is reduced by one compared to the original one.

Then, for the new periodic orbit, there are in total

$$(o_1 + o_{N-enc} - 1)(v_{o_1+o_{N_{enc}}-1} + 1)$$

encounter stretches, which can be cut in order to obtain again one of the considered trajectories. However, for computing the number of encounter structures with the same characteristic $\mathcal{N}(\mathbf{v})$, there is an additional factor given by the total number of links due to the freedom to choose the link that should be cut. This freedom is absent here, such that this procedure yields the equality [254]

$$\mathcal{N}_{o_1,o_{N_{enc}}}(\mathbf{v}) = \frac{(o_1 + o_{N_{enc}} - 1)\left(v_{o_1+o_{N_{enc}}-1} + 1\right)}{O-1}\mathcal{N}\left(\mathbf{v}^{[o_1,o_{N_{enc}}\to o_1+o_{N_{enc}}-1]}\right),$$

where the term $1/(O-1)$ cancels out the $O-1$ possibilities to cut a link of a periodic orbit with characteristic $\mathbf{v}^{[o_1,o_{N_{enc}}\to o_1+o_{N_{enc}}-1]}$.

Plugging in this result into Eq. (7.7) and writing it explicitly as a power series in $1/N$ yields

$$\begin{aligned}
&P^{(2\mathrm{ll})} + P^{(1\mathrm{ll})} + P^{(0\mathrm{ll})} = \\
&P^{(\mathrm{cl})} \sum_{m=1}^{\infty} \left(\frac{2\pi}{N}\right)^{(L-2)m} \frac{(t_f - t_i)^m}{m!\,\Omega^m} \sum_{\mathbf{v}:O-N_{enc}=m} \prod_{\alpha} (-o_\alpha) \\
&\times \left[ \sum_{o_1,o_{N_{enc}}} \frac{(o_1 + o_{N_{enc}} - 1)\left(v_{o_1+o_{N_{enc}}-1} + 1\right)}{(O-1)\,o_1 o_{N_{enc}}} \mathcal{N}\left(\mathbf{v}^{[o_1,o_{N_{enc}}\to o_1+o_{N_{enc}}-1]}\right) \right. \\
&\qquad \left. + \mathcal{N}(\mathbf{v}) - 2\frac{N_{enc}}{O}\mathcal{N}(\mathbf{v}) \right],
\end{aligned}$$

where the sum over characteristics runs over those with $O - N_{enc} = m$.

Now, since $\mathbf{v}^{[o_1,o_{N_{enc}}\to o_1+o_{N_{enc}}-1]}$ also satisfies $O - N_{enc} = m$, for the last term, the sum over $\mathbf{v}$ can easily be transformed into a sum over

$$\mathbf{v}' = \mathbf{v}^{[o_1,o_{N_{enc}}\to o_1+o_{N_{enc}}-1]}.$$

Then the factor $(o_1 + o_{N_{enc}} - 1)/(o_1 o_{N_{enc}})$ replaces the factor $o_1 o_{N_{enc}}$ in the product by $o' = o_1 + o_{N_{enc}} - 1$. Moreover, the sums over $o_1$ and

$o_{N_{enc}}$ affect only the term $v_{o_1+o_{N_enc}-1}+1=v'_{o_1+o_{N_enc}-1}$ and – as already mentioned – the total number of links is for $\mathbf{v}^{[o_1,o_{N_{enc}}\to o_1+o_{N_{enc}}-1]}$ reduced by one, such that

$$P^{(2ll)}+P^{(1ll)}+P^{(0ll)}= P^{(cl)}\sum_{m=1}^{\infty}\left(\frac{2\pi}{N}\right)^{(L-2)m}\frac{(t_f-t_i)^m}{m!\,\Omega^m}\sum_{\mathbf{v}:O-N_{enc}=m}\prod_{\alpha}(-o_\alpha) \times\left[\mathcal{N}(\mathbf{v})-2\frac{N_{enc}}{O}\mathcal{N}(\mathbf{v})-\frac{\mathcal{N}(\mathbf{v})}{O}\sum_{o,o'}v_{o+o'-1}\right].$$

The double sum in the last term can also be easily evaluated by substituting the sum over $o'$ by one over $j=o+o'-1$,

$$\sum_{o,o'}v_{o+o'-1}=\sum_{o\geq 2}\sum_{j>o}v_j=\sum_{j\geq 3}\sum_{o=2}^{j-1}v_j=\sum_{j\geq 3}v_j\,(j-2)$$

$$=\sum_{j\geq 2}v_j\,(j-2)=O-2N_{enc}.$$

This finally shows, as that the loop contributions for the transition probability indeed cancel,

$$P^{(2ll)}+P^{(1ll)}+P^{(0ll)}=0.$$

## 7.2 Weak Coupling Regime

The unperturbed quantum Hamiltonian here is given by the Bose-Hubbard Model with zero hopping amplitude, which describes a Mott-insulator [118, 119],

$$\hat{H}_0=\sum_{l=1}^{L}\left(\epsilon_l\hat{a}_l^\dagger\hat{a}_l+\frac{1}{2}\sum_{l'=1}^{L}V_{ll'}\hat{a}_l^\dagger\hat{a}_{l'}^\dagger\hat{a}_{l'}\hat{a}_l\right). \tag{7.8}$$

Obviously, any Fock state $|\mathbf{n}^{(i)}\rangle$ is an eigenstate of this Hamiltonian with eigenenergy

$$E_{\mathbf{n}^{(i)}}=\sum_{l=1}^{L}\left[\left(\epsilon_l-\frac{1}{2}V_{ll}\right)n_l^{(i)}+\frac{1}{2}\sum_{l'=1}^{L}V_{ll'}n_l^{(i)}n_{l'}^{(i)}\right],$$

such that the time evolution of an initial Fock state is given by

$$|\psi(t)\rangle \equiv \hat{K}(t)\,|\mathbf{n}^{(i)}\rangle = \exp\left(-\frac{\mathrm{i}}{\hbar}E_{\mathbf{n}^{(i)}}t\right)|\mathbf{n}^{(i)}\rangle\,.$$

The purpose of this section is, however, to describe the evolution of an initial Fock state under a Hamiltonian, determined by perturbing the Hamiltonian Eq. (7.8) by small hopping terms,

$$\hat{J} = -\sum_{\substack{l,l'=1\\ l\neq l'}}^{L} J_{l,l'}\hat{a}_l^\dagger\hat{a}_{l'} \tag{7.9}$$

with $J_{ll'} = J^*_{l'l}$.

This could in principle be done by treating the hopping term in semiclassical perturbation theory. However, as already discussed in section 2.3, within this framework, the perturbation does not alter the classical trajectories. Therefore, one can not start from the propagator in Fock state, since the unperturbed trajectories are diagonal in Fock space, *i.e.* they join the initial Fock state $\mathbf{n}^{(i)}$ only to the same final one $\mathbf{n}^{(f)} = \mathbf{n}^{(i)}$. On the other hand, as soon as hopping is introduced, the propagator is non-zero also for $\mathbf{n}^{(f)} \neq \mathbf{n}^{(i)}$. Therefore, it is necessary to start with the propagator in quadrature representation, apply the semiclassical perturbation theory, and only then perform the basis transformation to Fock states. This lifts the problem of the diagonality in Fock space, since the quadrature eigenstates are a superposition of Fock states.

### *7.2.1 The propagator in quadrature representation for diagonal Hamiltonians*

It turns out that the propagator in quadrature representation for the unperturbed Hamiltonian can be computed exactly by a stationary phase approximation if Hubbard-Stratonovich transformation (see Appendix G) is applied to the path integral. The Hubbard-Stratonovich transformation replaces the interactions by an additional time dependent field $\boldsymbol{\sigma}(t)$, which mimics the potential acting on one particle by the interaction with all the others. The propagator is thus after the Hubbard-Stratonovich transfor-

mation given by the path integral

$$K\left(\mathbf{q}^{(f)},\mathbf{q}^{(i)};t_f\right)=\frac{\int\mathcal{D}\left[\boldsymbol{\sigma}(t)\right]\mathrm{e}^{\frac{\mathrm{i}}{2\hbar}\int_0^{t_f}\mathrm{d}t\boldsymbol{\sigma}(t)V^{-1}\boldsymbol{\sigma}(t)}K_{\boldsymbol{\sigma}}\left(\mathbf{q}^{(f)},\mathbf{q}^{(i)};t_f\right)}{\int\mathcal{D}\left[\boldsymbol{\sigma}(t)\right]\mathrm{e}^{\frac{\mathrm{i}}{2\hbar}\int_0^{t_f}\mathrm{d}t\boldsymbol{\sigma}(t)V^{-1}\boldsymbol{\sigma}(t)}},\quad(7.10)$$

where $V$ is the matrix with elements $V_{ll'}$, the denominator ensures the correct normalization of the $\boldsymbol{\sigma}$-path integral and

$$K_{\boldsymbol{\sigma}}\left(\mathbf{q}^{(f)},\mathbf{q}^{(i)};t_f\right)=$$
$$\int_{\mathbf{q}(0)=\mathbf{q}^{(i)}}^{\mathbf{q}(t_f)=\mathbf{q}^{(f)}}\mathcal{D}\left[\mathbf{q}(t),\mathbf{p}(t)\right]\exp\left\{\frac{\mathrm{i}}{\hbar}\int_0^{t_f}\mathrm{d}t\left[\frac{\hbar}{2b}\mathbf{p}(t)\cdot\dot{\mathbf{q}}(t)-H_{\boldsymbol{\sigma}}\left(\boldsymbol{\psi}^*(t),\boldsymbol{\psi}(t);t\right)\right]\right\}$$

is the effective propagator under the external potential described by the field $\boldsymbol{\sigma}(t)$. Note that in Eq. (7.10) there are no boundary conditions imposed on $\boldsymbol{\sigma}(t)$. Again, $\boldsymbol{\psi}(t)=\mathbf{q}(t)+\mathrm{i}\mathbf{p}(t)$. Moreover, the effective Hamiltonian is given by

$$H_{\boldsymbol{\sigma}}\left(\boldsymbol{\psi}^*(t),\boldsymbol{\psi}(t);t\right)=\sum_{l=1}^{L}\left[\epsilon_l-\sigma_l(t)\right]\left(|\psi_l|^2-\frac{1}{2}\right).\quad(7.11)$$

Using the semiclassical approximation Eq. (4.10) for the effective propagator yields

$$K_{\boldsymbol{\sigma}}\left(\mathbf{q}^{(f)},\mathbf{q}^{(i)};t_f\right)=$$
$$\sqrt{\det\frac{1}{(-2\pi\mathrm{i}\hbar)}\frac{\partial^2R_\gamma\left(\mathbf{q}^{(f)},\mathbf{q}^{(i)};t_f\right)}{\partial\mathbf{q}^{(f)}\partial\mathbf{q}^{(i)}}}\exp\left[\frac{\mathrm{i}}{\hbar}R_\gamma\left(\mathbf{q}^{(f)},\mathbf{q}^{(i)};t_f\right)\right],\quad(7.12)$$

where the sum over classical trajectories has already been omitted in view of the fact that for the classical Hamiltonian Eq. (7.11), there is only one trajectory joining the initial and final quadratures. This very trajectory is denoted by $\gamma$ and is determined by the solution of the classical equations of motion

$$\mathrm{i}\hbar\frac{\partial\psi_l(t)}{\partial t}=\left[\epsilon_l-\sigma_l(t)\right]\psi_l(t)\quad(7.13)$$

under the boundary conditions

$$\Re\boldsymbol{\psi}(0)=\frac{1}{2b}\mathbf{q}^{(i)}\qquad\text{and}\qquad\frac{1}{2b}\Re\boldsymbol{\psi}(t_f)=\mathbf{q}^{(f)}.\quad(7.14)$$

It is easy to find the thus defined trajectory $\gamma$ and computing its action which is after a straight forward calculation (see Appendix D for details) given by

$$R_\gamma\left(\mathbf{q}^{(f)},\mathbf{q}^{(i)};t_f\right)= \frac{\hbar}{4b^2\sin A_l}\sum_{l=1}^{L}\left[-2q_l^{(f)}q_l^{(i)}+\left(q_l^{(i)^2}+q_l^{(f)^2}\right)\cos A_l\right]+\frac{\hbar}{2}\sum_{l=1}^{L}A_l \tag{7.15}$$

with

$$A_l=\frac{1}{\hbar}\int_{t_i}^{t_f}\mathrm{d}t\left[\epsilon_l-\sigma_l(t)\right].$$

Having determined the classical action, the propagator can be easily determined to be

$$K_{\boldsymbol{\sigma}}\left(\mathbf{q}^{(f)},\mathbf{q}^{(i)};t_f\right)= \prod_{l=1}^{L}\sqrt{\frac{1}{4b^2\mathrm{i}\pi\sin A_l}}\exp\left\{-\mathrm{i}\frac{2q_l^{(f)}q_l^{(i)}-\left(q_l^{(i)^2}+q_l^{(f)^2}\right)\cos A_l}{4b^2\sin A_l}+\frac{\mathrm{i}}{2}A_l\right\} \tag{7.16}$$

The hopping term Eq. (7.9) can now be included in semiclassical perturbation theory following section 2.3, *i.e.* a phase given by the classical analogue of the hopping integrated along the trajectory is added to the propagator. The classical analogue of an operator here is obtained by first expressing the creation and annihilation operators $\hat{a}_l^\dagger$ and $\hat{a}_l$ by quadrature operators $\hat{q}_l$ and $\hat{p}_l$, commuting all the $\hat{p}_l$'s to the left of all $\hat{q}_l$'s and then replacing the operators by real variables. For the operator Eq. (7.9), this prescription yields as classical analogue

$$J\left(\mathbf{p}(t),\mathbf{q}(t)\right)=-\frac{1}{4b^2}\sum_{\substack{l,l'=1\\ l\neq l'}}^{L}J_{ll'}\left(q_l(t)-\mathrm{i}p_l(t)\right)\left(q_{l'}(t)+\mathrm{i}p_{l'}(t)\right)$$

With this classical hopping, the effective propagator can be apprximated in semiclassical perturbation theory by

$$K_{\boldsymbol{\sigma}}\left(\mathbf{q}^{(f)},\mathbf{q}^{(i)};t_f\right) = \prod_{l=1}^{L}\sqrt{\frac{1}{4b^2\mathrm{i}\pi\sin A_l}}\exp\left\{-\mathrm{i}\frac{2q_l^{(f)}q_l^{(i)}-\left(q_l^{(i)^2}+q_l^{(f)^2}\right)\cos A_l}{4b^2\sin A_l}+\frac{\mathrm{i}}{2}A_l\right\} \times\exp\left[-\frac{\mathrm{i}}{\hbar}\int_{t_i}^{t_f}\mathrm{d}t J\left(\mathbf{p}(t),\mathbf{q}(t)\right)\right], \tag{7.17}$$

where $\mathbf{q}(t)$ and $\mathbf{p}(t)$ have to be evualuated along the trajectory.

The exponential of the effective propagator Eq. (7.17) is still a quadratic function of $\mathbf{q}^{(i)}$ and $\mathbf{q}^{(f)}$, which allows to perform the integrations for the basis transform to Fock states exactly. It should be noted that the basis transform does not affect the integration over the Hubbard-Stratonovich field $\boldsymbol{\sigma}(t)$, such that it is enough to transform the effective propagator. However, it turns out that the integrals are easiest, when first transforming to coherent states.

The basis transformation is rather cumbersome, which is why it is left for the Appendix D.2. The resulting effective propagator in Fock states turns out to be

$$K_{\boldsymbol{\sigma}}\left(\mathbf{n}^{(f)},\mathbf{n}^{(i)};t_f\right) = \sum_{\boldsymbol{\kappa}^{(1)}:\sum_{l=1}^{L}\kappa_l^{(1)}=n_1^{(f)}}\cdots\sum_{\boldsymbol{\kappa}^{(L)}:\sum_{l=1}^{L}\kappa_l^{(L)}=n_L^{(f)}}\delta_{\sum_{l'=1}^{L}\kappa_l^{(l')},n_l^{(i)}} \times\prod_{l=1}^{L}\binom{n_l^{(f)}}{\boldsymbol{\kappa}^{(l)}}\sqrt{\frac{n_l^{(i)}!}{n_l^{(f)}!}}\exp\left(-\mathrm{i}n_l^{(f)}A_l\right)\prod_{\substack{l'=1\\l'\neq l}}^{L}\left(-\frac{\mathrm{i}}{\hbar}J_{ll'}^{(\mathrm{eff})}\right)^{\kappa_{l'}^{(l)}}, \tag{7.18}$$

where

$$J_{l\neq l'}^{(\mathrm{eff})} = -J_{ll'}\int_{t_i}^{t_f}\mathrm{d}t\exp\left\{\frac{\mathrm{i}}{\hbar}\int_{t_i}^{t}\mathrm{d}t'\left[\epsilon_l-\epsilon_{l'}-\sigma_l(t')+\sigma_{l'}(t')\right]\right\}$$

is the effective hopping.

The interpretaion of Eq. (7.18) is quite simple. The sum over the vectors $\boldsymbol{\kappa}^{(1)}, \dots \boldsymbol{\kappa}^{(L)}$ runs over all possible combinations of hopping events, where $\kappa_l^{(l')}$ is for $l \neq l'$ the number of hopping events from $l$ to $l'$, while $\kappa_l^{(l)}$ is the number of particles, which stay at the same site during the whole time evolution. Note that these combinations also include those processes, where one particle hops from $l$ to $l''$ and another one from $l''$ to $l'$. The multinomial coefficient $\binom{n_l^{(f)}}{\boldsymbol{\kappa}^{(l)}}$ together with the square root containing the factorials of the initial and final occupations thereby account for the indistinguishability. Furthermore, each hopping event is weighted by its hopping probability $J_{ll'}^{(\mathrm{eff})}$ and the phase factor yields just the phase evolution due to the non-perturbed (Mott isolating) Hamiltonian. Finally, the Kronecker delta ensures that only those combinations of hopping events are taken into account, which connect the initial and final occupations correctly.

Inserting this expression for the effective propagator, Eq. (7.18), into Eq. (7.10) enables one to evaluate the integration over the auxiliary field $\boldsymbol{\sigma}(t)$ in stationary phase approximation. Since the exponent is quadratic in the auxiliary field, the stationary phase approximation is exact. In order to perform the integration, it is helpful to rewrite

$$\begin{aligned}
&\sum_{l\neq l'} \sum_{j=1}^{\kappa_{l'}^{(l)}} \int_0^{t_{ll'}^{(j)}} \mathrm{d}t \left(\sigma_l(t) - \sigma_{l'}(t)\right) \\
&\qquad = \int_0^{t_f} \mathrm{d}t \sum_{l=1}^{L} \sigma_l(t) \sum_{l'\neq l} \left[ \sum_{j=1}^{\kappa_{l'}^{(l)}} \theta\left(t_{ll'}^{(j)} - t\right) - \sum_{j=1}^{\kappa_l^{(l')}} \theta\left(t_{l'l}^{(j)} - t\right) \right] \\
&\qquad \equiv \int_0^{t_f} \mathrm{d}t \sum_{l=1}^{L} \sigma_l(t) \Theta_l(t).
\end{aligned}$$

Then, the stationary phase condition reads

$$\sum_{l'=1}^{L} V_{ll'}^{-1} \sigma_{l'}(t) + n_l^{(f)} - \Theta_l(t) = 0.$$

The integration over the oscillations around the stationary point is straight forward and just cancels the prefactor stemming from the Hubbard-Stratonovich transformation. Evaluating the exponent at the stationary point

finally yields after some simple transformations

$$
\begin{aligned}
K\left(\mathbf{n}^{(f)},\mathbf{n}^{(i)};t_f\right) = & \\
& \sum_{\boldsymbol{\kappa}^{(1)}:\sum_{l=1}^{L}\kappa_l^{(1)}=n_1^{(f)}} \cdots \sum_{\boldsymbol{\kappa}^{(L)}:\sum_{l=1}^{L}\kappa_l^{(L)}=n_L^{(f)}} \int_0^{t_f} \left( \prod_{l\neq l'} \prod_{j=1}^{\kappa_{l'}^{(l)}} \mathrm{d}t_{ll'}^{(j)} \right) \prod_{l=1}^{L} \delta_{\sum_{l'=1}^{L}\kappa_{l'}^{(l)},n_l^{(i)}} \\
& \times \binom{n_l^{(f)}}{\boldsymbol{\kappa}^{(l)}} \sqrt{\frac{n_l^{(i)}!}{n_l^{(f)}!}} \exp\left[ -\frac{\mathrm{i}}{\hbar} \left( \epsilon_l n_l^{(f)} + \frac{1}{2}\mathbf{n}^{(f)} V \mathbf{n}^{(f)} \right) t_f \right] \prod_{\substack{l'=1 \\ l'\neq l}}^{L} \left( -\frac{\mathrm{i}}{\hbar} J_{ll'} \right)^{\kappa_{l'}^{(l)}} \\
& \times \exp\left[ -\frac{\mathrm{i}}{2\hbar} \sum_{l''\neq l,l'''\neq l'}^{L} \left( V_{ll'} - V_{ll'''} - V_{l''l'} + V_{l''l'''} \right) \sum_{j=1}^{\kappa_{l''}^{(l)}} \sum_{j'=1}^{\kappa_{l'''}^{(l')}} \min\left( t_{ll''}^{(j)}, t_{l'l'''}^{(j')} \right) \right] \\
& \times \exp\left\{ -\frac{\mathrm{i}}{\hbar} \left[ \sum_{j=1}^{\kappa_{l'}^{(l)}} \left( \epsilon_l - \epsilon_{l'} \right) t_{ll'}^{(j)} - \sum_{l''\neq l'} \left( V_{ll'} - V_{ll''} \right) n_l^{(f)} \sum_{j=1}^{\kappa_{l''}^{(l')}} t_{l'l''}^{(j)} \right] \right\}
\end{aligned}
\tag{7.19}
$$

where $J_{ll}$ has been defined as $J_{ll} = \mathrm{i}\hbar$.

It is important to note that the constraints on the sums and the Kronecker deltas in Eq. (7.19) imply that the propagator is non-zero only if

$$N^{(i)} = \sum_{\alpha=1}^{l} n_\alpha^{(i)} = \sum_{\alpha=1}^{l} n_\alpha^{(f)} = N^{(f)}.$$

This can easily be seen by considering the sum over all $\kappa_l^{(l')}$. For each contribution, the constraints on the sums require that

$$N^{(f)} = \sum_{l=1}^{L}\sum_{l'=1}^{L} \kappa_{l'}^{(l)} = \sum_{l=1}^{L}\sum_{l'=1}^{L} \kappa_l^{(l')}. \tag{7.20}$$

On the other hand, due to the Kronecker deltas, the contribution of the sums is non-zero, only if the $l'$-sum on the right hand side of Eq. (7.20) is equal to $n_\alpha^{(i)}$ and therefore

$$N^{(f)} = \sum_{l=1}^{L} n_l^{(i)} = N^{(i)}.$$

Moreover, the result for the propagator Eq. (7.19) can be interpreted fairly easily. $\kappa_l^{(l')}$ denotes the number of hopping events from site $l$ to site $l'$ and one has to sum over all possible combinations of hopping events, which leave on one hand the number of particles within each site larger or equal to zero and on the other hand lead to the correct final state. The first condition is ensured by the Kronecker deltas, while the second one fulfilled due to the constrictions on the sums. Each hopping event contributes an additional factor of $-\mathrm{i}J_{ll'}^{(\mathrm{eff})}/\hbar$ and is weighted by the combinatorial factors accounting for the interchangeability of particles. The additional phase factor then accounts for the free propagation between two hopping events.

Finally, it is instructive to consider the case without hopping, $J_{ll'} = 0$. Then obviously the only non-vanishing contribution to the sums is

$$\kappa_l^{(l')} = \begin{cases} 0, & l \neq l' \\ n_l^{(f)}, & l = l' \end{cases}$$

However the Kronecker deltas then require that

$$n_l^{(i)} = \sum_{l'=1}^{L} \kappa_l^{(l')} = \kappa_l^{(l)} = n_l^{(f)}$$

and therefore in the diagonal case, *i.e.* if $J_{ll'} = 0$ the propagator reads

$$K\left(\mathbf{n}^{(f)}, \mathbf{n}^{(i)}; t_f\right) = \left(\prod_{l=1}^{L} \delta_{n_l^{(i)}, n_l^{(f)}}\right) \mathrm{e}^{-\frac{\mathrm{i}\left(t_f - t_i\right)}{\hbar} \sum\limits_{l=1}^{L} \left(\epsilon_l + \frac{1}{2} \sum\limits_{l'=1}^{L} V_{ll'} n_{l'}^{(i)}\right) n_l^{(i)}}, \tag{7.21}$$

which is equal to the exact quantum mechanical propagator for this case.

Finally, it is worth to notice that in the case that all particles interact equally no matter in which site they are, *i.e.* for $V_{ll'} = V$, the interaction enters only via a phase factor $\exp\left(-\mathrm{i}\mathbf{n}^{(f)} V \mathbf{n}^{(f)} t_f/\hbar\right)$ and thus do not affect the motion of the particles.

### *7.2.2 Transition probability for weak hopping*

From the propagator, Eq. (7.19), the transition probability from an intial to a final Fock state can be computed by simply taking its modulus square. For the case of a non-disordered ring of five magnetooptical traps with all on-site interactions 0, on-site interaction strength $V_{ll'} = 2\delta_{ll'}$ and

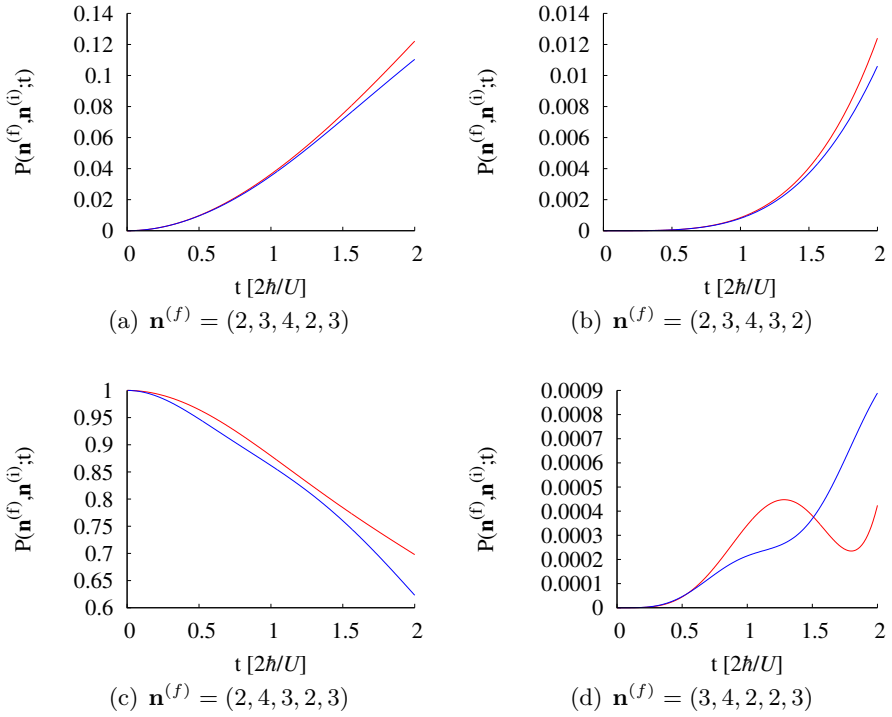


(a) $\mathbf{n}^{(f)} = (2,3,4,2,3)$ (b) $\mathbf{n}^{(f)} = (2,3,4,3,2)$

(c) $\mathbf{n}^{(f)} = (2,4,3,2,3)$ (d) $\mathbf{n}^{(f)} = (3,4,2,2,3)$

Figure 7.6: Comparison between the semiclassical weak coupling result for the transition probability up to fourth order in the hopping strength $J = 0.05$ (red) and the numerically obtained quantum mechanical one (blue) for zero on-site energies and on-site interactions $V = 2$.

a nearest-neighbor hopping strength $J = 0.05$, the result obtained from Eq. (7.19) as a function of time is compared with numerical ones in Fig. 7.6 for an initial state $\mathbf{n}^{(i)} = (2,4,3,2,3)$ and selected final ones. Note that in the semiclassical calculations only terms up to fourth order in the hopping strength are considered, *i.e.* the sums over the hopping events $\kappa_{l'}^{(l)}$ are restricted to those, which satisfy $\sum_{l \neq l'} \kappa_{l'}^{(l)} \leq 4$. It is obvious to see that this approximation holds differently good agreement for different final states. The best agreement seems to be for states which differ from the inital one by just one hopping event.

Finally, in Fig. 7.7 the transition probability obtained from the weak coupling limit, Eq. (7.19), is compared with the numerically obtained exact one for $J = 0.5$ and all other parameters being the same as above, *i.e.* in a regime, where a priori the weak coupling limit can not be assumed to hold.

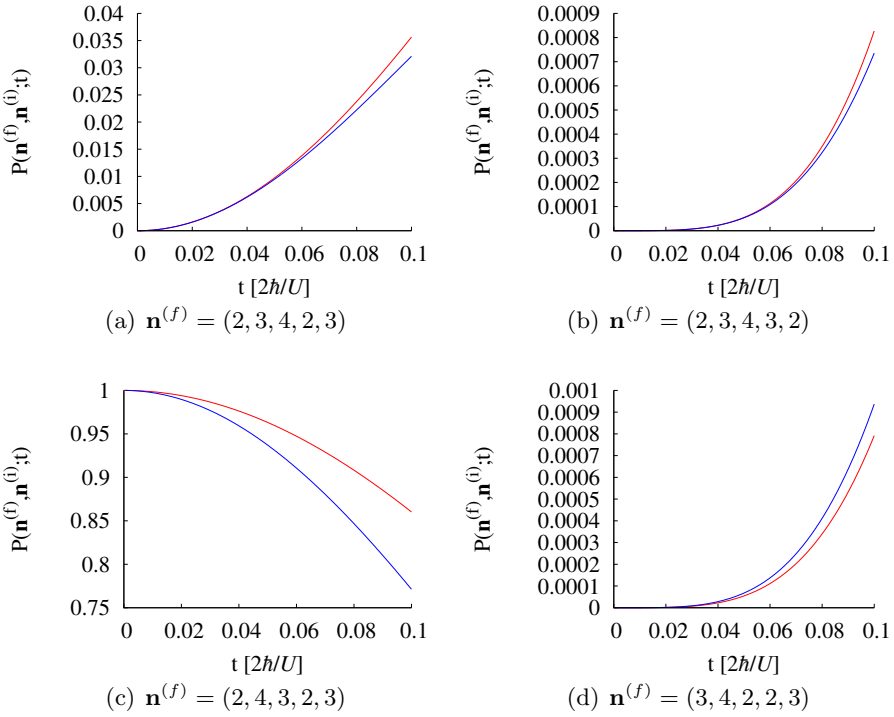


(a) $\mathbf{n}^{(f)} = (2, 3, 4, 2, 3)$ (b) $\mathbf{n}^{(f)} = (2, 3, 4, 3, 2)$

(c) $\mathbf{n}^{(f)} = (2, 4, 3, 2, 3)$ (d) $\mathbf{n}^{(f)} = (3, 4, 2, 2, 3)$

Figure 7.7: Comparison between the semiclassical weak coupling result for the transition probability up to fourth order in the hopping strength $J = 0.5$ (red) and the numerically obtained quantum mechanical one (blue) for zero on-site energies and on-site interactions $V = 2$.

However, for small enough propagation times, one still gets reasonable good agreement, although the approximation is much worse for $\mathbf{n}^{(f)} = \mathbf{n}^{(i)}$ than for all other final states. This suggests that the weak coupling limit at the same time also provides the small time limit.

CHAPTER 8

# Many-Body Transport

## 8.1 Formulation of many-body transport

In condensed matter physics there is another effect, called weak localization [19], which has the same origin as coherent backscattering [232]. Weak localization is the enhancement of the resistance an open cavity offers to article current due to constructive interference of time-reversed paths.

As it has been shown in Chapter 7 coherent backscattering is present in ultra-cold atom systems, too. The question naturally arises, whether weak localization can also be observed. In order to answer this question, in this chapter a typical transport setup, such as the one depicted in Fig. 8.1 will be considered, where interactions are turned off within the semi-infinite

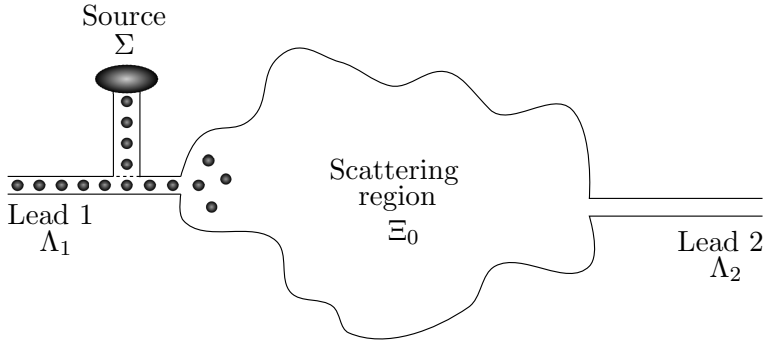


Figure 8.1: Schematic picture of the transport system with two leads.

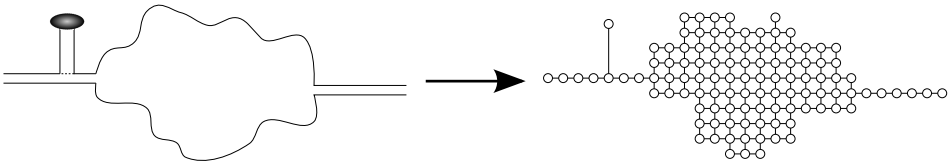

Figure 8.2: Discretization of the system for semiclassical and numerical treatment

leads $\Lambda = \{\Lambda_1, \Lambda_2, \ldots\}$. The source $\Sigma$, in which all the particles are located initially, and from which the particles are coupled either to a lead or to the scattering region $\Xi_0$, can for instance be realized by using an atom laser [255–261]. Finally, the interactions are assumed to be turned on within the scattering region $\Xi_0$, such that its classical limit, Eq. (4.7), is chaotic.

The semiclassical propagators derived in Chapter 4 require a discrete basis set of single-particle states. To this end, it is convenient to consider a discretization of the system as the one shown in Fig. 8.2, such that each site is described by one single-particle state. This discretization corresponds to an infinite network of magneto-optical traps coupled to each other with nearest neighbor hopping amplitudes $\hbar^2/(2m\Delta^2)$ [262], where $m$ is the mass of the atoms and $\Delta$ the lattice spacing, which eventually should be sent to zero.

After this discretization, the second quantized Hamiltonian can be written as

$$\hat{H} = \hat{H}^{(\Xi)} + \hat{H}^{(\Lambda)} + \hat{\mathbf{a}}_\Lambda^\dagger C \hat{\mathbf{a}}_\Xi + \hat{\mathbf{a}}_\Xi^\dagger C^\dagger \hat{\mathbf{a}}_\Lambda, \tag{8.1}$$

where $\hat{H}^{(\Xi)}$ is the Hamiltonian of the isolated *extended* scattering system $\Xi$, which consists of the scattering system $\Xi_0$ and the Source $\Sigma$. Moreover, the vector notation Eq. (3.2) for creation and annihilation operators for the extended scattering region $\hat{\mathbf{a}}_\Xi$ and the leads $\hat{\mathbf{a}}_\Lambda$ has been used and $C$ is the matrix containing the hopping amplitudes coupling the leads and the extended scattering system. Finally, $\hat{H}^{(\Lambda)}$ is the Hamiltonian of the isolated leads. For non-interacting leads it is given by

$$\hat{H}^{(\Lambda)} = \sum_{j=1}^{N_\Lambda} \sum_{l,l'=1}^{\infty} H_{ll'}^{(j)} \hat{a}_l^\dagger \hat{a}_{l'} = \hat{\mathbf{a}}_\Lambda^\dagger H^{(\Lambda)} \hat{\mathbf{a}}_\Lambda,$$

where $N_\Lambda$ is the number of leads, and the matrices $H^{(j)}$ are hermitian, which in turn implies that $H^{(\Lambda)}$ is also a hermitian matrix.

In order to get a stationary scattering state, there are two limits that have to be performed simultaneously. The first one is that the number of

particles $N$ goes to infinity. Since initially all particles are located in the source, the initial state can therefore be approximated to be the vacuum state within the scattering region and the leads and a coherent state $\psi^{(i)}$ with its modulus being given by the total number of particles $\left|\psi^{(i)}\right|^2 = N$, in the source,

$$|i\rangle = |0\rangle_\Lambda \; |0\rangle_{\Xi_0} \; \left|\psi^{(i)}\right\rangle_\Sigma .$$

The second limit is that the coupling between the source and the leads or the scattering region has to go to zero, such that the product of this coupling with the total number of particles stays constant. Under these conditions, one expects that in the long time limit single-particle observables, which can be written as a linear hermitian combination of

$$\mathcal{O}_{ll'} = \left\langle i \left| \hat{K}^\dagger \left(t_f, t_i\right) \hat{a}_l^\dagger \hat{a}_{l'} \hat{K} \left(t_f, t_i\right) \right| i \right\rangle \tag{8.2}$$

are independent of the final time $t_f$ when the measurement takes place.

## 8.2 Exact treatment of the leads

Eq. (8.2) explicitly contains the propagator of the *full* system, which in the limit of large total number of particles can safely be replaced by its semiclassical approximation. Since the initial state is a Fock state within the leads and the scattering region, it is tempting to use the semiclassical propagator in Fock basis,

$$\begin{aligned} K\left(\mathbf{N}^{(f)}, \mathbf{N}^{(i)}; \mathbf{n}^{(f)}, \mathbf{n}^{(i)}; t_f, t_i\right) &= \left\langle \mathbf{N}^{(f)}, \mathbf{n}^{(f)} \left| \hat{K}\left(t_f, t_i\right) \right| \mathbf{N}^{(i)}, \mathbf{n}^{(i)} \right\rangle \\ &= \left\langle \mathbf{N}^{(f)}, \mathbf{n}^{(f)} \left| \hat{\mathcal{T}} \exp\left[ -\frac{\mathrm{i}}{\hbar} \int_{t_i}^{t_f} \mathrm{d}t \hat{H}\left(t\right) \right] \right| \mathbf{N}^{(i)}, \mathbf{n}^{(i)} \right\rangle, \end{aligned}$$

where $\hat{\mathcal{T}}$ is the time ordering operator. Here, capital letters refer to single-particle states of the leads, while small ones to those within the scattering region, *i.e.*

$$|\mathbf{N}, \mathbf{n}\rangle = |\mathbf{N}\rangle_\Lambda \; |\mathbf{n}\rangle_\Xi .$$

However, as discussed in section 4.4.1, the semiclassical treatment is valid for large occupation numbers, only, while here, for almost all sites, the initial occupations are zero. Therefore, one can not use the Fock state

representation directly, but has to use a different basis at first and perform the transformation to Fock states later on. Moreover, the techniques developed in semiclassics in the past decades [18, 28, 30–38], which have been adjusted to the Fock space approach in Appendix F, require that the semiclassical propagator is given by a real action, which rules out the usage of coherent states, too. This leaves only the quadrature representation,

$$K\left(\mathbf{Q}^{(f)},\mathbf{Q}^{(i)};\mathbf{q}^{(f)},\mathbf{q}^{(i)};t_f,t_i\right)= \left\langle \mathbf{Q}^{(f)},\mathbf{q}^{(f)}\left|\hat{\mathcal{T}}\exp\left[-\frac{\mathrm{i}}{\hbar}\int\limits_{t_i}^{t_f}\mathrm{d}t\hat{H}\left(t\right)\right]\right|\mathbf{Q}^{(i)},\mathbf{q}^{(i)}\right\rangle .$$

Furthermore, the loop contributions require an ergodic system [28, 33, 38]. Thus it is desirable to treat the leads exactly, such that finally one can restrict oneself to an (effective) closed system, which may depend on some external parameters dictated by the state in the leads. Therefore, the first aim in the derivation of the semiclassical approximation of the propagator has to be to split off the leads. This is possible by first of all introducing the propagator for the (isolated) leads,

$$\hat{K}^{(\Lambda)}\left(t_f,t_i\right)=\hat{\mathcal{T}}\exp\left[-\frac{\mathrm{i}}{\hbar}\int\limits_{t_i}^{t_f}\mathrm{d}t\hat{H}^{(\Lambda)}\left(t\right)\right]$$

and then formally introducing the effective propagator for the scattering region $\hat{K}^{(\Xi)}\left(t_f,t_i\right)$ such that the full propagator can be written as

$$\hat{K}\left(t_f,t_i\right)=\hat{K}^{(\Lambda)}\left(t_f,t_i\right)\hat{K}^{(\Xi)}\left(t_f,t_i\right).$$

Due to this decomposition, the final result for the semiclassical propagator in quadrature representation will also be given by a product of the propagator of the leads and an effective propagator of the scattering region. This program is akin to the "trace over the leads" approach in one-particle systems. Since interactions are assumed to be switched off within the leads, the semiclassical approximation for the propagator of the leads is not an approximation but exact and has been derived in section 6.1.1 as

$$K^{(\Lambda)}\left(\mathbf{Q}^{(f)},t_f;\mathbf{Q}^{(i)},t_i\right)= {}_{\Lambda}\left\langle \mathbf{Q}^{(f)}\right|\hat{K}^{(\Lambda)}\left|\mathbf{Q}^{(i)}\right\rangle_{\Lambda}= \frac{\exp\left\{-\frac{\mathrm{i}}{4b^2}\begin{pmatrix}\mathbf{Q}^{(i)}\\ \mathbf{Q}^{(f)}\end{pmatrix}\begin{pmatrix}{U^{(i)}}^{-1}U^{(r)} & -{U^{(i)}}^{-1}\\ -{U^{(i)}}^{\mathrm{T}-1} & U^{(r)}{U^{(i)}}^{-1}\end{pmatrix}\begin{pmatrix}\mathbf{Q}^{(i)}\\ \mathbf{Q}^{(f)}\end{pmatrix}\right\}}{\det\sqrt{2\pi b^2\left(1-U^{\mathrm{T}}\left(t_f,t_i\right)U\left(t,t_i\right)\right)}},$$

with the abbreviations $U^{(r)} = \Re U\left(t_f, t_i\right)$ and $U^{(i)} = \Im U\left(t_f, t_i\right)$ for the real and imaginary part of the classical propagator of the isolated leads,

$$\begin{aligned} \mathrm{i}\hbar \frac{\partial U_{ll'}\left(t, t_i\right)}{\partial t} &= \sum_{l''} H_{ll''}^{(\Lambda)}\left(t\right) U_{l''l'}\left(t, t_i\right), \\ U\left(t_i, t_i\right) &= \mathbb{I}. \end{aligned}$$

Note that since the leads are assumed to be decoupled, *i.e.* they have no direct link to one another, $U\left(t, t_i\right)$ is a block diagonal matrix, with each block corresponding to one lead. Moreover, for a semi-infinite one-dimensional lattice of non-interacting, an analytic formula for these classical propagators has been derived in Ref. [263].

After several technical steps (see Appendix E), the semiclassical propagator in quadrature representation is finally found to read

$$\begin{aligned} K\left(\mathbf{Q}^{(f)}, \mathbf{q}^{(f)}, t_f; \mathbf{Q}^{(i)}, \mathbf{q}^{(i)}, t_i\right) = \\ K^{(\Lambda)}\left(\mathbf{Q}^{(f)}, t_f; \mathbf{Q}^{(i)}, t_i\right) \sum_{\gamma:\mathbf{q}^{(i)}\to\mathbf{q}^{(f)}} \sqrt{\det \frac{1}{(-2\mathrm{i}\pi\hbar)} \frac{\partial^2 R_\gamma}{\partial \mathbf{q}^{(f)} \partial \mathbf{q}^{(i)}}} \\ \times \exp\left[\frac{\mathrm{i}}{\hbar} R_\gamma\left(\mathbf{q}^{(f)}, t_f; \mathbf{q}^{(f)}, t_i\right)\right], \end{aligned} \tag{8.3}$$

where the sum runs over all classical trajectories $\gamma$ joining $\mathbf{q}^{(i)}$ to $\mathbf{q}^{(f)}$. These trajectories are determined by the equations of motion

$$\begin{aligned} \mathrm{i}\hbar\dot{\boldsymbol{\psi}}(t) = -\frac{\mathrm{i}}{2b} C^\dagger\left(t\right) U\left(t, t_i\right) {U^{(i)}}^{-1} \mathbf{Q}^{(f)} + \frac{\mathrm{i}}{2b} C^\dagger\left(t\right) U^\dagger\left(t_f, t\right) {U^{(i)}}^{\mathrm{T}^{-1}} \mathbf{Q}^{(i)} \\ + \frac{\partial H^{(\Xi)}\left(\boldsymbol{\psi}^*\left(t\right) \boldsymbol{\psi}\left(t\right); t\right)}{\partial \boldsymbol{\psi}^*\left(t\right)} - \frac{\mathrm{i}}{\hbar} C^\dagger\left(t\right) \int_{t_i}^{t} \mathrm{d}t' U\left(t, t'\right) C\left(t'\right) \boldsymbol{\psi}\left(t'\right) \\ + \frac{\mathrm{i}}{\hbar} C^\dagger\left(t\right) U\left(t, t_i\right) {U^{(i)}}^{-1} \int_{t_i}^{t_f} \mathrm{d}t' \Im\left[U\left(t_f, t'\right) C\left(t'\right) \boldsymbol{\psi}\left(t'\right)\right] \end{aligned} \tag{8.4}$$

and the boundary conditions

$$\begin{aligned} \Re\psi_l\left(t_i\right) &= \frac{1}{2b} q_l^{(i)}, \\ \Re\psi_l\left(t_f\right) &= \frac{1}{2b} q_l^{(f)}. \end{aligned}$$

Here, $H^{(\Xi)}\left(\boldsymbol{\psi}^{*}\left(t\right),\boldsymbol{\psi}\left(t\right);t\right)$ is the classical Hamiltonian of the effective extended scattering system, which is determined according to Eq. (4.7)

It is important to notice that the trajectories parametrically depend on the initial and final quadrature eigenstates of the leads as well as on the evolution of the (isolated) classical trajectories within the leads, which is determined by the classical propagator of the leads $U\left(t,t_{i}\right)$.

The first and the last term of the equations of motion can be interpreted very easily. The first term, which is given by the derivative of the Hamiltonian simply describes the motion within the scattering region, while the last one accounts for particles leaving the scattering region at time $t'\leq t$, which are back reflected into the scattering region.

In order to get a better understanding of the remaining terms of the classical equations of motion, a short analysis of the classical evolution within the isolated leads bears a helping hand. More precisely, determining the corresponding initial state $\mathbf{Q}^{(i)}+\mathrm{i}\mathbf{P}$, satisfying $\Re\left[U\left(t_{f},t_{i}\right)\left(\mathbf{Q}^{(i)}+\mathrm{i}\mathbf{P}\right)\right]=\mathbf{Q}^{(f)}$ yields

$$\mathbf{P}=U^{(i)^{-1}}\left(U^{(r)}\mathbf{Q}^{(i)}-\mathbf{Q}^{(f)}\right),$$

which allows to express the second line of the equations of motion in terms of this initial state only, namely as

$$\frac{1}{2b}C^{\dagger}\left(t\right)U\left(t,t_{i}\right)\left(\mathbf{Q}^{(i)}+\mathrm{i}\mathbf{P}\right).$$

Also, one recognizes that the second term in the equations of motion has a similar form as the $\mathbf{P}$-dependent part. Indeed, as will become clear later, the actual initial state within the leads is not the one of the isolated leads, but also depends on the trajectory $\gamma$ and is given by

$$\mathbf{Q}^{(i)}+\mathrm{i}\left\{\mathbf{P}+\frac{2b}{\hbar}U^{(i)^{-1}}\int_{t_{i}}^{t_{f}}\mathrm{d}t\Im\left[U\left(t_{f},t\right)C\left(t\right)\boldsymbol{\psi}\left(t\right)\right]\right\}.$$

Therefore, the second term in the equations of motion accounts exactly for this correction of the initial state.

Finally, the classical action of the trajectory is given by

$$
\begin{aligned}
&R_\gamma\left(\mathbf{q}^{(f)},t_f;\mathbf{q}^{(i)},t_i\right)= \\
&\quad\frac{1}{b}\mathbf{Q}^{(f)}{U^{(i)}}^{\mathrm{T}-1}\Im\left[U^\dagger\left(t,t_i\right)C(t)\boldsymbol{\psi}\left(t\right)\right]-\frac{1}{b}\mathbf{Q}^{(i)}{U^{(i)}}^{-1}\Im\left[U\left(t_f,t\right)C\left(t\right)\boldsymbol{\psi}\left(t\right)\right] \\
&+\int_{t_i}^{t_f}\mathrm{d}t\Bigg\{\frac{2}{\hbar}\Im\left[\boldsymbol{\psi}^*\left(t\right)C^\dagger\left(t\right)U^\dagger\left(t_f,t\right)\right]{U^{(i)}}^{-1}\int_{t_i}^{t}\mathrm{d}t'\Im\left[U^\dagger\left(t',t_i\right)C\left(t'\right)\boldsymbol{\psi}\left(t'\right)\right] \\
&\qquad\qquad+\frac{\hbar}{2b^2}\mathbf{p}\left(t\right)\cdot\dot{\mathbf{q}}\left(t\right)-H^{(\Xi)}\left(\boldsymbol{\psi}^*\left(t\right)\boldsymbol{\psi}\left(t\right);t\right)\Bigg\},
\end{aligned}
$$

where

$$
\begin{aligned}
\mathbf{q}\left(t\right)&=2b\Re\boldsymbol{\psi}\left(t\right), \\
\mathbf{p}\left(t\right)&=2b\Im\boldsymbol{\psi}\left(t\right).
\end{aligned}
$$

Later on, also the derivatives of the action with respect to the intial and final quadrature will be needed. Using the equations of motion, these can be shown to satisfy

$$
\begin{aligned}
\frac{\partial R_\gamma\left(\mathbf{q}^{(f)},t_f;\mathbf{q}^{(i)},t_i\right)}{\partial\mathbf{q}^{(i)}}&=-\frac{\hbar}{2b^2}\mathbf{p}\left(t_i\right), \\
\frac{\partial R_\gamma\left(\mathbf{q}^{(f)},t_f;\mathbf{q}^{(i)},t_i\right)}{\partial\mathbf{q}^{(f)}}&=\frac{\hbar}{2b^2}\mathbf{p}\left(t_f\right).
\end{aligned}
$$

## 8.3 Calculating Observables

### *8.3.1 A semiclassical formula for expectation values of single-particle observables*

The semiclassical propagator Eq. (8.3) is the key ingredient to determine expectation values of linear hermitian combinations of Eq. (8.2). In order to plug in Eq. (8.3), first of all one has to introduce unit operators in terms of quadrature eigenstates, Eq. (3.14c) to the left and to the right of each propagator.

Applying furthermore Eq. (3.16) yields – after a partial integration – derivatives of the semiclassical propagator for the effective extended scattering system. Typically, derivatives of the semiclassical prefactors can be

neglected compared to those of the phase [15]. Therefore, one is allowed to let the derivative act on the exponential only, which finally yields

$$\begin{aligned}\mathcal{O}_{ll'} = \int \mathrm{d}^{L_\Xi} q^{(1)} \int \mathrm{d}^{L_\Xi} q^{(2)} \int \mathrm{d}^{L_\Xi} q \int \prod_{l\in\Lambda} \frac{\mathrm{d}Q_l}{\left(\sqrt{2\pi} b\right)} \int \prod_{l\in\Lambda} \mathrm{d}\mathbf{Q}_l^{(1)} \int \prod_{l\in\Lambda} \mathrm{d}\mathbf{Q}_l^{(2)} \\ \exp\left\{-\frac{1}{4b^2}\left[\mathbf{Q}^{(2)^2} + \mathbf{Q}^{(1)^2} + \mathbf{q}_{\Xi_0}^{(1)^2} + \mathbf{q}_{\Xi_0}^{(2)^2}\right]\right\} {}_\Sigma\!\left\langle \mathbf{q}^{(1)} \,\middle|\, \psi^{(i)} \right\rangle_\Sigma \\ \times {}_\Sigma\!\left\langle \psi^{(i)} \,\middle|\, \mathbf{q}^{(2)} \right\rangle_\Sigma K^{(\Lambda)^*}\left(\mathbf{Q}, \mathbf{Q}^{(2)}; t_f, t_i\right) K^{(\Lambda)}\left(\mathbf{Q}, \mathbf{Q}^{(1)}; t_f, t_i\right) \\ \times \sum_{\gamma:\mathbf{q}^{(1)}\to\mathbf{q}} \sum_{\gamma':\mathbf{q}^{(2)}\to\mathbf{q}} \frac{1}{\left[(2\pi)^{\frac{3}{2}} b\hbar\right]^{L_{\Xi_0}}} \sqrt{\det \frac{\partial^2 R_\gamma}{\partial \mathbf{q}^{(1)} \partial \mathbf{q}}} \sqrt{\det \frac{\partial^2 R_{\gamma'}}{\partial \mathbf{q}^{(2)} \partial \mathbf{q}}}^* \\ \times \exp\left[\frac{\mathrm{i}}{\hbar}\left(R_\gamma - R_{\gamma'}\right)\right] \left[\psi_l^{(\gamma')^*}(t_f)\psi_{l'}^{(\gamma)}(t_f) - \frac{1}{2}\delta_{ll'}\right],\end{aligned} \tag{8.5}$$

where $\boldsymbol{\psi}^{(\gamma/\gamma')}$ are the solutions of the equations of motion corresponding to the trajectory $\gamma$ and $\gamma'$, respectively. Here, $\gamma$ depends parametrically on $\mathbf{Q}^{(1)}$ and $\mathbf{Q}$, while $\gamma'$ depends on $\mathbf{Q}^{(2)}$ and $\mathbf{Q}$. For the leads and the scattering region, the overlaps between quadrature eigenstate and the vacuum have already been evaluated according to Eq. (3.12).

Applying furthermore Eq. (3.19) for the overlap between a coherent state and a quadrature eigenstate to the source, shows that the main contributions to the integrals in (8.5) stem mainly from those regions wit $\mathbf{q}^{(1)} \approx \mathbf{q}^{(2)}$ and $\mathbf{Q}^{(1)} \approx \mathbf{Q}^{(2)}$. This allows to replace the trajectories $\gamma$ and $\gamma'$ by (nearby) trajectories $\bar{\gamma}$ and $\bar{\gamma}'$, respectively, which both start at $2b\mathbf{q}^{(0)} = \left(\mathbf{q}^{(1)} + \mathbf{q}^{(2)}\right)/2$ and depend parametrically on $2b\mathbf{Q}^{(0)} = \left(\mathbf{Q}^{(2)} + \mathbf{Q}^{(1)}\right)/2$ instead of $\mathbf{Q}^{(1)}$ and $\mathbf{Q}^{(2)}$ themselves. At the same time, in accordance with semiclassical perturbation theory one has to expand the corresponding actions $R_\gamma$ and $R_{\gamma'}$ in the exponential up to first order in $\mathbf{q}^{(1)}$, $\mathbf{q}^{(2)}$, $\mathbf{Q}^{(1)}$ and

$\mathbf{Q}^{(2)}$, respectively, *i.e.*

$$R_\gamma\left(\mathbf{q},t_f;\mathbf{q}^{(1)},t_i\right)\approx R_{\bar\gamma}\left(\mathbf{q},t_f;2b\mathbf{q}^{(0)},t_i\right)-\frac{\hbar}{2b^2}\mathbf{p}^{(\bar\gamma)}\cdot\left(\mathbf{q}^{(1)}-2b\mathbf{q}^{(0)}\right)$$
$$-\frac{\mathrm{i}}{\hbar b}\left(\mathbf{Q}^{(1)}-2b\mathbf{Q}^{(0)}\right)\left(U^{(i)}\right)^{-1}\int_{t_i}^{t_f}\mathrm{d}t\Im\left[U\left(t_f,t\right)C\left(t\right)\boldsymbol{\psi}^{(\bar\gamma)}\left(t\right)\right],$$
$$R_{\gamma'}\left(\mathbf{q},t_f;\mathbf{q}^{(2)},t_i\right)\approx R_{\bar\gamma'}\left(\mathbf{q},t_f;2b\mathbf{q}^{(0)},t_i\right)-\frac{\hbar}{2b^2}\mathbf{p}^{(\bar\gamma')}\cdot\left(\mathbf{q}^{(2)}-2b\mathbf{q}^{(0)}\right)$$
$$-\frac{\mathrm{i}}{\hbar b}\left(\mathbf{Q}^{(2)}-2b\mathbf{Q}^{(0)}\right)\left(U^{(i)}\right)^{-1}\int_{t_i}^{t_f}\mathrm{d}t\Im\left[U\left(t_f,t\right)C\left(t\right)\boldsymbol{\psi}^{(\bar\gamma')}\left(t\right)\right],$$

while in the semiclassical prefactor, $\mathbf{q}^{(1)}$ and $\mathbf{q}^{(2)}$ are simply replaced by $2b\mathbf{q}^{(0)}$.

After that, one can substitute the integrations over $\mathbf{q}^{(1)}$ and $\mathbf{Q}^{(1)}$ by integrals over $\mathbf{q}^{(0)}$ and $\mathbf{Q}^{(0)}$, respectively and perform the integrals over $\mathbf{q}^{(2)}$ and $\mathbf{Q}^{(2)}$, giving

$$\mathcal{O}_{ll'}=\frac{1}{(\pi b)^{L_\Xi}}\int\prod_{l\in\Lambda}\mathrm{d}Q_l^{(0)}\int\prod_{l\in\Lambda}\frac{\mathrm{d}P_l}{\pi b}\int\mathrm{d}^{L_\Xi}q^{(0)}\int\mathrm{d}^{L_\Xi}q\sum_{\bar\gamma,\bar\gamma':2b\mathbf{q}^{(0)}\to\mathbf{q}}$$
$$\sqrt{\det\frac{\partial\mathbf{p}^{(\bar\gamma)}(t_i)}{\partial\mathbf{q}}}\sqrt{\det\frac{\partial\mathbf{p}^{(\bar\gamma')}(t_i)}{\partial\mathbf{q}}}^{*}\left[\psi_l^{(\bar\gamma')*}(t_f)\psi_{l'}^{(\bar\gamma)}(t_f)-\frac{1}{2}\delta_{ll'}\right]$$
$$\exp\left\{-2\mathbf{Q}^{(0)^2}-2\sum_{l\in\Xi_0}q_l^{(0)^2}-\frac{1}{8b^2}\sum_{l\in\Xi_0}\left(p_l^{(\bar\gamma)}(t_i)+p^{(\bar\gamma')}(t_i)\right)^2\right.\quad(8.6)$$
$$-2\mathbf{P}^{(0)}-\frac{1}{2}\sum_{l\in\Sigma}\left|2q_l^{(0)}+\frac{\mathrm{i}}{2b}\left(p_l^{(\bar\gamma)}(t_i)+p_l^{(\bar\gamma')}(t_i)\right)-2\phi_l^{(i)}\right|^2$$
$$\left.+\frac{\mathrm{i}}{\hbar}\left(R_{\bar\gamma}-R_{\bar\gamma'}\right)\right\},$$

where

$$\mathbf{P}^{(0)}=\frac{1}{2b}\mathbf{P}+\frac{1}{\hbar}U^{(i)}\int_{t_i}^{t_f}\mathrm{d}s\Im\left(U(t_f,s)C(s)\boldsymbol{\psi}^{(\gamma)}(s)\right)$$

and the integration over $\mathbf{Q}$ has been transformed into one over

$$\mathbf{P}=\left(U^{(i)}\right)^{-1}\left(2bU^{(r)}\mathbf{Q}^{(0)}-\mathbf{Q}\right).$$

Note that with the definition of $\mathbf{q}^{(0)}$, the initial condition for the trajectories reads

$$\Re\boldsymbol{\psi}\left(t_i\right) = \mathbf{q}^{(0)}.$$

### *8.3.2 Diagonal approximation: Rederiving the Truncated Wigner Approximation*

Most of the trajectories $\bar{\gamma}$ are uncorrelated, such that when performing a disorder average most terms in the double sum in (8.6) strongly oscillate and tend to cancel each other. The only contributions that survive this average are those trajectory pairs that are correlated. The most obvious and easiest possibility to get pairs of correlated trajectories is again to choose identical ones, $\bar{\gamma} = \bar{\gamma}'$. This procedure is called diagonal approximation and yields

$$\begin{aligned}\mathcal{O}_{ll'}^{(da)} = & \\ & \int \prod_{l''\in\Lambda} \mathrm{d}Q_{l''}^{(0)} \int \prod_{l''\in\Lambda} \frac{\mathrm{d}P_{l''}}{\pi b} \int \frac{\mathrm{d}^{L_\Xi} q^{(0)}}{(\pi b)^{L_\Xi}} \int \mathrm{d}^{L_\Xi} q \sum_{\bar{\gamma}:2b\mathbf{q}^{(0)}\to\mathbf{q}} \left|\det \frac{\partial \mathbf{p}^{(\bar{\gamma})}(t_i)}{\partial \mathbf{q}}\right| \\ & \exp\left(-2{\mathbf{Q}^{(0)}}^2 - 2\mathbf{P}(0) - 2\sum_{l\in\Xi_0}\left|\psi_l^{(\bar{\gamma})}(t_i)\right|^2 - 2\sum_{l\in\Sigma}\left|\psi_l^{(\bar{\gamma})}(t_i) - \phi_l^{(i)}\right|^2\right) \\ & \left[{\psi_l^{(\bar{\gamma})}}^*(t_f)\psi_{l'}^{(\bar{\gamma})}(t_f) - \frac{1}{2}\delta_{ll'}\right].\end{aligned} \tag{8.7}$$

Just as in the case of the coherent backscattering in section 7.1, using the properties of the Dirac delta one can easily verify the sum rule

$$\int \mathrm{d}^{L_\Xi} q \sum_{\bar{\gamma}:2b\mathbf{q}^{(0)}\to\mathbf{q}} \frac{1}{(2b)^{L_\Xi}} \left|\det \frac{\partial \mathbf{p}^{(\bar{\gamma})}\left(t_i\right)}{\partial \mathbf{q}}\right| F\left[\boldsymbol{\psi}^{(\bar{\gamma})}\left(t\right)\right] = \int \mathrm{d}^{L_\Xi} p^{(0)} F\left[\boldsymbol{\psi}\left(t\right)\right],$$

where $F$ is an arbitrary functional of $\boldsymbol{\psi}(t)$, and $\boldsymbol{\psi}\left(t\right)$ is the time evolution of $\boldsymbol{\psi}\left(t_i\right) = \mathbf{q}^{(0)} + \mathrm{i}\mathbf{p}^{(0)}$ according to the equations of motion (8.4) with $\mathbf{Q}^{(i)} = 2b\mathbf{Q}^{(0)}$ and $\mathbf{Q}^{(f)} = 2bU^{(r)}\mathbf{Q}^{(0)} - U^{(i)}\mathbf{P}$.

Finally, transforming the integration over $\mathbf{P}$ to one over $\mathbf{P}^{(0)}$ yields the

truncated Wigner result

$$\mathcal{O}_{ll'}^{(da)} = \int \prod_{l''\in\Lambda} \mathrm{d}Q_{l''}^{(0)} \int \prod_{l''\in\Lambda} \frac{\mathrm{d}P_{l''}^{(0)}}{\pi/2} \int \frac{\mathrm{d}^{L_\Xi} q^{(0)}}{(\pi/2)^{L_\Xi}} \int \mathrm{d}^{L_\Xi} p^{(0)} \left(\psi_l^*(t_f)\psi_{l'}(t_f) - \frac{1}{2}\delta_{ll'}\right) \exp\left[-2\mathbf{Q}^{(0)^2} - 2\mathbf{P}^{(0)^2} - 2\sum_{l''\in\Xi_0} \psi_{l''}^{(0)^2} - 2\sum_{l''\in S} \left|\psi_{l''}^{(0)} - \phi_{l''}^{(i)}\right|^2\right].$$

with $\psi_l^{(0)} = q_l^{(0)} + \mathrm{i}p_l^{(0)}$.

It is important to notice that in the variables $\mathbf{Q}^{(0)}$ and $\mathbf{P}^{(0)}$, the equations of motion read

$$\mathrm{i}\hbar\dot{\boldsymbol{\psi}}(t) = \frac{\partial H^\Xi(\boldsymbol{\psi}(t);t)}{\partial \boldsymbol{\psi}^*(t)} + C^\dagger(t)U(t,t_i)\left(\mathbf{Q}^{(0)} + \mathrm{i}\mathbf{P}^{(0)}\right) - \frac{\mathrm{i}}{\hbar}C^\dagger(t)\int_{t_i}^{t} \mathrm{d}t' U(t,t')C(t')\boldsymbol{\psi}(t').$$

These equations of motion can also be obtained from the standard mean field equations corresponding to the exact quantum Hamiltonian Eq. (8.1), and are therefore exactly the same as the ones obtained in the Truncated Wigner approach [263].

However, in the same way as for the transition probabilities between Fock states, the Truncated Wigner approximation only yields the leading order - and therefore classical - contribution to single-particle observables in a transport setup as the one described here, while the loop contributions yield the quantum corrections.

### *8.3.3 Interference effects: Sieber-Richter Pairs and One-Leg-Loops*

The first order corrections stem from two- and one-leg-loops with one two-encounter. In order to compute them, one first of all needs to find out, whether and for which ranges of the parameters $\mathbf{Q}^{(0)}$, $\mathbf{P}$, $\mathbf{q}^{(0)}$ and $\mathbf{q}$ these trajectory pairs exist. To this end, recall the structure of a Sieber-Richter pair. Suppose, the trajectory $\bar{\gamma}$ leaves the encounter region after its first traversal at time $T_1$ and enters it again at $T_2$. Then, the fact that within the encounter, the trajectory has to be close to its time reverse requires that $\boldsymbol{\psi}^{(\bar{\gamma})}(T_1) \approx \boldsymbol{\psi}^{(\bar{\gamma})^*}(T_2)$. Moreover, its partner trajectory $\bar{\gamma}'$ can be

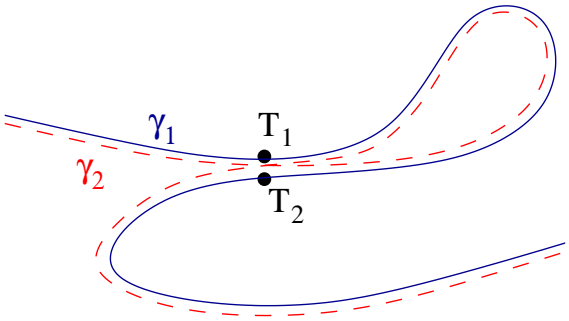


Figure 8.3: A sketch of (the two-dimensional projection) of a Sieber-Richter pair

apprximated as

$$\psi^{(\gamma')}(t) \approx \begin{cases} \psi^{(\gamma)}(t) & \text{for} \quad t_i \le t < T_1 - t_{enc} \\ \psi^{(\gamma')}(t) & \text{for} \quad T_1 - t_{enc} \le t < T_1 \\ \psi^{(\gamma)*}(T_2 + T_1 - t) & \text{for} \quad T_1 \le t \le T_2 \\ \psi^{(\gamma')}(t) & \text{for} \quad T_2 < t \le T_2 + t_{enc} \\ \psi^{(\gamma)}(t) & \text{for} \quad T_2 + t_{enc} < t \le t_f \end{cases} \tag{8.8}$$

where $t_{enc}$ is the time, the trajectories spend inside the encounter region. The second and third line account for the difference of the trajectories $\bar{\gamma}$ and $\bar{\gamma}'$ within the encounter region. Note that this parametrization also includes one-leg-loops by choosing either $T_1 = t_i + t$ or $T_2 = t_f - t$, with $t \in [0, t_{enc}]$.

By plugging (8.8) into the equations of motion (8.4) and checking their validity for $t \in [t_i, T_1 - t_{enc}]$ and $t \in [T_2 + t_{enc}]$, on finds that $\bar{\gamma}$ and $\bar{\gamma}'$ have to satisfy

$$\int_{T_1 - t_{enc}}^{T_2 + t_{enc}} \mathrm{d}t U(t_f, t)\, C(t) \psi^{(\bar{\gamma}')}(t) = \int_{T_1 - t_{enc}}^{T_2 + t_{enc}} \mathrm{d}t U(t_f, t)\, C(t) \psi^{(\bar{\gamma})}(t),$$

Indeed, using the equations of motion in the (isolated leads), as well as partial integrations, one can show that

$$\int_{T_1}^{T_2} \mathrm{d}t U(t_f, t)\, C(t) \psi^{(\bar{\gamma}')}(t) - \int_{T_1}^{T_2} \mathrm{d}t U(t_f, t)\, C(t) \psi^{(\bar{\gamma})}(t),$$

is of the same order as the integrals over the encounter durations, and can therefore be canceled by them.

Next, one has to check, whether $\boldsymbol{\psi}^{(\bar{\gamma})^*}(T_2+T_1-t)$ solves the equations of motion of $\boldsymbol{\psi}^{(\bar{\gamma}')}(t)$ for $T_1 \leq t \leq T_2$. This requires that the Hamiltonians $H^{(\Lambda)}$ and $H^{(\Xi)}$ as well as the coupling $C$ are real and time independent. Moreover, a further condition is found, which can be written as

$$\begin{aligned} C^{\mathrm{T}} U\left(t-t_i\right)\left[U^*\left(T_2+T_1-2t_i\right)\left(\mathbf{Q}^{(0)}-\mathrm{i}\mathbf{P}^{(0)}\right)-\left(\mathbf{Q}^{(0)}+\mathrm{i}\mathbf{P}^{(0)}\right)\right] = \\ -\frac{\mathrm{i}}{\hbar} C^{\mathrm{T}} U\left(t-t_i\right)\Bigg\{U^*\left(T_2+T_1-2t_i\right)\int_{t_i}^{T_2}\mathrm{d}t' U\left(t'-t_i\right) C\boldsymbol{\psi}^{(\gamma)^*}(t') \\ +\int_{T_1-t_{enc}}^{T_1}\mathrm{d}t' U^*\left(t'-t_i\right) C\boldsymbol{\psi}^{(\gamma')}(t')+\int_{t_i}^{T_1-t_{enc}}\mathrm{d}t' U^*\left(t'-t_i\right) C\boldsymbol{\psi}^{(\gamma)}(t')\Bigg\}, \end{aligned}$$

which actually just says that when following the classical trajectory in the extended scattering region once in each direction and subtracting the change in the number of particles in the extended scattering region, the result has to be minus the value obtained by following the classical trajectory in the leads once in each direction and subtracting the change in the number of particles in the leads.

Here, as in the diagonal approximation,

$$\mathbf{P}^{(0)}=\frac{1}{2b}\mathbf{P}+\frac{1}{\hbar}\left(U^{(i)}\right)^{-1}\int_{t_i}^{t_f}\mathrm{d}t\Im\left(U\left(t_f,t\right) C\boldsymbol{\psi}^{(\gamma)}(t)\right).$$

Since this has to be valid for any $t \in [T_1, T_2]$, one can omit the coupling matrix and multiply the whole expression with $U^\dagger(t-t_i)$, yielding

$$\begin{aligned} \mathrm{i}\hbar U^*\left(T_2+T_1-2t_i\right)\left(\mathbf{Q}^{(0)}-\mathrm{i}\mathbf{P}^{(0)}\right)-\mathrm{i}\hbar\left(\mathbf{Q}^{(0)}+\mathrm{i}\mathbf{P}^{(0)}\right) = \\ \int_{t_i}^{T_1-t_{enc}}\mathrm{d}t U^*\left(t-t_i\right) C\boldsymbol{\psi}^{(\gamma)}(t)+\int_{T_1-t_{enc}}^{T_1}\mathrm{d}t U^*\left(t-t_i\right) C\boldsymbol{\psi}^{(\gamma')}(t) \\ +\int_{t_i}^{T_2}\mathrm{d}t U^*\left(T_2+T_1-t-t_i\right) C\boldsymbol{\psi}^{(\gamma)^*}(t) \end{aligned} \tag{8.9}$$

On the other hand, $\boldsymbol{\psi}^{(\gamma)}$ at time $T_2$ has to be almost the time reverse of

itself at time $T_1$, such that

$$\begin{aligned}\dot{\boldsymbol{\psi}}^{(\gamma)}(T_1)+\dot{\boldsymbol{\psi}}^{(\gamma)^*}(T_2)=&\\ &\frac{\partial H^{(\Xi)}\left(\boldsymbol{\psi}^{(\gamma)}(T_1)\right)}{\partial\boldsymbol{\psi}^{(\gamma)^*}(T_1)}-\frac{\partial H^{(\Xi)}\left(\boldsymbol{\psi}^{(\gamma)}(T_2)\right)}{\partial\boldsymbol{\psi}^{(\gamma)}(T_2)}\\ &+C^{\mathrm{T}}\Bigg\{U(T_1-t_i)\left(\mathbf{Q}^{(0)}+\mathrm{i}\mathbf{P}^{(0)}\right)-U^*(T_2-t_i)\left(\mathbf{Q}^{(0)}-\mathrm{i}\mathbf{P}^{(0)}\right)\\ &-\frac{\mathrm{i}}{\hbar}\int_{t_i}^{T_1}\mathrm{d}tU(T_1-t)\,C\boldsymbol{\psi}^{(\gamma)}(t)-\frac{\mathrm{i}}{\hbar}\int_{t_i}^{T_2}\mathrm{d}tU^*(T_2-t)\,C\boldsymbol{\psi}^{(\gamma)}(t)^*\Bigg\}\end{aligned}\tag{8.10}$$

has to be very small.

Inserting (8.9) in (8.10) finally yields

$$\begin{aligned}\dot{\boldsymbol{\psi}}^{(\gamma)}(T_1)+\dot{\boldsymbol{\psi}}^{(\gamma)^*}(T_2)=-\frac{\mathrm{i}}{\hbar}C^{\mathrm{T}}\int_{T_1-t_enc}^{T_1}\mathrm{d}tU(T_1-t)\,C\left[\boldsymbol{\psi}^{(\gamma)}(t)-\boldsymbol{\psi}^{(\gamma')}(t)\right]&\\ +\frac{\partial H^{(\Xi)}\left(\boldsymbol{\psi}^{(\gamma)}(T_1)\right)}{\partial\boldsymbol{\psi}^{(\gamma)^*}(T_1)}-\frac{\partial H^{(\Xi)}\left(\boldsymbol{\psi}^{(\gamma)}(T_2)\right)}{\partial\boldsymbol{\psi}^{(\gamma)}(T_2)}.&\end{aligned}\tag{8.11}$$

Therefore, there is actually no condition on the parameters $\mathbf{Q}^{(0)}$, $\mathbf{P}$, $\mathbf{q}^{(0)}$ and $\mathbf{q}$. Instead, loop contributions will be present for any of these parameters.

This, however, means that one can perform the same steps of section 7.1.3, from which follows that the loop contributions all vanish. Therefore, the Truncated Wigner result presented in [262] is not only the classical limit, but actually exact within the semiclassical limit.

This is also in accordance with the fact that, for an infinite optical lattice with two energetical bariers between the scattering region and the leads but otherwise no disorder, the truncated Wigner approach showed very good agreement with the quantum mechanical calculation [263]. This agreement also shows that the integrations over initial conditions in Eq. (8.5) are already enough to justify the restriction to correlated pairs of trajectories, and a disorder average is not required.

CHAPTER 9

# The fidelity for interacting bosonic many-body systems

## 9.1 The Fidelity Amplitude

The concept of fidelity has been introduced first by Peres to study the stability and irreversibility of th motion of a quantum system [264]. There are actually two different equivalent pictures of the procedure. The first one is the one shown in Fig. 9.1 for the case of ultra-cold atoms in an optical lattice. In this picture, an initial quantum state is propagated forward until time $t$, then propagated backwards in time under a perturbed Hamiltonian and finally the overlap of the final state with the initial one is measured.

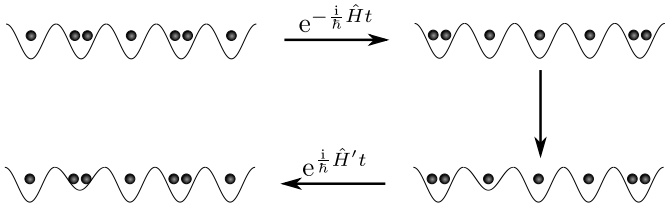


Figure 9.1: The procedure of the fidelity measurement considered here. The initial Fock state is evolved forward in time and after that backward in time under a Hamiltonian, for which one of the on-site energies is slightly perturbed. Finally the overlap between the initial and the final state is measured.

The second picture is to evolve one and the same initial quantum state in time under two different Hamiltonians, which differ in a small perturbation and measuring the overlap between the two evolved states. In both cases, the fidelity amplitude is given by

$$m(t) = \left\langle \mathbf{n} \left| \hat{K}'^{\dagger}(t)\hat{K}(t) \right| \mathbf{n} \right\rangle,$$

with $\hat{K}(t)$ being the propagator of the unperturbed many-body Hamiltonian $\hat{H}$, and $\hat{K}'(t)$ evolving the state according to the perturbed one, $\hat{H}'$.

Here a perturbation of one on-site energy, only, is considered *i.e.*

$$\hat{H}' = \hat{H} + \Delta\epsilon\hat{n}_l.$$

Inserting the semiclassical propagator in Fock state representation, (4.18), and treating $\Delta\epsilon$ in semiclassical perturbation theory, the fidelity becomes

$$m(t) \approx \sum_{\mathbf{m}}{}^{(N)} \sum_{\gamma,\gamma':\mathbf{n}\to\mathbf{m}} \mathcal{A}_\gamma \mathcal{A}^*_{\gamma'} \exp\left[ \frac{\mathrm{i}}{\hbar}\left( R_\gamma - R_{\gamma'} - \frac{1}{2}\Delta\epsilon t \right) + \frac{\mathrm{i}}{\hbar}\Delta\epsilon \int_0^t \mathrm{d}t' \left| \psi_l^{(\gamma')}(t') \right|^2 \right].$$

The last term in the first exponential stems from the constant terms in the classical limit of the Bose-Hubbard Hamitlonian, Eq. (4.9). Moreover, the superscript $(N)$ at the sum indicates that it runs over those Fock states with the total number of particles equal to the one of the initial state $\mathbf{n}$. Note that the Hamiltonian enters the action with a negative sign and thus the sign of the term in the second exponential is positive.

### *9.1.1 Disordered system*

In a disordered system, one can again restrict oneself to the diagonal approximation $\gamma' = \gamma$ and the coherent back-scattering contribution stemming from pairing time-reverse trajectories $\gamma' = \mathcal{T}\gamma$,

$$\langle m(t) \rangle \approx \sum_{\mathbf{m}}{}^{(N)} \left\langle \sum_{\gamma:\mathbf{n}\to\mathbf{m}} |\mathcal{A}_\gamma|^2 \exp\left\{ \frac{\mathrm{i}}{\hbar}\Delta\epsilon \int_0^t \mathrm{d}t' \left[ \left|\psi_l(t')\right|^2 - \frac{1}{2} \right] \right\} \right\rangle (1 + \delta_{\mathbf{nm}}). \tag{9.1}$$

Here, the term $\delta_{\mathbf{nm}}$ originates again from the pairing of time reverse trajectories. When performing the disorder average, one can assume that the perturbation will not be always the same, but rather uniformly distributed within a certain range, which here will be chosen to be $[\epsilon/2, -\epsilon/2]$.

Moreover, if the classical limit is chaotic the integral in the exponent in (9.1) can be interpreted as a sum over random variables. Hence, due to the central limit theorem it can be replaced by a gaussian distributed variable $X$. Then, the mean

$$\langle X \rangle = \left\langle \int_0^t \mathrm{d}t' \left[ |\psi_l(t)|^2 - \frac{1}{2} \right] \right\rangle = n_0 t \tag{9.2}$$

and the variance

$$\left\langle (X - \langle X \rangle)^2 \right\rangle = \left\langle \left\{ \int_0^t \mathrm{d}t' \left[ |\psi_l(t)|^2 - \frac{1}{2} \right] \right\}^2 \right\rangle - \langle X \rangle^2 = \sigma^2 t \tag{9.3}$$

are proportional to the time $t$. This behavior is expected due to the exponential decay of correlations in chaotic systems [265].

Furthermore, the mean can be easily estimated: thermalization [266–269] states that each site is on average equally occupied. The subtracted $1/2$ then cancels with the additional $1/2$ introduced by the boundary conditions (4.19) and therefore the mean is given by the average particle density multiplied by the time,

$$\langle X \rangle = n_0 t = \frac{N}{L} t.$$

Estimating $\sigma^2$, however, is a much more difficult task and has not been possible up to now. However, one can expect that

$$\sigma^2 = \left\langle \frac{1}{t} \int_0^t \mathrm{d}t' \int_{-t'}^{t-t'} \mathrm{d}\tau \left| \psi_l(t') \right|^2 \left| \psi_l(t' + \tau) \right|^2 \right\rangle - n_0 t - n_0^2 t - \frac{t}{4}.$$

is independent on the time $t$.

Evaluating the integrals over $X$ and $\Delta\epsilon$ arising due to the averaging are then straightforward and yield

$$\langle m(t) \rangle \approx \sqrt{\frac{2\pi}{t}} \frac{\hbar}{\epsilon\sigma} \exp\left( -\frac{n_0^2}{2\sigma^2} t \right) \Re\Phi\left( \frac{\epsilon\sigma^2 + 2\mathrm{i}\hbar n_0}{2\sqrt{2}\hbar\sigma} \sqrt{t} \right), \tag{9.4}$$

where

$$\Phi(x) = \frac{2}{\sqrt{\pi}} \int_0^x \mathrm{d}z \exp\left(-z^2\right)$$

is the error function. Moreover, in (9.4), the result of the transition probability has been used in order to replace

$$\sum_{\mathbf{m}}{}^{(N)} \left\langle \sum_{\gamma:\mathbf{n}\to\mathbf{m}} |\mathcal{A}_\gamma|^2 \right\rangle (1+\delta_{\mathbf{nm}}) = 1.$$

Using the asymptotic formula for the error function [270] then gives for the large time asymptotics, *i.e.* for $t \gg \frac{\hbar}{\sqrt{\epsilon^2\sigma^2+4\hbar^2 n_0^2/\sigma^2}}$

$$\langle m(t)\rangle \approx \frac{\hbar}{\epsilon}\left[\frac{4\hbar}{t}\frac{2n_0\hbar\sin\left(\frac{n_0\epsilon}{2\hbar}t\right)-\epsilon\sigma^2\cos\left(\frac{n_0\epsilon}{2\hbar}t\right)}{\epsilon^2\sigma^4+4n_0^2\hbar^2}\exp\left(-\frac{\epsilon^2\sigma^2}{8\hbar^2}t\right) + \sqrt{\frac{2\pi}{\sigma^2 t}}\exp\left(-\frac{n_0^2}{2\sigma^2}t\right)\right]. \tag{9.5}$$

### *9.1.2 Short Time Behavior*

On the other hand, as suggested by the results obtained in section 7.2, for short times the trajectory almost does not feel the disorder, but the particles stay at their individual sites and only the phase evolves, such that

$$\langle m(t)\rangle \approx \frac{1}{\epsilon}\int_{-\frac{\epsilon}{2}}^{\frac{\epsilon}{2}} \mathrm{d}\Delta\epsilon \exp\left(\frac{\mathrm{i}\Delta\epsilon}{\hbar}n_l t\right) = \frac{2\hbar\sin\left(\frac{\epsilon n_l t}{2\hbar}\right)}{\epsilon n_l t}, \tag{9.6}$$

which yields when expanding up to second order in time the well known quadratic initial decay [264]

$$\langle m(t)\rangle \approx 1 - \left(\frac{\epsilon n_l}{2\hbar}\right)^2 \frac{t^2}{6}. \tag{9.7}$$

The main observation here is that the decay becomes stronger when increasing the number of particles in the affected site. To the author's knowledge this is the first time that for a many-body system a prediction about the dependence of the fidelity on the number of particles has been made.

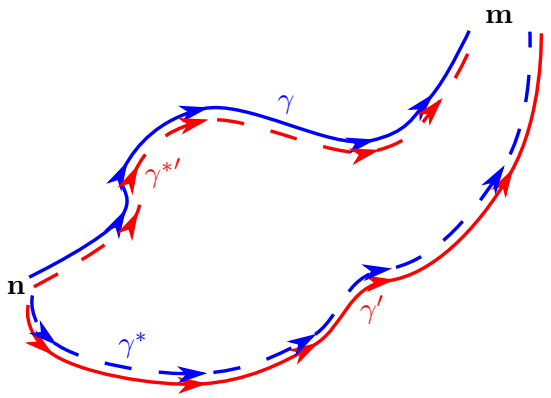


Figure 9.2: Trajectory pairs giving rise to the background contribution.

## 9.2 The Loschmidt echo

Following [25], the average Loschmidt echo, which is the average of the modulus of the fidelity, $M(t) = \left\langle |m(t)|^2 \right\rangle$ can be written in the semiclassical limit as a sum of two contributions. However, here due to the discreteness of the basis, a third background contribution arises such that

$$M(t) \approx M_{inc}(t) + M_{coh}(t) + M_{bg}. \tag{9.8}$$

In order to avoid confusion, the first term will be denoted as the incoherent and the second one as the coherent contribution. This notation will become clear in the following.

### *9.2.1 Background contribution*

The Loschmidt echo $M(t)$ in semiclassical perturbation theory is given by

$$M(t) = \sum_{\mathbf{m},\mathbf{m}'}{}^{(N)} \left\langle \sum_{\substack{\gamma,\gamma':\mathbf{n}\to\mathbf{m} \\ \gamma^*,\gamma^{*\prime}:\mathbf{n}\to\mathbf{m}'}} \mathcal{A}_\gamma \mathcal{A}^*_{\gamma'} \mathcal{A}^*_{\gamma^*} \mathcal{A}_{\gamma^{*\prime}} \exp\left\{ \frac{\mathrm{i}}{\hbar} \left( R_\gamma - R_{\gamma'} - R_{\gamma^*} + R_{\gamma^{*\prime}} + \Delta\epsilon \int_0^t \mathrm{d}t' \left[ \left| \psi_l^{(\gamma')}(t') \right|^2 - \left| \psi_l^{(\gamma^{*\prime})}(t') \right|^2 \right] \right) \right\} \right\rangle. \tag{9.9}$$

Here, the trajectories with and without an asterisk originate from the time evolution of $m^*(t)$ and $m(t)$, respectively. Moreover, a prime indicates that the trajectory corresponds to backward propagation. Here it becomes obvious that, apart from the usual (extended) diagonal pairing $\gamma^{(*)\prime} = \gamma^{(*)}$ and $\gamma^{(*)\prime} = \mathcal{T}\gamma^{(*)}$, one can also pair crosswise like in Fig. 9.2, *i.e.* $\gamma^{*\prime} = (\mathcal{T})\gamma'$ and $\gamma^* = (\mathcal{T})\gamma$ in order to get vanishing action differences. However, this pairing requires that $\mathbf{m}' = \mathbf{m}$. For a continuous basis, this would be a set of zero measure, and therefore these contributions did not arise in first quantized approaches [25, 45, 46]. However, in this case the basis is discrete, and thus this contribution should be taken into account.

One immediately sees that for this kind of pairing also the contribution arising due to the perturbation to the phase cancels and therefore the background contribution is given by

$$\begin{aligned} M_{bg}(t) &= \sum_{\mathbf{m}}{}^{(N)} \left\langle \sum_{\gamma,\gamma':\mathbf{n}\to\mathbf{m}} |\mathcal{A}_\gamma|^2 \left|\mathcal{A}_{\gamma'}\right|^2 \right\rangle (1+\delta_{\mathbf{nm}})^2 \\ &= \sum_{\mathbf{m}}{}^{(N)} \left[P^{(\mathrm{cl})}(\mathbf{m},\mathbf{n};t)\,(1+\delta_{\mathbf{nm}})\right]^2, \end{aligned} \tag{9.10}$$

where in the second step the sum rule Eq. (7.2) has been used in order to relate the background contribution with the classical transition probability $P^{(cl)}$. Since the disorder averaged classical transition probability becomes constant for large enough times $t$ the background contribution can also be assumed to be time independent.

### *9.2.2 Incoherent contribution*

Coming back to the usual pairing $\gamma' = \gamma$ or $\gamma' = \mathcal{T}\gamma$ and $\gamma^{(*)\prime} = \gamma^*$ or $\gamma^{(*)\prime} = \mathcal{T}\gamma^*$ (see Fig. 9.3), the incoherent contribution is given by considering those pairs of trajectories $\gamma^*$ and $\gamma^{*\prime}$ which generically are far away in phase space from $\gamma$ and $\gamma'$ and therefore explore different regions in phase space. Therefore, the evolution of this part of $m^*(t)$ is incoherent to the one of $m(t)$ and hence the denotation as incoherent contribution.

Since the trajectories for $m^*(t)$ and $m(t)$ are far away from each other, the diagonal approximation as well as the averaging over the time integral of $|\psi_l(t)|^2$ can be performed independently for $m^*(t)$ and $m(t)$. Following the above steps and again taking also into account the time reverse pairing,

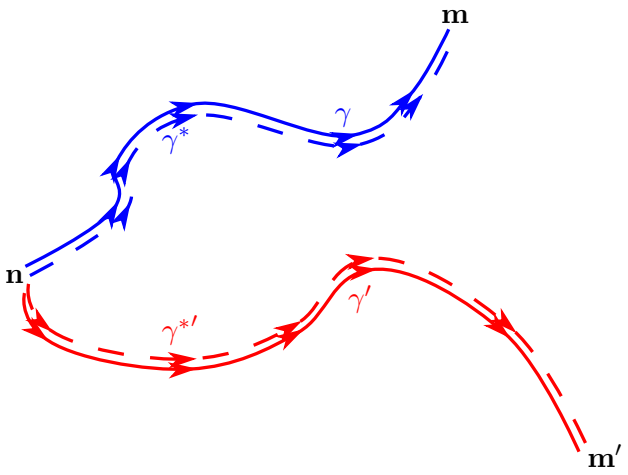


Figure 9.3: Trajectory pair determining the incoherent contribution.

this yields

$$M_{inc}(t) = \sum_{\mathbf{m},\mathbf{m}'}{}^{(N)} \left\langle \sum_{\substack{\gamma:\mathbf{n}\to\mathbf{m} \\ \gamma':\mathbf{n}\to\mathbf{m}'}}{}^{*} |\mathcal{A}_\gamma|^2 \left|\mathcal{A}_{\gamma'}\right|^2 \right\rangle (1+\delta_{\mathbf{n},\mathbf{m}}) \left(1+\delta_{\mathbf{n},\mathbf{m}'}\right) \times \sqrt{\frac{\pi}{t}} \frac{\hbar}{\epsilon\sigma} \Phi\left(\frac{\epsilon\sigma}{2\hbar}\sqrt{t}\right), \tag{9.11}$$

where the star at the double sum over trajectories indicates that only those pairs are taken into account, which explore different regions in phase space.

By introducing

$$x = \frac{\epsilon^2\sigma^2}{4\hbar^2} t,$$

as well as

$$M_{inc}^{(0)} = \sum_{\mathbf{m},\mathbf{m}'}{}^{(N)} \left\langle \sum_{\substack{\gamma:\mathbf{n}\to\mathbf{m} \\ \gamma':\mathbf{n}\to\mathbf{m}'}}{}^{*} |\mathcal{A}_\gamma|^2 \left|\mathcal{A}_{\gamma'}\right|^2 \right\rangle (1+\delta_{\mathbf{n},\mathbf{m}}) \left(1+\delta_{\mathbf{n},\mathbf{m}'}\right),$$

Eq. (9.11) can be written in the compact form

$$M_{inc}(t) = M_{inc}^{(0)} F(x),$$

with

$$F(x) = \frac{1}{2}\sqrt{\frac{\pi}{x}}\Phi\left(\sqrt{x}\right). \tag{9.12}$$

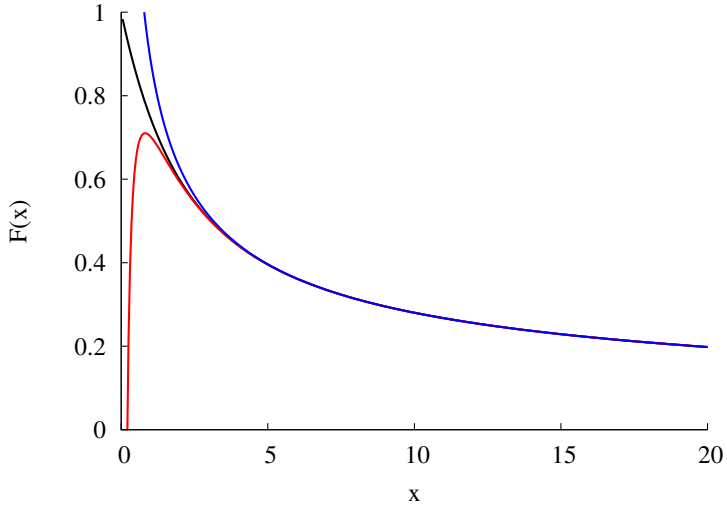


Figure 9.4: Comparison of the function $F(x)$, Eq. (9.12), (black) with its asymptotics $[\sqrt{\pi/x} - \exp(-x)/x]/2$ (red) and $\sqrt{\pi/x}/2$ (blue).

For large times, one can again use the asymptotic form of the error function [270], in order to get

$$F(x) \approx \frac{1}{2}\left[\sqrt{\frac{\pi}{x}} - \frac{1}{x}\exp(-x)\right] \approx \frac{1}{2}\sqrt{\frac{\pi}{x}}. \tag{9.13}$$

In Fig. 9.4 both approximations are compared with the exact expression for $F(x)$ showing that even the crude approximation $F(x) \approx \sqrt{\pi/x}/2$ is almost indistinguishable from the exact function $F(x)$ already for $x \approx 4$.

### *9.2.3 Coherent contribution*

Computing the coherent contribution is somewhat more elaborate, since if all four trajectories are correlated (see Fig. 9.5) one can not perform the averages over the time integrals in the second exponential in (9.9) independently. Instead, the difference should be computed by utilizing the linearized equations of motion around *e.g.* $\gamma'$.

It should also be noted that both time integrals are invariant under time-reversal. Thus in the following, it is enough to consider the pairing $\gamma' = \gamma$ and $\gamma^{*\prime} = \gamma^*$ with $\gamma^* \sim \gamma$ but $\gamma^* \neq \gamma$. The contributions of time reverse pairing can then be easily incorporated at the end of the analysis.

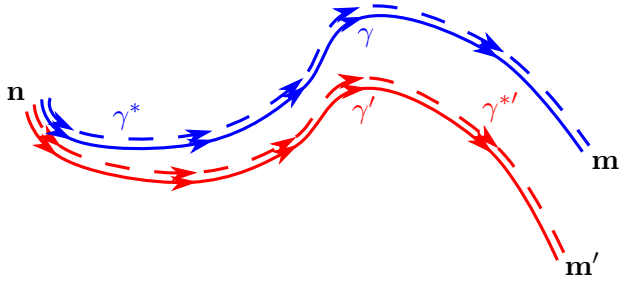


Figure 9.5: The coherent contribution is given by sets of four trajectories, which all stay close together during the whole time evolution.

The evolution determined by the linearized equations of motion are for long enough times exponentially with the Lyapunov exponent $\lambda$. Since the initial occupations of $\gamma$ and $\gamma^*$ are the same, but the final one have to be $\mathbf{m}$ and $\mathbf{m}'$, respectively, one finds [25]

$$\int_0^t \mathrm{d}t' \left[ \left| \psi_l^{(\gamma')}\left(t'\right) \right|^2 - \left| \psi_l^{(\gamma^*)}\left(t'\right) \right|^2 \right] \approx \left(m_l - m_l'\right) \int_0^t \mathrm{d}t' \exp\left[\lambda\left(t'-t\right)\right]$$
$$= \frac{m_l - m_l'}{\lambda}\left[1 - \exp\left(-\lambda t\right)\right].$$

After integrating over $\Delta\epsilon$ again, the coherent contribution reads

$$M_{coh}(t) = \sum_{\mathbf{m},\mathbf{m}'}{}^{(N)} \left\langle \sum_{\gamma:\mathbf{n}\to\mathbf{m}} |\mathcal{A}_\gamma|^4 \right\rangle \left(1 + \delta_{\mathbf{nm}} + \delta_{\mathbf{nm}'}\right) \times \frac{2\lambda\hbar \sin\left\{\frac{\epsilon}{2\lambda\hbar}\left[1 - \exp\left(-\lambda t\right)\right]\left(m_l - m_l'\right)\right\}}{\epsilon\left[1 - \exp\left(-\lambda t\right)\right]\left(m_l - m_l'\right)}, \tag{9.14}$$

where as usual the Kronecker deltas stem from pairing of time reverse paths.

For long enough times, the number of trajectories joining $\mathbf{n}$ with $\mathbf{m}$ typically increases exponentially, while at the same time, $|\mathcal{A}_\gamma|^2$ decreases exponentially with a rate given by the Lyapunov exponent. Thus,

$$\left\langle \sum_{\gamma:\mathbf{n}\to\mathbf{m}} |\mathcal{A}_\gamma|^4 \right\rangle \sim f(t) \exp\left(-\lambda t\right), \tag{9.15}$$

where $f(t)$ is some algebraic function of time. Finally, for long times in Eq. (9.14) one can approximate

$$1 - \exp\left(-\lambda t\right) \approx 1,$$

such that

$$M_{coh}(t) \sim \frac{2\lambda\hbar}{\epsilon} f(t) \exp(-\lambda t) \sum_{\Delta m_l} \frac{\sin\left(\frac{\epsilon}{2\lambda\hbar}\Delta m_l\right)}{\Delta m_l},$$

where the sum now runs only over the differences between the final occupations. Note that only differences up to a certain bound $\Delta \pm m_{max}$, which is assumed to be $\pm 1$, should be taken into account in order to ensure that all four trajectories stay close enough to each other, such that their contribution survives the averaging.

## 9.3 Discussion and comparison with numerical data

### *9.3.1 Fidelity*

The fact that the fidelity is given by an Error function with a complex argument, immediately leads to oscillations in the fidelity similar to those obtained in a Bose-Hubbard trimer, *i.e.* a three-site Bose-Hubbard system, without disorder [271]. However, the average fidelity even has exact zeros, given by those times, at which the Error function in Eq. (9.4) gets purely imaginary.

The semiclassical theory contains two parameters, which can be determined by fitting it to numerical data, namely the average occupation $n_0$ of the $l$-th site and the variance $\sigma$ introduced in Eq. (9.3). To this end, the fidelity has been computed for a Bose-Hubbard ring consisting of five sites with nearest neighbor hopping strength $J = 0.5$, interaction strength $U = 4J$ and disorder strength $W = 10J$ for a perturbation strength $\epsilon = 0.04J$. In these numerical calculations the initial state has been chosen to be $|2, 4, 3, 2, 3\rangle$ having in total $N = 14$ particles and the average runs over 24000 disorder realizations[1]. In addition, for every disorder realization, the site which is perturbed is chosen randomly.

As discussed in section section 9.1.1, the average occupation can be expected to be given approximately by the number of particles divided by the number of single-particle states, which in the chosen case would be $n_0 = 2.8$. Actually the mean value in Eq. (9.2) has been computed numerically by Julien Dujardin in Liége predicting a value of $n_0 = 2.77$.

1 Numerical data by courtesy of Peter Schlagheck

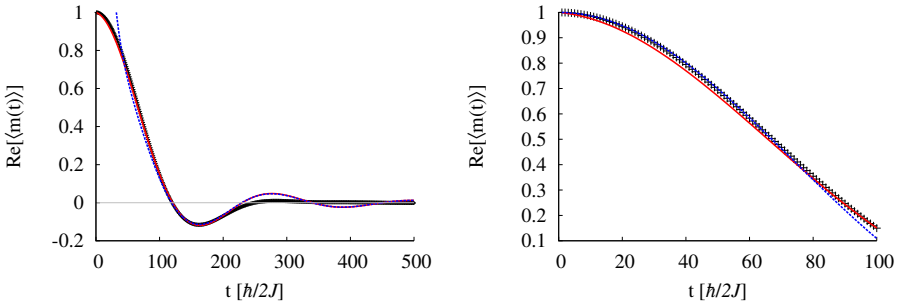


Figure 9.6: (a) Comparison of the numerical data (black) for the real part of the fidelity amplitude with the fitted semiclassical prediction (red line) as well as the corresponding long time asymptotics (blue dotted line). (b) Comparison of the numerical data (black) for the real part of the fidelity amplitude with the fitted semiclassical prediction (red line) and the short time formula Eq. (9.6) (blue dashed line).

The values obtained from fitting the semiclassical theory to the numerical data are

$$n_0 \approx 2.85, \tag{9.16a}$$

$$\sigma \approx 8.92, \tag{9.16b}$$

where the value obtained for $n_0$ is still in good agreement with the above estimate.

Fig. 9.6 shows that the semiclassical theory with the values given in Eq. (9.16) agrees very well with the numerical data for $\epsilon = 0.04J$.

It is worth to notice that both, the numerical data and the semiclassical theory, show the initial quadratic decay predicted by (9.7). Yet, in order to emphasize that the numerical data indeed initially has a quadratic behavior, Fig. 9.6(b) shows the numerical data in comparison with Eq. (9.6) for small times. Again, the agreement of both curves is very good. Note, however, that since in the numerical study the site which has been perturbed has been chosen randomly for each disorder realization, for a comparison one has to replace $n_l$ by $n_0$ in Eqns. (9.6,9.7).

It is obvious that the approximation Eq. (9.7) has to break down, before the first zero occurs. This is because this zero is related to the oscillations, which of course can not be covered by the quadratic approximation.

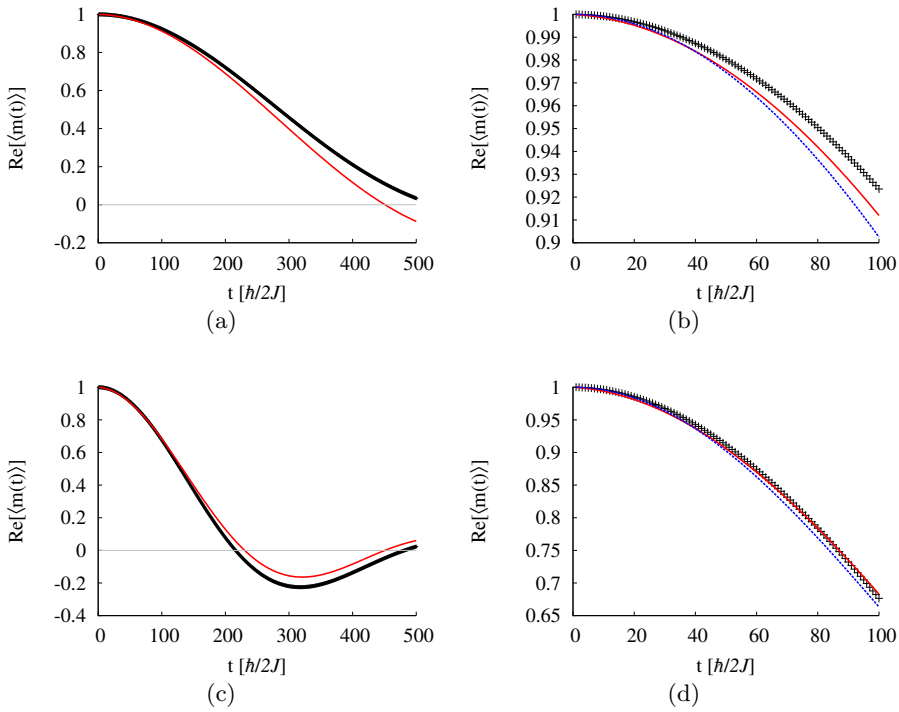


Figure 9.7: (a),(b) Comparison of the numerical data (black) for the real part of the fidelity amplitude with the fitted semiclassical prediction (red line) for $\epsilon = 0.01J$. (c),(d) Comparison of the numerical data (black) for the real part of the fidelity amplitude with the fitted semiclassical prediction (red line) for $\epsilon = 0.02J$ and the short time formula, Eq. (9.6) (blue dashed line).

Moreover, Fig. 9.6(a) also compares the numerical results with the long time behavior, Eq. (9.5). The cosine and sine in Eq. (9.5) indicate that the long time asymptotics may hold already before the fidelity becomes zero for the first time, since these terms are responsible for the oscillations. Indeed, the comparison in Fig. 9.6(a) holds good agreement already before the first zero occurs.

Finally, Fig. 9.7 shows a comparison of the semiclassical theory with the numerical data for perturbation strengths $\epsilon = 0.01J$ and $\epsilon = 0.02J$. In these figures for the semiclassical curves the parameters obtained from the fitting for $\epsilon = 0.04J$ have been used. However, in the numerical data, the average now runs over 200 disorder realizations only, which might explain

the stronger deviations compared to the plots shown in Fig. 9.6. Yet, the agreement between numerics and semiclassics is still very good.

As a matter of fact, Eq. (9.5) suggests that in principle, there might be two regimes, due to the decomposition into two terms, where each term decreases exponentially, however with different rates. For small perturbations, the second exponential decreases much slower and therefore this contribution will dominate. Thus, for small perturbation, the exponential decrease is determined by the perturbation strength.

For larger perturbation strengths however, the first term may eventually dominate and yield a decrease independent of the perturbation strength. Such a perturbation independent regime has been observed previously for the Loschmidt echo [25], but not yet for the fidelity. However, the perturbation independent regime for the decay of the Loschmidt echo typically decreases with a decay rate given by the Lyapunov exponent [25] – and is therefore called Lyapunov regime –, whereas here the decay rate is determined solely by the average occupation.

The perturbation strength, at which the first exponential starts to dominate can be estimated to be

$$\epsilon_c \approx \frac{2n_0\hbar}{\sigma^2}.$$

However, it remains the question, whether the above approach is still valid in this regime, since the perturbation strength already has to be pretty large, such that maybe the semiclassical perturbation theory is no longer justified.

### *9.3.2 Loschmidt echo*

The average Loschmidt echo also decreases quadratically for small times [272]. However, this quadratic decay can not be determined from the presented semiclassical approach. After this initial quadratic decay, there is a competition between the coherent and incoherent contribution, which determines its further decay. However, due to the asymptotic form, Eq. (9.13), the decay of the incoherent part Eq. (9.11) is algebraic, while the coherent part, Eq. (9.14), decays exponentially. Thus, in the scenario considered here, the incoherent contribution will always win for large enough times. This also explains the absence of the Lyapunov regime in the numerical calculations [272].

Finally, for even larger times, when the coherent and incoherent contributions are negligibly small, the Loschmidt echo enters the saturation regime determined by the background contribution Eq. (9.10), which is independent of time.

Assuming that in Eq. (9.15), $f(t) \sim t^{\beta}$, the Loschmidt echo Eq. (9.8) can be written as

$$M(t) = t^{\beta} \exp(-\lambda t) \sum_{\Delta m_l} b_{\Delta m_l} \frac{\sin\left\{\frac{\epsilon \Delta m_l}{2\lambda\hbar}\left[1-\exp(-\lambda t)\right]\right\}}{\frac{\epsilon \Delta m_l}{2\lambda\hbar}\left[1-\exp(-\lambda t)\right]} + a\sqrt{\frac{\pi}{t}}\frac{\hbar}{\epsilon\sigma}\Phi\left(\frac{\epsilon\sigma}{2\hbar}\sqrt{t}\right) + c, \tag{9.17}$$

where the fitting parameters

$$a = M_{inc}^{(0)} = \sum_{\mathbf{m},\mathbf{m}'}{}^{(N)} \left\langle \sum_{\substack{\gamma:\mathbf{n}\to\mathbf{m} \\ \gamma':\mathbf{n}\to\mathbf{m}'}}{}^{*} |\mathcal{A}_{\gamma}|^2 \left|\mathcal{A}_{\gamma'}\right|^2 \right\rangle \left(1+\delta_{\mathbf{n},\mathbf{m}}\right)\left(1+\delta_{\mathbf{n},\mathbf{m}'}\right),$$

$$b_{\Delta m_l} = \frac{\exp(\lambda t)}{t^{\beta}} \sum_{\mathbf{m}}{}^{(N)} \left\langle \sum_{\gamma:\mathbf{n}\to\mathbf{m}} |\mathcal{A}_{\gamma}|^4 \right\rangle \left(1+\delta_{\mathbf{nm}}+\delta_{\mathbf{nm}'}\right),$$

$$c = M_{bg} = \sum_{\mathbf{m}}{}^{(N)} \left\langle \sum_{\gamma,\gamma':\mathbf{n}\to\mathbf{m}} |\mathcal{A}_{\gamma}|^2 \left|\mathcal{A}_{\gamma'}\right|^2 \right\rangle \left(1+\delta_{\mathbf{nm}}\right)^2$$

have been introduced. Furthermore, $\sigma$, $\beta$ and $\lambda$ are obtained from fitting Eq. (9.17) to the numerical data. It is expected, however, that $b_{\Delta m_l} \approx b$ is roughly the same number for all values of $\Delta m_l$ smaller than or equal to an upper bound $m_{\max}$ for which the semiclassical perturbation theory remains valid and $b_{\Delta m_l} = 0$ for $\Delta m_l > m_{\max}$.

While the variance $\sigma$ has already been obtained from the fitting of the semiclassical prediction of the amplitude in section 9.3.1 and is given by Eq. (9.16b), the remaining parameters are obtained by two different fitting schemes.

Three-step fitting scheme

Here, it has been assumed that the maximum difference $m_{\max}$ in the final occupations for the coherent contribution has to be zero, in order for the semiclassical perturbation theory to be valid. Moreover, $\beta$ has been assumed to be zero. The remaining four fitting parameters are then obtained in two steps: First, for very long time, due to its exponential

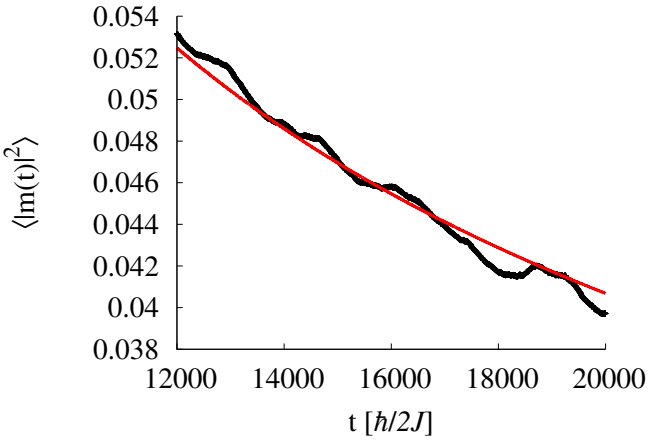


Figure 9.8: Comparison of the numerical (black) and semiclassical (red line) calculation of the Loschmidt echo for very long times. For the semiclassical curve, the coherent contribution has been neglected.

behavior the coherent contribution can be assumed to be negligibly small compared to the remaining two. The coefficients of the remaining two contributions are then obtained to be

$$a \approx 0.577. \tag{9.18a}$$

$$c \approx 0.000189, \tag{9.18b}$$

For long times, this step results in a very good agreement between the semiclassical theory and numerical calculation as shown in Fig. 9.8. The remaining two parameters $b$ and $\lambda$ are finally obtained from fitting the semiclassical theory to the numerical data for intermediate times while using the parameters obtained in Eqns. (9.16) and (9.18) yielding

$$b \approx 0.652, \tag{9.19a}$$

$$\lambda \approx 0.00105. \tag{9.19b}$$

One-step fitting scheme

The second fitting scheme is to fit all parameters at once using as many numerical points as possible. In this scenario $m_{\max}$ has been chosen to be one and $\beta$ has also been kept as a fitting parameter. Moreover, $b_1$ and $b_0$

| Fitting parameter | Three-step fitting | One-step fitting |
|---|---|---|
| $n_0$ | 2.85 | 2.87 |
| $\sigma$ | 8.92 | 9.01 |
| $a$ | 0.577 | 0.613 |
| $b_0$ | 0.652 | 0.611 |
| $b_1$ | – | 0.574 |
| $c$ | 0.000189 | $1.92 \times 10^{-11}$ |
| $\beta$ | – | $-0.0858$ |
| $\lambda$ | 0.00105 | 0.000625 |

Table 9.1: Comparison of the values for the fitting parameters of the Loschmidt echo obtained by the two different fitting schemes.

have been assumed to be independent fitting parameters, in order to still allow $m_{\max} = 0$, if this yields better results.

The parameters obtained from this fitting by using Eqns. (9.16), (9.18) and (9.19) as initial guesses are

$$n_0 \approx 2.87, \tag{9.20a}$$
$$\sigma \approx 9.01, \tag{9.20b}$$
$$a \approx 0.613, \tag{9.20c}$$
$$b_0 \approx 0.611 \tag{9.20d}$$
$$b_1 \approx 0.574 \tag{9.20e}$$
$$c \approx 1.92 \times 10^{-11}, \tag{9.20f}$$
$$\beta \approx -0.0858 \tag{9.20g}$$
$$\lambda \approx 0.000625, \tag{9.20h}$$

indicating that $m_{\max} = 1$ yields better agreement than $m_{\max} = 0$.

The values for the fitting parameters obtained from the two fitting schemes are compared in Table 9.1. While some of them are pretty similar, like for instance the mean occupation $n_0$, the variance $\sigma$, the obtained Lyapunov exponent $\lambda$ differs by a factor of roughly 2 and the magnitude of the background contribution is several orders of magnitude smaller for the one-step fitting scheme than for the three-step fitting. These discrepancies however are not yet understood.

Comparison with numerical results

Fig. 9.9 compares the thus obtained semiclassical predictions with the numerical results and shows a very good overall agreement (see Fig. 9.9(a)). As expected, for very long times, both fitting schemes as well as the numerical result agree with the long time asymptotics obtained from neglecting the coherent contribution. As can be easily seen in Fig. 9.9(c), for shorter times, the latter of course can not reproduce the correct results. Instead for $t \lesssim 2000\hbar/J$ the three-step fitting scheme gives the best agreement, while later on the one-step fitting scheme does (see Fig. 9.9(d)).

The shoulder the one-step fitting result shows below $t = 1000\hbar/J$ suggest that the reason for this behavior is a crossover from $m_{\max} = 0$ to $m_{\max} = 1$. This crossover can also be explained from a simple classical argument: In the coherent contributions, the two trajectories are assumed to be close enough to each other in phase space to allow a linearization of the motion of one of the trajectories around the other one. Then, due to ergodicity, the phase space distance between them increases exponentially in time. However, since the initial separation of the trajectories has to be small enough, there is a certain minimal time required in order for the two trajectories to end at *different* occupations. It is only after this minimal time that the $\Delta m_l = 1$ term has to be included in the coherent contribution. Including $\Delta m_l = 2$, on the other hand, seems not to be necessary, because at the time, at which the classical motion would allow for such large deviations of the trajectories, the coherent contribution is already negligible.

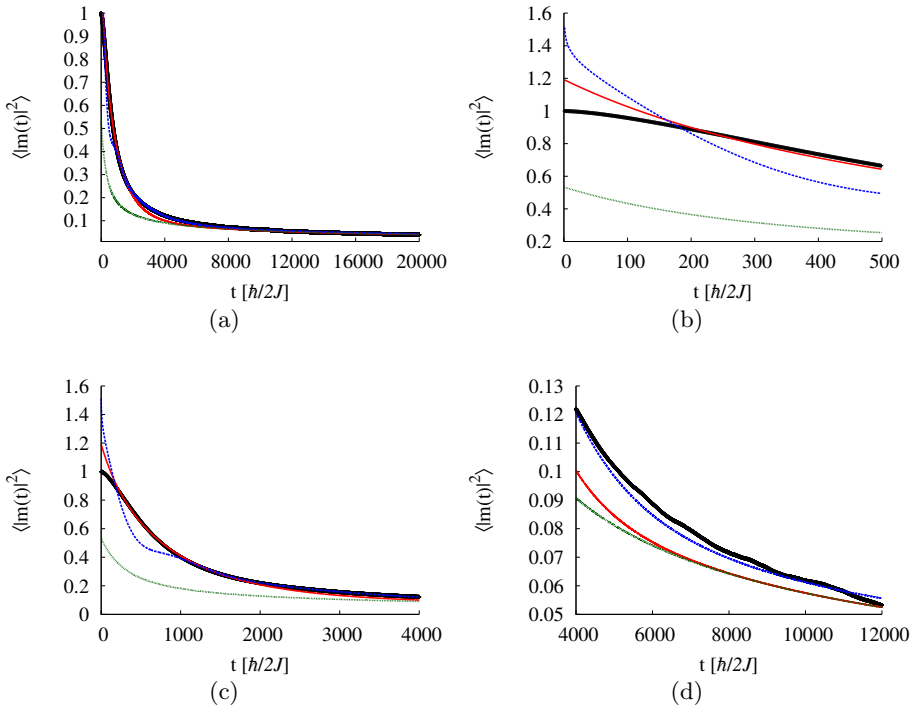


Figure 9.9: Comparison of the numerical result (black), the three-step fitting scheme (red line), the one-step fitting scheme (blue dotted line) and the long time asymptotics obtained from fitting the semiclassical theory without the coherent contribution to the numerical data for long times (green dotted line).

# Part IV

# Interference Effects in Fermionic Fock Space

CHAPTER 10

# The Transition Probability for Fermionic Systems

In section 7.1, it was shown that for a chaotic, bosonic many-body system which is prepared in the Fock state $\mathbf{n}^{(i)}$, the probability to measure at time $t_f$ the Fock state $\mathbf{n}^{(f)}$ is enhanced by a factor of two compared to the classical (Truncated Wigner) result if $\mathbf{n}^{(f)} = \mathbf{n}^{(i)}$, while for all other $\mathbf{n}^{(f)}$ the classical and quantum probability coincide.

Now that a semiclassical propagator for fermionic systems has been derived, one can ask, whether there is an analogous effect for fermions. To address this question, consider a spin-$\frac{1}{2}$ system with some spin-coupling (*e.g.* Rashba spin-orbit interaction). Such a system may be for example the Fermi-Hubbard model with Rashba spin-orbit interaction $\alpha$, described by the Hamiltonian

$$\begin{aligned}\hat{H} = \sum_{l=1}^{L} \Big[ \sum_{\sigma=\downarrow,\uparrow} \left( \epsilon_l \hat{c}^\dagger_{l,\sigma}\hat{c}_{l,\sigma} - J\hat{c}^\dagger_{l,\sigma}\hat{c}_{l+1,\sigma} - J^*\hat{c}^\dagger_{l+1,\sigma}\hat{c}_{l,\sigma} \right) + U\hat{c}^\dagger_{l,\uparrow}\hat{c}^\dagger_{l,\downarrow}\hat{c}_{l,\downarrow}\hat{c}_{l,\uparrow} \\ + \alpha \left( \hat{c}^\dagger_{l,\downarrow}\hat{c}_{l+1,\uparrow} - \hat{c}^\dagger_{l+1,\downarrow}\hat{c}_{l,\uparrow} \right) + \alpha^* \left( \hat{c}^\dagger_{l+1,\uparrow}\hat{c}_{l,\downarrow} - \hat{c}^\dagger_{l,\uparrow}\hat{c}_{l+1,\downarrow} \right) \Big].\end{aligned} \tag{10.1}$$

Inserting the semiclassical propagator, (5.14), the transition probability is given by

$$P\left(\mathbf{n}^{(f)},\mathbf{n}^{(i)};t_f,t_i\right)=\left|\langle\mathbf{n}^{(f)}|\,\hat{K}\left(t_f,t_i\right)|\mathbf{n}^{(i)}\rangle\right|^2$$
$$\approx\sum_{\gamma,\gamma'}\mathcal{A}_\gamma\mathcal{B}_\gamma\mathcal{A}^*_{\gamma'}\mathcal{B}_{\gamma'}{}^*\exp\left[\frac{\mathrm{i}}{\hbar}\left(R_\gamma-R_{\gamma'}\right)\right]$$

With the same arguments as in section 7.1, under disorder average, one can restrict the double sum over trajectories by one sum over trajectories $\gamma$ and a second one over partner trajectories $\gamma'$, which give rise to generic action differences $R_\gamma - R_{\gamma'}$, *i.e.* to action differences, which are independent on the disorder realization.

## 10.1 Diagonal approximation

The most obvious partner causing a generic action difference is of course again $\gamma'=\gamma$ leading to the diagonal approximation. Obviously, the actions of $\gamma$ and $\gamma'$ as well as the prefactors $\mathcal{B}_\gamma$ and $\mathcal{B}_{\gamma'}$ are equal. The sum rule (7.2) is valid for fermions, too, and therefore, the diagonal approximation to the transition probability for fermions is given by what will be called the classical transition probability,

$$P^{(\mathrm{cl})}\left(\mathbf{n}^{(f)},t_f;\mathbf{n}^{(i)},t_i\right)=$$
$$\int_0^{2\pi}\frac{\mathrm{d}^{N-1}\theta^{(i)}}{(2\pi)^{N-1}}\delta^{N-1}\left[\mathcal{P}_0^{(f)}\mathbf{n}\left(\mathbf{n}^{(i)},\boldsymbol{\theta}^{(i)};t_f\right)-\mathcal{P}_0^{(f)}\mathbf{n}^{(f)}\right]\left|\mathcal{B}\left(\mathbf{n}^{(i)},\boldsymbol{\theta}^{(i)}\right)\right|^2.$$

Here, $\mathbf{n}\left(\mathbf{n}^{(i)},\boldsymbol{\theta}^{(i)};t\right)$ is the vector containing the modulus squares of the time evolution of the initial state with the components

$$\phi^{(i)}_{l,\sigma}=\sqrt{n^{(i)}_{l,\sigma}}\exp\left(\mathrm{i}\theta^{(i)}_{l,\sigma}\right).$$

Moreover, $\mathcal{B}\left(\mathbf{n}^{(i)},\boldsymbol{\theta}^{(i)}\right)$ is given by $\mathcal{B}_\gamma$ defined in Eq. (5.15) for the trajectory $\gamma$ with initial phases $\boldsymbol{\theta}^{(i)}$ and can be considered as a renormalization of the classical probability due to vacuum fluctuations.

## 10.2 Coherent backscattering like contribution

For time reversal symmetric systems, a second possibility to chose the partner trajectory $\gamma'$, is the time reversed trajectory of $\gamma$, *i.e.* $\gamma' = \mathcal{T}\gamma$. In the example stated in Eq. (10.1), time reversal is achieved, if $J$ is real. However, here one has to be more careful with the time reversal operator as for bosonic systems, because it depends on the choice of the coupling $\alpha$. On the one hand, if $\alpha = 0$, which corresponds to having two copies of one and the same system of spinless fermions, the time reversal operator is - just as in the bosonic case - identical to complex conjugation, and one can follow section 7.1.2 to find that the transition probability is twice the classical one, if $\mathbf{n}^{(f)} = \mathbf{n}^{(i)}$, and equal to the classical one otherwise.

On the other hand in the presence of spin-orbit coupling, *i.e.* if $\alpha \neq 0$, the time reversal operator is given by

$$\mathcal{T} = -\mathrm{i}\sigma_y \hat{\mathcal{C}},$$

where $\sigma_y$ is the (many-body) $y$-Pauli matrix acting on spin space, and $\hat{\mathcal{C}}$ is complex conjugation in site-$|+z\rangle, |-z\rangle$ representation. Thus the time reverse of the trajectory $\gamma$ is achieved by the replacement

$$\begin{pmatrix} \phi_{l,\uparrow}(t_i + t) \\ \phi_{l,\downarrow}(t_i + t) \end{pmatrix} \longrightarrow \begin{pmatrix} -{\phi_{l,\downarrow}}^*(t_f - t) \\ {\phi_{l,\uparrow}}^*(t_f - t) \end{pmatrix}.$$

In particular this implies that the time reverse of the trajectory $\gamma$ starts at $\mathcal{X}\mathbf{n}^{(f)}$ and ends at $\mathcal{X}\mathbf{n}^{(i)}$, where $\mathcal{X}$ is the matrix, which exchanges the spin-up and spin-down components, while its initial and final phases satisfy

$$\begin{aligned} \theta_{l,\uparrow}^{(\mathcal{T}\gamma,i)} &= \pi - \theta_{l,\downarrow}^{(\gamma,f)} \\ \theta_{l,\downarrow}^{(\mathcal{T}\gamma,i)} &= -\theta_{l,\uparrow}^{(\gamma,f)} \\ \theta_{l,\uparrow}^{(\mathcal{T}\gamma,f)} &= \pi - \theta_{l,\downarrow}^{(\gamma,i)} \\ \theta_{l,\downarrow}^{(\mathcal{T}\gamma,f)} &= -\theta_{l,\uparrow}^{(\gamma,i)}. \end{aligned} \tag{10.2}$$

Similar to the bosonic case, pairing the trajectory $\gamma$ with its time reverse is only possible, if the final Fock state is the spin reversed of the initial one. Therefore, one has again to replace the trajectories $\gamma$ by nearby ones, which connect spin reversed Fock states. However, here the trajectories $\tilde{\gamma}$ used to replace $\gamma$ will be chosen somewhat differently than in the bosonic case, namely to start at $\mathbf{n}^{(i)}$ and end at $\mathcal{X}\mathbf{n}^{(f)}$, because in this way the origin of the final result is more transparent.

Using the relations of the initial and final phases of the time reversed trajectory with the ones of the original one, Eq. (10.2), leads to the action difference

$$R_\gamma - R_{\gamma'} \approx R_{\tilde{\gamma}} - R_{\mathcal{T}\tilde{\gamma}} + \hbar \left(\boldsymbol{\theta}^{(\tilde{\gamma},f)} - \boldsymbol{\theta}^{(\tilde{\gamma},i)}\right) \cdot \left(\mathbf{n}^{(f)} - \mathcal{X}\mathbf{n}^{(i)}\right).$$

Reminding oneself of the derivation of the semiclassical prefactors in section 5.2.2, it is clear that $\mathcal{B}_\gamma$ is the same for $\gamma$ and its time reverse $\mathcal{T}\gamma$, just as the second derivative of the action with respect to the initial and final occupation numbers is. Therefore

$$\begin{aligned} P^{(\mathrm{cbs})}\left(\mathbf{n}^{(f)}, t_f; \mathbf{n}^{(i)}, t_i\right) = \\ \frac{\delta_{TRI}}{(2\pi)^{N-1}} \sum_{\tilde{\gamma}:\mathbf{n}^{(i)}\to\mathcal{X}\mathbf{n}^{(i)}} |\mathcal{B}_{\tilde{\gamma}}|^2 \left|\det \frac{\partial P_0^{(i)} \boldsymbol{\theta}^{(\tilde{\gamma},i)}}{\partial\left(P_0^{(f)}\mathcal{X}\mathbf{n}^{(i)}\right)}\right| \exp\left[\frac{\mathrm{i}}{\hbar}\left(R_{\tilde{\gamma}} - R_{\mathcal{T}\tilde{\gamma}}\right)\right] \\ \exp\left[\mathrm{i}\left(\boldsymbol{\theta}^{(\gamma,f)} - \boldsymbol{\theta}^{(\gamma',i)}\right)\left(\mathbf{n}^{(f)} - \mathcal{X}\mathbf{n}^{(i)}\right)\right]. \end{aligned} \tag{10.3}$$

The next step is to determine the action difference $R_{\tilde{\gamma}} - R_{\mathcal{T}\tilde{\gamma}}$. Since the Hamiltonian is the same for a trajectory and its time reverse, this action difference is determined by the kinetic parts only,

$$\begin{aligned} R_{\tilde{\gamma}} - R_{\mathcal{T}\tilde{\gamma}} &= \hbar \int_\gamma \mathrm{d}\mathbf{n}\cdot\boldsymbol{\theta} - \hbar \int_{\mathcal{T}\gamma} \mathrm{d}\mathbf{n}\cdot\boldsymbol{\theta} \\ &= \hbar \int_\gamma \mathrm{d}\mathbf{n}\cdot\boldsymbol{\theta} - \hbar \sum_{l=1}^{L} \left[ \int_{t_i}^{t_f} \mathrm{d}t \left[\pi - \theta_{l,\uparrow}(T-t)\right] \frac{\partial}{\partial t} n_{l,\uparrow}(T-t) \right. \\ &\qquad \left. + \int_{t_i}^{t_f} \mathrm{d}t \left[-\theta_{l,\downarrow}(T-t)\right] \frac{\partial}{\partial t} n_{l,\downarrow}(T-t) \right] \\ &= \hbar\pi \sum_{l=1}^{L} \left(n_{l,\uparrow}^{(f)} - n_{l,\uparrow}^{(i)}\right), \end{aligned} \tag{10.4}$$

where $T = t_f + t_i$. Finally, for $\mathbf{n}^{(f)} = \mathcal{X}\mathbf{n}^{(i)}$, the action difference is given by

$$R_\gamma - R_{\mathcal{T}\gamma} = \pi\hbar \sum_{l=1}^{L} \left(n_{l,\downarrow}^{(i)} - n_{l,\uparrow}^{(i)}\right) = \pi\hbar N - 2\pi\hbar N^{(\uparrow)},$$

with $N^{(i,\uparrow)}$ the initial total number of spin-up particles. We find then that the action difference is equal to $\hbar\pi$ times an even (odd) number, if the total number of particles is even (odd). Thus, under disorder average, after averaging over the final phases, the coherent backscattering-like contribution to the transition probability for spin-$\frac{1}{2}$ particles becomes

$$P^{(\mathrm{cbs})}\left(\mathbf{n}^{(f)},t_f;\mathbf{n}^{(i)},t_i\right) = (-1)^N \delta_{TRI}\delta_{\mathbf{n}_\uparrow^{(f)},\mathbf{n}_\downarrow^{(i)}}\delta_{\mathbf{n}_\downarrow^{(f)},\mathbf{n}_\uparrow^{(i)}} P^{(\mathrm{cl})}\left(\mathbf{n}^{(f)},t_f;\mathbf{n}^{(i)},t_i\right),$$

and summing up the two leading order contributions yields

$$P\left(\mathbf{n}^{(f)},t_f;\mathbf{n}^{(i)},t_i\right) \approx \left[1+(-1)^N\delta_{TRI}\delta_{\mathbf{n}^{(f)},\mathcal{X}\mathbf{n}^{(i)}}\right] P^{(\mathrm{cl})}\left(\mathbf{n}^{(f)},t_f;\mathbf{n}^{(i)},t_i\right). \tag{10.5}$$

All in all, the average transition probability can be written as

$$P\left(\mathbf{n}^{(f)},t_f;\mathbf{n}^{(i)},t_i\right) \approx P^{(\mathrm{cl})}\left(\mathbf{n}^{(f)},t_f;\mathbf{n}^{(i)},t_i\right) \begin{cases} 1 & \text{GUE} \\ 1+\delta_{\mathbf{n}^{(f)}\mathbf{n}^{(i)}} & \text{GOE} \\ 1+(-1)^N\delta_{\mathbf{n}^{(f)},\mathcal{X}\mathbf{n}^{(i)}} & \text{GSE,} \end{cases}$$

where the notation of Random matrix symmetry classes [273] has been implied with GUE (gaussian unitary ensemble) denoting systems without time reversal invariance, GOE (gaussian orthogonal ensemble) time reversal symmetric systems without spin-orbit coupling and GSE (gaussian symplectic ensemble) those with both, time reversal symmetry and spin-orbit coupling. This result and the pairing of trajectories for each symmetry class is also summarized in Fig. 10.1.

## 10.3 Discussion

Eq. (10.5) says that the probability to measure a final Fock state which is the spin reversed of the initial one is zero if the total number of particles is odd, while it is twice the classical one if the total number of particles is even. As already stated above, this holds only if the system is time reversal symmetric and there is a spin coupling mechanism which allows the transformation of spin-up to spin-down particles and no further discrete symmetries exist. Without spin coupling, the result would be given by

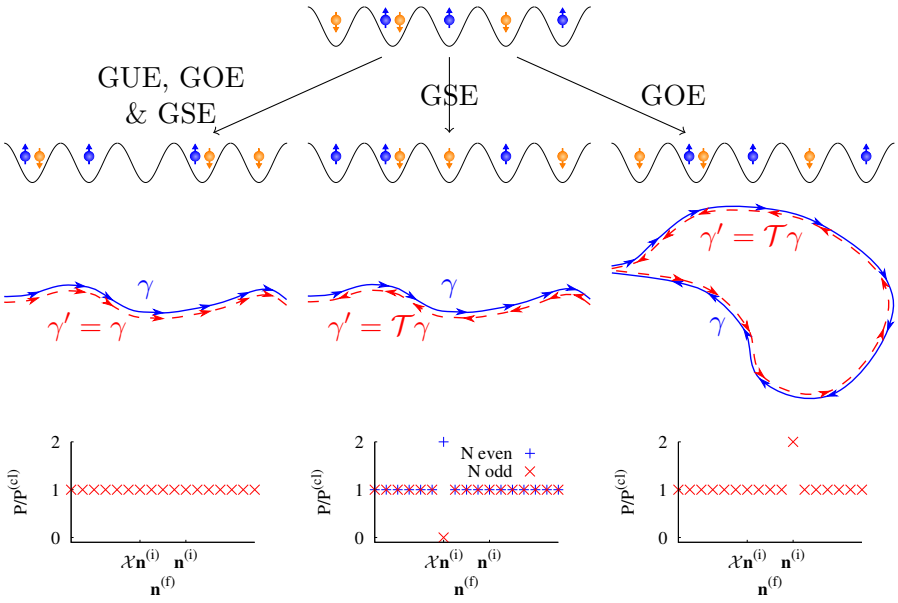


Figure 10.1: Summary of the transition probabilities. The diagonal pairing (left) is always possible, while the time reverse pairing (center and right) require time reversal symmetry and a certain final occupation. This final occupation has to be the same as the initial one for GOE (right) and the spin-reverse for the GUE (center) case. The three diagrams at the bottom show schematicaly the expected result of a measurement of the transition probability for (from left to right) GUE, GSE and GOE. In the GSE case, the result depends on whether the total number $N$ of particles is even or odd. If it is even, the probability gets enhanced by a factor of two for the spin-reverse of the initial state, while for odd $N$, the same transition is forbidden.

(7.3). The fact that for $\mathbf{n}^{(f)} = \mathcal{X}\mathbf{n}^{(i)}$, *i.e.* if the final Fock state is the spin-flipped version of the initial one, the averaged transition probability is zero and the transition probability itself is by construction a non-negative quantity, already implies that the transition probability is zero for every disorder realization. In fact, it can be shown exactly for any quantum system with a time-reversal operator, which squares to minus one, $\mathcal{T}^2 = -1$, that the transition probability between time reversed states is zero:

$$\begin{aligned}\langle \mathcal{T}\phi | \exp\left(-\frac{\mathrm{i}}{\hbar}\hat{H}t\right) |\phi\rangle &= \left\langle \mathcal{T}^2\phi \middle| \mathcal{T}\exp\left(-\frac{\mathrm{i}}{\hbar}\hat{H}t\right)\phi \right\rangle^* \\ &= (-1)^N \left\langle \phi \middle| \exp\left(\frac{\mathrm{i}}{\hbar}\hat{H}t\right)\mathcal{T}\phi \right\rangle^* \\ &= (-1)^N \langle \mathcal{T}\phi | \exp\left(-\frac{\mathrm{i}}{\hbar}\hat{H}t\right) |\phi\rangle .\end{aligned}$$

Therefore, for odd total number of particles

$$\langle \mathcal{T}\phi | \exp\left(-\frac{\mathrm{i}}{\hbar}\hat{H}t\right) |\phi\rangle = 0.$$

which is a much easier and more general way to show that for an odd number of half-integer spin systems the transition from an initial state to its time reverse (spin reverse) state vanishes. However, Eq. (10.5) on one hand shows that the semiclassical technique introduced here can reproduce the delicate phase coherences that produce even such an fundamental quantum mechanical result, although the classical probability for this transition may be non-zero. On the other hand, it is able to predict the result for an even number of particles, in which case the above argument tells nothing about the transition probability.

## 10.4 Further discrete symmetries

If the spin-orbit coupling strength fulfills further conditions, additional discrete symmetries may occur. For example, if $\alpha^* = \alpha$, the system is invariant under replacing all spin-up components by the negative of the spin-down ones and simultaneously replacing the spin-up by the spin-down components. If initially $n_{l,\uparrow}^{(i)} = n_{l,\downarrow}^{(i)}$ for every site $l$, which is possible only for an even total number of particles, there are two further possible partners for each trajectory, while in all the other cases there is one additional possible

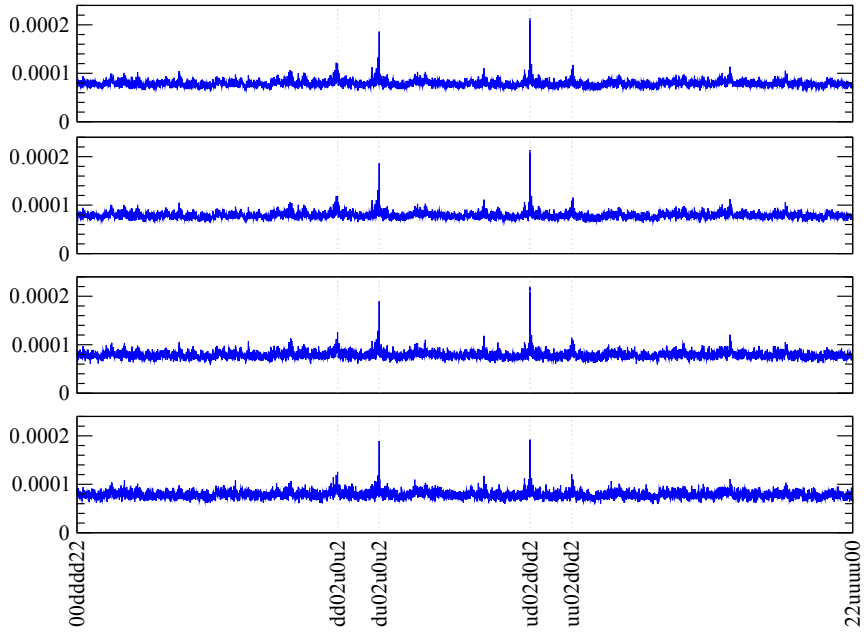


Figure 10.2: Numerical result for the transition probabilities after at $t = 50\hbar/(2J)$ for $N = 8$ particles in an 8-site Fermi-Hubbard-system, Eq. (10.1), with disorder strength $W = 2J$, interaction strength $U = J$, hopping strength $J = 0.5$ and spin orbit coupling strength $|\alpha| = J/5$. The phase of the spin orbit coupling was chosen to be (from top to bottom) $\varphi = 0$, $\pi/2$ , $\pi/4$ and $0.6214\pi$. The initial state was chosen to be given by the sequence ud02d02d2, where u and d stand for a spin-up and spin-down particle, respectively, in the corresponding site, 0 for an empty site and 2 for a doubly occupied one. The enhancement at the initial and its spin-flipped state are clearly visible. Figure by courtesy of Peter Schlagheck.

partner, determined by complex conjugating the trajectory and replacing $t$ by $t_f + t_i - t$. Following the above steps for this discrete symmetry, too, one finds

$$P\left(\mathbf{n}^{(f)}, t_f; \mathbf{n}^{(i)}, t_i\right) = \left[1 + (-1)^N \delta_{\mathbf{n}^{(f)}, \mathcal{X}\mathbf{n}^{(i)}} + \delta_{\mathbf{n}^{(i)}, \mathcal{X}\mathbf{n}^{(i)}} \delta_{\mathbf{n}^{(f)} \mathcal{X}\mathbf{n}^{(f)}} + \delta_{\mathbf{n}^{(f)}, \mathbf{n}^{(i)}}\right] \times P^{(\mathrm{cl})}\left(\mathbf{n}^{(f)}, t_f; \mathbf{n}^{(i)}, t_i\right). \tag{10.6}$$

In the same way, if $\alpha$ is completely imaginary, there is a symmetry towards exchanging spin-up and spin-down components if at the same time one of

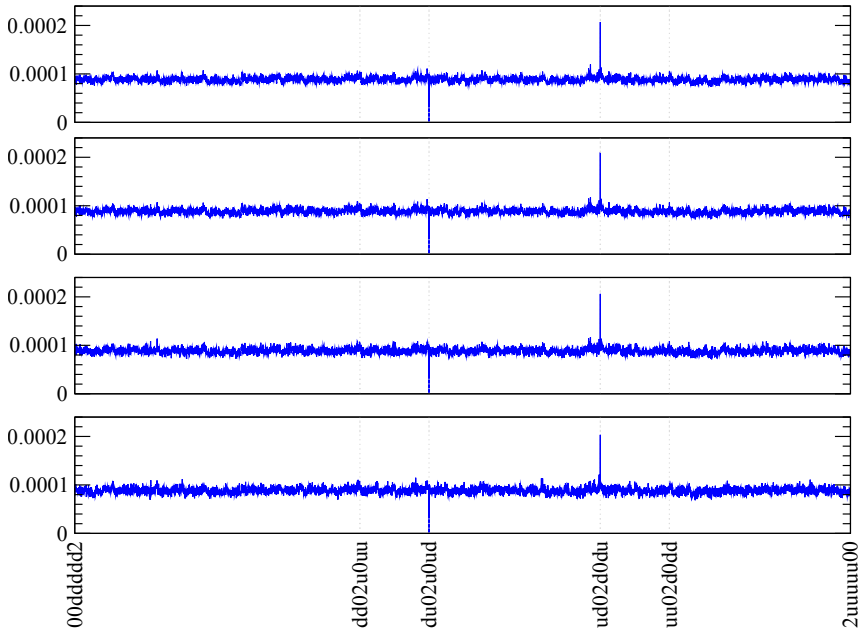


Figure 10.3: Numerical result for the transition probabilities at time $t = 50\hbar/(2J)$ for $N = 7$ particles in an 8-site Fermi-Hubbard-system, Eq. (10.1), with disorder strength $W = 2J$, interaction strength $U = J$, hopping strength $J = 0.5$ and spin orbit coupling strength $|\alpha| = J/5$. The phase of the spin orbit coupling was chosen to be (from top to bottom) $\varphi = 0$, $\pi/2$ , $\pi/4$ and $0.6214\pi$. The initial state was chosen to be given by the sequence ud02d02d2, where u and d stand for a spin-up and spin-down particle, respectively, in the corresponding site, 0 for an empty site and 2 for a doubly occupied one. The enhancement at the initial state as well as the vanishing probability for its spin-flipped version are clearly visible. Figure by courtesy of Peter Schlagheck.

the two components gets multiplied by $-1$. This leads again to additional partner trajectories and finally to Eq. (10.6).

In fact, the result keeps the same for any phase $\varphi$ of the coupling strength $\alpha = |\alpha| \exp(\mathrm{i}\varphi)$ as long as it does not become site dependent. This is because the classical Hamiltonian is invariant under the transformation

$$\begin{pmatrix} \boldsymbol{\psi}_\uparrow \\ \boldsymbol{\psi}_\downarrow \end{pmatrix} \to \begin{pmatrix} \boldsymbol{\psi}_\downarrow \mathrm{e}^{\mathrm{i}\varphi} \\ \boldsymbol{\psi}_\uparrow \mathrm{e}^{-\mathrm{i}\varphi} \end{pmatrix}.$$

As shown in Figs. 10.2 and 10.3, this prediction is nicely confirmed by numerical calculations obtained by Peter Schlagheck.

In general, each discrete symmetry will give rise to further partner trajectories (and therefore further additive terms in the transition probability), which require certain conditions on the initial and final Fock state. In the averaged transition probability, this condition will be reflected in a Kronecker delta. Moreover, the phase of this contribution will be determined by the difference in the kinetic parts of the actions. Since the result has to be a real number, this phase will either be an integer multiple of $\pi$ or each symmetry related partner will come in pairs such that each pair adds up to a real number.

CHAPTER 11

# Many-Body Spin Echo

## 11.1 The spin-echo setup

Since the prohibition of a transition from an initial Fock state to the one which is the spin reversed one for an odd number of spin-$\frac{1}{2}$ particles is no dynamical effect, and can be proven without any loss of generality by using $\mathcal{T}^2 = -1$, only the transition probability for fermions is a very nice check of the validity of the semiclassical approach presented here, but not more.

On the other hand, there is a very famous effect in single-particle systems based on constructive interference for spin-$\frac{1}{2}$ particles, namely the spin (or Hahn) echo [275], which is depicted in Fig. 11.1. In this spin-echo experiment, spins are first of all aligned in $z$-direction along a constant magnetic field (Fig. 11.1a). An intermediately applied radio frequency field then rotates the spins into $x$-direction (Fig. 11.1b), such that they start to precess around the $z$-axes (Fig. 11.1c). After some time $t$, again a radio-frequency field is applied, in order to ratate the spins by 180° around the $y$-axes (Fig. 11.1d). After letting the spins precess again for time $t$ (Fig. 11.1e), all the spins point again into the same direction (Fig. 11.1f), independently on the different local magnetic field.

It is expected that due to relaxation processes and spin decoherence, the echo signal at time $2t$, *i.e.* the enhancement of the probability of all spins pointing into the same direction shows a gaussian decay [276–279]. Many-body effects have been included up to now only by means of spin-

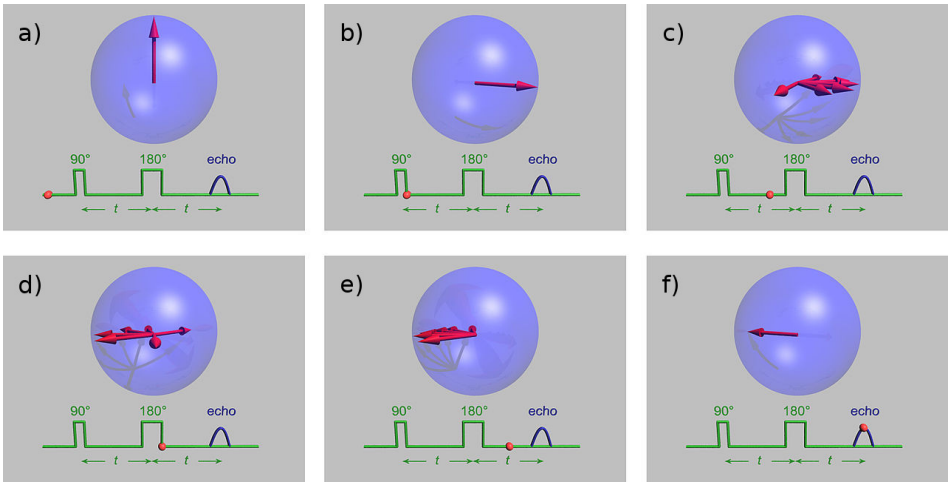


Figure 11.1: Conventional spin echo experiment (cf. [274])

chains [280, 281], while spin-orbit interactions have not been considered at all.

Here, these last two points will be adressed. The focus of this section is on an interacting fermionic many-body system with spin-orbit coupling. However, in contrast to the conventional spin echo experiment [275], time reversal invariant systems will be considered. To this end, a system described for instance by the Hamiltonian Eq. (10.1) is considered, with the parameters chosen such that the classical limit Eq. (5.2) is chaotic.

It is furthermore assumed that the system is initially prepared in a Fock state $\mathbf{n}^{(i)}$, for which the single-particle states are ordered such that for each orbital state the spin-down state follows the spin-up state,

$$|\mathbf{n}\rangle = |n_{1,\uparrow}, n_{1,\downarrow}, \ldots, n_{L,\uparrow}, n_{L,\downarrow}\rangle \,. \tag{11.1}$$

This initial Fock state is then evolved for some time $t_1$, after which, for a number $F$ of the single-particle states, labeled by $l_1, \ldots, l_F$, the spins are reversed without measuring the number of particles within this state. Mathematically, this spin flip can be described by the operator

$$\hat{A} = \prod_{j=1}^{F} \left[ \left(1 - \hat{n}_{l_j,\uparrow}\right) \left(1 - \hat{n}_{l_j,\downarrow}\right) + \hat{n}_{l_j,\uparrow}\hat{n}_{l_j,\downarrow} + \hat{c}^{\dagger}_{l_j,\uparrow}\hat{c}_{l_j,\downarrow} + \hat{c}^{\dagger}_{l_j,\downarrow}\hat{c}_{l_j,\uparrow} \right] . \tag{11.2}$$

In order to check that this linear operator indeed gives the correct spin-flip, one has to apply it to a Fock state $|\mathbf{n}\rangle$. Thereby, the $j$-th factor in

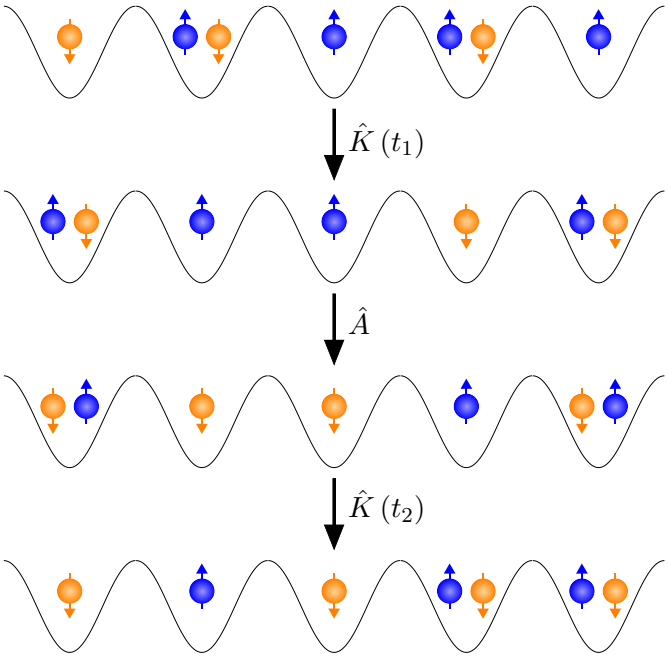


Figure 11.2: Schematic sketch of the procedure of the spin-echo experiment

the product acts on the $l_j$-th site only. The first term then is zero, if the $l_j$-th site is occupied, and equal to the unity operator on this site if it is empty. In the same way, the second term is equal to unity, if the $l_j$-th site is fully, *i.e.* doubly, occupied, and zero else. Now, the last two terms are zero if the corresponding site is fully occupied or empty, while if it is singly occupied, the spin-up and spin-down component are exchanged. Therefore, the operator $\hat{A}$ indeed resembles the desired spin flip. However, one has to keep in mind that due to the antisymmetric nature of fermions, this operator will also yield an additional sign, which depends on the Fock state, it is applied to and the choice of the ordering. Luckily, by the ordering chosen here, Eq. (11.1), these signs vanish.

The system is then let to evolve again for a time $t_2$ and the resulting Fock state is measured. For the example of spin-orbit coupled fermionic ultra-cold atoms in an optical lattice this procedure is depicted in Fig. 11.2. However, the system does not need to be an ultra-cold atom system, but can be any fermionic many-body system with spin-orbit interactions. The only requirements that will be made are the ergodicity of the classical Hamiltonian system and the invariance under the time reversal operator

$$\mathcal{T} = -\mathrm{i}\sigma_y \hat{\mathcal{C}},$$

where $\sigma_y$ is the Pauli matrix in $y$-direction and $\hat{\mathcal{C}}$ denotes complex conjugation.

## 11.2 Leading order contributions

The quantity analogous to the spin echo signal is the probability to measure a certain final Fock state $\mathbf{n}^{(f)}$, which is given by

$$P_{mbse}\left(\mathbf{n}^{(f)}, \mathbf{n}^{(i)}\right) = \left| \langle \mathbf{n}^{(f)} | \, \hat{K}\left(t_2\right) \hat{A} \hat{K}\left(t_1\right) | \mathbf{n}^{(i)} \rangle \right|^2,$$

where $\hat{K}(t)$ is the propagator of the system. Inserting a unity operator in terms of Fock states between $\hat{A}$ and $\hat{K}\left(t_1\right)$ and inserting the semiclassical approximation for the propagator, Eq. (5.14), then yields a four-fold sum over trajectories,

$$P_{mbse}\left(\mathbf{n}^{(f)}, \mathbf{n}^{(i)}\right) \approx \sum_{\mathbf{m},\mathbf{m}'} \sum_{\substack{\gamma_1:\mathbf{n}^{(i)}\to\mathbf{m} \\ \gamma_2:B\mathbf{m}\to\mathbf{n}^{(f)} \\ \gamma_3:\mathbf{n}^{(i)}\to\mathbf{m}' \\ \gamma_4:B\mathbf{m}'\to\mathbf{n}^{(f)}}} \mathcal{A}_{\gamma_1}\mathcal{B}_{\gamma_1}\mathcal{A}_{\gamma_2}\mathcal{B}_{\gamma_2}{\mathcal{A}_{\gamma_3}}^*{\mathcal{B}_{\gamma_3}}^*{\mathcal{A}_{\gamma_4}}^*{\mathcal{B}_{\gamma_4}}^*$$
$$\times \exp\left[\frac{\mathrm{i}}{\hbar}\left(R_{\gamma_1} + R_{\gamma_2} - R_{\gamma_3} - R_{\gamma_4}\right)\right],$$

where $B$ is the matrix, which exchanges the spin-up and spin-down components for those sites, for which the spin is flipped in between,

$$B = \begin{pmatrix} b_1 & & \\ & \ddots & \\ & & b_L \end{pmatrix}$$

$$b_l = \begin{cases} \begin{pmatrix} 1 & 0 \\ 0 & 1 \end{pmatrix} & \text{if} \quad l \notin \{l_1, \ldots, l_F\} \\ \begin{pmatrix} 0 & 1 \\ 1 & 0 \end{pmatrix} & \text{if} \quad l \in (l_1, \ldots, l_F) \end{cases}$$

Under disorder average, one has to find those combinations of trajectories such that a trajectory contributing with a positive sign to the action difference in the exponential is paired by one, which contributes with a negative

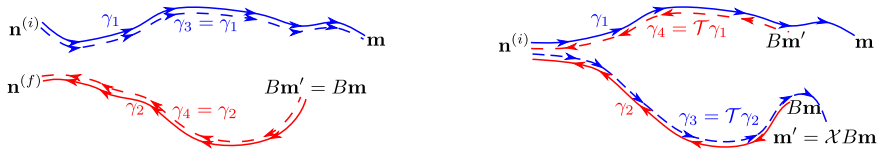


Figure 11.3: Leading order contributions to the many-body spin-echo probability.

sign. Neglecting all loop contributions, which have been introduced very briefly in section 7.1.3 and are discussed in more detail in Appendix F, this leaves in total eight possibilities for pairing. However, there are only two possibilities, for which one of the sums over intermediate occupations $\mathbf{m}$ and $\mathbf{m}'$ survives, and which therefore yield the leading order contribution. These two possibilities, which will be called incoherent and coherent contribution, are shown in Fig. 11.3. Note that the labeling as incoherent and coherent contribution refers only to the many-body coherence, which is not incorporated in the classical limit.

The incoherent contribution, Fig. 11.3(a) is the diagonal approximation obtained by pairing $\gamma_1 = \gamma_3$ and $\gamma_2 = \gamma_4$, which is obviously only possible, if the intermediate occupations are equal, $\mathbf{m}' = \mathbf{m}$, but does not require any further conditions.

Using the definition of the classical transition probability in section 10.1, the diagonal approximation yields the classical or incoherent many-body spin-echo probability

$$\begin{aligned} P_{mbse}^{(\mathrm{incoh})}\left(\mathbf{n}^{(f)}, \mathbf{n}^{(i)}; t_1, t_2\right) &= \sum_{\mathbf{m}} P^{(\mathrm{cl})}\left(\mathbf{n}^{(f)}, \mathbf{m}; t_2\right) P^{(\mathrm{cl})}\left(\mathbf{m}, \mathbf{n}^{(i)}; t_1\right) \\ &= P_{mbse}^{(\mathrm{cl})}\left(\mathbf{n}^{(f)}, \mathbf{n}^{(i)}; t_1, t_2\right), \end{aligned}$$

which can be assumed to be approximately constant for all combinations of $\mathbf{n}^{(f)}$, $\mathbf{n}^{(i)}$, $t_1$ and $t_2$, as long as the initial and final occupations are such that the particles are sufficiently distributed and $t_1$ and $t_2$ are large enough that the particles have been able to move.

The crosswise pairing shown in Fig. 11.3(b) of $\gamma_1$ with the time reverse of $\gamma_4$ as well as $\gamma_2$ with the time reverse of $\gamma_3$ is possible only if the two times $t_1$ and $t_2$ are comparable. Therefore the coherent contribution arises only for $t_1 \sim t_2$. Moreover, it requires that the final Fock state is the time reverse version of the initial one, $\mathbf{n}^{(f)} = \mathcal{X}\mathbf{n}^{(i)}$, where $\mathcal{X}$ is the matrix,

which flips all spins,

$$\mathcal{X} = \begin{pmatrix} 0 & 1 & & & \\ 1 & 0 & & & \\ & & \ddots & & \\ & & & 0 & 1 \\ & & & 1 & 0 \end{pmatrix}. \tag{11.3}$$

In other words, the final occupations have to be equal to the initial one with all spin-up and spin-down particles exchanged. Moreover, according to Eq. (10.4), the phase accumulated by this pairing is given by

$$R_{\gamma_1} - R_{\mathcal{T}\gamma_1} + R_{\gamma_2} - R_{\mathcal{T}\gamma_2} = \hbar \sum_{l=1}^{L} \left[ m_{l,\uparrow} - n_{l,\uparrow}^{(i)} + n_{l,\uparrow}^{(f)} - (B\mathbf{m})_{l,\uparrow} \right]$$

such that, to leading order for $t_1 = t_2$, the many-body spin echo probability is given by

$$P_{mbse}^{(\mathrm{coh})}\left(\mathbf{n}^{(f)}, \mathbf{n}^{(i)}; t_1, t_2 = t_1\right) = \delta_{\mathbf{n}^{(f)}, \mathcal{X}\mathbf{n}^{(i)}} \sum_{\mathbf{m}} P_{mbse}^{(\mathrm{cl})}\left(\mathbf{n}^{(f)}, \mathbf{n}^{(i)}; t_1, t_2\right) \times (-1)^{N + \sum_{j=1}^{F} \left(m_{l_j,\uparrow} - m_{l_j,\downarrow}\right)},$$

where the fact that $m_{l,\uparrow} - (B\mathbf{m})_{l,\uparrow} = 0$ for $l \notin \{l_1, \ldots, l_F\}$ as well as that the difference in the total number of spin-up and spin-down particles is odd, if and only if the total number of particles is odd has been used. Thus, the sign of the coherent contribution to the leading order many-body spin-echo is negative if either the total number of particles is even and the number of intermediately flipped spins is odd or vice versa, and positive otherwise.

Assuming that, following classical ergodicity, the classical transition probability is independent of the intermediate state $\mathbf{m}$, one can easily estimate the overall size of the second term by simple combinatorics. For this, it is convenient to get rid of the $N$-dependence, which is possible by using

$$\sum_{j=1}^{F} m_{l_j,\downarrow} = N - \sum_{j=1}^{F} m_{l_j,\uparrow} - \sum_{l \notin \{l_1,\ldots,l_F\}} (m_{l,\uparrow} + m_{l,\downarrow}).$$

Thus, the second term contributes with a positive sign if the number of particles whose spins are not flipped is even, and is negative otherwise. Thus, one only has to count the numbers $\mathcal{N}_{even}$ and $\mathcal{N}_{odd}$ of possible occupations

**m**, for which the number of particles to which the spin-flip is not applied if even and odd, respectively. These numbers are given by

$$\begin{aligned}\mathcal{N}_{odd} &= \sum_{k=1}^{\lceil \frac{N}{2} \rceil} \binom{2(L-F)}{2k-1} \binom{2F}{N-2k+1}, \\ \mathcal{N}_{even} &= \sum_{k=0}^{\lfloor \frac{N}{2} \rfloor} \binom{2(L-F)}{2k} \binom{2F}{N-2k},\end{aligned} \tag{11.4}$$

and thus give the coherent contribution for $t_1 = t_2$

$$P^{(\mathrm{coh})}_{mbse}\left(\mathbf{n}^{(f)}, \mathbf{n}^{(i)}; t_1, t_2 = t_1\right) = \delta_{\mathbf{n}^{(f)}, \mathcal{X}\mathbf{n}^{(i)}} P^{(\mathrm{cl})}_{mbse}\left(\mathbf{n}^{(f)}, \mathbf{n}^{(i)}; t_1, t_1\right) \times \frac{(\mathcal{N}_{even} - \mathcal{N}_{odd})}{\mathcal{N}}$$

with $\mathcal{N} = \mathcal{N}_{even} + \mathcal{N}_{odd}$ being the number of occupations $\mathbf{m}$ with total number of particles $N$.

What is left now is the time dependence of the coherent contribution to the echo signal, *i.e.* the dependence on the echo time $\tau = t_2 - t_1$ if $\tau \neq 0$. In this case the pairing of the trajectories requires to replace the trajectories $\gamma_2$ and $\gamma_4$ by trajectories, which evolve for time $t_1$ instead of $t_2$ and expand their actions in the exponential up to first order in $\tau$. Using

$$\frac{\partial R_\gamma\left(\mathbf{n}^{(f)}, \mathbf{n}^{(i)}; t\right)}{\partial t} = -E_\gamma,$$

which can be proven using the equations of motion and the fact that the final occupations of both trajectories have to be the same, yields an additional phase $\exp\left(\mathrm{i}\Delta E\tau/\hbar\right)$ for the coherent contribution, where $\Delta E$ is the difference between the hopping terms in the energies of $\gamma_3$ and $\gamma_1$. This difference solely stems from the different final phases of the two trajectories, and therefore can be assumed to be on average uniformly distributed between $\pm\mathcal{E}$. For a chain with nearest neighbor-hopping, $\mathcal{E}$ is given then by

$$\mathcal{E} = 2\kappa \sum_{l=1}^{L-1} \sum_{\sigma=\uparrow,\downarrow} \sqrt{n_{l,\sigma} n_{l+1,\sigma}} \exp(-n_{l,\sigma} - n_{l+1,\sigma}),$$

where $\kappa$ is the hopping parameter. This finally yields the leading order many-body spin-echo probability for small enough $\tau$,

$$P_{mbse}\left(\mathbf{n}^{(f)},\mathbf{n}^{(i)};t_1,t_2=t_1+\tau\right)= \left[1+\frac{(\mathcal{N}_{even}-\mathcal{N}_{odd})}{\mathcal{N}}\frac{\sin\left(\frac{\mathcal{E}}{\hbar}\tau\right)}{\frac{\mathcal{E}}{\hbar}\tau}\delta_{\mathbf{n}^{(f)},\mathcal{X}\mathbf{n}^{(i)}}\right]P^{(\mathrm{cl})}_{mbse}\left(\mathbf{n}^{(f)},\mathbf{n}^{(i)};t_1,t_1\right). \tag{11.5}$$

Thus as in the conventional spin echo, there is an echo signal, which is an change of the probability to measure a certain Fock state compared to all the others, if the second evolution time $t_2$ is of the same order as the first one $t_1$. The time width during which the probability is enhanced, can be expected to be typically inverse proportional to the total number of particles through $\mathcal{E}$.

With this result at hand, one can consider the special case that no spins are flipped, *i.e.* $F=0$. In this case, $B$ becomes the $2L\times 2L$ unit matrix, $B=\mathbb{I}_{2L}$, and it is easy to see that the many body spin echo probability, Eq. (11.5), recovers for $\tau=0$ the result for the transition probability for GSE, Eq. (10.5). For $\tau\neq 0$, on the other hand, this is no longer true. At first glance, this seems to be a contradiction to the result of Chapter 10, which yields for long enough times a time independent result. Thus, in the absence of spin-flips, the coherent contribution should be treated somewhat differently, in order to obtain the semigroup property.

## 11.3 No spin-flips: Semigroup property

In order to recover the semigroup property, the crosswise pairing has to be done in the way depicted in Fig. 11.4, *i.e.* by pairing $\gamma_1=\mathcal{T}\gamma_4$ and $\gamma_2=\mathcal{T}\gamma_3$. Note that in this case, the durations of the paired trajectories are in general not equal. Thus if $t_1\neq t_2$, the pairing $\gamma_1=\mathcal{T}\gamma_4$ should be understood as chosing the initial conditions of $\gamma_4$ equal to the time reverse of the final conditions of $\gamma_1$,

$$\boldsymbol{\psi}^{(\gamma_4)}(0)=\mathcal{X}\boldsymbol{\psi}^{(\gamma_1)^*}(t_1),$$

where $\mathcal{X}$ is given by Eq. (11.3). This initial condition $\boldsymbol{\psi}^{(\gamma_4)}(0)$ is then classically evolved up to time $t_2$. The same construction holds for $\gamma_3$. Note that this procedure is not possible in the case with spin flips, since a spin

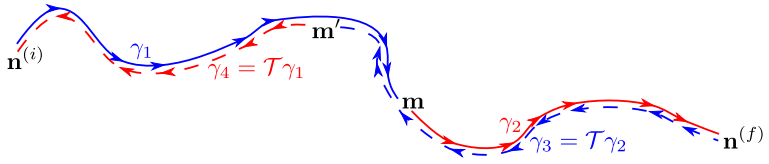


Figure 11.4: Coherent contribution to the many-body spin echo without spin flips.

flip would move the starting points of $\gamma_2$ and $\gamma_4$ away from the ending points of $\gamma_1$ and $\gamma_3$, respectively.

As can be seen from Fig. 11.4, this construction then requires that the trajectory $\gamma_2$ is the continuation of $\gamma_1$ and $\gamma_4$ the continuation of $\gamma_3$. In that way, this pairing coincides with the usual proof of the semigroup property for the semiclassical propagator by means of a stationary phase approximation [15, 282, 283], where the stationarity condition selects those trajectories, where the second is the continuation of the first one.

However, this in turn means that for instance if $t_1 > t_2$ the trajectory $\gamma_1$, which is fixed by the occupations $\mathbf{n}^{(i)}$ and $\mathbf{m}$, already determines $\mathbf{m}' = \mathcal{X}\mathbf{n}^{(\gamma_1)}(t_2)$, where $n_l^{(\gamma)}(t) = \left|\psi_l^{(\gamma)}(t)\right|$. The thus determined $\mathbf{m}'$, on the other hand, does not have to have integer entries. Therefore in order to pair in the discussed way, $\gamma_3$ and $\gamma_4$ will have to be replaced by nearby trajectories with final and initial occupations given by $\mathcal{X}\mathbf{n}^{(\gamma_1)}(t_2)$. During this replacement, the action in the phase of the propagator would have to be expanded up to first order in the difference $\mathbf{m}' - \mathcal{X}\mathbf{n}^{(\gamma_1)}(t_2)$, which however cancels, since $\boldsymbol{\psi}^{(\gamma_4)}(0) = \boldsymbol{\psi}^{(\gamma_3)}(t_2)$.

Finally, this kind of pairing requires that the initial occupation is the time reverse version of the final one, $\mathbf{n}^{(f)} = \mathcal{X}\mathbf{n}^{(i)}$, such that following section 10.2, the contribution of the crosswise time-reverse pairing is given by

$$P^{(coh)}\left(\mathbf{n}^{(f)}, \mathbf{n}^{(i)}; t_1, t_2\right) = (-1)^N \sum_{\mathbf{m}} P^{(cl)}\left(\mathbf{n}^{(f)}, \mathbf{m}; t_2\right) P^{(cl)}\left(\mathbf{m}, \mathbf{n}^{(i)}; t_1\right) \delta_{\mathbf{n}^{(f)}, \mathcal{X}\mathbf{n}^{(i)}},$$

such that to leading order the transition probability, Eq. (10.5), is obtained, yielding the validity of the semigroup property of the semiclassical propagator in fermionic Fock sapce.

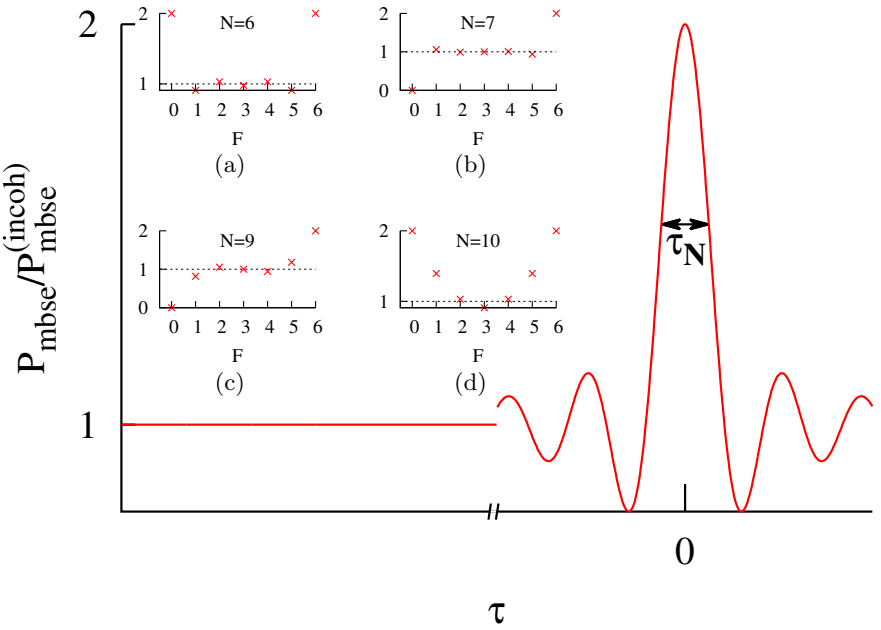


Figure 11.5: Time dependence of the the many-body spin echo for the case of flipping all spins and $\mathbf{n}^{(f)} = \mathcal{X}\mathbf{n}^{(i)}$. Insets: Size of the coherent contribution at $t_2 = t_1$ for a six single-particle states with (a) six, (b) seven, (c) nine and (d) ten particles. as a function of the number $F$ of single-particle states, for which the spins are flipped.

## 11.4 Discussion of the results

With the peace of mind we get since the result Eq. (11.5) does not contradict with the calculations of the transition probability, one can continue to discuss the results. To this end, let's start with the second obvious case of $F = L$, in which all the spins are flipped, such that also $B = \mathcal{X}$. Then, obviously, the coherent contribution has a positive sign for every intermediate occupation $\mathbf{m}$ no matter whether the total number of particles is even or odd, and the probability to measure at time $2t_1$ the spin-reverse of the initial Fock state is twice the classical one,

$$P_{mbse}\left(\mathbf{n}^{(f)}, \mathbf{n}^{(i)}; t_1, t_2 = t_1 + \tau\right) = \left[1 + \frac{\sin\left(\frac{\mathcal{E}}{\hbar}\tau\right)}{\frac{\mathcal{E}}{\hbar}\tau}\delta_{\mathbf{n}^{(f)}, T\mathbf{n}^{(i)}}\right] P^{(incoh)}_{mbse}\left(\mathbf{n}^{(f)}, \mathbf{n}^{(i)}; t_1, t_1\right).$$

One might then expect that the size of the coherent contribution changes for an odd number of particles monotonous from $-P_{mbse}^{(incoh)}$ to $+P_{mbse}^{(incoh)}$, when increasing the number of single-particle states, for which the spins are flipped. For an even number of particles, one might expect that it first decreases monotonously until it reaches a minimum and then increases again. However, $\mathcal{N}_{even} - \mathcal{N}_{odd}$ depends highly non-linearly on $F$. In fact, it may jump from positive to negative when changing $F$ to $F+1$ and again to positive when flipping a further single-particle state as is demonstrated for the case of six single-particle states by the insets (a) and (b) of Fig. 11.5 for six and seven particles, respectively. Finally it is worth to note that even for an even number of particles, it is possible to chose $L$ and $F$ in such a way that the coherent contribution becomes negative such as for the case of six and ten particles in six single-particle states (see insets (a) and (d) of Fig. 11.5). However, the negative value is often very small, such that it is questionable whether this reduction can indeed be observed. For some combinations, it is even possible to get a vanishing coherent contribution, as shown in insets (b) and (c) of Fig. 11.5.

Another remarkable observation is that the time dependence is given by an oscillatory function, although again it is not clear, whether the approximations made in order to obtain this time dependence are still valid for large enough $\tau$, in order to see these oscillations. However, the fact that the coherent contribution is only present in a time window, with a width decreasing when increasing the total number of particles (see Fig. 11.5), clearly identifies the observed effect as an echo.

## 11.5 Concluding remarks

### *11.5.1 Higher order contributions*

It is furthermore surprising that to leading order, only the probability for $\mathbf{n}^{(f)} = \mathcal{X}\mathbf{n}^{(i)}$ is affected, while all the others stay constant. Thus, in presence of spin-flips, the many-body spin-echo probability in Eq. (11.5) is clearly not correctly normalized: when summing over all possible $\mathbf{n}^{(f)}$, the result will be different from one. However, the difference between this sum and 1 is typically small and of the order of the sum over the next-to-leading order contributions.

Similar issues arised in single particle semiclassics, among them the normalization of the transmission coefficients of an open cavity. There, the

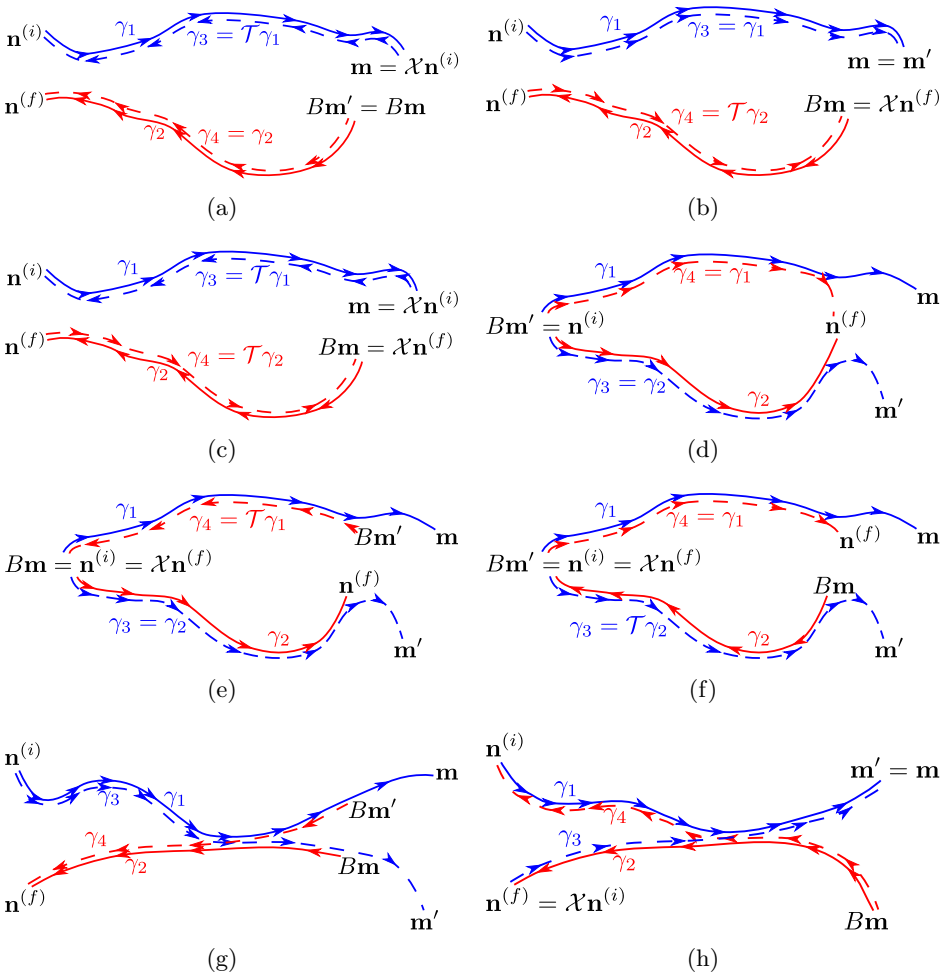


Figure 11.6: Next-to-leading order contributions to the many-body spin-echo probability

loop contributions have been found to solve this problem [21].

These next-to-leading order contributions stem from the six remaining diagrams, where ever two trajectories are the same or time reverse of each other (see Figs. 11.6(a)-(f)), as well as the two diagrams with a two-encounter, for which the sum over the intermediate occupations survives, Figs. 11.6(g),(h).

Concerning the loop contributions, *i.e.* the latter two, it should be noted that one-leg- and no-leg-loops (see Appendix F) do not arise here, since – after replacing $\gamma_2$ and $\gamma_4$ by nearby trajectories with propagation time $t_1$

– all four trajectories are evolved for the same time, which in turn requires that if one trajectory starts or ends during traversing the encounter the remaining three also do. However, this case is already included in the remaining eight diagrams, Figs. 11.3,11.6(a)-(f).

The contributions from the diagonal like diagrams can be easily calculated in the same way as the incoherent and coherent contribution above, while the computation of the loop contributions needs a little bit more care, since now there are two sources of action difference, which are the pairing of time reverse links on the one hand, and the encounter itself on the other. Consider for example diagram 11.6(g), where $\gamma_2$ follows the time reverse of $\gamma_3$ and $\gamma_4$ the time reverse of $\gamma_1$ from the initial until the time, where they enter the encounter, which shall be denoted as $t_0$. The action difference stemming from these two links is according to Eq. (10.4) given by

$$\pi\hbar \sum_{l=1}^{L} \left[ \left| \psi_{l,\uparrow}^{(\gamma_2)}(t_0) \right|^2 - (B\mathbf{m})_{l,\uparrow} - \left| \psi_{l,\uparrow}^{(\mathcal{T}\gamma_1)}(t_0) \right|^2 + \left(B\mathbf{m}'\right)_{l,\uparrow} \right].$$

The differences between $\gamma_4$ and $\gamma_2$ within the encounter, however are small, such that one can neglect the difference in their occupations, when entering the encounter,

$$\left| \psi_{l,\uparrow}^{(\gamma_2)}(t_0) \right|^2 - \left| \psi_{l,\uparrow}^{(\mathcal{T}\gamma_1)}(t_0) \right|^2 \approx 0.$$

Furthermore using the condition on the intermediate occupations required by this diagram, $\mathcal{X}B\mathbf{m}' = \mathbf{m}$, the action difference originating from the links is given by

$$\pi\hbar \sum_{l=1}^{L} \left[ (\mathcal{X}\mathbf{m})_{l,\uparrow} - (B\mathbf{m})_{l,\uparrow} \right].$$

In order to evaluate the contribution of the encounter, one has to keep in mind that, as discussed above, on the one hand all four links need to have positive duration, and on the other hand, if one link vanishes, the second vanishes, too. Thus the density of phase space separations, Eq. (F.12), here has to be replaced by

$$w(\mathbf{s}, \mathbf{u}) = \frac{t_1 - t_{enc}}{\Omega_N t_{enc}}$$

which yields for the contribution of Fig. 11.6(g)

$$P^{(\mathrm{g})}_{mbse}\left(\mathbf{n}^{(f)},\mathbf{n}^{(i)};t_1,t_2\right) = \sum_{\mathbf{m}} (-1)^{\sum_{l=1}^{L}[(\mathcal{X}-B)\mathbf{m}]_{l,\uparrow}} P^{(\mathrm{cl})}\left(\mathbf{n}^{(f)},B\mathbf{m};t_2\right) P^{(\mathrm{cl})}\left(\mathbf{m},\mathbf{n}^{(i)};t_1\right) \times \int_{-c}^{c} \mathrm{d}^{2L-2}u \int_{-c}^{c} \mathrm{d}^{2L-2}s \frac{t_1-t_{enc}}{\Omega_N t_{enc}} \exp\left(\mathrm{i}N\mathbf{s}\cdot\mathbf{u}\right).$$

The integral over the stable and unstable components can then be performed following section 7.1.3, and the contribution of Fig. 11.6(h) can be calculated similarly.

The next-to-leading order contributions are therefore found to read

$$P^{(\mathrm{a})}_{mbse}\left(\mathbf{n}^{(f)},\mathbf{n}^{(i)};t_1,t_2\right)=P^{(\mathrm{cl})}\left(\mathbf{n}^{(f)},B\mathcal{X}\mathbf{n}^{(i)};t_2\right)P^{(\mathrm{cl})}\left(\mathcal{X}\mathbf{n}^{(i)},\mathbf{n}^{(i)};t_1\right)\times(-1)^N$$

$$P^{(\mathrm{b})}_{mbse}\left(\mathbf{n}^{(f)},\mathbf{n}^{(i)};t_1,t_2\right)=P^{(\mathrm{cl})}\left(\mathbf{n}^{(f)},\mathcal{X}\mathbf{n}^{(f)};t_2\right)P^{(\mathrm{cl})}\left(B\mathcal{X}\mathbf{n}^{(f)},\mathbf{n}^{(i)};t_1\right)\times(-1)^N$$

$$P^{(\mathrm{c})}_{mbse}\left(\mathbf{n}^{(f)},\mathbf{n}^{(i)};t_1,t_2\right)=P^{(\mathrm{cl})}\left(\mathbf{n}^{(f)},\mathcal{X}\mathbf{n}^{(f)};t_2\right)P^{(\mathrm{cl})}\left(T\mathbf{n}^{(i)},\mathbf{n}^{(i)};t_1\right)\times\delta_{\mathbf{n}^{(f)},B\mathbf{n}^{(i)}}$$

$$P^{(\mathrm{d})}_{mbse}\left(\mathbf{n}^{(f)},\mathbf{n}^{(i)};t_1,t_2\right)=P^{(\mathrm{cl})}\left(\mathbf{n}^{(f)},\mathbf{n}^{(i)};t_2\right)P^{(\mathrm{cl})}\left(\mathbf{n}^{(f)},\mathbf{n}^{(i)};t_1\right)\times\frac{\sin\left(\frac{\mathcal{E}}{\hbar}\tau\right)}{\frac{\mathcal{E}}{\hbar}\tau}\delta_{\mathbf{n}^{(f)},B\mathbf{n}^{(i)}}$$

$$P^{(\mathrm{e})}_{mbse}\left(\mathbf{n}^{(f)},\mathbf{n}^{(i)};t_1,t_2\right)=P^{(\mathrm{cl})}\left(\mathbf{n}^{(f)},\mathbf{n}^{(i)};t_2\right)P^{(\mathrm{cl})}\left(B\mathbf{n}^{(i)},\mathbf{n}^{(i)};t_1\right)\times(-1)^{\sum_{l=1}^{L}\left[(B-\mathbb{I}_{2L})\mathbf{n}^{(i)}\right]_{l,\uparrow}}\frac{\sin\left(\frac{\mathcal{E}}{\hbar}\tau\right)}{\frac{\mathcal{E}}{\hbar}\tau}\delta_{\mathbf{n}^{(f)},\mathcal{X}\mathbf{n}^{(i)}}$$

$$P^{(\mathrm{f})}_{mbse}\left(\mathbf{n}^{(f)},\mathbf{n}^{(i)};t_1,t_2\right)=P^{(\mathrm{cl})}\left(\mathbf{n}^{(f)},B\mathbf{n}^{(f)};t_2\right)P^{(\mathrm{cl})}\left(\mathbf{n}^{(f)},\mathbf{n}^{(i)};t_1\right)\times(-1)^{\sum_{l=1}^{L}\left[(\mathbb{I}_{2L}-B)\mathbf{n}^{(f)}\right]_{l,\uparrow}}\frac{\sin\left(\frac{\mathcal{E}}{\hbar}\tau\right)}{\frac{\mathcal{E}}{\hbar}\tau}\delta_{\mathbf{n}^{(f)},\mathcal{X}\mathbf{n}^{(i)}}$$

$$P^{(\mathrm{g})}_{mbse}\left(\mathbf{n}^{(f)},\mathbf{n}^{(i)};t_1,t_2\right)=-\sum_{\mathbf{m}}P^{(\mathrm{cl})}\left(\mathbf{n}^{(f)},B\mathbf{m};t_2\right)P^{(\mathrm{cl})}\left(\mathbf{m},\mathbf{n}^{(i)};t_1\right)\times(-1)^{\sum_{l=1}^{L}[(\mathcal{X}-B)\mathbf{m}]_{l,\uparrow}}\left(\frac{2\pi}{N}\right)^{2L-2}\frac{1}{2\Omega_N}\frac{\sin\left(\frac{\mathcal{E}}{\hbar}\tau\right)}{\frac{\mathcal{E}}{\hbar}\tau}$$

$$P^{(\mathrm{h})}_{mbse}\left(\mathbf{n}^{(f)},\mathbf{n}^{(i)};t_1,t_2\right)=-\left(\frac{2\pi}{N}\right)^{2L-2}\frac{(-1)^N}{2\Omega_N}P^{(\mathrm{cl})}_{mbse}\left(\mathbf{n}^{(f)},\mathbf{n}^{(i)};t_1,t_2\right)\times\delta_{\mathbf{n}^{(f)},\mathcal{X}\mathbf{n}^{(i)}}$$

One can expect that

$$\sum_{\mathbf{m}}^{(N)}\left(\frac{2\pi}{N}\right)^{2L-2}\frac{1}{2\Omega_N}=\mathcal{O}(1),$$

which a posteriori justifies, the consideration of the diagrams 11.6(g),(h), in the next-to leading order. When considering the normalization of the

many-body spin-echo probability, this assumption becomes even more evident by noticing that when summing over the final occupations, only the diagrams 11.6(a),(b) and (g) can be of next-to-leading order and therefore of the same order as the coherent contribution. Futhermore, from these three contributions only the last one has the same time-dependence as the coherent contribution, and can therefore cancel it. The remaining two contributions $P^{((a))}_{mbse}$ and $P^{((b))}_{mbse}$ then restore the original value of the normalization up to next-to-leading order.

### *11.5.2 Incomplete spin flips*

Since the occupations should not be measured when applying the spin flip, it may be that it is incomplete, *i.e.* that the spins are not completely flipped but brought into a superposition of up and down, such that the measured object is given by

$$\begin{aligned} P'_{mbse}\left(\mathbf{n}^{(f)},\mathbf{n}^{(i)};t_2,t_1\right) &= \left|\langle\mathbf{n}^{(f)}|\,\hat{K}\left(t_2\right)\left(\alpha+\beta\hat{A}\right)\hat{K}\left(t_1\right)|\mathbf{n}^{(i)}\rangle\right|^2 \\ &= |\alpha|^2\,P\left(\mathbf{n}^{(f)},\mathbf{n}^{(i)};t_1+t_2\right)+|\beta|^2\,P_{mbse}\left(\mathbf{n}^{(f)},\mathbf{n}^{(i)};t_1,t_2\right) \\ &\quad + 2\Re\alpha\beta^*\left\langle\mathbf{n}^{(f)}\left|\,\hat{K}\left(t_2+t_1\right)\right|\mathbf{n}^{(i)}\right\rangle\left\langle\mathbf{n}^{(f)}\left|\,\hat{K}\left(t_2\right)\hat{A}\hat{K}\left(t_1\right)\right|\mathbf{n}^{(i)}\right\rangle^*, \end{aligned}$$

with $0\leq|\alpha|,|\beta|\leq 1$ as well as $|\alpha+\beta|^2=1$. Here, $P(\mathbf{n}^{(f)},\mathbf{n}^{(i)};t_2+t_1)$ is the transition probability from $\mathbf{n}^{(i)}$ to $\mathbf{n}^{(f)}$ when evolving the system for time $t_1+t_2$ according to Chapter 10, and $P_{mbse}$ is the many-body spin-echo probability computed before in Eq. (11.5). Thus, one only has to determine the last term which after inserting the semiclassical approximation for the propagator, Eq. (5.14), is given by a sum over three trajectories,

$$\begin{aligned} &\left\langle\mathbf{n}^{(f)}\left|\,\hat{K}\left(t_2+t_1\right)\right|\mathbf{n}^{(i)}\right\rangle\left\langle\mathbf{n}^{(f)}\left|\,\hat{K}\left(t_2\right)\hat{A}\hat{K}\left(t_1\right)\right|\mathbf{n}^{(i)}\right\rangle^* = \\ &\qquad\sum_{\mathbf{m}}\sum_{\gamma_0:\mathbf{n}^{(i)}\to\mathbf{n}^{(f)}}\sum_{\substack{\gamma_1:\mathbf{n}^{(i)}\to\mathbf{m}\\ \gamma_2:B\mathbf{m}\to\mathbf{n}^{(f)}}}\mathcal{A}_{\gamma_0}\mathcal{A}^*_{\gamma_1}\mathcal{A}^*_{\gamma_2}\mathcal{B}_{\gamma_0}\mathcal{B}^*_{\gamma_1}\mathcal{B}^*_{\gamma_2} \\ &\qquad\qquad\times\exp\left[\frac{\mathrm{i}}{\hbar}\left(R_{\gamma_0}-R_{\gamma_1}-R_{\gamma_2}\right)\right]. \end{aligned}$$

Here, $\gamma_0$ is propagated for time $t_1+t_2$, while $\gamma_1$ is evolved for time $t_1$ and $\gamma_2$ for time $t_2$ only. Thus, pairing in such a way that all three trajectories

have correlated actions is possible, only if $\gamma_2$ is the continuation of $\gamma_1$, which obviously requires that

$$B\mathbf{m} = \mathbf{m}.$$

However, having the extended trajectory $\tilde{\gamma}$, which results from joining $\gamma_1$ and $\gamma_2$ and pairing $\tilde{\gamma} = \gamma_0$ or $\tilde{\gamma} = \mathcal{T}\gamma_0$ produces contributions, which survive the averaging. Then $\mathbf{m}$ is again fixed by $\gamma_0$. Moreover, according to section 11.3, the remaining (single) sum over trajectories $\gamma_0$ yields together with the three semiclassical prefactors the classical transition probability. This yields for the incomplete many-body spin-echo probability

$$\begin{aligned} P'_{mbse}\left(\mathbf{n}^{(f)}, \mathbf{n}^{(i)}; t_2, t_1\right) = \\ |\alpha|^2 P\left(\mathbf{n}^{(f)}, \mathbf{n}^{(i)}; t_1 + t_2\right) + |\beta|^2 P_{mbse}\left(\mathbf{n}^{(f)}, \mathbf{n}^{(i)}; t_1, t_2\right) \\ + 2\Re\alpha\beta^* \left[1 + (-1)^N \delta_{\mathbf{n}^{(f)}, \mathcal{X}\mathbf{n}^{(i)}}\right] P^{(\mathrm{cl})}\left(\mathbf{n}^{(f)}, \mathbf{n}^{(i)}; t_2 + t_1\right) \mathcal{N}_{B,N}, \end{aligned} \tag{11.6}$$

where the additional factor

$$\mathcal{N}_{B,N} = \frac{\sum_{\mathbf{m}}^{(N)} \delta_{B\mathbf{m},\mathbf{m}}}{\sum_{\mathbf{m}}^{(N)} 1}$$

has been included, in order to account for the fact that only those intermediate occupations contribute, which are eigenvectors of the flipping matrix $B$. It is obvious that for $B = \mathbb{I}_{2L}$, *i.e.* when no spin is flipped, $\mathcal{N}_{B,N} = 1$, such that when inserting the semiclassical results Eq. (10.5) for the transition probability and Eq. (11.5) for the many-body spin-echo probability due to $|\alpha + \beta|^2 = 1$, the incomplete many-body spin-echo probability is equal to the transition probability,

$$P'_{mbse}\left(\mathbf{n}^{(f)}, \mathbf{n}^{(i)}; t_2, t_1\right) = \left[1 + (-1)^N \delta_{\mathbf{n}^{(f)}, \mathcal{X}\mathbf{n}^{(i)}}\right] P^{(\mathrm{cl})}\left(\mathbf{n}^{(f)}, \mathbf{n}^{(i)}; t_2 + t_1\right),$$

which is in accordance with the semigroup property.

Moreover, if the total number of particles is odd and all spins are flipped, *i.e.* $B = \mathcal{X}$, the condition $\mathcal{X}\mathbf{m} = \mathbf{m}$ can never be fulfilled and therefore, this term vanishes, yielding

$$\begin{aligned} P'_{mbse}\left(\mathbf{n}^{(f)}, \mathbf{n}^{(i)}; t_2, t_1\right) = \\ |\alpha|^2 P\left(\mathbf{n}^{(f)}, \mathbf{n}^{(i)}; t_1 + t_2\right) + |\beta|^2 P_{mbse}\left(\mathbf{n}^{(f)}, \mathbf{n}^{(i)}; t_1, t_2\right). \end{aligned}$$

Assuming that

$$\sum_{\mathbf{m}} P^{(\mathrm{cl})}\left(\mathbf{n}^{(f)}, B\mathbf{m}; t_2\right) P^{(\mathrm{cl})}\left(\mathbf{m}, \mathbf{n}^{(i)}\right) \approx P^{(\mathrm{cl})}\left(\mathbf{n}^{(f)}, \mathbf{n}^{(i)}; t_2 + t_1\right),$$

for equal propagation times before and after the spin flip, this probability can be written to leading order as

$$P'_{mbse}\left(\mathbf{n}^{(f)}, \mathbf{n}^{(i)}; t_2, t_1\right) = P^{(\mathrm{cl})}\left(\mathbf{n}^{(f)}, \mathbf{n}^{(i)}; t_1 + t_2\right)\left[|\alpha|^2 + |\beta|^2 + \delta_{\mathbf{n}^{(f)}, \mathcal{X}\mathbf{n}^{(i)}}\left(|\beta|^2 - |\alpha|^2\right)\right]$$

Thus, for the case of flipping all spins and an odd number of particles, the incomplete many-body spin-echo probability interpolates between the cases $\beta = 0$ and $\beta = 1$. Interestingly, for $|\alpha| = |\beta|$, the resulting probability is equal to the classical one, and therefore all interference effects vanish to leading order.

CHAPTER 12

# Many-Body Spin Fidelity

Reverting all the spins in a many-body system with spin-orbit coupling is *almost* the time reversal operation. The fact that it is not exactly time reversal resembles itself in the non-vanishing probability to get $\mathbf{n}^{(f)} \neq \mathbf{n}^{(i)}$ in the many-body spin echo introduced in Chapter 11.

In analogy to this spin echo, this chapter deals with what will be called the many-body spin fidelity, which differs from the spin echo by propagating the system backwards in time after applying the spin flip, *i.e.* the observable of interest here is the spin-fidelity defined as

$$M_F(t) = \left| \langle \mathbf{n}^{(f)} | \hat{K}^\dagger(t) \hat{A} \hat{K}(t) | \mathbf{n}^{(i)} \rangle \right|^2,$$

with $\hat{A}$ given by (11.2). Since the evaluation of the spin fidelity is pretty similar to the one of the spin echo, it will be kept somewhat shorter here.

After inserting the semiclassical propagator (5.14), the spin-fidelity becomes a four fold sum over classical trajectories,

$$M_F(t) \approx \tag{12.1}$$

Again, when performing a disorder average for large total number of particles, the actions in the exponential give rise to large oscillations which will cancel on average, as long as the trajectories are not pairwise correlated. Those trajectory pairs, which exhibit at most one 2-encounter are shown in Figs. 12.1 and 12.2. Their contributions to the spin-fidelity are shown in Table 12.1 and 12.2.

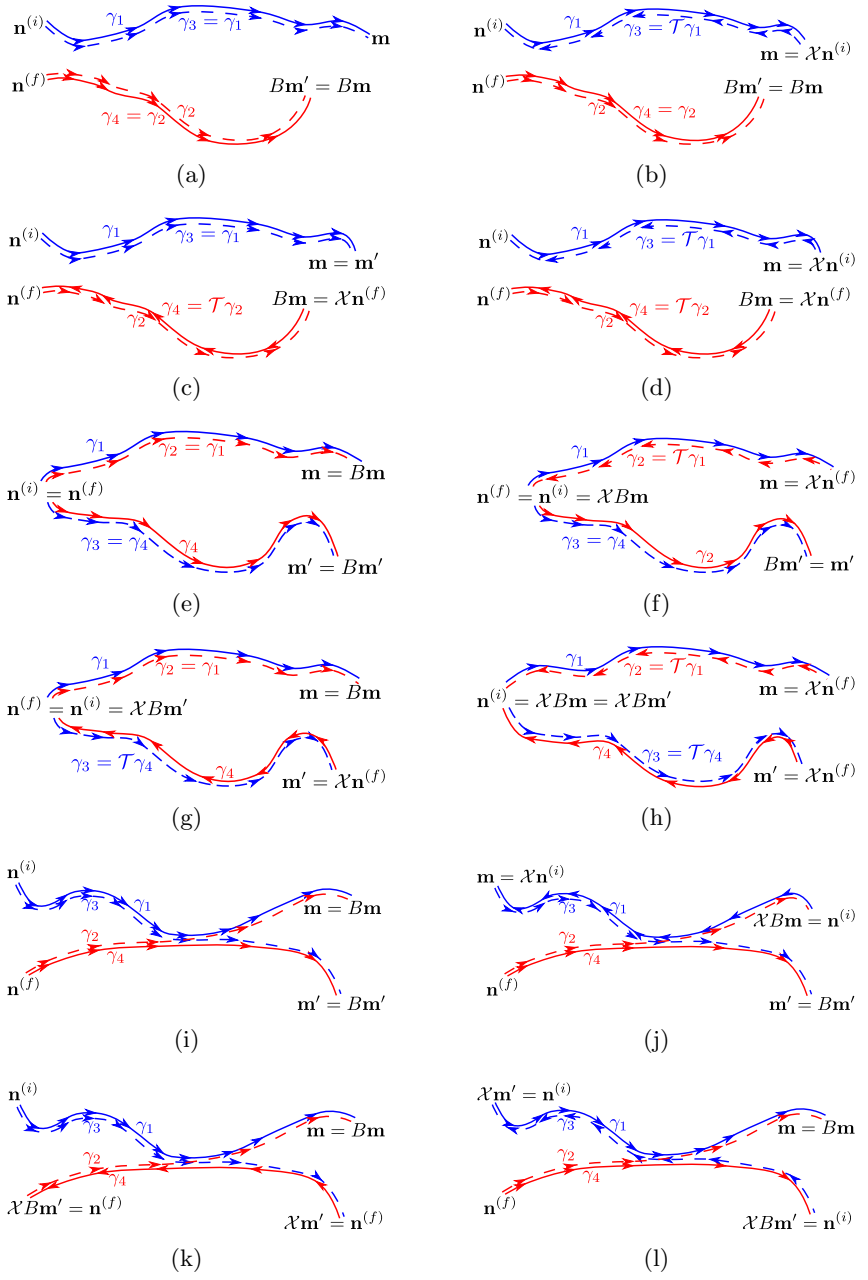


Figure 12.1: First part of diagrams contributing to the spin fidelity, Eq. (12.1), with at most one 2-encounter.

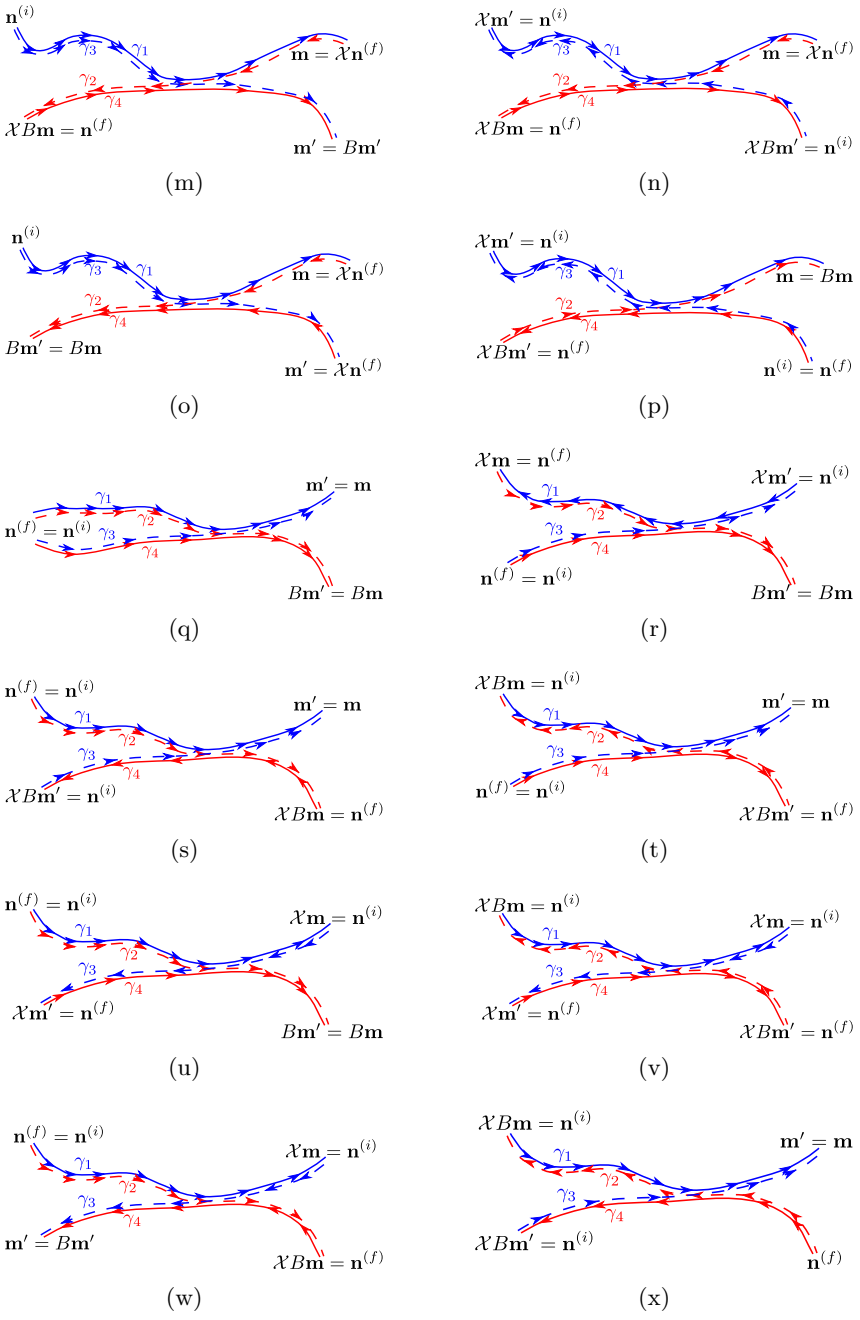


Figure 12.2: Second part of diagrams contributing to the spin fidelity, Eq. (12.1), with at most one 2-encounter.

$$M_F^{(a)}(t) = \sum_{\mathbf{m}} P^{(\mathrm{cl})}\left(B\mathbf{m}, \mathbf{n}^{(f)}\right) P^{(\mathrm{cl})}\left(\mathbf{m}, \mathbf{n}^{(i)}\right)$$

$$M_F^{(b)}(t) = (-1)^N P^{(\mathrm{cl})}\left(B\mathcal{X}\mathbf{n}^{(i)}, \mathbf{n}^{(f)}\right) P^{(\mathrm{cl})}\left(\mathcal{X}\mathbf{n}^{(i)}, \mathbf{n}^{(i)}\right)$$

$$M_F^{(c)}(t) = (-1)^N P^{(\mathrm{cl})}\left(\mathcal{X}\mathbf{n}^{(f)}, \mathbf{n}^{(f)}\right) P^{(\mathrm{cl})}\left(B\mathcal{X}\mathbf{n}^{(f)}, \mathbf{n}^{(i)}\right)$$

$$M_F^{(d)}(t) = P^{(\mathrm{cl})}\left(\mathcal{X}\mathbf{n}^{(f)}, \mathbf{n}^{(f)}\right) P^{(\mathrm{cl})}\left(\mathcal{X}\mathbf{n}^{(i)}, \mathbf{n}^{(i)}\right) \delta_{\mathbf{n}^{(f)}, B\mathbf{n}^{(i)}}$$

$$M_F^{(e)}(t) = \sum_{\mathbf{m},\mathbf{m}'} P^{(\mathrm{cl})}\left(\mathbf{m}', \mathbf{n}^{(i)}\right) P^{(\mathrm{cl})}\left(\mathbf{m}, \mathbf{n}^{(i)}\right) \delta_{\mathbf{m},B\mathbf{m}}\delta_{\mathbf{m}',B\mathbf{m}'}\delta_{\mathbf{n}^{(f)},\mathbf{n}^{(i)}}$$

$$M_F^{(f)}(t) = \sum_{\mathbf{m}} (-1)^N P^{(\mathrm{cl})}\left(\mathbf{m}, \mathbf{n}^{(f)}\right) P^{(\mathrm{cl})}\left(\mathcal{X}\mathbf{n}^{(i)}, \mathbf{n}^{(i)}\right) \delta_{\mathbf{m},B\mathbf{m}} \times \delta_{\mathbf{n}^{(f)},B\mathbf{n}^{(f)}}\delta_{\mathbf{n}^{(i)},\mathbf{n}^{(f)}}$$

$$M_F^{(g)}(t) = \sum_{\mathbf{m}} (-1)^N P^{(\mathrm{cl})}\left(\mathcal{X}\mathbf{n}^{(f)}, \mathbf{n}^{(f)}\right) P^{(\mathrm{cl})}\left(\mathbf{m}, \mathbf{n}^{(i)}\right) \delta_{\mathbf{m},B\mathbf{m}} \times \delta_{\mathbf{n}^{(f)},B\mathbf{n}^{(f)}}\delta_{\mathbf{n}^{(f)},\mathbf{n}^{(i)}}$$

$$M_F^{(h)}(t) = P^{(\mathrm{cl})}\left(\mathcal{X}\mathbf{n}^{(i)}, \mathbf{n}^{(f)}\right) P^{(\mathrm{cl})}\left(\mathcal{X}\mathbf{n}^{(f)}, \mathbf{n}^{(i)}\right) \delta_{\mathbf{n}^{(f)},B\mathbf{n}^{(i)}}$$

$$M_F^{(i)}(t) = -\left(\frac{2\pi}{N}\right)^{2L-3} \frac{1}{\Omega_N} \sum_{\mathbf{m},\mathbf{m}'} P^{(\mathrm{cl})}\left(\mathbf{m}', \mathbf{n}^{(f)}\right) P^{(\mathrm{cl})}\left(\mathbf{m}, \mathbf{n}^{(i)}\right) \times \delta_{\mathbf{m},B\mathbf{m}}\delta_{\mathbf{m}',B\mathbf{m}'}$$

$$M_F^{(j)}(t) = -\left(\frac{2\pi}{N}\right)^{2L-3} \frac{(-1)^N}{\Omega_N} \sum_{\mathbf{m}} P^{(\mathrm{cl})}\left(\mathbf{m}, \mathbf{n}^{(f)}\right) P^{(\mathrm{cl})}\left(\mathcal{X}\mathbf{n}^{(i)}, \mathbf{n}^{(i)}\right) \times \delta_{\mathbf{m},B\mathbf{m}}\delta_{\mathbf{n}^{(i)},B\mathbf{n}^{(i)}}$$

$$M_F^{(k)}(t) = -\left(\frac{2\pi}{N}\right)^{2L-3} \frac{(-1)^N}{\Omega_N} \sum_{\mathbf{m}} P^{(\mathrm{cl})}\left(\mathcal{X}\mathbf{n}^{(f)}, \mathbf{n}^{(f)}\right) P^{(\mathrm{cl})}\left(\mathbf{m}, \mathbf{n}^{(i)}\right) \times \delta_{\mathbf{m},B\mathbf{m}}\delta_{\mathbf{n}^{(f)},B\mathbf{n}^{(f)}}$$

$$M_F^{(l)}(t) = -\left(\frac{2\pi}{N}\right)^{2L-3} \frac{(-1)^N}{\Omega_N} \sum_{\mathbf{m}} P^{(\mathrm{cl})}\left(\mathcal{X}\mathbf{n}^{(i)}, \mathbf{n}^{(f)}\right) P^{(\mathrm{cl})}\left(\mathbf{m}, \mathbf{n}^{(i)}\right) \times \delta_{\mathbf{m},B\mathbf{m}}\delta_{\mathbf{n}^{(i)},B\mathbf{n}^{(i)}}$$

Table 12.1: Contributions of the diagrams in Fig. 12.1 to the spin-fidelity. The upper index of each contributions corresponds to the label of its diagram in Fig. 12.1.

$$M_F^{(m)}(t) = -\left(\frac{2\pi}{N}\right)^{2L-3} \frac{(-1)^N}{\Omega_N} \sum_{\mathbf{m}} P^{(\mathrm{cl})}\left(\mathbf{m}, \mathbf{n}^{(f)}\right) P^{(\mathrm{cl})}\left(\mathcal{X}\mathbf{n}^{(f)}, \mathbf{n}^{(i)}\right) \times \delta_{\mathbf{m},B\mathbf{m}} \delta_{\mathbf{n}^{(f)},B\mathbf{n}^{(f)}}$$

$$M_F^{(n)}(t) = -\left(\frac{2\pi}{N}\right)^{2L-3} \frac{1}{\Omega_N} P^{(\mathrm{cl})}\left(\mathcal{X}\mathbf{n}^{(i)}, \mathbf{n}^{(f)}\right) P^{(\mathrm{cl})}\left(\mathcal{X}\mathbf{n}^{(f)}, \mathbf{n}^{(i)}\right) \times \delta_{\mathbf{n}^{(i)},B\mathbf{n}^{(i)}} \delta_{\mathbf{n}^{(f)},B\mathbf{n}^{(f)}}$$

$$M_F^{(o)}(t) = -\left(\frac{2\pi}{N}\right)^{2L-3} \frac{(-1)^N}{\Omega_N} P^{(\mathrm{cl})}\left(B\mathcal{X}\mathbf{n}^{(f)}, \mathbf{n}^{(f)}\right) P^{(\mathrm{cl})}\left(\mathcal{X}\mathbf{n}^{(f)}, \mathbf{n}^{(i)}\right)$$

$$M_F^{(p)}(t) = -\left(\frac{2\pi}{N}\right)^{2L-3} \frac{(-1)^N}{\Omega_N} \sum_{\mathbf{m}} P^{(\mathrm{cl})}\left(\mathcal{X}\mathbf{n}^{(f)}, \mathbf{n}^{(f)}\right) P^{(\mathrm{cl})}\left(\mathbf{m}, \mathbf{n}^{(i)}\right) \times \delta_{\mathbf{n}^{(f)},\mathbf{n}^{(i)}} \delta_{\mathbf{n}^{(f)},B\mathbf{n}^{(f)}} \delta_{\mathbf{m},B\mathbf{m}}$$

$$M_F^{(q)}(t) = -\left(\frac{2\pi}{N}\right)^{2L-3} \frac{1}{\Omega_N} \sum_{\mathbf{m}} P^{(\mathrm{cl})}\left(B\mathbf{m}, \mathbf{n}^{(f)}\right) P^{(\mathrm{cl})}\left(\mathbf{m}, \mathbf{n}^{(i)}\right) \delta_{\mathbf{n}^{(f)},\mathbf{n}^{(i)}}$$

$$M_F^{(r)}(t) = -\left(\frac{2\pi}{N}\right)^{2L-3} \frac{(-1)^N}{\Omega_N} P^{(\mathrm{cl})}\left(\mathcal{X}B\mathbf{n}^{(i)}, \mathbf{n}^{(f)}\right) P^{(\mathrm{cl})}\left(\mathcal{X}\mathbf{n}^{(i)}, \mathbf{n}^{(i)}\right) \times \delta_{\mathbf{n}^{(f)},\mathbf{n}^{(i)}}$$

$$M_F^{(s)}(t) = -\left(\frac{2\pi}{N}\right)^{2L-3} \frac{(-1)^N}{\Omega_N} P^{(\mathrm{cl})}\left(\mathcal{X}\mathbf{n}^{(i)}, \mathbf{n}^{(f)}\right) P^{(\mathrm{cl})}\left(\mathcal{X}B\mathbf{n}^{(i)}, \mathbf{n}^{(i)}\right) \times \delta_{\mathbf{n}^{(f)},\mathbf{n}^{(i)}}$$

Table 12.2: Contributions of the diagrams in Fig. 12.2 to the spin-fidelity. The upper index of each contributions corresponds to the label of its diagram in Fig. 12.2.

$$M_F^{(t)}(t) = -\left(\frac{2\pi}{N}\right)^{2L-3} \frac{(-1)^N}{\Omega_N} P^{(\mathrm{cl})}\left(\mathcal{X}\mathbf{n}^{(f)}, \mathbf{n}^{(f)}\right) P^{(\mathrm{cl})}\left(\mathcal{X}B\mathbf{n}^{(i)}, \mathbf{n}^{(i)}\right) \times\delta_{\mathbf{n}^{(i)},\mathbf{n}^{(f)}}$$

$$M_F^{(u)}(t) = -\left(\frac{2\pi}{N}\right)^{2L-3} \frac{(-1)^N}{\Omega_N} P^{(\mathrm{cl})}\left(\mathcal{X}B\mathbf{n}^{(i)}, \mathbf{n}^{(f)}\right) P^{(\mathrm{cl})}\left(\mathcal{X}\mathbf{n}^{(i)}, \mathbf{n}^{(i)}\right) \times\delta_{\mathbf{n}^{(f)},\mathbf{n}^{(i)}}$$

$$M_F^{(v)}(t) = -\left(\frac{2\pi}{N}\right)^{2L-3} \frac{1}{\Omega_N} P^{(\mathrm{cl})}\left(\mathcal{X}\mathbf{n}^{(f)}, \mathbf{n}^{(f)}\right) P^{(\mathrm{cl})}\left(\mathcal{X}\mathbf{n}^{(i)}, \mathbf{n}^{(i)}\right) \times\delta_{\mathbf{n}^{(i)},B\mathbf{n}^{(i)}}\delta_{\mathbf{n}^{(f)},B\mathbf{n}^{(f)}}$$

$$M_F^{(w)}(t) = -\left(\frac{2\pi}{N}\right)^{2L-3} \frac{(-1)^N}{\Omega_N} \sum_{\mathbf{m}} P^{(\mathrm{cl})}\left(\mathbf{m}, \mathbf{n}^{(f)}\right) P^{(\mathrm{cl})}\left(\mathcal{X}\mathbf{n}^{(i)}, \mathbf{n}^{(i)}\right) \times\delta_{\mathbf{m},B\mathbf{m}}\delta_{\mathbf{n}^{(i)},\mathbf{n}^{(f)}}\delta_{\mathbf{n}^{(f)},B\mathbf{n}^{(f)}}$$

$$M_F^{(x)}(t) = -\left(\frac{2\pi}{N}\right)^{2L-3} \frac{(-1)^N}{\Omega_N} P^{(\mathrm{cl})}\left(\mathcal{X}\mathbf{n}^{(i)}, \mathbf{n}^{(f)}\right) P^{(\mathrm{cl})}\left(\mathcal{X}B\mathbf{n}^{(i)}, \mathbf{n}^{(i)}\right)$$

Table 12.3: Contributions of the diagrams in Fig. 12.2 to the spin-fidelity. The upper index of each contributions corresponds to the label of its diagram in Fig. 12.2.

The order of each diagram can be determined by the number of sums over the intermediate occupations, which survive the averaging. However, although a proof of this is missing, it is assumed that $\left(\frac{N}{2\pi}\right)^{2L-3}\Omega_N$, where

$$\Omega_N = \int \mathrm{d}^{4L}\psi\delta\left(\theta_{1,\uparrow}\right)\delta\left(N - \sum_{l=1}^{L}\sum_{\sigma=\uparrow,\downarrow}|\psi_{l,\sigma}|^2\right).$$

is the phase space volume for fixed total number $N$ of particles, is of the same order as the sum over occupations,

$$\left(\frac{N}{2\pi}\right)^{2L-3}\Omega_N \sim \sum_{\mathbf{m}}\delta_{\sum\limits_{l,\sigma} m_{l,\sigma},N}. \tag{12.2}$$

Thus, diagram 12.1(q) is for instance of the same order of magnitude as diagram 12.1(d). Restricting oneself to leading and next to leading order, the

many-body spin-fidelity is given by diagrams 12.1(a), (e)-(g) and 12.1(i),

$$M_F(t) \approx \sum_{\mathbf{m}} P^{(\mathrm{cl})^2} \Bigg\{ 1 + \delta_{\mathbf{m},B\mathbf{m}} \Bigg[ 2\,(-1)^N \delta_{\mathbf{n}^{(f)},B\mathbf{n}^{(f)}} \delta_{\mathbf{n}^{(f)},\mathbf{n}^{(i)}} + \sum_{\mathbf{m}'} \delta_{\mathbf{m}',B\mathbf{m}'} \left( \delta_{\mathbf{n}^{(f)},\mathbf{n}^{(i)}} - \left( \frac{2\pi}{N} \right)^{2L-3} \frac{1}{\Omega_N} \right) \Bigg] \Bigg\}. \tag{12.3}$$

At this point it should be noted that only those encounter diagrams involving all four trajectories are taken into account since those which involve only two trajectories have been shown to cancel in section 7.1.3. Moreover, in the situation considered here, there are no one-leg-loops formed by all four trajectories, since the fact that the propagation times are the same requires that if one link vanishes a second one also has to vanish thus forming again one of the diagrams in Fig. 12.1.

## 12.1 Unitarity

Before discussing the result, Eq. (12.3), in more detail consider the case of no spin flips, *i.e.* $\hat{A} = 1$, which also implies $B = \mathbb{I}_{2L}$. In this case, due to unitarity of the propagator, the spin-fidelity obviously should be $M_F(t) = \delta_{\mathbf{n}^{(i)},\mathbf{n}^{(f)}}$. Comparing Eq. (12.3) with this expectation further affirms the assumption Eq. (12.2), which leads to a cancellation of the first and the last term for $F = 0$ and therefore leads to a result proportional to a Kronecker delta in the initial and final occupations. Therefore, encounter diagrams have indeed to be taken into account and can be of the same order of magnitude as diagrams without encounter.

Consider now the next-to-next-to-leading order diagrams. In order to show the unitarity within this order, one has to recognize that the diagrams 12.1(j) and (l) ((k) and (m)) are of the same order as Fig. 12.1(b) ((c)). However, since the sum over trajectories $\gamma_1$ ($\gamma_4$) for the diagonal terms include both, $\gamma_1$ ($\gamma_4$) and $\mathcal{T}\gamma_1$ ($\mathcal{T}\gamma_4$), there are twice as many contributions corresponding to the diagram 12.1(b) (12.1(c)) than those corresponding to the diagrams 12.1(j) and (l) (Figure 12.1(k) and (m)), respectively. Therefore, these contributions again cancel out for $\hat{A} = 1$.

The remaining diagrams are, for $B = 1$, either proportional to $\delta_{\mathbf{n}^{(f)},\mathbf{n}^{(i)}}$ or of even higher order. Therefore, the semiclassical result is again consistent with the exact quantum mechanical one for the case that actually no

spin-flip was applied. Therefore one can expect that the result obtained for $\hat{A} \neq 1$ is also reasonable.

## 12.2 General Results

### *12.2.1 Odd number of particles*

Let us continue with the contrary case, namely that every spin is flipped, *i.e.* $B = \mathcal{X}$. For odd number of particles, the conditions $\mathbf{m} = B\mathbf{m}$ can not be fulfilled, since there is at least one singly occupied single-particle state. Therefore, the result Eq. (12.3) reduces to

$$\sum_{\mathbf{m}} P^{(\mathrm{cl})}\left(\mathcal{X}\mathbf{m}, \mathbf{n}^{(f)}\right) P^{(\mathrm{cl})}\left(\mathbf{m}, \mathbf{n}^{(i)}\right),$$

which can be assumed, to be approximately constant for each combination of $\mathbf{n}^{(i)}$ and $\mathbf{n}^{(f)}$.

The next-to-next-to-leading order result also stems solely from the extended diagonal approximation, since the contributing diagrams consisting of an encounter are again zero, such that finally

$$M_L(t) \approx \sum_{\mathbf{m}} \left[1 + (-1)^N \delta_{\mathbf{m},\mathcal{X}\mathbf{n}^{(i)}}\right] \left[1 + (-1)^N \delta_{\mathbf{m},\mathbf{n}^{(f)}}\right] P^{(\mathrm{cl})}\left(\mathcal{X}\mathbf{m}, \mathbf{n}^{(f)}\right) P^{(\mathrm{cl})}\left(\mathbf{m}, \mathbf{n}^{(i)}\right) + \delta_{\mathbf{n}^{(f)},\mathcal{X}\mathbf{n}^{(i)}} P^{(\mathrm{cl})}\left(\mathbf{n}^{(f)}, \mathbf{n}^{(f)}\right) P^{(\mathrm{cl})}\left(\mathbf{n}^{(i)}, \mathbf{n}^{(i)}\right),$$

giving a small enhancement of the probability to measure $\mathcal{X}\mathbf{n}^{(i)}$ compared to all the other probabilities.

If not all spins are flipped, *i.e.* $F \neq L$, the result is – surprise, surprise – somewhere in between the two extreme cases $F = L$ and $F = 0$. More importantly, the result is more or less independent on the exact choice of sites where the spin is flipped, but depends only on the number of flipped sites. The height of the peak at $\mathbf{n}^{(f)} = \mathbf{n}^{(i)}$ can thereby be measured by the number of available vectors $\mathbf{m}$ satisfying $\mathbf{m} = B\mathbf{m}$,

$$\#\left(\mathbf{m} = B\mathbf{m}\right) = \sum_{j=0}^{F} \binom{2L-2F}{N-2j} \binom{F}{j},$$

which decreases monotonously, when increasing $F$.

### *12.2.2 Even number of particles*

The situation for an even number of particles is essentially the same as for odd number of particles, except that an enhancement for $\mathbf{n}^{(f)} = \mathbf{n}^{(i)}$ remains for $F = L$, since those intermediate occupations, where each single-particle state is doubly occupied or empty still contribute.

CHAPTER 13

# Summary & Outlook

## 13.1 Summary

The fact that for many indistinguishable particles, symmetrization renders first quantized approaches very extensive, together with the fact that semiclassics has been very successfully applied to various single-particle problems [246, 284], was the main motivation to develop a semiclassical approach for quantum fields in the sense of van Vleck and Gutzwiller in Fock space. This very thesis is of course not the first attempt to develop such (see *e.g.* [66, 67] for bosons and [216, 217] for fermions). However, to the author's knowledge, it is the first time that a semiclassical van-Vleck-Gutzwiller like propagator in Fock space with real trajectories and real actions has been derived rigorously by applying the stationary phase approximation to the exact path integral.

While previous approaches for Bosons were based on the coherent state path integral, which requires in a semiclassical approximation to complexify the classical trajectories, thus hidding interference effects, the approach presented in Chapter 4 is based on quadrature eigenstates. In contrast to the coherent state approach, this fixes only the initial and final real part of the trajectory, does not require complexification and therefore makes interference manifest. Furthermore, starting from the semiclassical propagator in quadrature representation it has been shown, how a basis transformation from quadrature to Fock states can be performed, yielding a propagator given by a sum over trajectories with fixed initial and final occupations. Furthermore, in the same chapter, it is shown that the semiclassical prop-

agator fulfills the semigroup property by means of a stationary phase approximation.

In the subsequent chapter, the propagator in fermionic Fock space has been considered, which is a considerably more difficult problem due to the antisymmetry of Fermionic many-body states. However, we managed to derive an exact path integral in commuting complex rather than anticommuting Grassmann variables – for the first time to the authors knowledge. Since a path integral explicitly contains the corresponding classical Hamiltonian, one can also read off the classical limit of the exact quantum theory. Of course, a classical limit based on complex variables can not account for the antisymmetry and the Pauli exclusion principle implied by it exactly, yet it is approximated by additional factors, for which there is a certain freedom of choice. These additional factors incorporate the Pauli principle approximately either by penalizing hopping events which lead to larger occupations, or by means of nonlinear dependencies of the on-site energies on the occupation, leading to an energetical hindering of higher occupations. The latter possibilities can be regarded as the inclusion of a so called Pauli potential [285–288], which usage up to now seems to have been always heuristic.

It should be noted that at least one of the possible classical Hamiltonians obtained by this rigorous construction corresponds to the one obtained for a two-level system by means of truncation of the Holstein-Primakoff transformation in Ref. [215].

It is furthermore remarkable that the path integral and therefore the classical limit can also be obtained in what can be regarded as a hole picture. In this picture, the roles of occupied and unoccupied single-particle states interchange, such that sites occupied in the (conventional) particle picture are unoccupied in the hole picture and vise versa. In order to understand this analogy better, it should also be mentioned that each single-particle state is here determined by both, the orbital and spin state, such that for Fermions each single-particle state can indeed be occupied by at most one particle, and therefore the correspondence of an empty single-particle state and a hole is indeed one-to-one.

In Chapter 5 it is then furthermore shown how to derive, starting from this path integral, a semiclassical propagator in fermionic Fock state representation.

Just as the derivations of the semiclassical coherent state propagators did [65–67, 69], the derivations of the semiclassical propagators in Fock space representation for Bosons and Fermions show that the effective Planck is the inverse particle number $\hbar_{\text{eff}} = 1/N$, and the classical limit is

the corresponding mean field theory. It is furthermore in agreement with previous coherent state approaches [65–67, 69, 235–238] that, in both cases – Bosons and Fermions – adds an additional phase the semiclassical propagator, which is nowadays known as the Kochetov-Solari phase [65, 235]. The exact form, and for Bosons even the presence, of this additional phase, depends on the chosen ordering of the creation and annihilation operators. In the bosonic case, it is absent for the symmetric Weyl-ordering [235]. For Fermions, however, it seems that due to the additional factors in the Hamiltonian, which make for the approximate antisymmetry and Pauli exclusion, it is in general not possible to get rid of this phase.

In Chapter 6, first of all the integrable case of non-interacting Bosons is considered. In this case, the semiclassical propagator in quadrature representation is exact and can be evaluated easily, yielding a closed expression. The resulting propagator has also been transformed to coherent state representation, in order to compare results obtained by using quadratures on the one, and coherent states on the other hand.

In Chapter 7, the focus is finally turned towards interacting disordered systems, we study the transition probability from one Fock state to another one, *i.e.* the probability that after fixing a certain occupation of the single-particle states at initial time and evolving the system a certain final occupation is measured. It turns out that for time reversal invariant systems in the chaotic regime the probability to observe the initial Fock state again is enhanced by a factor of two of compared to all the other Fock states. This enhancement is furthermore predicted to be absent if time reversal symmetry is broken (see Fig. 13.1(a)). Our analytical result for this enhancement, which is typically denoted as coherent backscattering [232], are also in perfect agreement with numerical calculations.

After that, the transition probability for systems for which the hopping strength is small compared to the interaction strength is considered. A special case is the one of vanishing hopping strengths, in which the exact quantum mechanical result is reproduced by the semiclassical propagator. For small, but non-vanishing hopping strengths, again agreement with numerical data is found.

In single-particle transport, coherent backscattering gives rise to weak localization [19, 21, 233]. Driven by this fact, in Chapter 8 bosonic many-body transport has been considered. Assuming that the system is infinitely large with interactions only within a closed region, and only one site initially occupied it has been found, however, that the contributions usually responsible for weak localization cancel when considering single-particle observables like the occupation of a single site, or the single-particle current.

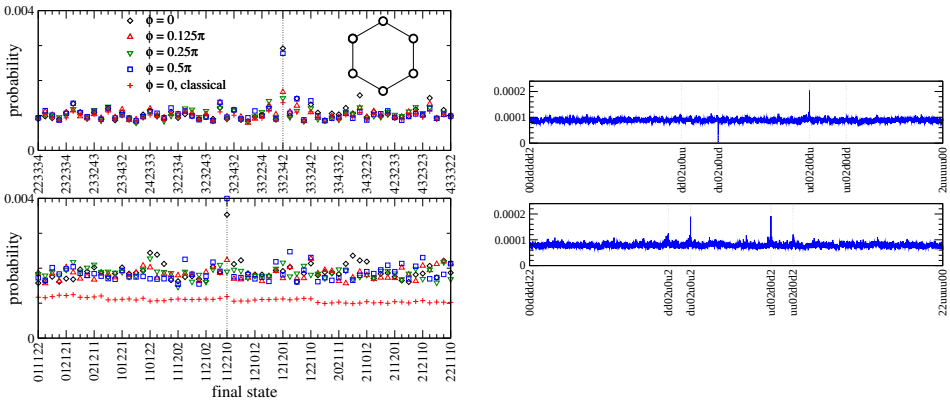


Figure 13.1: Numerical results for the transition probability in Fock space for (a) a six-site Bose-Hubbard ring and (a) a eight-site Fermi-Hubbard ring with spin-orbit coupling and an odd (top) and even (bottom) number of particles.

This implies that these quantities can be computed using the Truncated Wigner method [289–292], which is shown to be the classical limit of the quantum theory.

For the fidelity considered in Chapter 9, the classical theory will not give correct results, however. This is, because the quantity considered is the interference between two quantum mechanical wave functions, which are evolved under slightly different Hamiltonian. The classical limit then will not be able to reproduce this interference completely. In contrast to the fidelity in first quantization [25], the semiclassical approach in Fock space not only reproduces the long-time decay, but also the quadratic decay for small times [264, 293] as well as the saturation regime [264, 294–297]. Using the presented methods, even the absence of the Lyapunov regime, *i.e.* the perturbation independent dacay which is determined by the Lyapunov exponent only, can be explained. Our analytical results are in good agreement with numerical calculations [272]. It is worth to note that although the fidelity has been considered here for Bosons only, with the semiclassical propagator for Fermions derived in Chapter 5 together with the transition probability for Fermions considered in Chapter 10 it is straight forward to transfer the results to fermionic systems.

The results for the transition probability for Fermions in the chaotic disordered case is somewhat richer than those for Bosons. First of all,

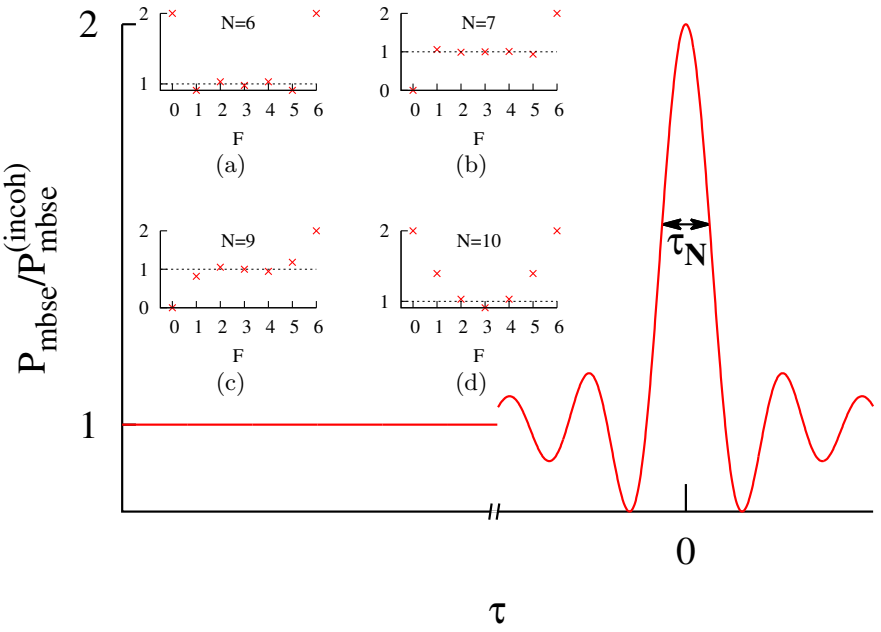


Figure 13.2: Time dependence of the the many-body spin echo for the case of flipping all spins and $\mathbf{n}^{(f)} = \mathcal{X}\mathbf{n}^{(i)}$. Insets: Size of the coherent contribution at $t_2 = t_1$ for a six single-particle states with (a) six, (b) seven, (c) nine and (d) ten particles. as a function of the number $F$ of single-particle states, for which the spins are flipped.

if spin-orbit coupling – or any other spin-mixing mechanism – is absent, they behave apart from the Pauli exclusion like Bosons and show coherent backscattering. In the presence of *e.g.* spin-orbit coupling, however, the result depends very much on whether the total number of particles is even or odd. In both cases, the transition probability from the initial Fock state to its spin-reversed counterpart differs in time reversal invariant systems from the flat background. If now the total number of particles is odd, this transition is completely forbidden, which is actually a consequence of Kramer's degeneracy. For an even number of particles on the other hand, this transition is twice as probable as all the others. Additionally, if the spin-orbit coupling is site-independent, there is also an enhancement for the initial state. All this is shown in Fig. 13.1(b). Again, when destroying time reversal symmetry this enhancement and prohibition, respectively, vanish.

However, as shown in Chapter 11, it turns out that for an odd number of particles the prohibited transition can be turned into a favored one, by

applying an intermediate extrinsic spin flip. Yet, it should be noted that if the spin flip does not take place roughly at half the evolution time, the observed probability is just roughly the same for every Fock state, without any enhancement or reduction for certain final occupations. When flipping all spins, both for even and odd total number of particles, the probability to observe the spin reversed of the initial state is twice as large as the one for any other Fock state, while if the spins are flipped only for certain single-particle states, it changes non-monotonically with the number of single-particle states chosen for the flips. It is furthermore remarkable that for even number of particles, by the right choices, the enhancement can be turned into a reduction, though it would be very small. All this is again graphically summarized in Fig. 13.2.

Moreover, note that the spin-echo calculation presented in Chapter 11 also contains the semigroup property of the semiclassical propagator as a special case, just as Chapter 12 contains the unitarity as a special case of the sequence forward evolution – spin-flip – backward evolution. For lack of a better name, this process has been denoted as spin-fidelity. In this process, the probability to measure the spin-reverse of the initial Fock state again is slightly enhanced compared to the other ones, with the height of the enhancement given roughly by the inverse number of accessible Fock states if all spins are flipped. If it happens that not all spins are flipped, but only those of a subset of all single-particle states, the result changes monotonously from the result for the complete flip to unitarity.

The consideration of the semigroup property and the unitarity of the semiclassical propagator as special cases of the spin-echo and spin-fidelity, has to the author's knowledge been the first time to proof these properties on the level of transition probabilities without using a stationary phase approximation. Instead, it turns out that especially for the unitarity also loop contributions have to be taken into account, in order to obtain the correct result.

To summarize, this thesis represents a further step in the development and improvement of semiclassical theories, and transfers the concepts developed for single-particle systems [33, 38, 284] to Fock space, in order to allow a semiclassical treatment of interacting many-body systems. In order to show its applicability, a few first examples have been considered, some of them being justifications of existing and frequently used methods or proofs of the validity of the presented approach, others being completely new effects.

## 13.2 Outlook

To be sure, the many-body interference effects studied here can only be the beginning of a whole new field for semiclassics to explore. In general, one could expect that the approach developed here can be applied to any many-body system with a large number of particles, but also to quantum optics, where experiments are often performed with a single photon. The latter is due to the fact that in quantum optics, the Hamiltonian is quadratic, and therefore the semiclassical approximation in quadrature representation is exact.

Here, the semiclassical approach has been applied mainly to systems where some kind of average (mainly disorder average) has been implied, in order to get analytical results by pairing of trajectories. Yet, it is also possible to study systems without averaging *e.g.* numerically, where the main complication lies in the solution of a root search problem, which can be solved for example by using the Newton-Raphson approach [239–247], or by means of the initial value representation derived in section 4.3.3.

Currently under developement is for instance a semiclassical many-body scattering theory [298] similar to the one used in single-particle transport [284]. Such a many-body scattering theory would allow for instance to study many-body analogues of weak localization [19–21] and weak antilocalization [22, 23].

Furthermore many-body effects on general single-particle observables are under investigation.

Apart from these current projects, it is planed to apply the presented approach to nonlinear laser theory and spin chains. Moreover, one could also think about applications to quantum optics and to the investigation of many-body localization *e.g.* along the lines of Ref. [299].

# List of Publications

1. Published articles

   - Thomas Engl, Julien Dujardin, Arturo Argüelles, Peter Schlagheck, Klaus Richter and Juan Diego Urbina
     *Coherent Backscattering in Fock Space: a Signature of Quantum Many-Body Interference in Interacting Bosonic Systems.*
     Physical Review Letters 112, 140403 (2014).
   - Thomas Engl, Peter Plößl, Juan Diego Urbina and Klaus Richter
     *The semiclassical propagator in fermionic Fock space.*
     Theoretical Chemistry Accounts 133, 1563 (2014).

2. To be submitted

   - Julien Dujardin, Thomas Engl, Klaus Richter and Peter Schlagheck
     *A truncated Wigner approach to bosonic transport in atom lasers.*
   - Thomas Engl, Juan Diego Urbina and Klaus Richter
     *Many-Body Spin Echo.*
     arxiv:1409.5684

3. In preparation

   - Julien Dujardin, Thomas Engl, Juan Diego Urbina and Peter Schlagheck
     *Describing many-body bosonic waveguide scattering with the truncated Wigner method.*
   - Thomas Engl, Juan Diego Urbina and Klaus Richter
     *Semiclassical theory of Boson Sampling*

# Acknowledgements

First of all, I would like to thank my supervisor Klaus Richter for giving me the opportunity for this PhD thesis and guiding, supporting and advising me in my research during the last years. Also I'm thankful for additional support and supervision by Juan Diego Urbina and Peter Schlagheck. Furthermore, I thank the University of Regensburg, the Université de Liège and the Deutsche Forschungsgesellschaft for the financial support.

Almost all the time of my thesis I collaborated with Juan Diego Urbina, who always helped me setting the obtained results into the right scientific context and supported me by providing literature whenever necessary to overcome difficulties in my scientific work. Furthermore, the parts on the bosonic transition probability, the fidelity and the transition probability in fermionic Fock state were supported by Julien Dujardin, Peter Schlagheck and Arturo Argüelles who provided the numerical calculations. The part on the bosonic many-body transport came into being during my stay at Université de Liège in the group of Peter Schlagheck, who also brought the idea for this study to me. It was also him, who motivated me to the consideration of the fidelity and Loschmidt echo. The considerations on noninteracting Bosons originate mainly from discussions with Christine Silberhorn.

Moreover, I would like to thank everybody with whom I head very useful discussions, leading to a better understanding of my results and the physics behind them. In particular for the semiclassical propagator in Fock space and the transition probabilities these are Lena Simon, Walter Strunz, Stefan Fischer, Andreas Buchleitner, Regine Frank, Daniel Waltner and Sandro Wimberger for the bosonic as well as Sven Essert, Sergey Smirnov and Rodolfo Jalabert and Thomas Guhr for the fermionic case.

About the Loschmidt echo and the many-body spin echo, I discussed a lot with Rodolfo Jalabert, Horacio Pastawski, Arseni Goussev, Diego Wisniacki, Daniel Waltner, Sven Essert, Cord Mller and Tomaž Prosen.

In addition, the research projects of Andrea Spichtinger, Emilie Tisserond, Michael Nicklas and Peter Plöessl where very helpful in better understanding the classical limit of the many-body theory. In addition, I thank Jack Kuipers, who was the co-supervisor of my diploma thesis, where I learned essentially everything I know about semiclassical loop contributions.

Futhermore, I would like to thank Josef Michl, Juan Diego Urbina and Ming-Hao Liu for their very thorough proof reading of this thesis.

Finally, I want to thank everybody who helped making my stay at the University of Regensburg and Université de Liège as comfortable as possible. Most importantly, these are our secretaries Angela Reisser and Toni Bienert. Also, my officemates Dmitry Ryndyk and Sven Essert provided a sometimes quiet but otherwise positive and friendly atmosphere, and the joint excursions and Schweinshaxn days, which were mostly initiated and organized by Viktor Krückl, Josef Michl and Ming-Hao Liu, helped me to stay motivated for all these years.

Surely the list of people mentioned here is far from being complete. So I would like to finish with thanking all those I have not mentioned here explicitly – including my family and friends – but supported me in any way during my PhD, no matter whether it was by brightening up my mood with a joke, feedback to my work, pointing out mistakes or sharing a beer with me.

# Appendix

APPENDIX A

# The Semiclassical Propagator for Bosons

## A.1 The classical Hamiltonian for a Bose-Hubbard systems in quadrature representation

One possible way to determine the classical Hamiltonian, Eq. (4.7) corresponding to a quantum Hamiltonian of the form

$$\hat{H} = \sum_{l_1,l_2=1}^{L} H^{(0)}_{l_1 l_2} \hat{a}^\dagger_{l_1} \hat{a}_{l_2} + \frac{1}{2} \sum_{l_1,l_2,l_3,l_4=1}^{L} V_{l_1 l_2 l_3 l_4} \hat{a}^\dagger_{l_1} \hat{a}^\dagger_{l_2} \hat{a}_{l_3} \hat{a}_{l_4},$$

is to use coherent states, since the action of an annihilation operator on a coherent state is fairly easy.

Note that due to the Hermiticity of the Hamiltonian $H^{(0)}$, which is the matrix with elements $H^{(0)}_{ll'}$, also has to be hermitian, and the interaction coefficients have to satisfy $V_{l_1 l_2 l_3 l_4} = V^*_{l_4 l_3 l_2 l_1}$. Moreover, one is free to choose

$$V_{l_1 l_2 l_3 l_4} = V_{l_2 l_1 l_3 l_4} = V_{l_1 l_2 l_4 l_3} = V_{l_2 l_1 l_4 l_3}.$$

Inserting a unit operator in terms of coherent states, Eq. (3.18), to the left

and to the right of the exponential yields

$$\left\langle \mathbf{p} \left| \exp\left(-\frac{\mathrm{i}\tau}{\hbar}\hat{H}\right) \right| \mathbf{q} \right\rangle = \frac{1}{\pi^{2L}} \int \mathrm{d}^{2L}\phi \int \mathrm{d}^{2L}\mu \, \langle \mathbf{p} \,|\, \boldsymbol{\mu} \rangle \left\langle \boldsymbol{\mu} \left| \exp\left(-\frac{\mathrm{i}\tau}{\hbar}\hat{H}\right) \right| \boldsymbol{\phi} \right\rangle \langle \boldsymbol{\phi} \,|\, \mathbf{q} \rangle ,$$

where the evaluation of the matrix elements straight forward, and the overlaps of a coherent state and an quadrature eigenstate is given by Eq. (3.19). Here, the notation $\mathrm{d}^{2L}\phi = \mathrm{d}^{L}\Re\phi \mathrm{d}^{L}\Im\phi$, is used. However, the interaction term in the Hamiltonian gives rise for quartic terms in $\boldsymbol{\phi}$ and $\boldsymbol{\mu}$. Therefore, in order to evaluate these integrals exactly, it is advantageous to use a Hubbard Stratonovich transformation (see Appendix G) in order to get rid of these quartic terms, yielding

$$\begin{aligned}\left\langle \mathbf{p} \left| \exp\left(-\frac{\mathrm{i}\tau}{\hbar}\hat{H}\right) \right| \mathbf{q} \right\rangle = \\ \frac{1}{\pi^{2L}\sqrt{2\pi b^2}^{L}} \left[ \int \mathrm{d}^{2L\times 2L}\eta \exp\left( \frac{\mathrm{i}\tau}{2\hbar} \sum_{l_1,l_2,l_3,l_4=1}^{L} \eta_{l_1 l_2} \left(V^{-1}\right)_{l_1 l_3 l_2 l_4} \eta_{l_3 l_4} \right) \right]^{-1} \\ \int \mathrm{d}^{2L}\phi \int \mathrm{d}^{2L}\mu \int \mathrm{d}^{2L\times 2L}\sigma \exp\Bigg\{ -|\boldsymbol{\phi}|^2 - |\boldsymbol{\mu}|^2 + \frac{(\boldsymbol{\phi}^*)^2}{2} - \frac{\boldsymbol{\mu}^2}{2} + \boldsymbol{\mu}^* \cdot \boldsymbol{\phi} \\ + \frac{\mathrm{i}\tau}{2\hbar} \sum_{l_1,l_2,l_3,l_4=1}^{L} \sigma_{l_1 l_2} \left(V^{-1}\right)_{l_1 l_3 l_2 l_4} \sigma_{l_3 l_4} - \frac{\mathrm{i}\tau}{\hbar} \boldsymbol{\mu}^* \cdot H_\sigma \boldsymbol{\phi} \\ - \left(\frac{\mathbf{q}}{2b} - \boldsymbol{\phi}^*\right)^2 - \left(\frac{\mathbf{p}}{2b} - \mathrm{i}\boldsymbol{\mu}\right)^2 \Bigg\},\end{aligned}$$

where the integration over $\sigma$ runs over all hermitian $L \times L$ matrices, $V^{-1}$ is defined such that

$$\sum_{ll'=1}^{L} \left(V^{-1}\right)_{ll_1 l'l_2} V_{ll_3 l'l_4} = \delta_{l_1 l_3}\delta_{l_2 l_4},$$

and

$$H_\sigma = H^{(0)} - \sigma$$

is the effective single-particle hamiltonian.

Performing the integrations over $\boldsymbol{\mu}$ and $\boldsymbol{\phi}$ is then cumbersome, but otherwise straight forward and yields

$$\begin{aligned}
&\left\langle \mathbf{p} \left| \exp\left(-\frac{\mathrm{i}\tau}{\hbar}\hat{H}\right) \right| \mathbf{q} \right\rangle = \\
&\frac{1}{\sqrt{4\pi b^2}^L} \left[ \int \mathrm{d}^{2L\times 2L}\eta \exp\left( \frac{\mathrm{i}\tau}{2\hbar} \sum_{l_1,l_2,l_3,l_4=1}^{L} \eta_{l_1 l_2} \left(V^{-1}\right)_{l_1 l_3 l_2 l_4} \eta_{l_3 l_4} \right) \right]^{-1} \\
&\qquad \int \mathrm{d}^{2L\times 2L}\sigma \frac{\exp\left( \frac{\mathrm{i}\tau}{2\hbar} \sum_{l_1,l_2,l_3,l_4=1}^{L} \sigma_{l_1 l_2} \left(V^{-1}\right)_{l_1 l_3 l_2 l_4} \sigma_{l_3 l_4} \right)}{\sqrt{\det\left[\mathbb{I}_L - \frac{\mathrm{i}\tau}{\hbar}\Re H_\sigma - \frac{\tau^2}{2\hbar^2} H_\sigma^* H_\sigma\right]}} \\
&\qquad\qquad \exp\left[ -\frac{\mathbf{q}^2}{4b^2} - \frac{\mathbf{p}}{4b^2} + \frac{1}{2b^2} \begin{pmatrix} \mathbf{q} \\ -\mathrm{i}\mathbf{q} \\ -\mathrm{i}\mathbf{p} \\ \mathbf{p} \end{pmatrix} A^{-1} \begin{pmatrix} \mathbf{q} \\ -\mathrm{i}\mathbf{q} \\ -\mathrm{i}\mathbf{p} \\ \mathbf{p} \end{pmatrix} \right],
\end{aligned}$$

where the $4L \times 4L$-matrix $A$ is given by

$$A = \begin{pmatrix} 3\mathbb{I}_L & -\mathrm{i}\mathbb{I}_L & -\mathbb{I}_L + \frac{\mathrm{i}\tau}{\hbar} H_\sigma^* & \mathrm{i}\mathbb{I}_L + \frac{\tau}{\hbar} H_\sigma^* \\ -\mathrm{i}\mathbb{I}_L & \mathbb{I}_L & -\mathrm{i}\mathbb{I}_L - \frac{\tau}{\hbar} H_\sigma^* & -\mathbb{I}_L + \frac{\mathrm{i}\tau}{\hbar} H_\sigma^* \\ -\mathbb{I}_L + \frac{\mathrm{i}\tau}{\hbar} H_\sigma & -\mathrm{i}\mathbb{I}_L - \frac{\tau}{\hbar} H_\sigma & \mathbb{I}_L & -\mathrm{i}\mathbb{I}_L \\ \mathrm{i}\mathbb{I}_L + \frac{\tau}{\hbar} H_\sigma & -\mathbb{I}_L + \frac{\mathrm{i}\tau}{\hbar} H_\sigma & -\mathrm{i}\mathbb{I}_L & 3\mathbb{I}_L \end{pmatrix}$$

Since eventually $\tau$ will go to zero, the determinant in the denominator in the third line can be approximated by an exponential,

$$\begin{aligned}
\det\left[\mathbb{I}_L - \frac{\mathrm{i}\tau}{\hbar}\Re H_\sigma - \frac{\tau^2}{2\hbar^2} H_\sigma^* H_\sigma\right] &\approx \det \exp\left[-\frac{\mathrm{i}\tau}{\hbar}\Re H_\sigma\right] \\
&= \exp\left[-\frac{\mathrm{i}\tau}{\hbar}\mathrm{Tr} H_\sigma\right],
\end{aligned}$$

where the real part could be omitted in the last step, since $H_\sigma$ is hermitian, and therefore its diagonal entries are real.

Moreover, the inverse of $A$ can be approximated by its Taylor series up

to first order in $\tau$ using $(\mathbb{I}_{4L}+\tau X)^{-1}\approx\mathbb{I}_{4L}-\tau X$, which finally yields

$$\left\langle \mathbf{p}\left|\exp\left(-\frac{\mathrm{i}\tau}{\hbar}\hat{H}\right)\right|\mathbf{q}\right\rangle = \frac{1}{\sqrt{4\pi b^2}^{L}}\left[\int \mathrm{d}^{2L\times 2L}\eta \exp\left(\frac{\mathrm{i}\tau}{2\hbar}\sum_{l_1,l_2,l_3,l_4=1}^{L}\eta_{l_1l_2}\left(V^{-1}\right)_{l_1l_3l_2l_4}\eta_{l_3l_4}\right)\right]^{-1} \int \mathrm{d}^{2L\times 2L}\sigma \exp\left\{\frac{\mathrm{i}\tau}{2\hbar}\sum_{l_1,l_2,l_3,l_4=1}^{L}\sigma_{l_1l_2}\left(V^{-1}\right)_{l_1l_3l_2l_4}\sigma_{l_3l_4} -\frac{\mathrm{i}}{2b^2}\mathbf{p}\cdot\mathbf{q}-\frac{\mathrm{i}\tau}{\hbar}\boldsymbol{\psi}^{*}H_{\sigma}\boldsymbol{\psi}+\frac{\mathrm{i}\tau}{2\hbar}\mathrm{Tr}H_{\sigma}\right\}$$

Performing the integration over $\sigma$ by substituting

$$\sigma_{ll'}=\sigma'_{ll'}+\sum_{l_1,l_2=1}^{L}V_{ll_1l'l_2}\left[\frac{1}{2}\delta_{l_1l_2}-\psi^{*}_{l_1}\psi_{l_2}\right]$$

yields

$$\left\langle \mathbf{p}\left|\exp\left(-\frac{\mathrm{i}\tau}{\hbar}\hat{H}\right)\right|\mathbf{q}\right\rangle = \frac{1}{\sqrt{4\pi b^2}}\exp\left(-\frac{\mathrm{i}}{2b^2}\mathbf{p}\cdot\mathbf{q}-\frac{\mathrm{i}\tau}{\hbar}H^{(\mathrm{cl})}\left(\mathbf{q}-\mathrm{i}\mathbf{p},\mathbf{q}+\mathrm{i}\mathbf{p}\right)\right),$$

where the classical Hamiltonian is given by Eq. (4.9).

## A.2 The stationary phase approximation to the bosonic propagator in quadrature representation

The stationary phase approximation to the propagator for bosonic systems in quadrature representation starts from (*c.f.* Eq. (4.6))

$$K\left(\mathbf{q}^{(f)},\mathbf{q}^{(i)};t_f,t_i\right) = \lim_{M\to\infty}\int \mathrm{d}^{L}q^{(1)}\cdots\int \mathrm{d}^{L}q^{(M-1)}\int \mathrm{d}^{L}p^{(1)}\cdots\int \mathrm{d}^{L}p^{(M)}\prod_{m=1}^{M}\frac{1}{(4\pi b^2)^{L}} \exp\left\{\frac{\mathrm{i}}{\hbar}\left[\frac{\hbar}{2b^2}\mathbf{p}^{(m)}\left(\mathbf{q}^{(m)}-\mathbf{q}^{(m-1)}\right)-\tau H^{(\mathrm{cl})}\left(\boldsymbol{\psi}^{(m)*},\boldsymbol{\psi}^{(m)};t_i+m\tau\right)\right]\right\},$$

While the determination of the stationary points of the exponential is straight forward and stated in section 4.3.1, the integration over fluctuations are more elaborate. These integrals are given by

$$\lim_{M\to\infty}\int \mathrm{d}^L\delta q^{(1)}\cdots\int \mathrm{d}^L\delta q^{(M-1)}\int \mathrm{d}^L\delta p^{(1)}\cdots\int \mathrm{d}^L\delta p^{(M)}\frac{1}{(4\pi b^2)^{ML}}\exp\left[\frac{\mathrm{i}\delta\mathbf{p}^{(1)}\delta\mathbf{q}^{(1)}}{2b^2}\right.$$
$$+\frac{\mathrm{i}}{2b^2}\sum_{m=2}^{M}\begin{pmatrix}\delta\mathbf{q}^{(m-1)}\\ \delta\mathbf{p}^{(m)}\end{pmatrix}\begin{pmatrix}0 & 0\\ \mathbb{I}_L & 0\end{pmatrix}\begin{pmatrix}\delta\mathbf{q}^{(m)}\\ \delta\mathbf{p}^{(m+1)}\end{pmatrix}-\frac{\mathrm{i}\tau}{2\hbar}\delta\mathbf{p}^{(1)}\frac{\partial^2 H^{(1)}}{\partial\mathbf{p}^{(1)2}}\delta\mathbf{p}^{(1)}$$
$$\left.-\frac{\mathrm{i}\tau}{2\hbar}\sum_{m=2}^{M}\begin{pmatrix}\delta\mathbf{q}^{(m-1)}\\ \delta\mathbf{p}^{(m)}\end{pmatrix}\begin{pmatrix}\frac{\partial^2 H^{(m)}}{\partial\mathbf{q}^{(m-1)2}} & \frac{\hbar}{2b^2\tau}+\frac{\partial^2 H^{(m)}}{\partial\mathbf{q}^{(m-1)}\mathbf{p}^{(m)}}\\ \frac{\hbar}{2b^2\tau}+\frac{\partial^2 H^{(m)}}{\partial\mathbf{p}^{(m)}\mathbf{q}^{(m-1)}} & \frac{\partial^2 H^{(m)}}{\partial\mathbf{p}^{(m)2}}\end{pmatrix}\begin{pmatrix}\delta\mathbf{q}^{(m-1)}\\ \delta\mathbf{p}^{(m)}\end{pmatrix}\right],$$

which can after the substitutions $\delta\mathbf{q}^{(m)}=2b\mathbf{x}^{(m)}$, $\delta\mathbf{p}^{(m)}=2b\mathbf{y}^{(m)}$ also be written as

$$\lim_{M\to\infty}\int \mathrm{d}^L x^{(1)}\cdots\int \mathrm{d}^L x^{(M-1)}\int \mathrm{d}^L y^{(1)}\cdots\int \mathrm{d}^L y^{(M)}\frac{\exp\left(\mathrm{i}\Phi/\hbar\right)}{\pi^{ML}\left(2b\right)^{L}}$$
$$\times\exp\left\{\mathrm{i}\sum_{m=1}^{M-1}\left[\begin{pmatrix}\mathbf{x}^{(m)}\\ \mathbf{y}^{(m)}\end{pmatrix}\begin{pmatrix}-\frac{2b^2\tau}{\hbar}\frac{\partial^2 H^{(m+1)}}{\partial\mathbf{q}^{(m)2}} & \mathbb{I}_L\\ \mathbb{I}_L & -\frac{2b^2\tau}{\hbar}\frac{\partial^2 H^{(m)}}{\partial\mathbf{p}^{(m)2}}\end{pmatrix}\begin{pmatrix}\mathbf{x}^{(m)}\\ \mathbf{y}^{(m)}\end{pmatrix}\right.\right.$$
$$\left.-2\mathrm{i}\begin{pmatrix}\mathbf{x}^{(m)}\\ \mathbf{y}^{(m)}\end{pmatrix}\begin{pmatrix}0 & \mathbb{I}_L+\frac{2b^2\tau}{\hbar}\frac{\partial^2 H^{(m+1)}}{\partial\mathbf{q}^{(m)}\partial\mathbf{p}^{(m+1)}}\\ 0 & 0\end{pmatrix}\begin{pmatrix}\mathbf{x}^{(m+1)}\\ \mathbf{y}^{(m+1)}\end{pmatrix}\right]$$
$$\left.-\frac{2\mathrm{i}b^2\tau}{\hbar}\mathbf{y}^{(M)}\frac{\partial^2 H^{(M)}}{\partial\mathbf{p}^{(M)2}}\mathbf{y}^{(M)}\right\},$$

where the result has to be evaluated at $\mathbf{x}^{(M)}=0$.

Step by step integrating out $\mathbf{x}^{(1)},\mathbf{y}^{(1)},\mathbf{x}^{(2)},\mathbf{y}^{(2)},\mathbf{x}^{(3)},\mathbf{y}^{(3)},\ldots$ indicates that it is convenient to introduce recursively

$$X^{(m+1)}=$$
$$-\frac{2b^2\tau}{\hbar}\frac{\partial^2 H^{(m+1)}}{\partial\mathbf{p}^{(m+1)2}}$$
$$+\left(\mathbb{I}_L+\frac{2b^2\tau}{\hbar}\frac{\partial^2 H^{(m+1)}}{\partial\mathbf{p}^{(m+1)}\partial\mathbf{q}^{(m)}}\right)\left(-\frac{2b^2\tau}{\hbar}\frac{\partial^2 H^{(m+1)}}{\partial\mathbf{q}^{(m)2}}-X^{(m)-1}\right)^{-1}$$
$$\times\left(\mathbb{I}_L+\frac{2b^2\tau}{\hbar}\frac{\partial^2 H^{(m+1)}}{\partial\mathbf{q}^{(m)}\partial\mathbf{p}^{(m+1)}}\right)$$

with the initial condition

$$X^{(1)} = -\frac{2b^2\tau}{\hbar}\frac{\partial^2 H^{(1)}}{\partial \mathbf{p}^{(1)^2}}.$$

Expanding Eq. (A.2) up to linear order in $\tau$ yields

$$\begin{aligned} X^{(m+1)} = X^{(m)} &- \frac{2b^2\tau}{\hbar}\frac{\partial^2 H^{(m+1)}}{\partial \mathbf{p}^{(m+1)^2}} + \frac{2b^2\tau}{\hbar}\frac{\partial^2 H^{(m+1)}}{\partial \mathbf{p}^{(m+1)}\partial \mathbf{q}^{(m)}}X^{(m)} \\ &+ \frac{2b^2\tau}{\hbar}X^{(m)}\frac{\partial^2 H^{(m+1)}}{\partial \mathbf{q}^{(m)}\partial \mathbf{p}^{(m+1)}} - \frac{2b^2\tau}{\hbar}X^{(m)}\frac{\partial^2 H^{(m+1)}}{\partial \mathbf{q}^{(m)^2}}X^{(m)}. \end{aligned}$$

In continuous limit $\tau \to 0$, the recursion relation for $X$ gets transformed into a first order differential equation,

$$\dot{X} = -\frac{2b^2}{\hbar}\frac{\partial^2 H}{\partial \mathbf{p}^2} + \frac{2b^2}{\hbar}\frac{\partial^2 H}{\partial \mathbf{p}\partial \mathbf{q}}X + \frac{2b^2}{\hbar}X\frac{\partial^2 H}{\partial \mathbf{q}\partial \mathbf{p}} - \frac{2b^2}{\hbar}X\frac{\partial^2 H}{\partial \mathbf{q}^2}X$$

with initial condition $X(t_i) = 0$ and is solved by

$$X = -\frac{\partial \mathbf{q}}{\partial \mathbf{p}(t_i)}\left(\frac{\partial \mathbf{p}}{\partial \mathbf{p}(t_i)}\right)^{-1}$$

Therefore, the integral over the fluctuations yields

$$\begin{aligned} &\lim_{M\to\infty}\int \frac{\mathrm{d}^L y^{(M)}}{(2\pi b)^L}\exp\left(\mathrm{i}\Phi/\hbar + \mathrm{i}\mathbf{y}^{(M)}X^{(M)}\mathbf{y}^{(M)}\right) \\ &\quad\times\prod_{m=1}^{M-1}\left[\det \mathrm{i}\begin{pmatrix} -\frac{2b^2\tau}{\hbar}\frac{\partial^2 H^{(m+1)}}{\partial \mathbf{q}^{(m)^2}} & \mathbb{I}_L \\ \mathbb{I}_L & X^{(m)} \end{pmatrix}\right]^{-\frac{1}{2}} \\ &= \lim_{M\to\infty}\frac{\exp\left(\frac{\mathrm{i}}{\hbar}\Phi\right)}{\sqrt{\det\left(-4\mathrm{i}b^2\pi X^{(M)}\right)}}\prod_{m=1}^{M-1}\left[\det\left(\mathbb{I}_L + \frac{2b^2\tau}{\hbar}\frac{\partial^2 H^{(m+1)}}{\partial \mathbf{q}^{(m)^2}}X^{(m)}\right)\right]^{-\frac{1}{2}} \\ &= \lim_{M\to\infty}\frac{\exp\left(\frac{\mathrm{i}}{\hbar}\Phi\right)}{\sqrt{\det\left(-4\mathrm{i}b^2\pi X^{(M)}\right)}}\exp\left(-\frac{b^2\tau}{\hbar}\sum_{m=1}^{M-1}\mathrm{Tr}\frac{\partial^2 H^{(m+1)}}{\partial \mathbf{q}^{(m)^2}}X^{(m)}\right) \\ &= \frac{\exp\left(\frac{\mathrm{i}}{\hbar}\Phi\right)}{\sqrt{\det\left(-4\mathrm{i}b^2\pi X(t_f)\right)}}\exp\left(-\frac{b^2}{\hbar}\int_{t_i}^{t_f}\mathrm{d}t\mathrm{Tr}\frac{\partial^2 H}{\partial \mathbf{q}^2}X\right). \end{aligned}$$

Using the differential equation for $\partial\mathbf{q}/\partial\mathbf{p}(t_i)$, the exponent can be written as

$$\begin{aligned}\frac{b^2}{\hbar}\int_{t_i}^{t_f}\mathrm{d}t\mathrm{Tr}\frac{\partial^2 H}{\partial\mathbf{q}^2}X &= -\frac{b^2}{\hbar}\int_{t_i}^{t_f}\mathrm{d}t\mathrm{Tr}\frac{\partial^2 H}{\partial\mathbf{q}^2}\frac{\partial\mathbf{q}}{\partial\mathbf{p}(t_i)}\left(\frac{\partial\mathbf{p}}{\partial\mathbf{p}(t_i)}\right)^{-1}\\ &=\frac{1}{2}\int_{t_i}^{t_f}\mathrm{d}t\mathrm{Tr}\left(\frac{\mathrm{d}}{\mathrm{d}t}\frac{\partial\mathbf{p}}{\partial\mathbf{p}(t_i)}\right)\left(\frac{\partial\mathbf{p}}{\partial\mathbf{p}(t_i)}\right)^{-1}+\frac{b^2}{\hbar}\int_{t_i}^{t_f}\mathrm{d}t\mathrm{Tr}\frac{\partial^2 H}{\partial\mathbf{q}\partial\mathbf{p}}\\ &=\frac{1}{2}\mathrm{Tr}\ln\frac{\partial\mathbf{p}(t_f)}{\partial\mathbf{p}(t_i)}.\end{aligned}$$

Thus, the semiclassical prefactor of the bosonic propagator in quadrature representation is given by the van-Vleck-Gutzwiller determinant

$$\sqrt{\det\left[\frac{1}{-4\mathrm{i}b^2\pi}\left(-\frac{\partial\mathbf{p}(t_i)}{\partial\mathbf{q}^{(f)}}\right)\right]}=\sqrt{\det\left[\frac{1}{-2\pi\mathrm{i}\hbar}\frac{\partial^2 R_\gamma}{\partial\mathbf{q}^{(f)}\partial\mathbf{q}^{(i)}}\right]}.$$

## A.3 The basis change from Quadratures to Fock states for the semiclassical propagator

The propagator in Fock state representation is related to the propagator in quadrature representation via

$$\begin{aligned}&K\left(\mathbf{n}^{(f)},\mathbf{n}^{(i)};t_f,t_i\right)=\left\langle\mathbf{n}^{(f)}\right|\hat{K}\left(t_f,t_i\right)\left|\mathbf{n}^{(i)}\right\rangle\\ &=\int\mathrm{d}^L q^{(f)}\int\mathrm{d}^L q^{(i)}\left\langle\mathbf{n}^{(f)}\middle|\mathbf{q}^{(f)}\right\rangle\left\langle\mathbf{q}^{(f)}\right|\hat{K}\left(t_f,t_i\right)\left|\mathbf{q}^{(i)}\right\rangle\left\langle\mathbf{q}^{(i)}\middle|\mathbf{n}^{(i)}\right\rangle\\ &=\int\mathrm{d}^L q^{(f)}\int{}^L q^{(i)}\left\langle\mathbf{n}^{(f)}\middle|\mathbf{q}^{(f)}\right\rangle\left\langle\mathbf{q}^{(i)}\middle|\mathbf{n}^{(i)}\right\rangle K\left(\mathbf{q}^{(f)},\mathbf{q}^{(i)};t_f,t_i\right).\end{aligned}$$

We plug in the semiclassical propagator (4.10), as well as the asymptotic expression of the overlap between a Fock and a quadrature state for large occupation number (3.13). Furthermore, for simplicity of writing, we introduce

$$F(q,n)=\frac{q}{4b^2}\sqrt{4b^2\left(n+\frac{1}{2}\right)-q^2}-\left(n+\frac{1}{2}\right)\arccos\left(\frac{q}{2b\sqrt{n+\frac{1}{2}}}\right)+\frac{\pi}{4},$$

which can be interpreted as generating function for the basis transform from $q$ and $p$ to $n$ and $\theta$, where $n$ is the modulus square and $\theta$ the phase of the mean field wave function. This can be seen by noticing that,

$$\frac{\partial F\left(q,n\right)}{\partial q}=\frac{\sqrt{n+\frac{1}{2}+\frac{q^2}{4b^2}}}{b}\equiv\frac{p}{2b} \tag{A.1}$$

$$\frac{\partial F\left(q,n\right)}{\partial n}=-\arccos\left(\frac{q}{2b\sqrt{n+\frac{1}{2}}}\right)\equiv-\theta. \tag{A.2}$$

Using this definition, the semiclassical propagator in Fock state representation can be written as

$$\begin{aligned}
&K\left(\mathbf{n}^{(f)},\mathbf{n}^{(i)};t_f,t_i\right)=\\
&\int \mathrm{d}^L q^{(f)}\int \mathrm{d}^L q^{(i)}\sum_{\mathbf{s}^{(i)},\mathbf{s}^{(f)}\in\{-1,1\}^L}\left[\prod_{l=1}^{L}\sqrt{\frac{\partial^2 F\left(q_l^{(f)},n_l^{(f)}\right)}{\partial q_l^{(f)}\partial n_l^{(f)}}\frac{\partial^2 F\left(q_l^{(i)},n_l^{(i)}\right)}{\partial q_l^{(i)}\partial n_l^{(i)}}}\right]\\
&\quad\times\sum_{\gamma:\mathbf{q}^{(i)}\to\mathbf{q}^{(f)}}\sqrt{\det\frac{1}{(-8\pi^3\mathrm{i}\hbar)}\frac{\partial^2 R_\gamma\left(\mathbf{q}^{(f)},\mathbf{q}^{(i)};t_f,t_i\right)}{\partial\mathbf{q}^{(f)}\partial\mathbf{q}^{(i)}}}\mathrm{e}^{\frac{\mathrm{i}}{\hbar}R_\gamma\left(\mathbf{q}^{(f)},\mathbf{q}^{(i)};t_f,t_i\right)}\\
&\quad\times\exp\left\{\mathrm{i}\sum_{l=1}^{L}\left[s_l^{(i)}F\left(q_l^{(i)},n_l^{(i)}\right)-s_l^{(f)}F\left(q_l^{(f)},n_l^{(f)}\right)\right]+\frac{\mathrm{i}}{\hbar}\Phi\left(t_f,t_i\right)\right\}.
\end{aligned} \tag{A.3}$$

Since the asymptotic formula for the overlap is valid only for the oscillating region $|q|<2b\sqrt{n+\frac{1}{2}}$, one can substitute

$$\begin{aligned}
q_1^{(i)}=&2b\sqrt{n_1^{(i)}+\frac{1}{2}}\cos\theta_1^{(i)},\\
q_l^{(i)}=&2b\sqrt{n_l^{(i)}+\frac{1}{2}}\cos\left(\theta_l^{(i)}+\theta_1^{(i)}\right) &&\text{for} l=2,\ldots,L,\\
q_l^{(f)}=&2b\sqrt{n_l^{(f)}+\frac{1}{2}}\cos\left(\theta_l^{(f)}+\theta_1^{(i)}\right) &&\text{for} l=1,\ldots,L.
\end{aligned}$$

In the following, for reasons that will become obvious after the stationary phase conditions, we will refere to the $\theta_l^{(i/f)}$'s as "phases". Note that these definitions correspond to the definitions of the phases by (A.2). Together

with the sums over $\mathbf{s}^{(i)}$ and $\mathbf{s}^{(f)}$, the integrals over $\theta_l^{(i/f)}$ then run from $-\pi$ to $\pi$ and the phase $\theta_1^{(i)}$ does not enter in the hamiltonian part of the action. Moreover, it will turn out to be a global phase, dropping out of the equations of motion. Therefore, the integral over $\theta_1^{(i)}$ can not be evaluated in stationary phase approximation, since it is an integral over a continuous family of trajectories.

However, the remaining $2L-1$ integrals can be evaluated in stationary phase approximation. Here, we will do the two integrations over the final and initial quadratures one after another, starting with the final ones.

The stationary phase condition for the integration over the final phases is given by

$$p_l^{(f)} = 2b\sqrt{n_l^{(f)} + \frac{1}{2}}\sin\left(\theta_l^{(f)} + \theta_1^{(i)}\right)$$

Thus, the stationary phase approximation selects those classical trajectories $\boldsymbol{\psi}(t)$ satisfying the boundary conditions

$$|\psi_l(t_f)|^2 = n_l^{(f)} + \frac{1}{2}, \tag{A.4}$$

and therefore justifies that we called the $\theta_l^{(f)}$'s "phases", since the solutions of the stationary phase conditions are the trajectories with the final phases equal to them.

The evaluation of the exponent at the stationary point will be postponed to when we derived the stationary phase condition for the initial phases.

The second derivative of the exponent in (A.3) with respect to the initial and final phases at the stationary point yields

$$\begin{aligned}
&\frac{\partial^2}{\partial\theta_l^{(f)}\partial\theta_{l'}^{(f)}}\left\{\frac{1}{\hbar}R_\gamma\left(\mathbf{q}^{(f)},\mathbf{q}^{(i)};t_f,t_i\right) + \sum_{m=1}^{L}\left[\left(n_m^{(f)}+\frac{1}{2}\right)\left(\theta_m^{(f)}+\theta_1^{(i)}\right)\right.\right.\\
&\qquad\left.\left.-\sqrt{n_m^{(f)}+\frac{1}{2}}\cos\left(\theta_m^{(f)}+\theta_1^{(i)}\right)\sin\left(\theta_m^{(f)}+\theta_1^{(i)}\right)\right]\right\}\\
&= \sqrt{n_l^{(f)}+\frac{1}{2}}\sin\left(\theta_l^{(f)}+\theta_1^{(i)}\right)\left[2\delta_{ll'}\sqrt{n_l^{(f)}+\frac{1}{2}}\cos\left(\theta_l^{(f)}+\theta_1^{(i)}\right) - \frac{1}{b}\frac{\partial p_l^{(f)}}{\partial\theta_{l'}^{(f)}}\right]\\
&= -\frac{\partial}{\partial\theta_{l'}^{(f)}}\frac{1}{4b^2}\left[\left(q_l^{(f)}\right)^2+\left(p_l^{(f)}\right)^2\right] = -\left(\frac{\partial\theta_{l'}^{(f)}}{\partial n_l^{(f)}}\right)^{-1}.
\end{aligned}$$

Therefore, together with the prefactor given by the second derivative of the generating function, the semiclassical prefactor after performing the integration over the final phases is given by

$$\sqrt{\prod_{l=1}^{L}\frac{\partial q_l^{(i)}}{\partial\theta_l^{(i)}}}\sqrt{\frac{1}{(-4\pi^2\mathrm{i}\hbar)^L}\det\frac{\partial^2 R_\gamma\left(\mathbf{n}^{(f)},\mathbf{q}^{(i)};t_f,t_i\right)}{\partial\mathbf{n}^{(f)}\partial\mathbf{q}^{(i)}}}, \tag{A.5}$$

where we defined

$$\begin{aligned}R_\gamma\left(\mathbf{n}^{(f)},\mathbf{q}^{(i)};t_f,t_i\right) = \\ R_\gamma\left(\mathbf{q}^{(f)},\mathbf{q}^{(i)};t_f,t_i\right)+\hbar\sum_{l=1}^{L}\Bigg[\left(n_l^{(f)}+\frac{1}{2}\right)\left(\theta_l^{(f)}+\theta_1^{(i)}\right) \\ -\sqrt{n_l^{(f)}+\frac{1}{2}}\cos\left(\theta_l^{(f)}+\theta_1^{(i)}\right)\sin\left(\theta_l^{(f)}+\theta_1^{(i)}\right)\Bigg]\end{aligned}$$

evaluated at the stationary point.

Noticing that

$$\frac{\partial R_\gamma\left(\mathbf{n}^{(f)},\mathbf{q}^{(i)};t_f,t_i\right)}{\partial\mathbf{n}^{(f)}} = \hbar\left(\boldsymbol{\theta}^{(f)}+\theta_1^{(i)}\mathbf{1}\right),$$

where $\mathbf{1}$ is the vector, which every entry is equal to one, one can write (A.5) also as

$$\sqrt{\det\frac{1}{(-4\pi^2\mathrm{i})}\frac{\partial\left(\boldsymbol{\theta}^{(f)}+\theta_1^{(i)}\mathbf{1}\right)}{\partial\boldsymbol{\theta}^{(i)}}}.$$

Now, the stationary phase condition for the integration over the initial phases, save for $\theta_1^{(i)}$, yields

$$p_l^{(i)} = 2b\sqrt{n_l^{(i)}+\frac{1}{2}}\sin\left(\theta_l^{(i)}+\theta_1^{(i)}\right),$$

which corresponds to

$$|\psi_l(t_i)|^2 = n_l^{(i)}+\frac{1}{2}. \tag{A.6}$$

Note that with (A.4) and (A.6) the conservation of the total number of particles together with the fact that $q_1^{(i)} = \sqrt{n_1^{(i)}+1/2}\cos\theta_1^{(i)}$ already requires that

$$\psi_1(t_i) = \sqrt{n_1^{(i)}+\frac{1}{2}}\exp\left(\mathrm{i}\theta_1^{(i)}\right). \tag{A.7}$$

Moreover, we see that $\theta_1^{(i)}$ indeed is a global phase, which does neither enter the equations of motion, nor the Hamiltonian. Therefore, the solutions to the equations of motion under the boundary conditions (A.4), (A.6) and (A.7) are the trajectories with the initial phase of the first component fixed to a certain $\varphi$, *e.g.* $\varphi = 0$, and multiplied by a global phase factor $\exp\left(\mathrm{i}\theta_1^{(i)} - \mathrm{i}\varphi\right)$.

With this, one can now evaluate the exponent at the stationary points, which will then give the classical action in Fock representation. Substituting

$$\begin{aligned} q_l(t) =& 2b\sqrt{n_l(t) + \frac{1}{2}}\cos\left(\theta_l(t) + \theta_1^{(i)}\right), \\ p_l(t) =& 2b\sqrt{n_l(t) + \frac{1}{2}}\sin\left(\theta_l(t) + \theta_1^{(i)}\right) \end{aligned}$$

in the kinetic part of the action, in consideration of the preservation of the total number of particles by the classical equations of motion yields for the classical action in Fock state representation

$$R_\gamma\left(\mathbf{n}^{(f)}, \mathbf{n}^{(i)}; t_f, t_i\right) = \int_{t_i}^{t_f} \mathrm{d}t \left[\hbar\boldsymbol{\theta}(t)\cdot\dot{\mathbf{n}}(t) - H^{(\mathrm{cl})}\left(\boldsymbol{\psi}^*(t), \boldsymbol{\psi}(t); t\right)\right].$$

Analoguous to above,

$$\begin{aligned} \frac{\partial^2}{\partial\theta_l^{(i)}\partial\theta_{l'}^{(i)}}\Bigg\{\frac{1}{\hbar}R\left(\mathbf{n}^{(f)}, \mathbf{q}^{(i)}; t_f, t_i\right) - \sum_{m=1}^{L}\Bigg[\left(n_m^{(i)} + \frac{1}{2}\right)\left(\theta_m^{(i)} + \theta_1^{(i)}\right) \\ - \sqrt{n_m^{(i)} + \frac{1}{2}}\cos\left(\theta_m^{(i)} + \theta_1^{(i)}\right)\sin\left(\theta_m^{(i)} + \theta_1^{(i)}\right)\Bigg]\Bigg\} \\ = \left(\frac{\partial\theta_{l'}^{(i)}}{\partial n_l^{(i)}}\right)^{-1}. \end{aligned}$$

Therefore, we find

$$K\left(\mathbf{n}^{(f)},\mathbf{n}^{(i)};t_f,t_i\right)=$$
$$\frac{1}{2\pi}\int_0^{2\pi}\mathrm{d}\theta_1^{(i)}\sum_{\gamma:\mathbf{n}^{(f)}\to\mathbf{n}^{(i)}}\sqrt{\frac{1}{-2\pi\mathrm{i}}\det\left(\frac{\partial\theta_l^{(i)}}{\partial n_{l'}^{(i)}}\right)_{l,l'=2,\ldots,L}\det\frac{\partial\left(\boldsymbol{\theta}^{(f)}+\theta_1^{(i)}\mathbf{1}\right)}{\partial\boldsymbol{\theta}^{(i)}}}$$
$$\times\exp\left[\frac{\mathrm{i}}{\hbar}R_\gamma\left(\mathbf{n}^{(f)},\mathbf{n}^{(i)};t_f,t_i\right)+\frac{\mathrm{i}}{\hbar}\Phi\left(t_f,t_i\right)\right]. \tag{A.8}$$

It is important to notice that the two matrices in the prefactor have different dimensions. The first one is a $(L-1)\times(L-1)$-matrix, while the second one is $L\times L$ dimensional. However, since $\boldsymbol{\theta}^{(f)}$ does not depend on $\theta_1^{(i)}$, the second one has the form

$$\begin{pmatrix}\mathbf{1} & \dfrac{\partial\boldsymbol{\theta}^{(f)}}{\partial\tilde{\boldsymbol{\theta}}^{(i)}},\end{pmatrix}$$

where $\tilde{\boldsymbol{\theta}}^{(i)}$ is the vector resulting from $\boldsymbol{\theta}^{(i)}$ by skipping its first entry. Moreover, we can match the dimensions of the two matrices by using

$$\det\left(\frac{\partial\tilde{\boldsymbol{\theta}}^{(i)}}{\partial\tilde{\mathbf{n}}^{(i)}}\right)=\det\begin{pmatrix}1 & 0\\ 0 & \dfrac{\partial\tilde{\boldsymbol{\theta}}^{(i)}}{\partial\tilde{\mathbf{n}}^{(i)}}\end{pmatrix}$$

Then,

$$\begin{pmatrix}\mathbf{1} & \dfrac{\partial\boldsymbol{\theta}^{(f)}}{\partial\tilde{\boldsymbol{\theta}}^{(i)}},\end{pmatrix}\begin{pmatrix}1 & 0\\ 0 & \dfrac{\partial\tilde{\boldsymbol{\theta}}^{(i)}}{\partial\tilde{\mathbf{n}}^{(i)}}\end{pmatrix}=\begin{pmatrix}\mathbf{1} & \dfrac{\partial\boldsymbol{\theta}^{(f)}}{\partial\tilde{\mathbf{n}}^{(i)}}\end{pmatrix}.$$

The determinant of this matrix however can be further simplified by using Sylvester's determinant theorem, which states that for an $n\times m$ matrix $A$ and an $m\times n$ matrix $B$

$$\det\left(\mathbb{I}_n+AB\right)=\det\left(\mathbb{I}_m+BA\right),$$

where $\mathbb{I}_n$ is the $n\times n$ unit matrix and applying it to the right hand side of

$$\det\begin{pmatrix}1 & \dfrac{\partial\theta_1^{(f)}}{\partial\tilde{\mathbf{n}}^{(i)}}\\ \mathbf{1} & \dfrac{\partial\tilde{\boldsymbol{\theta}}^{(f)}}{\partial\tilde{\mathbf{n}}^{(i)}}\end{pmatrix}=$$
$$\det\begin{pmatrix}1 & \dfrac{\partial\theta_1^{(f)}}{\partial\tilde{\mathbf{n}}^{(i)}}\\ \mathbf{0} & \dfrac{\partial\tilde{\boldsymbol{\theta}}^{(f)}}{\partial\tilde{\mathbf{n}}^{(i)}}\end{pmatrix}\left[\mathbb{I}_L+\begin{pmatrix}-\dfrac{\partial\theta_1^{(f)}}{\partial\tilde{\mathbf{n}}^{(i)}}\left(\dfrac{\partial\tilde{\boldsymbol{\theta}}^{(f)}}{\partial\tilde{\mathbf{n}}^{(i)}}\right)^{-1}\mathbf{1} & \mathbf{0}^{\mathrm{T}}\\ \left(\dfrac{\partial\tilde{\boldsymbol{\theta}}^{(f)}}{\partial\tilde{\mathbf{n}}^{(i)}}\right)^{-1}\mathbf{1} & 0\end{pmatrix}\right]$$

With this, one can show that

$$\det\begin{pmatrix}\mathbf{1} & \dfrac{\partial\boldsymbol{\theta}^{(f)}}{\partial\tilde{\mathbf{n}}^{(i)}}\end{pmatrix} = \det\frac{\partial\tilde{\boldsymbol{\theta}}^{(f)}}{\partial\tilde{\mathbf{n}}^{(i)}} = \det\hbar\frac{\partial^2 R_\gamma\left(\mathbf{n}^{(f)},\mathbf{n}^{(i)};t_f,t_i\right)}{\partial\tilde{\mathbf{n}}^{(f)}\partial\tilde{\mathbf{n}}^{(i)}}.$$

Finally, we see that the integrand in (A.8) is independent of $\theta_1^{(i)}$, such that the final result reads

$$K\left(\mathbf{n}^{(f)},\mathbf{n}^{(i)};t_f,t_i\right) = \sum_{\gamma:\mathbf{n}^{(i)}\to\mathbf{n}^{(f)}}\sqrt{\det\frac{1}{(-2\pi\mathrm{i}\hbar)}\frac{\partial^2 R_\gamma\left(\mathbf{n}^{(f)},\mathbf{n}^{(i)};t_f,t_i\right)}{\partial\tilde{\mathbf{n}}^{(f)}\partial\tilde{\mathbf{n}}^{(i)}}}$$
$$\times\exp\left\{\frac{\mathrm{i}}{\hbar}\left[R_\gamma\left(\mathbf{n}^{(f)},\mathbf{n}^{(i)};t_f,t_i\right)+\Phi\left(t_f,t_i\right)\right]\right\}.$$

APPENDIX B

# The Feynman Path Integral for Fermions using complex variables

The starting point for the derivation of a complex path integral representation of the fermionic propagator is, *cf.* (5.1)

$$
\begin{aligned}
&K\left(\mathbf{n}^{(f)},\mathbf{n}^{(i)};t_f,t_i\right) = \\
&\quad\lim_{M\to\infty}\int \mathrm{d}^{2L}\zeta^{(0)}\int \mathrm{d}^{2L}\chi^{(0)}\cdots\int \mathrm{d}^{2L}\zeta^{(M)}\int \mathrm{d}^{2L}\chi^{(M)}\left\langle \mathbf{n}^{(f)}\,\middle|\,\boldsymbol{\chi}^{(M)}\right\rangle \\
&\qquad\times\left\langle \boldsymbol{\chi}^{(M)}\,\middle|\,\boldsymbol{\zeta}^{(M)}\right\rangle\left\{\prod_{m=0}^{M-1}\langle\boldsymbol{\zeta}^{(m+1)}|\,\mathrm{e}^{-\frac{\mathrm{i}\tau}{\hbar}\hat{H}^{(m)}}\,|\boldsymbol{\chi}^{(m)}\rangle\left\langle \boldsymbol{\chi}^{(m)}\,\middle|\,\boldsymbol{\zeta}^{(m)}\right\rangle\right\} \\
&\qquad\qquad\times\left\langle \boldsymbol{\zeta}^{(0)}\,\middle|\,\mathbf{n}^{(i)}\right\rangle,
\end{aligned}
$$

which after expanding the exponential up to first order in $\tau$ and evaluating the overlaps yields

$$
\begin{aligned}
K\left(\mathbf{n}^{(f)},\mathbf{n}^{(i)};t_f,t_i\right) = & \\
\lim_{M\to\infty}\int \mathrm{d}^{2L}\zeta^{(0)}\int \mathrm{d}^{2L}\chi^{(0)}\cdots\int \mathrm{d}^{2L}\zeta^{(M)}\int \mathrm{d}^{2L}\chi^{(M)}\left[\prod_{l=0}^{L-1}\left(\chi_{L-l}^{(M)}\right)^{n_{L-l}^{(f)}}\right] & \\
\times\exp\left[-\sum_{m=0}^{M}\left(\boldsymbol{\zeta}^{(m)^*}\cdot\boldsymbol{\zeta}^{(m)}+\boldsymbol{\chi}^{(m)^*}\cdot\boldsymbol{\chi}^{(m)}\right)\right]\left[\prod_{l=1}^{L}\left(1+\chi_l^{(M)^*}\zeta_l^{(M)}\right)\right] & \\
\times\left\{\prod_{m=0}^{M-1}\left[1-\frac{\mathrm{i}\tau}{\hbar}\sum_{\alpha,\beta=1}^{L}\left(h_{\alpha\beta}^{(m)}\zeta_\alpha^{(m+1)^*}\chi_\beta^{(m)}+U_{\alpha\beta}^{(m)}\zeta_\alpha^{(m+1)^*}\zeta_\beta^{(m+1)^*}\chi_\beta^{(m)}\chi_\alpha^{(m)}\right)\right]\right. & \\
\left.\times\left[\prod_{l=1}^{L}\left(1+\zeta_l^{(m+1)^*}\chi_l^{(m)}\right)\left(1+\chi_l^{(m)^*}\zeta_l^{(m)}\right)\right]\right\} & \\
\times\left[\prod_{l=1}^{L}\left(\zeta_l^{(0)^*}\right)^{n_l^{(i)}}\right]. &
\end{aligned}
$$

The fact that for (positiv) integer $j, j'$

$$
\int_0^{2\pi}\mathrm{d}\theta\int \mathrm{d}^2\phi\exp\left(-|\phi|^2+\phi^*\mathrm{e}^{\mathrm{i}\theta}-\mathrm{i}j\theta\right)\phi^{j'} = 2\pi^2\delta_{j,j'} \tag{B.1a}
$$

$$
\int \mathrm{d}^2\phi\int \mathrm{d}^2\mu\exp\left(-|\phi|^2-|\mu|^2+\phi^*\mu\right)\phi^j\,(\mu^*)^{j'} = \pi^2 j!\,\delta_{j,j'}, \tag{B.1b}
$$

where $\mathrm{d}^2\mu = \mathrm{d}\Re\mu\mathrm{d}\Im\mu$, allows to insert these integrals such that $\boldsymbol{\zeta}^{(m+1)}$ and $\boldsymbol{\zeta}^{(m)}$ appear decoupled only. For this, it is best to first of all expand the factors of the product over the individual time steps according to

$$
\begin{aligned}
&\left[\prod_{l=1}^{L}\left(1+\chi_l^{(m)^*}\zeta_l^{(m)}\right)\right] \\
&\times\left[1-\frac{\mathrm{i}\tau}{\hbar}\sum_{\alpha,\beta=1}^{L}\left(h_{\alpha\beta}^{(m-1)}\zeta_\alpha^{(m)^*}\chi_\beta^{(m-1)}+U_{\alpha\beta}^{(m-1)}\zeta_\alpha^{(m)^*}\zeta_\beta^{(m)^*}\chi_\beta^{(m-1)}\chi_\alpha^{(m-1)}\right)\right] \\
&=\left[a^{(m)}-\frac{\mathrm{i}\tau}{\hbar}b^{(m)}-\frac{\mathrm{i}\tau}{\hbar}c^{(m)}-\frac{\mathrm{i}\tau}{\hbar}d^{(m)}\right],
\end{aligned}
$$

with

$$a^{(m)} = \prod_{l=1}^{L} \left(1 + \chi_l^{(m)^*} \zeta_l^{(m)}\right)$$

$$b^{(m)} = \Theta\,(m-1) \left[\prod_{l=1}^{L} \left(1 + \chi_l^{(m)^*} \zeta_l^{(m)}\right)\right] \sum_{\alpha=1}^{L} h_{\alpha\alpha}^{(m-1)} \zeta_\alpha^{(m)} \chi_\alpha^{(m-1)}$$

$$c^{(m)} = \Theta\,(m-1) \left[\prod_{l=1}^{L} \left(1 + \chi_l^{(m)^*} \zeta_l^{(m)}\right)\right] \sum_{\substack{\alpha,\beta=1 \\ \alpha\neq\beta}}^{L} h_{\alpha\beta}^{(m-1)} \zeta_\alpha^{(m)} \chi_\beta^{(m-1)}$$

$$d^{(m)} =$$

$$\Theta(m-1) \left[\prod_{l=1}^{L} \left(1 + \chi_l^{(m)^*} \zeta_l^{(m)}\right)\right] \sum_{\substack{\alpha,\beta=1 \\ \alpha\neq\beta}}^{L} U_{\alpha\beta}^{(m-1)} \zeta_\alpha^{(m)} \zeta_\beta^{(m)} \chi_\beta^{(m-1)} \chi_\alpha^{(m-1)}$$

and then considering one by one each factor starting with $m = 0$. For $m = 0$, (B.1a) is used in order to replace

$$\int \mathrm{d}^{2L}\zeta^{(0)} \exp\left(-\boldsymbol{\zeta}^{(0)^*} \cdot \boldsymbol{\zeta}^{(0)}\right) \left[\prod_{l=1}^{L} \left(1 + \chi_l^{(0)^*} \zeta_l^{(0)}\right)\right] \prod_{l=1}^{L} \left(\zeta_l^{(0)^*}\right)^{n_l^{(i)}} =$$

$$\int \mathrm{d}^{2N^{(i)}}\phi^{(0)} \int_0^{2\pi} \mathrm{d}^{N^{(i)}}\theta^{(i)} \int \mathrm{d}^{2L}\zeta^{(0)} \mathrm{e}^{-\boldsymbol{\zeta}^{(0)^*}\cdot\boldsymbol{\zeta}^{(0)} - \left|\boldsymbol{\phi}^{(0)}\right|^2 + \boldsymbol{\phi}^{(0)^*}\cdot\boldsymbol{\mu}^{(0)}}$$

$$\times \left[\prod_{l=1}^{L} \left(1 + \chi_l^{(0)^*} \phi_l^{(0)}\right)\right] \left[\prod_{l=0}^{L-1} \left(1 + \zeta_{L-l}^{(0)} \mu_{L-l}^{(0)^*}\right)\right] \frac{\prod_{l=1}^{L} \left(\zeta_l^{(0)^*}\right)^{n_l^{(i)}}}{\left(2\pi^2\right)^{N^{(i)}}},$$

with $\mu_l^{(0)} = n_l^{(i)} \exp\left(\mathrm{i}\theta_l^{(i)}\right)$ for all $l \in \{1, \ldots, L\}$. Note that here, for the initially unoccupied sites, the phases $\theta_l^{(i)}$ are arbitrary but fixed, *e.g.* to zero.

For the $N^{(i)} = \sum_{l=1}^{L} n_l^{(i)}$ occupied sites, the identity follows directly from (B.1a), while for the unoccupied ones, it is important to notice that the term $\chi_l^{(0)^*} \zeta_l^{(0)}$ does vanish when integrating over $\boldsymbol{\zeta}^{(0)}$. This is because of the properties of the Grassmann integrals (3.20) and the fact that there is no $\zeta_l^{(0)^*}$ for those components, for which $n_l^{(i)} = 0$.

For $m > 0$, using (B.1b) leads to

$$
\begin{aligned}
a^{(m)} = & \int \mathrm{d}^{2L}\mu^{(m)} \int \frac{2L\phi^{(m)}}{\pi^{2L}} \mathrm{e}^{-\left|\boldsymbol{\phi}^{(m)}\right|^2 - \left|\boldsymbol{\mu}^{(m)}\right|^2 + \boldsymbol{\phi}^{(m)*}\cdot\boldsymbol{\mu}^{(m)}} \\
& \times \left[\prod_{l=1}^{L}\left(1+\chi_l^{(m)*}\phi_l^{(m)}\right)\right] \prod_{l=0}^{L-1}\left[1+\zeta_{L-l}^{(m)}\sum_{j=1}^{\infty}\frac{1}{j!}\left(\mu_{L-l}^{(m)*}\right)^j\left(\phi_{L-l}^{(m-1)}\right)^{j-1}\right] \\
b^{(m)} = & \int \mathrm{d}^{2L}\mu^{(m)} \int \frac{2L\phi^{(m)}}{\pi^{2L}} \mathrm{e}^{-\left|\boldsymbol{\phi}^{(m)}\right|^2 - \left|\boldsymbol{\mu}^{(m)}\right|^2 + \boldsymbol{\phi}^{(m)*}\cdot\boldsymbol{\mu}^{(m)}} \left[\prod_{l=1}^{L}\left(1+\chi_l^{(m)*}\phi_l^{(m)}\right)\right] \\
& \times \sum_{\alpha=1}^{L} h_{\alpha\alpha}^{(m-1)}\zeta_\alpha^{(m)*}\chi_\alpha^{(m-1)} \prod_{l=0}^{L-1}\left[1+\zeta_{L-l}^{(m)}\sum_{j=1}^{\infty}\frac{\left(\mu_{L-l}^{(m)*}\right)^j\left(\phi_{L-l}^{(m-1)}\right)^{j-1}}{(j-\delta_{L-l,\alpha})\,!}\right] \\
c^{(m)} = & \int \mathrm{d}^{2L}\mu^{(m)} \int \frac{2L\phi^{(m)}}{\pi^{2L}} \mathrm{e}^{-\left|\boldsymbol{\phi}^{(m)}\right|^2 - \left|\boldsymbol{\mu}^{(m)}\right|^2 + \boldsymbol{\phi}^{(m)*}\cdot\boldsymbol{\mu}^{(m)}} \\
& \times \left[\prod_{l=1}^{L}\left(1+\chi_l^{(m)*}\phi_l^{(m)}\right)\right] \sum_{\substack{\alpha,\beta=1 \\ \alpha\neq\beta}}^{L} h_{\alpha\beta}^{(m-1)}\zeta_\alpha^{(m)*}\chi_\beta^{(m-1)} \\
& \times \left\{\prod_{l=0}^{L-\max(\alpha,\beta)-1}\left[1+\zeta_{L-l}^{(m)}\sum_{j=1}^{\infty}\frac{1}{j!}\left(\mu_{L-l}^{(m)*}\right)^j\left(\phi_{L-l}^{(m-1)}\right)^{j-1}\right]\right\} \\
& \times \left(1+\zeta_{\max(\alpha,\beta)}^{(m)}{\mu_{\max(\alpha,\beta)}^{(m)}}^*\right) \\
& \times \left\{\prod_{l=L-\max(\alpha,\beta)+1}^{L-\min(\alpha,\beta)-1}\left[1+\zeta_{L-l}^{(m)}\sum_{j=1}^{\infty}\frac{2j-1}{j!}\left(\mu_{L-l}^{(m)*}\right)^j\left(\phi_{L-l}^{(m-1)}\right)^{j-1}\right]\right\} \\
& \times \left(1+\zeta_{\min(\alpha,\beta)}^{(m)}{\mu_{\min(\alpha,\beta)}^{(m)}}^*\right) \\
& \times \prod_{l=L-\min(\alpha,\beta)+1}^{L-1}\left[1+\zeta_{L-l}^{(m)}\sum_{j=1}^{\infty}\frac{1}{j!}\left(\mu_{L-l}^{(m)*}\right)^j\left(\phi_{L-l}^{(m-1)}\right)^{j-1}\right] \\
d^{(m)} = & \int \mathrm{d}^{2L}\mu^{(m)} \int \frac{2L\phi^{(m)}}{\pi^{2L}} \mathrm{e}^{-\left|\boldsymbol{\phi}^{(m)}\right|^2 - \left|\boldsymbol{\mu}^{(m)}\right|^2 + \boldsymbol{\phi}^{(m)*}\cdot\boldsymbol{\mu}^{(m)}} \\
& \times \left[\prod_{l=1}^{L}\left(1+\chi_l^{(m)*}\phi_l^{(m)}\right)\right] \sum_{\substack{\alpha,\beta=1 \\ \alpha\neq\beta}}^{L} U_{\alpha\beta}^{(m-1)}\zeta_\alpha^{(m)*}\zeta_\beta^{(m)*}\chi_\beta^{(m-1)}\chi_\alpha^{(m-1)} \\
& \times \prod_{l=0}^{L-1}\left[1+\zeta_{L-l}^{(m)}\sum_{j=1}^{\infty}\frac{1}{(j-\delta_{L-l,\alpha}-\delta_{L-l,\beta})\,!}\left(\mu_{L-l}^{(m)*}\right)^j\left(\phi_{L-l}^{(m-1)}\right)^{j-1}\right]
\end{aligned}
$$

It has been possible to insert the additional terms $\left(\phi_l^{(m-1)}\right)^{j-1}$, since these variables are already defined by the integrals introduced for smaller $m$, and the integration over $\boldsymbol{\mu}^{(m)}$ and $\boldsymbol{\phi}^{(m)}$ selects the $j = 1$ term only.

Finally, for $m = M$, a similar argument as for $m = 0$ allows to restrict the integrals over $\boldsymbol{\phi}^{(M)}$ again to those $N^{(f)} = \sum_{l=1}^{L} n_l^{(f)}$ components with $n_l^{(f)} = 1$, while setting all the other components of $\boldsymbol{\phi}^{(M)}$ to zero.

After this, the propagator reads

$$
\begin{aligned}
&K\left(\mathbf{n}^{(f)},\mathbf{n}^{(i)};t_f,t_i\right)=\\
&\lim_{M\to\infty}\int \mathrm{d}^{2L}\zeta^{(0)}\int \mathrm{d}^{2L}\chi^{(0)}\cdots\int \mathrm{d}^{2L}\zeta^{(M)}\int \mathrm{d}^{2L}\chi^{(M)}\int_0^{2\pi}\mathrm{d}^{N^{(i)}}\theta^{(i)}\int \mathrm{d}^{2L}\phi^{(0)}\\
&\int \mathrm{d}^{2L}\phi^{(1)}\int \mathrm{d}^{2L}\mu^{(1)}\cdots\int \mathrm{d}^{2L}\phi^{(M-1)}\int \mathrm{d}^{2L}\mu^{(M-1)}\int \mathrm{d}^{2L}\mu^{(M)}\int \mathrm{d}^{2N^{(f)}}\phi^{(M)}\\
&\mathrm{e}^{\sum_{m=0}^{M}\left[-\boldsymbol{\zeta}^{(m)*}\cdot\boldsymbol{\zeta}^{(m)}-\boldsymbol{\chi}^{(m)*}\cdot\boldsymbol{\chi}^{(m)}-\left|\boldsymbol{\phi}^{(m)}\right|^2-\left|\boldsymbol{\mu}^{(m)}\right|^2+\boldsymbol{\phi}^{(m)*}\cdot\boldsymbol{\mu}^{(m)}\right]+N^{(i)}}\\
&\times\frac{1}{2^{N^{(i)}}\pi^{N^{(i)}+N^{(f)}+2ML}}\left[\prod_{l=0}^{L-1}\left(\chi_{L-l}^{(M)}\right)^{n_{L-l}^{(f)}}\right]\left[\prod_{l=1}^{L}\left(1+\chi_l^{(M)*}\phi_l^{(M)}\right)\right]\\
&\times\left\{\prod_{m=0}^{M-1}\left[\prod_{l=0}^{L-1}\left(1+\zeta_{L-l}^{(m+1)}\sum_{j=1}^{\infty}\frac{1}{j!}\left(\mu_{L-l}^{(m+1)*}\right)^j\left(\phi_{L-l}^{(m)}\right)^{j-1}\right)\right.\right.\\
&\quad-\frac{\mathrm{i}\tau}{\hbar}\sum_{\alpha=1}^{L}h_{\alpha\alpha}^{(m)}\zeta_{\alpha}^{(m+1)*}\chi_{\alpha}^{(m)}\prod_{l=0}^{L-l}\left(1+\zeta_{L-l}^{(m+1)}\sum_{j=1}^{\infty}\frac{\left(\mu_{L-l}^{(m+1)*}\right)^j\left(\phi_{L-l}^{(m)}\right)^{j-1}}{(j-\delta_{L-l,\alpha})\,!}\right)\\
&\quad-\frac{\mathrm{i}\tau}{\hbar}\sum_{\substack{\alpha,\beta=1\\ \alpha\neq\beta}}^{L}h_{\alpha\beta}^{(m)}\zeta_{\alpha}^{(m+1)*}\chi_{\beta}^{(m)}\\
&\qquad\times\left(\prod_{l=0}^{L-\max(\alpha,\beta)-1}\left\{1+\zeta_{L-l}^{(m+1)}\sum_{j=1}^{\infty}\frac{\left(\mu_{L-l}^{(m+1)*}\right)^j\left(\phi_{L-l}^{(m)}\right)^{j-1}}{j!}\right\}\right)\\
&\qquad\times\left(1+\zeta_{\max(\alpha,\beta)}^{(m+1)}{\mu_{\max(\alpha,\beta)}^{(m+1)}}^{*}\right)\\
&\qquad\times\left(\prod_{l=L-\max(\alpha,\beta)+1}^{L-\min(\alpha,\beta)-1}\left\{1+\zeta_{L-l}^{(m+1)}\sum_{j=1}^{\infty}\frac{2j-1}{j!}\left(\mu_{L-l}^{(m+1)*}\right)^j\left(\phi_{L-l}^{(m)}\right)^{j-1}\right\}\right)\\
&\qquad\times\left(1+\zeta_{\min(\alpha,\beta)}^{(m+1)}{\mu_{\min(\alpha,\beta)}^{(m+1)}}^{*}\right)\\
&\qquad\times\prod_{l=L-\min(\alpha,\beta)+1}^{L-1}\left(1+\zeta_{L-l}^{(m+1)}\sum_{j=1}^{\infty}\frac{1}{j!}\left(\mu_{L-l}^{(m+1)*}\right)^j\left(\phi_{L-l}^{(m)}\right)^{j-1}\right)\\
&\quad-\frac{\mathrm{i}\tau}{\hbar}\sum_{\substack{\alpha,\beta=1\\ \alpha\neq\beta}}^{L}U_{\alpha\beta}^{(m)}\zeta_{\alpha}^{(m+1)*}\zeta_{\beta}^{(m+1)*}\chi_{\beta}^{(m)}\chi_{\alpha}^{(m)}\\
&\qquad\times\left.\left.\prod_{l=0}^{L-l}\left(1+\zeta_{L-l}^{(m+1)}\sum_{j=1}^{\infty}\frac{\left(\mu_{L-l}^{(m+1)*}\right)^j\left(\phi_{L-l}^{(m)}\right)^{j-1}}{(j-\delta_{L-l,\alpha}-\delta_{L-l,\beta})\,!}\right)\right]\left[\prod_{l=1}^{L}\left(1+\zeta_l^{(m+1)*}\chi_l^{(m)}\right)\right]\right.\\
&\left.\times\prod_{l=1}^{L}\left[1+\chi_l^{(m)*}\phi_l^{(m)}\right]\right\}\left[\prod_{l=0}^{L-1}\left(1+\zeta_{L-l}^{(0)}{\mu_{L-l}^{(0)}}^{*}\right)\right]\prod_{l=1}^{L}\left(\zeta_l^{(0)*}\right)^{n_l^{(i)}},
\end{aligned}
$$

with $\mu_l^{(0)} = n_l^{(i)} \exp\left(\mathrm{i}\theta_l^{(i)}\right)$.

Since the $m$-th factor in the product over the timesteps only depends on $\boldsymbol{\zeta}^{(m+1)}$ and $\boldsymbol{\chi}^{(m)}$, one can easily integrate out the intermediate Grassmann

variables $\boldsymbol{\zeta}^{(1)},\ldots,\boldsymbol{\zeta}^{(M)}$ and $\boldsymbol{\chi}^{(0)},\ldots,\boldsymbol{\chi}^{(M-1)}$ by using

$$\begin{aligned}
&\int \mathrm{d}^{2L}\zeta^{(m+1)} \int \mathrm{d}^{2L}\chi^{(m)} \mathrm{e}^{-\boldsymbol{\zeta}^{(m+1)^*}\cdot\boldsymbol{\zeta}^{(m+1)}-\boldsymbol{\chi}^{(m)^*}\cdot\boldsymbol{\chi}^{(m)}} \\
&\qquad \times \left[\prod_{l=0}^{L-1}\left(1+\zeta_{L-l}^{(m+1)} f_{L-l}^{(m)}\right)\right]\left[\prod_{l=1}^{L}\left(1+\zeta_l^{(m+1)^*}\chi_l^{(m)}\right)\right] \\
&\qquad \times \prod_{l=1}^{L}\left(1+\chi_l^{(m)^*}\phi_l^{(m)}\right) \\
&\quad = \prod_{l=1}^{L}\left(1+f_l^{(m)}\phi_l^{(m)}\right), \\
&\int \mathrm{d}^{2L}\zeta^{(m+1)} \int \mathrm{d}^{2L}\chi^{(m)} \mathrm{e}^{-\boldsymbol{\zeta}^{(m+1)^*}\cdot\boldsymbol{\zeta}^{(m+1)}-\boldsymbol{\chi}^{(m)^*}\cdot\boldsymbol{\chi}^{(m)}} \zeta_\alpha^{(m+1)^*}\chi_\beta^{(m)} \\
&\qquad \times \left[\prod_{l=0}^{L-1}\left(1+\zeta_{L-l}^{(m+1)} f_{L-l}^{(m)}\right)\right]\left[\prod_{l=1}^{L}\left(1+\zeta_l^{(m+1)^*}\chi_l^{(m)}\right)\right] \\
&\qquad \times \prod_{l=1}^{L}\left(1+\chi_l^{(m)^*}\phi_l^{(m)}\right) \\
&\quad = f_\alpha^{(m)}\phi_\beta^{(m)}\left[\prod_{l=1}^{\min(\alpha,\beta)-1}\left(1+f_l^{(m)}\phi_l^{(m)}\right)\right] \\
&\qquad \times \left[\prod_{l=\max(\alpha,\beta)+1}^{L}\left(1+f_l^{(m)}\phi_l^{(m)}\right)\right]\prod_{l=\min(\alpha,\beta)+1}^{\max(\alpha,\beta)-1}\left(1-f_l^{(m)}\phi_l^{(m)}\right), \\
&\int \mathrm{d}^{2L}\zeta^{(m+1)} \int \mathrm{d}^{2L}\chi^{(m)} \mathrm{e}^{-\boldsymbol{\zeta}^{(m+1)^*}\cdot\boldsymbol{\zeta}^{(m+1)}-\boldsymbol{\chi}^{(m)^*}\cdot\boldsymbol{\chi}^{(m)}} \zeta_\alpha^{(m+1)^*}\zeta_\beta^{(m+1)^*} \\
&\qquad \times \chi_\beta^{(m)}\chi_\alpha^{(m)}\left[\prod_{l=0}^{L-1}\left(1+\zeta_{L-l}^{(m+1)} f_{L-l}^{(m)}\right)\right]\left[\prod_{l=1}^{L}\left(1+\zeta_l^{(m+1)^*}\chi_l^{(m)}\right)\right] \\
&\qquad \times \prod_{l=1}^{L}\left(1+\chi_l^{(m)^*}\phi_l^{(m)}\right) \\
&\quad = f_\alpha^{(m)} f_\beta^{(m)}\phi_\beta^{(m)}\phi_\alpha^{(m)} \prod_{\substack{l=1 \\ l\neq\alpha,\beta}}^{l}\left(1+f_l^{(m)}\phi_l^{(m)}\right).
\end{aligned}$$

Moreover, the integrals over $\boldsymbol{\zeta}^{(0)}$ and $\boldsymbol{\chi}^{(M)}$ yield

$$\int \mathrm{d}^{2L}\zeta^{(0)}\mathrm{e}^{-\boldsymbol{\zeta}^{(0)*}\cdot\boldsymbol{\zeta}^{(0)}}\left[\prod_{l=0}^{L-1}\left(1+\zeta_{L-l}^{(0)}{\mu_{L-l}^{(0)}}^{*}\right)\right]\prod_{l=1}^{L}\left(\zeta_l^{(0)*}\right)^{n_l^{(i)}} = \prod_{j=1}^{N^{(i)}}\mu_{l_j^{(i)}}^{(0)\,*}$$

$$\int \mathrm{d}^{2L}\chi^{(M)}\mathrm{e}^{-\boldsymbol{\chi}^{(M)*}\cdot\boldsymbol{\chi}^{(M)}}\left[\prod_{l=0}^{L-1}\left(\chi_{L-l}^{(M)}\right)^{n_{L-l}^{(f)}}\right]\prod_{l=1}^{L}\left(1+\chi_l^{(M)}\phi_l^{(M)*}\right) = \prod_{j=1}^{N^{(f)}}\phi_{l_j^{(f)}}^{(M)}$$

After performing these integrals, one notices that the inserted integrals have been chosen such that the resulting sums can be performed, yielding exponentials, and finds the propagator to read

$$\begin{aligned}K\left(\mathbf{n}^{(f)},\mathbf{n}^{(i)};t_f,t_i\right) = \lim_{M\to\infty}\int \mathrm{d}^{2L}\phi^{(0)}\int \mathrm{d}^{2L}\phi^{(1)}\int \mathrm{d}^{2L}\mu^{(1)}\cdots\int \mathrm{d}^{2L}\phi^{(M-1)}\int \mathrm{d}^{2L}\mu^{(M-1)}\\ \int \mathrm{d}^{2L}\mu^{(M)}\int \mathrm{d}^{2N^{(f)}}\phi^{(M)}\int_0^{2\pi}\mathrm{d}^{N^{(i)}}\theta^{(i)}\left(\prod_{j=1}^{N^{(f)}}\phi_{l_j^{(f)}}^{(M)}\right)\exp\left\{\sum_{m=0}^{M}\left[-\left|\boldsymbol{\phi}^{(m)}\right|^2\right.\right.\\ \left.\left.-\left|\boldsymbol{\mu}^{(m)}\right|^2+\boldsymbol{\phi}^{(m)*}\cdot\boldsymbol{\mu}^{(m)}\right]+N^{(i)}-\mathrm{i}\sum_{j=1}^{N^{(i)}}\theta_{l_j^{(i)}}^{(i)}+\sum_{m=0}^{M-1}\boldsymbol{\mu}^{(m+1)*}\cdot\boldsymbol{\phi}^{(m)}\right\}\\ \times\frac{\prod_{m=0}^{M-1}\left[1-\frac{\mathrm{i}\tau}{\hbar}H^{(\mathrm{cl})(k)}\left(\boldsymbol{\mu}^{(m+1)*},\boldsymbol{\phi}^{(m)}\right)\right]}{2^{N^{(i)}}\pi^{N^{(i)}+N^{(f)}+2ML}},\end{aligned}$$

with

$$H^{(\mathrm{cl})(k)}\left(\boldsymbol{\mu}^*,\boldsymbol{\phi}\right) = \sum_{\alpha=1}^{L} h^{(k)}_{\alpha\alpha}\mu^*_\alpha\phi_\alpha + \sum_{\substack{\alpha,\beta=1\\ \alpha\neq\beta}}^{L} U^{(k)}_{\alpha\beta}\mu^*_\alpha\mu^*_\beta\phi_\beta\phi_\alpha + \sum_{\substack{\alpha,\beta=1\\ \alpha\neq\beta}}^{L} h^{(k)}_{\alpha\beta}\mu^*_\alpha\phi_\beta \exp\left(-\mu^*_\alpha\phi_\alpha - \mu^*_\beta\phi_\beta\right) \prod_{l=\min(\alpha,\beta)+1}^{\max(\alpha,\beta)-1} \left(1-2\mu^*_l\phi_l\right).$$

Now, one can also integrate out $\boldsymbol{\mu}^{(1)},\ldots,\boldsymbol{\mu}^{(M)}$ as well as $\boldsymbol{\phi}^{(0)}$ and redo the expansion in $\tau$ to obtain the final path integral expression,

$$K\left(\mathbf{n}^{(f)},\mathbf{n}^{(i)};t_f,t_i\right) = \lim_{M\to\infty}\int_0^{2\pi} \mathrm{d}^{N^{(i)}}\theta^{(i)} \int \mathrm{d}^{2L}\phi^{(1)}\ldots\int \mathrm{d}^{2L}\phi^{(M-1)} \int \mathrm{d}^{2N^{(f)}}\phi^{(M)} \left(\prod_{j=1}^{N^{(f)}} \phi^{(M)}_{l^{(f)}_j}\right) \frac{\mathrm{e}^{\sum_{m=1}^{M}\left[-\left|\boldsymbol{\phi}^{(m)}\right|^2+\boldsymbol{\phi}^{(m)*}\cdot\boldsymbol{\phi}^{(m-1)}-\frac{\mathrm{i}\tau}{\hbar}H^{(\mathrm{cl})(m-1)}\left(\boldsymbol{\phi}^{(m)*},\boldsymbol{\phi}^{(m-1)}\right)\right]-\mathrm{i}\sum_{j=1}^{N^{(i)}}\theta^{(i)}_{l^{(i)}_j}}}{(2\pi)^{N^{(i)}}\,\pi^{N^{(f)}+(M-1)L}}.$$

APPENDIX C

# Semiclassical propagator for Fermions

## C.1 Derivation of the semiclassical prefactor

After the substitution $\phi_l^{(m)} = \sqrt{J_l^{(m)}} \exp\left[\mathrm{i}\left(\theta_l^{(m)} - \theta_{l_1^{(i)}}^{(i)}\right)\right]$ and integration over $\theta_{l_1^{(i)}}^{(i)}$, the propagator is given by

$$
\begin{aligned}
&K\left(\mathbf{n}^{(f)}, \mathbf{n}^{(i)}; t_f, t_i\right) = \\
&\delta_{N^{(i)},N^{(f)}} \lim_{M\to\infty} \int_0^{2\pi} \mathrm{d}^{N-1}\theta^{(i)} \int_0^{2\pi} \mathrm{d}^{L}\theta^{(1)} \int_0^{\infty} \mathrm{d}^{L}J^{(1)} \cdots \int_0^{2\pi} \mathrm{d}^{L}\theta^{(M-1)} \int_0^{\infty} \mathrm{d}^{L}J^{(M-1)} \\
&\int_0^{2\pi} \mathrm{d}^{N}\theta^{(M)} \int_0^{\infty} \mathrm{d}^{N}J^{(M)} \frac{\exp\left[\mathrm{i}\left(\mathbf{n}^{(f)}\cdot\boldsymbol{\theta}^{(M)} - \mathbf{n}^{(i)}\boldsymbol{\theta}^{(i)}\right)\right]}{(2\pi)^{2N-1+(M-1)L}} \left(\prod_{j=1}^{N} \sqrt{J_{l_j^{(f)}}^{(M)}}\right) \\
&\exp\left\{\sum_{m=1}^{M}\left[-\left|\boldsymbol{\phi}^{(m)}\right|^2 + \boldsymbol{\phi}^{(m)*}\cdot\boldsymbol{\phi}^{(m-1)} - \frac{\mathrm{i}\tau}{\hbar} H^{(\mathrm{cl})(m-1)}\left(\boldsymbol{\phi}^{(m)*}, \boldsymbol{\phi}^{(m-1)}\right)\right]\right\},
\end{aligned}
$$

where now (and in the following) $\theta_{l_1^{(i)}}^{(i)} = 0$. For simplicity of writing the initial and final phases for the non-occupied states are also set to zero, *i.e.* $\theta_l^{(i)} = 0$ for all $l \in \{1,\ldots,L\} \setminus \left\{l_2^{(i)},\ldots,l_{N^{(i)}}^{(i)}\right\}$ as well as $\theta_l^{(f)} = 0$ for all

$l \in \{1,\dots,L\} \setminus \left\{l_1^{(f)},\dots,l_{N^{(f)}}^{(f)}\right\}$. When performing the stationary phase approximation, the additional factor

$$\prod_{j=1}^{N}\sqrt{J^{(M)}_{l_j^{(f)}}} = \exp\left(\frac{1}{2}\sum_{j=1}^{N}\log J^{(M)}_{l_j^{(f)}}\right)$$

has to be included in the stationary phase analysis as well.

The stationary phase conditions are then found by taking the derivative of the exponent with respect to all the $J_l^{(m)}$ and $\theta_l^{(m)}$ individually and are given by

$$\begin{aligned}
-\exp\left(-\mathrm{i}\theta^{(i)}_{l_j^{(i)}}\right) + {\phi^{(1)}_{l_j^{(i)}}}^{*} - \frac{\mathrm{i}\tau}{\hbar}\frac{\partial {H^{(\mathrm{cl})}}^{(0)}}{\partial \phi^{(0)}_{l_j^{(i)}}} &= 0\\
\left(\phi_l^{(m-1)} - \frac{\mathrm{i}\tau}{\hbar}\frac{\partial {H^{(\mathrm{cl})}}^{(m-1)}}{\partial {\phi_l^{(m)}}^{*}}\right)\frac{\partial {\phi_l^{(m)}}^{*}}{\partial J_l^{(m)}} + \left({\phi_l^{(m+1)}}^{*} - \frac{\mathrm{i}\tau}{\hbar}\frac{\partial {H^{(\mathrm{cl})}}^{(m)}}{\partial \phi_l^{(m)}}\right)\frac{\partial \phi_l^{(m)}}{\partial J_l^{(m)}} &= 1\\
\left(\phi_l^{(m-1)} - \frac{\mathrm{i}\tau}{\hbar}\frac{\partial {H^{(\mathrm{cl})}}^{(m-1)}}{\partial {\phi_l^{(m)}}^{*}}\right)\frac{\partial {\phi_l^{(m)}}^{*}}{\partial \theta_l^{(m)}} + \left({\phi_l^{(m+1)}}^{*} - \frac{\mathrm{i}\tau}{\hbar}\frac{\partial {H^{(\mathrm{cl})}}^{(m)}}{\partial \phi_l^{(m)}}\right)\frac{\partial \phi_l^{(m)}}{\partial \theta_l^{(m)}} &= 0\\
\left(\frac{1}{\sqrt{J^{(M)}_{l_j^{(f)}}}} - 2\sqrt{J^{(M)}_{l_j^{(f)}}}\right)\exp\left(\mathrm{i}\theta^{(M)}_{l_j^{(f)}}\right) + \phi^{(M-1)}_{l_j^{(f)}} - \frac{\mathrm{i}\tau}{\hbar}\frac{\partial {H^{(\mathrm{cl})}}^{(M-1)}}{\partial {\phi^{(M)}_{l_j^{(f)}}}^{*}} &= 0\\
\frac{\exp\left(\mathrm{i}\theta^{(M)}_{l_j^{(f)}}\right)}{\sqrt{J^{(M)}_{l_j^{(f)}}}} - \left(\phi^{(M-1)}_{l_j^{(f)}} - \frac{\mathrm{i}\tau}{\hbar}\frac{\partial {H^{(\mathrm{cl})}}^{(M-1)}}{\partial {\phi^{(M)}_{l_j^{(f)}}}^{*}}\right) &= 0
\end{aligned}$$

with the short hand notation ${H^{(\mathrm{cl})}}^{(m)} = {H^{(\mathrm{cl})}}^{(m)}\left(\boldsymbol{\phi}^{(m+1)^*}, \boldsymbol{\phi}^{(m)}\right)$. The second and third equation are found for all $m \in \{1,\dots,M-1\}$. Keeping in mind that $\phi_l^{(0)} = n_l^{(i)}\exp\left(\mathrm{i}\theta_l^{(i)}\right)$, these stationary phase conditions can be written as

$$\begin{aligned}
\frac{\boldsymbol{\phi}^{(m)} - \boldsymbol{\phi}^{(m-1)}}{\tau} &= -\tfrac{\mathrm{i}}{\hbar}\frac{\partial {H^{(\mathrm{cl})}}^{(m-1)}}{\partial {\boldsymbol{\phi}^{(m)}}^{*}} \quad 1 \le m \le M\\
\frac{{\boldsymbol{\phi}^{(m)}}^{*} - {\boldsymbol{\phi}^{(m-1)}}^{*}}{\tau} &= \tfrac{\mathrm{i}}{\hbar}\frac{\partial {H^{(\mathrm{cl})}}^{(m-1)}}{\partial \boldsymbol{\phi}^{(m-1)}} \quad 1 \le m \le M\\
J^{(M)}_{l_j^{(f)}} &= n^{(f)}_{l_j^{(f)}}.
\end{aligned}$$

Therefore, in the continuous limit $\tau \to 0$, the stationary phase approximation selects the classical trajectories from $\mathbf{n}^{(i)}$ to $\mathbf{n}^{(f)}$, which are defined as the solutions of the equations of motion

$$\mathrm{i}\hbar\dot{\boldsymbol{\phi}} = \frac{\partial H^{(\mathrm{cl})}}{\partial \boldsymbol{\phi}^*}.$$

with

$$\begin{aligned} H^{(\mathrm{cl})} = & \\ & \sum_{\alpha=1}^{L} h_{\alpha\alpha}(t)\left|\phi_\alpha(t)\right|^2 + \sum_{\substack{\alpha,\beta=1 \\ \alpha\neq\beta}}^{L} U_{\alpha\beta}(t)\left|\phi_\alpha(t)\right|^2\left|\phi_\beta(t)\right|^2 \\ & + \sum_{\substack{\alpha,\beta=1 \\ \alpha\neq\beta}}^{L} h_{\alpha\beta}(t)\phi_\alpha^*(t)\phi_\beta(t)\mathrm{e}^{-\left|\phi_\alpha(t)\right|^2-\left|\phi_\beta(t)\right|^2} \prod_{l=\min(\alpha,\beta)+1}^{\max(\alpha,\beta)-1}\left(1-2\left|\phi_l(t)\right|^2\right) \end{aligned}$$

under the boundary conditions

$$\begin{aligned} \left|\phi_l\left(t_i\right)\right|^2 =& n_l^{(i)} \\ \left|\phi_l\left(t_f\right)\right|^2 =& n_l^{(f)} \end{aligned}$$

and $\phi_{l_1^{(i)}}\left(t_i\right) = 1$.

The semiclassical propagator in Fock state representation for Fermions is then given by a sum over these classical trajectories,

$$K\left(\mathbf{n}^{(f)}, \mathbf{n}^{(i)}; t_f, t_i\right) = \sum_{\gamma:\mathbf{n}^{(i)}\to\mathbf{n}^{(f)}} \exp\left(\frac{\mathrm{i}}{\hbar}R_\gamma\right) K_{\mathrm{red}}^{(\gamma)},$$

with the classical action

$$R_\gamma = \int_{t_i}^{t_f} \mathrm{d}t\left[\hbar\boldsymbol{\theta}(t)\cdot\dot{\mathbf{J}}(t) - H^{(\mathrm{cl})}\left(\boldsymbol{\phi}^*(t), \boldsymbol{\phi}(t); t\right)\right].$$

The reduced propagator is given by the remaining integrals over the fluc-

tuations,

$$
\begin{aligned}
&K_{\mathrm{red}}^{(\gamma)} = \\
&\lim_{M\to\infty} \frac{1}{(2\pi)^{2N-1+(M-1)L}} \int \mathrm{d}^{N-1}\delta\theta^{(0)} \int \mathrm{d}^{N}\delta J^{(M)} \int \mathrm{d}^{N}\delta\theta^{(M)} \\
&\int \mathrm{d}^{L}\delta J^{(1)} \int \mathrm{d}^{L}\delta\theta^{(1)} \cdots \int \mathrm{d}^{L}\delta J^{(M-1)} \int \mathrm{d}^{L}\delta\theta^{(M-1)} \\
&\exp\left\{ -\frac{1}{2}\delta\boldsymbol{\theta}^{(0)} P_0^{(i)} \left( A_1^{(0)} + C_1^{(0)} \right) {P_0^{(i)}}^{\mathrm{T}} \delta\boldsymbol{\theta}^{(0)} \right. \\
&- \frac{1}{2} \begin{pmatrix} \delta\boldsymbol{\theta}^{(M)} P^{(f)} \\ \delta\mathbf{J}^{(M)} P^{(f)} \end{pmatrix} \begin{pmatrix} B_1^{(M)} + D_1^{(M)} & B_2^{(M)} + D_2^{(M)} \\ B_2^{(M)} + D_2^{(M)\mathrm{T}} & B_3^{(M)} + D_3^{(M)} \end{pmatrix} \begin{pmatrix} {P^{(f)}}^{\mathrm{T}} \delta\boldsymbol{\theta}^{(M)} \\ {P^{(f)}}^{\mathrm{T}} \delta\mathbf{J}^{(M)} \end{pmatrix} \\
&- \frac{1}{2} \sum_{m=1}^{M-1} \begin{pmatrix} \delta\boldsymbol{\theta}^{(m)} \\ \delta\mathbf{J}^{(m)} \end{pmatrix} \left[ \begin{pmatrix} A_1^{(m)} + B_1^{(m+1)} & A_2^{(m)} - B_2^{(m+1)} \\ A_2^{(m)} - B_2^{(m+1)} & A_3^{(m)} + B_3^{(m+1)} \end{pmatrix} \right. \\
&\qquad \left. + \begin{pmatrix} C_1^{(m)} + D_1^{(m)} & C_2^{(m)} + D_2^{(m)} \\ C_2^{(m)\mathrm{T}} + D_2^{(m)\mathrm{T}} & C_3^{(m)} + D_3^{(m)} \end{pmatrix} \right] \begin{pmatrix} \delta\boldsymbol{\theta}^{(m)} \\ \delta\mathbf{J}^{(m)} \end{pmatrix} \\
&+ \begin{pmatrix} \delta\boldsymbol{\theta}^{(1)} \\ \delta\mathbf{J}^{(1)} \end{pmatrix} \begin{pmatrix} E_1^{(0)} \\ E_3^{(0)} \end{pmatrix} {P_0^{(i)}}^{\mathrm{T}} \delta\boldsymbol{\theta}^{(0)} \\
&+ \begin{pmatrix} \delta\boldsymbol{\theta}^{(M)} P^{(f)} \\ \delta\mathbf{J}^{(M)} P^{(f)} \end{pmatrix} \begin{pmatrix} E_1^{(M-1)} & E_2^{(M-1)} \\ E_3^{(M-1)} & E_4^{(M-1)} \end{pmatrix} \begin{pmatrix} \delta\boldsymbol{\theta}^{(m)} \\ \delta\mathbf{J}^{(m)} \end{pmatrix} \\
&\left. + \sum_{m=1}^{M-2} \begin{pmatrix} \delta\boldsymbol{\theta}^{(m+1)} \\ \delta\mathbf{J}^{(m+1)} \end{pmatrix} \begin{pmatrix} E_1^{(m)} & E_2^{(m)} \\ E_3^{(m)} & E_4^{(m)} \end{pmatrix} \begin{pmatrix} \delta\boldsymbol{\theta}^{(m)} \\ \delta\mathbf{J}^{(m)} \end{pmatrix} \right\}
\end{aligned}
\tag{C.1}
$$

where $P^{(i/f)}$ and $P_0^{(i/f)}$ are defined in the same way as in section 5.2.2, namely as the $(N-1)\times L$ and, respectively, $N\times L$-matrices, which project onto the subspace of initially and finally occupied sites, with the latter excluding the first occupied one,

$$
\begin{aligned}
\left(P^{(i/f)}\right)_{jl'} &= \delta_{l_j^{(i/f)},l'} \\
\left(P_0^{(i/f)}\right)_{jl'} &= \delta_{l_{j+1}^{(i/f)},l'}
\end{aligned}
$$

For later reference, their complements $\bar{P}^{(i/f)}$ and $\bar{P}_0^{(i/f)}$ are also defined, as well as

$$
Q^{(i/f)} = \begin{pmatrix} \bar{P}^{(i/f)} \\ P^{(i/f)} \end{pmatrix}
$$

which are the (orthogonal) matrices, which put the components corresponding to initially and finally unoccupied sites, respectively to the first $L - N^{(i/f)}$ positions, and those correspondig to occupied sites to the last $N^{(i/f)}$ positions, see (5.11).

Furthermore,

$$\begin{aligned}
\left(A_1^{(m)}\right)_{ll'} =& \delta_{ll'}\phi_l^{(m)}\left[\phi_l^{(m+1)^*} - \frac{\mathrm{i}\tau}{\hbar}\frac{\partial H^{(\mathrm{cl})(m)}}{\partial \phi_l^{(m)}}\right] \\
\left(A_2^{(m)}\right)_{ll'} =& \delta_{ll'}\frac{\mathrm{i}\phi_l^{(m)}}{2J_l^{(m)}}\left[\phi_l^{(m+1)^*} - \frac{\mathrm{i}\tau}{\hbar}\frac{\partial H^{(\mathrm{cl})(m)}}{\partial \phi_l^{(m)}}\right] \\
\left(A_3^{(m)}\right)_{ll'} =& \delta_{ll'}\frac{\phi_l^{(m)}}{4{J_l^{(m)}}^2}\left[\phi_l^{(m+1)^*} - \frac{\mathrm{i}\tau}{\hbar}\frac{\partial H^{(\mathrm{cl})(m)}}{\partial \phi_l^{(m)}}\right] \\
\left(B_1^{(m)}\right)_{ll'} =& \delta_{ll'}\phi_l^{(m)^*}\left[\phi_l^{(m-1)} - \frac{\mathrm{i}\tau}{\hbar}\frac{\partial H^{(\mathrm{cl})(m-1)}}{\partial \phi_l^{(m)^*}}\right] \\
\left(B_2^{(m)}\right)_{ll'} =& \delta_{ll'}\frac{\mathrm{i}\phi_l^{(m)^*}}{2J_l^{(m)}}\left[\phi_l^{(m-1)} - \frac{\mathrm{i}\tau}{\hbar}\frac{\partial H^{(\mathrm{cl})(m-1)}}{\partial \phi_l^{(m)^*}}\right] \\
\left(B_3^{(m)}\right)_{ll'} =& \delta_{ll'}\frac{\phi_l^{(m)^*}}{4{J_l^{(m)}}^2}\left[2n_l^{(f)}\delta_{m,M} + \phi_l^{(m-1)} - \frac{\mathrm{i}\tau}{\hbar}\frac{\partial H^{(\mathrm{cl})(m-1)}}{\partial \phi_l^{(m)^*}}\right] \\
\left(C_1^{(m)}\right)_{ll'} =& \frac{\mathrm{i}\tau}{\hbar}\frac{\partial \phi_l^{(m)}}{\partial \theta_l^{(m)}}\frac{\partial^2 H^{(\mathrm{cl})(m)}}{\partial \phi_l^{(m)}\phi_{l'}^{(m)}}\frac{\partial \phi_{l'}^{(m)}}{\partial \theta_{l'}^{(m)}} \\
\left(C_2^{(m)}\right)_{ll'} =& \frac{\mathrm{i}\tau}{\hbar}\frac{\partial \phi_l^{(m)}}{\partial \theta_l^{(m)}}\frac{\partial^2 H^{(\mathrm{cl})(m)}}{\partial \phi_l^{(m)}\phi_{l'}^{(m)}}\frac{\partial \phi_{l'}^{(m)}}{\partial J_{l'}^{(m)}} \\
\left(C_3^{(m)}\right)_{ll'} =& \frac{\mathrm{i}\tau}{\hbar}\frac{\partial \phi_l^{(m)}}{\partial J_l^{(m)}}\frac{\partial^2 H^{(\mathrm{cl})(m)}}{\partial \phi_l^{(m)}\phi_{l'}^{(m)}}\frac{\partial \phi_{l'}^{(m)}}{\partial J_{l'}^{(m)}}
\end{aligned}$$

as well as

$$
\begin{aligned}
\left(D_1^{(m)}\right)_{ll'} =& \frac{\mathrm{i}\tau}{\hbar}\frac{\partial\phi_l^{(m)*}}{\partial\theta_l^{(m)}}\frac{\partial^2 H^{(\mathrm{cl})\,(m-1)}}{\partial\phi_l^{(m)*}\phi_{l'}^{(m)*}}\frac{\partial\phi_{l'}^{(m)*}}{\partial\theta_{l'}^{(m)}}\\
\left(D_2^{(m)}\right)_{ll'} =& \frac{\mathrm{i}\tau}{\hbar}\frac{\partial\phi_l^{(m)*}}{\partial\theta_l^{(m)}}\frac{\partial^2 H^{(\mathrm{cl})\,(m-1)}}{\partial\phi_l^{(m)*}\phi_{l'}^{(m)*}}\frac{\partial\phi_{l'}^{(m)*}}{\partial J_{l'}^{(m)}}\\
\left(D_3^{(m)}\right)_{ll'} =& \frac{\mathrm{i}\tau}{\hbar}\frac{\partial\phi_l^{(m)*}}{\partial J_l^{(m)}}\frac{\partial^2 H^{(\mathrm{cl})\,(m-1)}}{\partial\phi_l^{(m)*}\phi_{l'}^{(m)*}}\frac{\partial\phi_{l'}^{(m)*}}{\partial J_{l'}^{(m)}}\\
\left(E_1^{(m)}\right)_{ll'} =& \frac{\partial\phi_l^{(m+1)*}}{\partial\theta_l^{(m+1)}}\left[\delta_{ll'}-\frac{\mathrm{i}\tau}{\hbar}\frac{\partial^2 H^{(\mathrm{cl})\,(m)}}{\partial\phi_l^{(m+1)*}\partial\phi_{l'}^{(m)}}\right]\frac{\partial\phi_{l'}^{(m)}}{\partial\theta_{l'}^{(m)}}\\
\left(E_2^{(m)}\right)_{ll'} =& \frac{\partial\phi_l^{(m+1)*}}{\partial\theta_l^{(m+1)}}\left[\delta_{ll'}-\frac{\mathrm{i}\tau}{\hbar}\frac{\partial^2 H^{(\mathrm{cl})\,(m)}}{\partial\phi_l^{(m+1)*}\partial\phi_{l'}^{(m)}}\right]\frac{\partial\phi_{l'}^{(m)}}{\partial J_{l'}^{(m)}}\\
\left(E_3^{(m)}\right)_{ll'} =& \frac{\partial\phi_l^{(m+1)*}}{\partial J_l^{(m+1)}}\left[\delta_{ll'}-\frac{\mathrm{i}\tau}{\hbar}\frac{\partial^2 H^{(\mathrm{cl})\,(m)}}{\partial\phi_l^{(m+1)*}\partial\phi_{l'}^{(m)}}\right]\frac{\partial\phi_{l'}^{(m)}}{\partial\theta_{l'}^{(m)}}\\
\left(E_4^{(m)}\right)_{ll'} =& \frac{\partial\phi_l^{(m+1)*}}{\partial J_l^{(m+1)}}\left[\delta_{ll'}-\frac{\mathrm{i}\tau}{\hbar}\frac{\partial^2 H^{(\mathrm{cl})\,(m)}}{\partial\phi_l^{(m+1)*}\partial\phi_{l'}^{(m)}}\right]\frac{\partial\phi_{l'}^{(m)}}{\partial J_{l'}^{(m)}}.
\end{aligned}
$$

These matrices have to be evaluated at the stationary points, which means that one can use the equations of motion to simplify

$$
\begin{aligned}
\left(A_1^{(m)}\right)_{ll'} = \left(B_1^{(m)}\right)_{ll'} =& \delta_{ll'}J_l^{(m)}\\
\left(A_2^{(m)}\right)_{ll'} = \left(B_2^{(m)}\right)_{ll'} =& \delta_{ll'}\frac{\mathrm{i}}{2}\\
\left(A_3^{(m)}\right)_{ll'} = \left(B_3^{(m)}\right)_{ll'} =& \delta_{ll'}\frac{1}{4J_l^{(m)}}
\end{aligned}
$$

With this, (C.1) can be written as

$$
\begin{aligned}
&K_{\mathrm{red}}^{(\gamma)} = \\
&\lim_{M\to\infty} \frac{1}{(2\pi)^{2N-1+(M-1)L}} \int \mathrm{d}^{N-1}\delta\theta^{(0)} \int \mathrm{d}^{N}\delta J^{(M)} \int \mathrm{d}^{N}\delta\theta^{(M)} \\
&\int \mathrm{d}^{L}\delta J^{(1)} \int \mathrm{d}^{L}\delta\theta^{(1)} \cdots \int \mathrm{d}^{L}\delta J^{(M-1)} \int \mathrm{d}^{L}\delta\theta^{(M-1)} \\
&\exp\left\{ -\frac{1}{2}\delta\boldsymbol{\theta}^{(0)} P_0^{(i)} \frac{\partial\boldsymbol{\phi}^{(0)}}{\partial\boldsymbol{\theta}^{(i)}} \left[ -\mathrm{e}^{-2\mathrm{i}\mathrm{diag}\left(\boldsymbol{\theta}^{(i)}\right)} + \frac{\mathrm{i}\tau}{\hbar} \frac{\partial^2 H^{(\mathrm{cl})(0)}}{\partial\boldsymbol{\phi}^{(0)\,2}} \right] \frac{\partial\boldsymbol{\phi}^{(0)}}{\partial\boldsymbol{\theta}^{(i)}} P_0^{(i)\,\mathrm{T}} \delta\boldsymbol{\theta}^{(0)} \right. \\
&- \frac{1}{2} \begin{pmatrix} \delta\boldsymbol{\theta}^{(M)} P^{(f)} \\ \delta\mathbf{J}^{(M)} P^{(f)} \end{pmatrix} \mathcal{O}^{(M)\,\mathrm{T}} \begin{pmatrix} \mathrm{e}^{-2\mathrm{i}\mathrm{diag}\left(\boldsymbol{\theta}^{(M)}\right)} & \mathbb{I}_L \\ \mathbb{I}_L & \frac{\mathrm{i}\tau}{\hbar} \frac{\partial^2 H^{(\mathrm{cl})(M-1)}}{\partial\boldsymbol{\phi}^{(M)*\,2}} \end{pmatrix} \mathcal{O}^{(M)} \begin{pmatrix} P^{(f)\,\mathrm{T}} \delta\boldsymbol{\theta}^{(M)} \\ P^{(f)\,\mathrm{T}} \delta\mathbf{J}^{(M)} \end{pmatrix} \\
&- \frac{1}{2} \sum_{m=1}^{M-1} \begin{pmatrix} \delta\boldsymbol{\theta}^{(m)} \\ \delta\mathbf{J}^{(m)} \end{pmatrix} \mathcal{O}^{(m)\,\mathrm{T}} \begin{pmatrix} \frac{\mathrm{i}\tau}{\hbar} \frac{\partial^2 H^{(\mathrm{cl})(m)}}{\partial\boldsymbol{\phi}^{(m)\,2}} & \mathbb{I}_L \\ \mathbb{I}_L & \frac{\mathrm{i}\tau}{\hbar} \frac{\partial^2 H^{(\mathrm{cl})(m-1)}}{\partial\boldsymbol{\phi}^{(m)*\,2}} \end{pmatrix} \mathcal{O}^{(m)} \begin{pmatrix} \delta\boldsymbol{\theta}^{(m)} \\ \delta\mathbf{J}^{(m)} \end{pmatrix} \\
&+ \begin{pmatrix} \delta\boldsymbol{\theta}^{(1)} \\ \delta\mathbf{J}^{(1)} \end{pmatrix} \mathcal{O}^{(1)\,\mathrm{T}} \begin{pmatrix} 0 \\ \mathbb{I}_L - \frac{\mathrm{i}\tau}{\hbar} \frac{\partial^2 H^{(\mathrm{cl})(0)}}{\partial\boldsymbol{\phi}^{(1)*}\partial\boldsymbol{\phi}^{(0)}} \end{pmatrix} \frac{\partial\boldsymbol{\phi}^{(0)}}{\partial\boldsymbol{\theta}^{(i)}} P_0^{(i)\,\mathrm{T}} \delta\boldsymbol{\theta}^{(i)} \\
&+ \begin{pmatrix} \delta\boldsymbol{\theta}^{(M)} P^{(f)} \\ \delta\mathbf{J}^{(M)} P^{(f)} \end{pmatrix} \mathcal{O}^{(M)\,\mathrm{T}} \begin{pmatrix} 0 & 0 \\ \mathbb{I}_L - \frac{\mathrm{i}\tau}{\hbar} \frac{\partial^2 H^{(\mathrm{cl})(M-1)}}{\partial\boldsymbol{\phi}^{(M)*}\partial\boldsymbol{\phi}^{(M-1)}} & 0 \end{pmatrix} \mathcal{O}^{(M-1)} \begin{pmatrix} \delta\boldsymbol{\theta}^{(M-1)} \\ \delta\mathbf{J}^{(M-1)} \end{pmatrix} \\
&\left. + \sum_{m=1}^{M-2} \begin{pmatrix} \delta\boldsymbol{\theta}^{(m)} \\ \delta\mathbf{J}^{(m)} \end{pmatrix} \mathcal{O}^{(m)\,\mathrm{T}} \begin{pmatrix} 0 & 0 \\ \mathbb{I}_L - \frac{\mathrm{i}\tau}{\hbar} \frac{\partial^2 H^{(\mathrm{cl})(m)}}{\partial\boldsymbol{\phi}^{(m+1)*}\partial\boldsymbol{\phi}^{(m)}} & 0 \end{pmatrix} \mathcal{O}^{(m)} \begin{pmatrix} \delta\boldsymbol{\theta}^{(m)} \\ \delta\mathbf{J}^{(m)} \end{pmatrix} \right\}
\end{aligned}
\tag{C.2}
$$

with

$$
\mathcal{O}^{(m)} = \begin{pmatrix} \dfrac{\partial\boldsymbol{\phi}^{(m)}}{\partial\boldsymbol{\theta}^{(m)}} & \dfrac{\partial\boldsymbol{\phi}^{(m)}}{\partial\mathbf{J}^{(m)}} \\ \dfrac{\partial\boldsymbol{\phi}^{(m)*}}{\partial\boldsymbol{\theta}^{(m)}} & \dfrac{\partial\boldsymbol{\phi}^{(m)*}}{\partial\mathbf{J}^{(m)}} \end{pmatrix}
$$

and $\mathrm{diag}\,(\mathbf{v})$ the diagonal $d\times d$-matrix for which the $(j,j)$-th entry is equal to $v_j$, where $d$ is the dimensionality of the vector $\mathbf{v}$.

The integral over $\delta\boldsymbol{\theta}^{(0)}$ is given by

$$\begin{aligned}
&\int \frac{\mathrm{d}^{N-1}\delta\theta^{(0)}}{(2\pi)^{N-1}} \exp\left\{ \frac{1}{2}\delta\boldsymbol{\theta}^{(0)} P_0^{(i)} \frac{\partial\boldsymbol{\phi}^{(0)}}{\partial\boldsymbol{\theta}^{(i)}} \left[ \mathrm{e}^{-2\mathrm{idiag}\left(\boldsymbol{\theta}^{(i)}\right)} - \frac{\mathrm{i}\tau}{\hbar} \frac{\partial^2 H^{(\mathrm{cl})(0)}}{\partial\boldsymbol{\phi}^{(0)^2}} \right] \frac{\partial\boldsymbol{\phi}^{(0)}}{\partial\boldsymbol{\theta}^{(i)}} {P_0^{(i)}}^{\mathrm{T}} \delta\boldsymbol{\theta}^{(0)} \right. \\
&\quad - \frac{1}{2} \begin{pmatrix} \delta\boldsymbol{\theta}^{(1)} \\ \delta\mathbf{J}^{(1)} \end{pmatrix} {\mathcal{O}^{(1)}}^{\mathrm{T}} \begin{pmatrix} \frac{\mathrm{i}\tau}{\hbar}\frac{\partial^2 H^{(\mathrm{cl})(1)}}{\partial\boldsymbol{\phi}^{(1)^2}} & \mathbb{I}_L \\ \mathbb{I}_L & \frac{\mathrm{i}\tau}{\hbar}\frac{\partial^2 H^{(\mathrm{cl})(0)}}{\partial\boldsymbol{\phi}^{(1)*2}} \end{pmatrix} \mathcal{O}^{(1)} \begin{pmatrix} \delta\boldsymbol{\theta}^{(1)} \\ \delta\mathbf{J}^{(1)} \end{pmatrix} \\
&\quad \left. + \begin{pmatrix} \delta\boldsymbol{\theta}^{(1)} \\ \delta\mathbf{J}^{(1)} \end{pmatrix} {\mathcal{O}^{(1)}}^{\mathrm{T}} \begin{pmatrix} 0 \\ \mathbb{I}_L - \frac{\mathrm{i}\tau}{\hbar}\frac{\partial^2 H^{(\mathrm{cl})(0)}}{\partial\boldsymbol{\phi}^{(1)*}\partial\boldsymbol{\phi}^{(0)}} \end{pmatrix} \frac{\partial\boldsymbol{\phi}^{(0)}}{\partial\boldsymbol{\theta}^{(i)}} {P_0^{(i)}}^{\mathrm{T}} \delta\boldsymbol{\theta}^{(i)} \right\} \\
&= \frac{1}{\sqrt{2\pi}^{N-1}} \left\{ \det\left[ \mathbb{I}_L - \frac{\partial^2 H^{(\mathrm{cl})(0)}}{\partial\left(P^{(i)}\boldsymbol{\phi}^{(0)}\right)^2} \exp\left[ 2\mathrm{idiag}\left(\boldsymbol{\theta}^{(i)}\right)\right]\right]\right\}^{-1} \\
&\quad \times \exp\left\{ -\frac{1}{2} \begin{pmatrix} \delta\boldsymbol{\theta}^{(1)} \\ \delta\mathbf{J}^{(1)} \end{pmatrix} {\mathcal{O}^{(1)}}^{\mathrm{T}} \begin{pmatrix} \frac{\mathrm{i}\tau}{\hbar}\frac{\partial^2 H^{(\mathrm{cl})(1)}}{\partial\boldsymbol{\phi}^{(1)^2}} & \mathbb{I}_L \\ \mathbb{I}_L & X^{(1)} \end{pmatrix} \mathcal{O}^{(1)} \begin{pmatrix} \delta\boldsymbol{\theta}^{(1)} \\ \delta\mathbf{J}^{(1)} \end{pmatrix} \right\},
\end{aligned}$$

where $X^{(1)}$ is defined as

$$\begin{aligned}
X^{(1)} &= \frac{\mathrm{i}\tau}{\hbar} \frac{\partial^2 H^{(\mathrm{cl})(0)}}{\partial\boldsymbol{\phi}^{(1)^{*2}}} \\
&\quad + \left( \mathbb{I}_L - \frac{\mathrm{i}\tau}{\hbar} \frac{\partial^2 H^{(\mathrm{cl})(0)}}{\partial\boldsymbol{\phi}^{(1)^*}\partial\boldsymbol{\phi}^{(0)}} \right) {P_0^{(i)}}^{\mathrm{T}} \left\{ \mathrm{e}^{-2\mathrm{idiag}\left(P_0^{(i)}\boldsymbol{\theta}^{(i)}\right)} - \frac{\mathrm{i}\tau}{\hbar} \frac{\partial^2 H^{(\mathrm{cl})(0)}}{\partial\left(P_0^{(i)}\boldsymbol{\phi}^{(0)}\right)^2} \right\}^{-1} \\
&\qquad \times P_0^{(i)} \left( \mathbb{I}_L - \frac{\mathrm{i}\tau}{\hbar} \frac{\partial^2 H^{(\mathrm{cl})(0)}}{\partial\boldsymbol{\phi}^{(0)}\partial\boldsymbol{\phi}^{(1)^*}} \right)
\end{aligned} \tag{C.3}$$

It can be shown that eq. (C.3) can also be written as

$$\begin{aligned}
X^{(1)} =& \frac{\mathrm{i}\tau}{\hbar} \frac{\partial^2 H^{(\mathrm{cl})(0)}}{\partial\boldsymbol{\phi}^{(1)^{*2}}} \\
&+ \left( \mathbb{I}_L - \frac{\mathrm{i}\tau}{\hbar} \frac{\partial^2 H^{(\mathrm{cl})(0)}}{\partial\boldsymbol{\phi}^{(1)^*}\partial\boldsymbol{\phi}^{(0)}} \right) X^{(0)} \left( \mathbb{I}_L - \frac{\mathrm{i}\tau}{\hbar} \frac{\partial^2 H^{(\mathrm{cl})(0)}}{\partial\boldsymbol{\phi}^{(0)^2}} X^{(0)} \right)^{-1} \\
&\qquad \times \left( \mathbb{I}_L - \frac{\mathrm{i}\tau}{\hbar} \frac{\partial^2 H^{(\mathrm{cl})(0)}}{\partial\boldsymbol{\phi}^{(0)}\partial\boldsymbol{\phi}^{(1)^*}} \right),
\end{aligned}$$

with

$$X^{(0)} = {R^{(i)}}^{\mathrm{T}} \begin{pmatrix} 0 & \\ & \exp\left[ 2\mathrm{idiag}\left(P_0^{(i)}\boldsymbol{\theta}^{(i)}\right)\right] \end{pmatrix} R^{(i)}.$$

Now, consider the integral

$$
\begin{aligned}
&\int \mathrm{d}^L \delta J^{(m)} \int \frac{\mathrm{d}^L \delta\theta^{(m)}}{(2\pi)^L} \\
&\exp\left[ -\frac{1}{2} \begin{pmatrix} \delta\boldsymbol{\theta}^{(m)} \\ \delta\mathbf{J}^{(m)} \end{pmatrix} \mathcal{O}^{(m)\mathrm{T}} \begin{pmatrix} \frac{\mathrm{i}\tau}{\hbar} \frac{\partial^2 H^{(\mathrm{cl})(m)}}{\partial \boldsymbol{\phi}^{(m)2}} & \mathbb{I}_L \\ \mathbb{I}_L & X^{(m)} \end{pmatrix} \mathcal{O}^{(m)} \begin{pmatrix} \delta\boldsymbol{\theta}^{(m)} \\ \delta\mathbf{J}^{(m)} \end{pmatrix} \right. \\
&+ \begin{pmatrix} \delta\boldsymbol{\theta}^{(m+1)} \\ \delta\mathbf{J}^{(m+1)} \end{pmatrix} \mathcal{O}^{(m+1)\mathrm{T}} \begin{pmatrix} 0 & 0 \\ \mathbb{I}_L - \frac{\mathrm{i}\tau}{\hbar} \frac{\partial^2 H^{(\mathrm{cl})(m)}}{\partial \boldsymbol{\phi}^{(m+1)*} \partial \boldsymbol{\phi}^{(m)}} & 0 \end{pmatrix} \mathcal{O}^{(m)} \begin{pmatrix} \delta\boldsymbol{\theta}^{(m)} \\ \delta\mathbf{J}^{(m)} \end{pmatrix} \\
&\left. -\frac{1}{2} \begin{pmatrix} \delta\boldsymbol{\theta}^{(m+1)} \\ \delta\mathbf{J}^{(m+1)} \end{pmatrix} \mathcal{O}^{(m+1)\mathrm{T}} \begin{pmatrix} \frac{\mathrm{i}\tau}{\hbar} \frac{\partial^2 H^{(\mathrm{cl})(m+1)}}{\partial \boldsymbol{\phi}^{(m+1)2}} & \mathbb{I}_L \\ \mathbb{I}_L & \frac{\mathrm{i}\tau}{\hbar} \frac{\partial^2 H^{(\mathrm{cl})(m)}}{\partial \boldsymbol{\phi}^{(m+1)*2}} \end{pmatrix} \mathcal{O}^{(m+1)} \begin{pmatrix} \delta\boldsymbol{\theta}^{(m+1)} \\ \delta\mathbf{J}^{(m+1)} \end{pmatrix} \right] \\
&= \left\{ \det \left[ \mathbb{I}_L - \frac{\mathrm{i}\tau}{\hbar} \frac{\partial^2 H^{(\mathrm{cl})(m)}}{\partial \boldsymbol{\phi}^{(m)2}} X^{(m)} \right] \right\}^{-1} \\
&\times \exp\left[ - \begin{pmatrix} \delta\boldsymbol{\theta}^{(m+1)} \\ \delta\mathbf{J}^{(m+1)} \end{pmatrix} \mathcal{O}^{(m+1)\mathrm{T}} \begin{pmatrix} \frac{\mathrm{i}\tau}{2\hbar} \frac{\partial^2 H^{(\mathrm{cl})(m+1)}}{\partial \boldsymbol{\phi}^{(m+1)2}} & \frac{1}{2}\mathbb{I}_L \\ \frac{1}{2}\mathbb{I}_L & \frac{X^{(m+1)}}{2} \end{pmatrix} \mathcal{O}^{(m+1)} \begin{pmatrix} \delta\boldsymbol{\theta}^{(m+1)} \\ \delta\mathbf{J}^{(m+1)} \end{pmatrix} \right]
\end{aligned}
\tag{C.4}
$$

with

$$
\begin{aligned}
X^{(m+1)} = &\frac{\mathrm{i}\tau}{\hbar} \frac{\partial^2 H^{(\mathrm{cl})(m)}}{\partial \boldsymbol{\phi}^{(m+1)*2}} \\
&+ \left( \mathbb{I}_L - \frac{\mathrm{i}\tau}{\hbar} \frac{\partial^2 H^{(\mathrm{cl})(m)}}{\partial \boldsymbol{\phi}^{(m+1)*} \partial \boldsymbol{\phi}^{(m)}} \right) X^{(m)} \left( \mathbb{I}_L - \frac{\mathrm{i}\tau}{\hbar} \frac{\partial^2 H^{(\mathrm{cl})(m)}}{\partial \boldsymbol{\phi}^{(m)2}} X^{(m)} \right)^{-1} \\
&\times \left( \mathbb{I}_L - \frac{\mathrm{i}\tau}{\hbar} \frac{\partial^2 H^{(\mathrm{cl})(m)}}{\partial \boldsymbol{\phi}^{(m)} \partial \boldsymbol{\phi}^{(m+1)*}} \right).
\end{aligned}
$$

For $m = 1$ this is exactly the integral in (C.2) after integrating out $\delta\boldsymbol{\theta}^{(0)}$ and thus defines $X^{(2)}$. One then recognizes that after the $m$-th integration, the integral is again of the form of (C.4) up to the $(M-1)$-th integration.

With this observation, the reduced propagator is given by

$$
\begin{aligned}
&K_{\mathrm{red}}^{(\gamma)} \\
&= \lim_{M\to\infty} \int \frac{\mathrm{d}^N J^{(M)}}{\sqrt{2\pi}^{N-1}} \int \frac{\mathrm{d}^N \theta^{(M)}}{(2\pi)^N} \prod_{m=0}^{M-1} \sqrt{\det\left(\mathbb{I}_L - \frac{\mathrm{i}\tau}{\hbar}\frac{\partial^2 H^{(\mathrm{cl})(m)}}{\partial \boldsymbol{\phi}^{(m)^2}} X^{(m)}\right)}^{-1} \\
&\quad \times \mathrm{e}^{-\frac{1}{2}\begin{pmatrix} \delta\boldsymbol{\theta}^{(M)} P^{(f)} \\ \delta\mathbf{J}^{(M)} P^{(f)} \end{pmatrix} \mathcal{O}^{(M)^{\mathrm{T}}} \begin{pmatrix} \mathrm{e}^{-2\mathrm{idiag}\left(\boldsymbol{\theta}^{(M)}\right)} & \mathbb{I}_L \\ \mathbb{I}_L & X^{(M)} \end{pmatrix} \mathcal{O}^{(M)} \begin{pmatrix} P^{(f)^{\mathrm{T}}} \delta\boldsymbol{\theta}^{(M)} \\ P^{(f)^{\mathrm{T}}} \delta\mathbf{J}^{(M)} \end{pmatrix}} \\
&= \lim_{M\to\infty} \frac{1}{\sqrt{2\pi}^{N-1}} \left[\prod_{m=0}^{M-1} \sqrt{\det\left(\mathbb{I}_L - \frac{\mathrm{i}\tau}{\hbar}\frac{\partial^2 H^{(\mathrm{cl})(m)}}{\partial \boldsymbol{\phi}^{(m)^2}} X^{(m)}\right)}^{-1}\right] \\
&\quad \times \sqrt{\det\left(\mathbb{I}_N - \exp\left[-2\mathrm{idiag}\left(P^{(f)}\boldsymbol{\theta}^{(M)}\right)\right] P^{(f)} X^{(M)} P^{(f)^{\mathrm{T}}}\right)}^{-1}
\end{aligned}
$$

In the continuous limit, the discrete set of $X^{(m)}$ turns into a function of time $X(t)$, and (by expanding it up to first order in $\tau$) is given by (5.13) and the reduced propagator can be written in the form given in (5.12).

## C.2 Simplification of the semiclassical prefactor

Using the equations of motion for $\sigma(t)$,

$$
\begin{aligned}
&\exp\left[\frac{\mathrm{i}}{2\hbar}\int_{t_i}^{t_f} \mathrm{d}t \mathrm{Tr} \frac{\partial^2 H^{(\mathrm{cl})}}{\partial \boldsymbol{\phi}^2} X\right] \\
&\quad = \exp\left(-\frac{1}{2}\int_{t_i}^{t_f} \mathrm{d}t \mathrm{Tr} \dot{\sigma}(t)\sigma^{-1}(t) + \frac{\mathrm{i}}{2\hbar}\int_{t_i}^{t_f} \mathrm{d}t \mathrm{Tr} \frac{\partial^2 H^{(\mathrm{cl})}}{\partial\boldsymbol{\phi}\partial\boldsymbol{\phi}^*}\right) \\
&\quad = \exp\left(\frac{\mathrm{i}}{2\hbar}\int_{t_i}^{t_f} \mathrm{d}t \mathrm{Tr} \frac{\partial^2 H^{(\mathrm{cl})}}{\partial\boldsymbol{\phi}\partial\boldsymbol{\phi}^*}\right) \sqrt{\sigma\left(t_i\right)\sigma^{-1}\left(t_f\right)}
\end{aligned}
$$

and therefore

$$
\begin{aligned}
&K_{\mathrm{red}}^{(\gamma)} \\
&= \frac{1}{\sqrt{2\pi}^{N-1}} \exp\left(\frac{\mathrm{i}}{2\hbar}\int_{t_i}^{t_f} \mathrm{d}t \mathrm{Tr}\frac{\partial^2 H^{(\mathrm{cl})}}{\partial\boldsymbol{\phi}\partial\boldsymbol{\phi}^*}\right)\sqrt{\det\sigma\left(t_i\right)\sigma^{-1}\left(t_f\right)} \\
&\quad\times\sqrt{\det\left(\mathbb{I}_N + \mathrm{e}^{-2\mathrm{idiag}\left(P^{(f)}\boldsymbol{\theta}^{(f)}\right)}P^{(f)}\rho\left(t_f\right)\sigma^{-1}\left(t_f\right)P^{(f)\mathrm{T}}\right)}^{-1} \\
&= \frac{1}{\sqrt{2\pi}^{N-1}} \exp\left(\frac{\mathrm{i}}{2\hbar}\int_{t_i}^{t_f} \mathrm{d}t \mathrm{Tr}\frac{\partial^2 H^{(\mathrm{cl})}}{\partial\boldsymbol{\phi}\partial\boldsymbol{\phi}^*}\right)\sqrt{\det\sigma\left(t_i\right)\sigma^{-1}\left(t_f\right)} \\
&\quad\times\sqrt{\det\left[\mathbb{I}_L + \begin{pmatrix} 0 \\ P^{(f)} \end{pmatrix}\mathrm{e}^{-2\mathrm{idiag}\left(\boldsymbol{\theta}^{(f)}\right)}\rho\left(t_f\right)R^{(i)\mathrm{T}}R^{(i)}\sigma^{-1}\left(t_f\right)\begin{pmatrix} 0 & P^{(f)\mathrm{T}} \end{pmatrix}\right]}^{-1} \\
&= \frac{1}{\sqrt{2\pi}^{N-1}} \exp\left(\frac{\mathrm{i}}{2\hbar}\int_{t_i}^{t_f} \mathrm{d}t \mathrm{Tr}\frac{\partial^2 H^{(\mathrm{cl})}}{\partial\boldsymbol{\phi}\partial\boldsymbol{\phi}^*}\right)\sqrt{\det\sigma\left(t_i\right)\sigma^{-1}\left(t_f\right)} \\
&\quad\times\sqrt{\det\left[\mathbb{I}_L + \begin{pmatrix} 0 \\ P^{(f)} \end{pmatrix}\mathrm{e}^{-2\mathrm{idiag}\left(\boldsymbol{\theta}^{(f)}\right)}\rho\left(t_f\right)R^{(i)\mathrm{T}}R^{(i)}\sigma^{-1}\left(t_f\right)R^{(f)\mathrm{T}}\right]}^{-1} \\
&= \frac{1}{\sqrt{2\pi}^{N-1}} \exp\left(\frac{\mathrm{i}}{2\hbar}\int_{t_i}^{t_f} \mathrm{d}t \mathrm{Tr}\frac{\partial^2 H^{(\mathrm{cl})}}{\partial\boldsymbol{\phi}\partial\boldsymbol{\phi}^*}\right)\sqrt{\det\sigma\left(t_i\right)}\sqrt{\det R^{(f)}R^{(i)\mathrm{T}}} \\
&\quad\times\sqrt{\det\left[R^{(f)}\sigma\left(t_f\right)R^{(i)\mathrm{T}} + \begin{pmatrix} 0 \\ P^{(f)} \end{pmatrix}\mathrm{e}^{-2\mathrm{idiag}\left(\boldsymbol{\theta}^{(f)}\right)}\rho\left(t_f\right)R^{(i)\mathrm{T}}\right]}^{-1}
\end{aligned}
$$

The factor in the last line can be simplified as

$$
\begin{aligned}
&R^{(f)}\sigma\left(t_f\right)R^{(i)\mathrm{T}} + \begin{pmatrix} 0 \\ P^{(f)} \end{pmatrix}\exp\left[-2\mathrm{idiag}\left(\boldsymbol{\theta}^{(f)}\right)\right]\rho\left(t_f\right)R^{(i)\mathrm{T}} = \\
&\begin{pmatrix}
\frac{\partial\left(\bar{P}^{(f)}\boldsymbol{\phi}^*(t_f)\right)}{\partial\left(\bar{P}^{(i)}\boldsymbol{\phi}^*(t_i)\right)} & \frac{\partial\left(\bar{P}^{(f)}\boldsymbol{\phi}^*(t_f)\right)}{\partial\left(P^{(i)}\boldsymbol{\theta}^{(i)}\right)} \\
2\frac{\partial\left(P^{(f)}\boldsymbol{\phi}^*(t_f)\right)}{\partial\left(P^{(f)}\mathbf{J}^{(f)}\right)}\frac{\partial\left(P^{(f)}\mathbf{J}^{(f)}\right)}{\partial\left(\bar{P}^{(i)}\boldsymbol{\phi}^*(t_i)\right)} & 2\frac{\partial\left(P^{(f)}\boldsymbol{\phi}^*(t_f)\right)}{\partial\left(P^{(f)}\mathbf{J}^{(f)}\right)}\frac{\partial\left(P^{(f)}\mathbf{J}^{(f)}\right)}{\partial\left(P^{(i)}\boldsymbol{\theta}^{(i)}\right)}
\end{pmatrix}.
\end{aligned}
$$

And therefore, finally

$$K_{\mathrm{red}}^{(\gamma)} = \mathrm{e}^{\frac{\mathrm{i}}{2\hbar}\int_{t_i}^{t_f} \mathrm{d}t \mathrm{Tr}\frac{\partial^2 H^{(\mathrm{cl})}}{\partial\boldsymbol{\phi}\partial\boldsymbol{\phi}^*} + \frac{\mathrm{i}}{2}\left(\mathbf{n}^{(f)}\cdot\boldsymbol{\theta}^{(f)} - \mathbf{n}^{(i)}\cdot\boldsymbol{\theta}^{(i)}\right)} \sqrt{\det R^{(f)}R^{(i)}} \sqrt{\det \frac{1}{2\pi\mathrm{i}} \frac{\partial\left(P^{(i)}\boldsymbol{\theta}^{(i)}\right)}{\partial\left(J^{(f)}_{l_2^{(f)}},\ldots,J^{(f)}_{l_N^{(f)}}\right)}}$$

$$\times \left\{ \det \left[ \frac{\partial\left(\bar{P}^{(f)}\boldsymbol{\phi}^*(t_f), J^{(f)}_{l_1^{(f)}}\right)}{\partial\left(\bar{P}^{(i)}\boldsymbol{\phi}^*(t_i)\right)} \right.\right.$$

$$\left.\left. - \frac{\partial\left(\bar{P}^{(f)}\boldsymbol{\phi}^*(t_f), J^{(f)}_{l_1^{(f)}}\right)}{\partial\left(P^{(i)}\boldsymbol{\theta}^{(i)}\right)} \left(\frac{\partial\left(J^{(f)}_{l_2^{(f)}},\ldots,J^{(f)}_{l_N^{(f)}}\right)}{\partial\left(P^{(i)}\boldsymbol{\theta}^{(i)}\right)}\right)^{-1} \frac{\partial\left(J^{(f)}_{l_2^{(f)}},\ldots,J^{(f)}_{l_N^{(f)}}\right)}{\partial\left(\bar{P}^{(i)}\boldsymbol{\phi}^*(t_i)\right)} \right] \right\}^{-\frac{1}{2}}.$$

APPENDIX D

# The bosonic transition probability in the weak coupling regime

## D.1 Determination of the trajectory and its action

The solution of the equations of motion Eq. (7.13) for initial conditions $\Re\boldsymbol{\psi}(0) = \mathbf{q}^{(0)}/(2b)$ and $\Im\boldsymbol{\psi}(0) = \mathbf{p}^{(0)}/(2b)$ are obviously given by

$$\psi_l(t) = \frac{1}{2b}\left(q_l^{(0)} + \mathrm{i}p_l^{(0)}\right) \mathrm{e}^{-\frac{\mathrm{i}}{\hbar}\int_0^t \mathrm{d}t'[\epsilon_l - \sigma_l(t')]}. \tag{D.1}$$

Next, $\mathbf{q}^{(i)}$ and $\mathbf{p}^{(i)}$ have to be chosen such that the solution Eq. (D.1) satisfies the boundary conditions Eq. (7.14), which yields $\mathbf{q}^{(0)} = \mathbf{q}^{(i)}$ as well as

$$p_l^{(0)} = -q_l^{(i)} \cot\left(\frac{1}{\hbar}\int_0^{t_f} \mathrm{d}t\,[\epsilon_l - \sigma_l(t)]\right) + q_l^{(f)} \csc\left(\frac{1}{\hbar}\int_0^{t_f} \mathrm{d}t\,[\epsilon_l - \sigma_l(t)]\right). \tag{D.2}$$

For simplicity of writing we now define

$$A_l = \frac{1}{\hbar}\int_0^{t_f} \mathrm{d}t\left[\epsilon_l - \sigma_l\left(t\right)\right]. \tag{D.3}$$

The action in (7.12) is given by

$$\begin{aligned} &R_\gamma\left(\mathbf{q}^{(f)},\mathbf{q}^{(i)};t_f\right) = \\ &\quad\frac{\hbar}{2b^2}\int_0^{t_f}\mathrm{d}t\mathbf{p}(t)\dot{\mathbf{q}}(t) - \int_0^{t_f}\mathrm{d}t\sum_{l=1}^{L}\psi_l^*(t)\left[\epsilon_l-\sigma_l(t)\right]\psi_l(t) + \frac{\hbar}{2}\sum_{l=1}^{L}A_l, \end{aligned} \tag{D.4}$$

where

$$\mathbf{q}(t) = 2b\Re\boldsymbol{\psi}(t) \qquad \text{and} \qquad \mathbf{p}(t) = 2b\Im\boldsymbol{\psi}(t). \tag{D.5}$$

Let us first look to the first part of the action,

$$\begin{aligned} &\hbar p_l(t)\dot{q}_l(t) = \\ &\left(p_l^{(0)}\cos\left\{\frac{1}{\hbar}\int_0^t \mathrm{d}t'\left[\epsilon_l-\sigma_l\left(t'\right)\right]\right\} - q_l^{(i)}\sin\left\{\frac{1}{\hbar}\int_0^t \mathrm{d}t'\left[\epsilon_l-\sigma_l\left(t'\right)\right]\right\}\right)^2 \\ &\qquad\qquad\qquad\qquad\qquad\qquad\qquad\qquad\qquad\qquad\times\left[\epsilon_l-\sigma_l\left(t\right)\right]. \end{aligned}$$

One may note that this can also be written as

$$\begin{aligned} \hbar p_l(t)\dot{q}_l(t) = \frac{\partial}{\partial t}\Bigg[&\hbar p_l^{(0)}q_l^{(i)}\cos^2\left(\frac{1}{\hbar}\int_0^t \mathrm{d}t'\left[\epsilon_l-\sigma_l\left(t'\right)\right]\right) \\ &+\hbar\frac{{p_l^{(0)}}^2-{q_l^{(i)}}^2}{4}\sin\left(\frac{2}{\hbar}\int_0^t \mathrm{d}t'\left[\epsilon_l-\sigma_l\left(t'\right)\right]\right) \\ &+\frac{{q_l^{(i)}}^2+{p_l^{(0)}}^2}{2}\int_0^t \mathrm{d}t'\left[\epsilon_l-\sigma_l\left(t'\right)\right]\Bigg] \end{aligned} \tag{D.6}$$

such that

$$\begin{aligned} 2\hbar \int_0^{t_f} \mathrm{d}t p_l(t) \cdot \dot{q}_l(t) = \\ 2\hbar p_l^{(0)} q_l^{(i)} \left(\cos^2 A_l - 1\right) + \frac{\hbar}{2}\left(p_l^{(0)^2} - q_l^{(i)^2}\right) \sin 2A_l \\ + \left(q_l^{(i)^2} + p_l^{(0)^2}\right) A_l. \end{aligned} \tag{D.7}$$

and therefore

$$\begin{aligned} R_\gamma\left(\mathbf{q}^{(f)}, \mathbf{q}^{(i)}; t_f\right) = \\ \frac{\hbar}{4b^2} \sum_{l=1}^{L} \left[2p_l^{(0)} q_l^{(i)} \left(\cos^2 A_l - 1\right) + \left(p_l^{(0)^2} - q_l^{(i)^2}\right) \sin A_l \cos A_l\right] + \frac{\hbar}{2} \sum_{l=1}^{L} A_l. \end{aligned} \tag{D.8}$$

Plugging in (D.2) one finally finds the action to be

$$\begin{aligned} R_\gamma\left(\mathbf{q}^{(f)}, \mathbf{q}^{(i)}; t_f\right) = \\ \frac{\hbar}{4b^2 \sin A_l} \sum_{l=1}^{L} \left[-2q_l^{(f)} q_l^{(i)} + \left(q_l^{(i)^2} + q_l^{(f)^2}\right) \cos A_l\right] + \frac{\hbar}{2} \sum_{l=1}^{L} A_l. \end{aligned} \tag{D.9}$$

## D.2 Transformation to Fock states

In order to perform the integrations involved in the basis transform, one first has to determine the exact dependence of the hopping on the initial

and final quadratures. Evaluating the time integral over the hopping yields

$$
\begin{aligned}
&\int_{t_i}^{t_f} \mathrm{d}t J\left(\mathbf{p}(t), \mathbf{q}(t)\right) \\
&= -\frac{1}{4b^2} \sum_{l,l'} J_{ll'} \int_{t_i}^{t_f} \mathrm{d}t \left(q_l^{(i)} - \mathrm{i}p_l^{(0)}\right)\left(q_{l'}^{(i)} + \mathrm{i}p_{l'}^{(0)}\right) \mathrm{e}^{\frac{\mathrm{i}}{\hbar}\int_{t_i}^{t} \mathrm{d}t'[\epsilon_l - \epsilon_{l'} - \sigma_l(t') + \sigma_{l'}(t')]} \\
&= -\frac{1}{4b^2} \sum_{l,l'} J_{ll'} \int_{t_i}^{t_f} \mathrm{d}t \mathrm{e}^{\frac{\mathrm{i}}{\hbar}\int_{t_i}^{t} \mathrm{d}t'[\epsilon_l - \epsilon_{l'} - \sigma_l(t') + \sigma_{l'}(t')]} \\
&\quad \times \begin{pmatrix} q_l^{(i)} \\ q_l^{(f)} \end{pmatrix} \begin{pmatrix} (1+\mathrm{i}\cot A_l)(1-\mathrm{i}\cot A_{l'}) & \frac{\mathrm{i}(1+\mathrm{i}\cot A_l)}{\sin A_{l'}} \\ \frac{-\mathrm{i}(1-\mathrm{i}\cot A_{l'})}{\sin A_l} & \frac{1}{\sin A_l \sin A_{l'}} \end{pmatrix} \begin{pmatrix} q_{l'}^{(i)} \\ q_{l'}^{(f)} \end{pmatrix} \\
&= -\sum_{l,l'} J_{ll'} \int_{t_i}^{t_f} \mathrm{d}t \frac{\mathrm{e}^{\frac{\mathrm{i}}{\hbar}\int_{t_i}^{t} \mathrm{d}t'[\epsilon_l - \epsilon_{l'} - \sigma_l(t') + \sigma_{l'}(t')]}}{4b^2 \sin A_l \sin A_{l'}} \\
&\quad \times \begin{pmatrix} q_l^{(i)} \\ q_l^{(f)} \end{pmatrix} \begin{pmatrix} \mathrm{e}^{\mathrm{i}(A_{l'} - A_l)} & -\mathrm{e}^{-\mathrm{i}A_l} \\ -\mathrm{e}^{\mathrm{i}A_{l'}} & 1 \end{pmatrix} \begin{pmatrix} q_{l'}^{(i)} \\ q_{l'}^{(f)} \end{pmatrix}
\end{aligned} \tag{D.10}
$$

With this the effective propagator in quadrature representation with the hopping included via semiclassical perturbation theory can be written as

$$
\begin{aligned}
K_{\boldsymbol{\sigma}}\left(\mathbf{q}^{(f)}, \mathbf{q}^{(i)}; t_f\right) = \exp\Bigg\{ &\frac{\mathrm{i}}{4b^2} \begin{pmatrix} \mathbf{q}^{(i)} \\ \mathbf{q}^{(f)} \end{pmatrix} \Bigg[ \begin{pmatrix} \cot A & -\frac{1}{\sin A} \\ -\frac{1}{\sin A} & \cot A \end{pmatrix} \\
&- \frac{1}{\hbar} \begin{pmatrix} (\sin A)^{-1} \mathrm{e}^{-\mathrm{i}A} & 0 \\ 0 & (\sin A)^{-1} \end{pmatrix} \begin{pmatrix} J^{(\mathrm{eff})} & -J^{(\mathrm{eff})} \\ -J^{(\mathrm{eff})} & J^{(\mathrm{eff})} \end{pmatrix} \\
&\times \begin{pmatrix} (\sin A)^{-1} \mathrm{e}^{\mathrm{i}A} & 0 \\ 0 & (\sin A)^{-1} \end{pmatrix} \Bigg] \begin{pmatrix} \mathbf{q}^{(i)} \\ \mathbf{q}^{(f)} \end{pmatrix} \Bigg\} \frac{\mathrm{e}^{\frac{\mathrm{i}}{2}\sum_{\alpha=1}^{l} A_\alpha}}{\sqrt{\det 4b^2 \mathrm{i}\pi \sin A}}
\end{aligned} \tag{D.11}
$$

where $A$ is the diagonal matrix with entries $A_l$,

$$
A = \begin{pmatrix} A_1 & & \\ & \ddots & \\ & & A_l \end{pmatrix}
$$

and the effective hopping matrix $J^{(\mathrm{eff})}$ with entries

$$J^{(\mathrm{eff})}_{ll'} = -J_{ll'} \int_{t_i}^{t_f} \mathrm{d}t \mathrm{e}^{\frac{\mathrm{i}}{\hbar}\int_{t_i}^{t} \mathrm{d}t' [\epsilon_l - \epsilon_{l'} - \sigma_{l'}(t') + \sigma_k(t')]} .$$

With this expression for the effective propagator, one can perform the basis transform from the quadrature to the number representation. However it turns out to be easier not to go to the number representation directly but to make a detour over coherent states.

### *D.2.1 The coherent state propagator for weak hopping*

For the basis change one needs the overlap between a coherent state and a quadrature eigenstate, which is given by Eq. (3.19). This yields the effective propagator in coherent state representation,

$$\begin{aligned}
&K_{\boldsymbol{\sigma}}\left(\boldsymbol{\phi}^f, \boldsymbol{\phi}^{(i)}; t_f\right) = \int \mathrm{d}^l q^{(i)} \int \mathrm{d}^l q^{(f)} \, \langle \boldsymbol{\phi}^{(f)} | \mathbf{q}^{(f)} \rangle \, K_{\boldsymbol{\sigma}}\left(\mathbf{q}^{(f)}, \mathbf{q}^{(i)}; t_f\right) \langle \mathbf{q}^{(i)} | \boldsymbol{\phi}^{(i)} \rangle \\
&= \frac{1}{\sqrt{\det \frac{\mathrm{i}}{2} \sin A \mathrm{e}^{-\mathrm{i}A}}} \det \left[ 1 - \mathrm{i} \begin{pmatrix} \cot A & -\frac{1}{\sin A} \\ -\frac{1}{\sin A} & \cot A \end{pmatrix} \right. \\
&\left. + \frac{\mathrm{i}}{\hbar} \begin{pmatrix} (\sin A)^{-1} \mathrm{e}^{-\mathrm{i}A} & 0 \\ 0 & (\sin A)^{-1} \end{pmatrix} \begin{pmatrix} J^{(\mathrm{eff})} & -J^{(\mathrm{eff})} \\ -J^{(\mathrm{eff})} & J^{(\mathrm{eff})} \end{pmatrix} \begin{pmatrix} (\sin A)^{-1} \mathrm{e}^{\mathrm{i}A} & 0 \\ 0 & (\sin A)^{-1} \end{pmatrix} \right]^{-\frac{1}{2}} \\
&\times \exp \left\{ -\frac{\left|\boldsymbol{\phi}^{(f)}\right|^2}{2} - \frac{\left|\boldsymbol{\phi}^{(i)}\right|^2}{2} - \frac{\boldsymbol{\phi}^{(f)*2}}{2} - \frac{\boldsymbol{\phi}^{(i)2}}{2} + \begin{pmatrix} \boldsymbol{\phi}^{(i)} \\ \boldsymbol{\phi}^{(f)*} \end{pmatrix} \left[ 1 - \mathrm{i} \begin{pmatrix} \cot A & -\frac{1}{\sin A} \\ -\frac{1}{\sin A} & \cot A \end{pmatrix} \right. \right. \\
&\left. + \frac{\mathrm{i}}{\hbar} \begin{pmatrix} (\sin A)^{-1} \mathrm{e}^{-\mathrm{i}A} & 0 \\ 0 & (\sin A)^{-1} \end{pmatrix} \begin{pmatrix} J^{(\mathrm{eff})} & -J^{(\mathrm{eff})} \\ -J^{(\mathrm{eff})} & J^{(\mathrm{eff})} \end{pmatrix} \begin{pmatrix} (\sin A)^{-1} \mathrm{e}^{\mathrm{i}A} & 0 \\ 0 & (\sin A)^{-1} \end{pmatrix} \right]^{-1} \\
&\left. \times \begin{pmatrix} \boldsymbol{\phi}^{(i)} \\ \boldsymbol{\phi}^{(f)*} \end{pmatrix} \right\}.
\end{aligned}$$

Doing the semiclassical perturbation theory on the level of the coherent state propagator now corresponds to setting $J^{(\mathrm{eff})} = 0$ in the prefactor and expanding the exponent up to first order in $J^{(\mathrm{eff})}$. For the expansion of the

exponent we will need

$$
\begin{aligned}
&\begin{pmatrix} 1-\mathrm{i}\cot A & \mathrm{i}\,(\sin A)^{-1} \\ \mathrm{i}\,(\sin A)^{-1} & 1-\mathrm{i}\cot A \end{pmatrix}^{-1} \\
&\quad = \mathrm{i}\begin{pmatrix} \sin A & 0 \\ 0 & \sin A \end{pmatrix}\begin{pmatrix} \mathrm{e}^{\mathrm{i}A} & -1 \\ -1 & \mathrm{e}^{\mathrm{i}A} \end{pmatrix}^{-1} \\
&\quad = \mathrm{i}\begin{pmatrix} \sin A & 0 \\ 0 & \sin A \end{pmatrix}\begin{pmatrix} \left(\mathrm{e}^{2\mathrm{i}A}-1\right)^{-1}\mathrm{e}^{\mathrm{i}A} & \left(\mathrm{e}^{2\mathrm{i}A}-1\right)^{-1} \\ \left(\mathrm{e}^{2\mathrm{i}A}-1\right)^{-1} & \left(\mathrm{e}^{2\mathrm{i}A}-1\right)^{-1}\mathrm{e}^{\mathrm{i}A} \end{pmatrix} \\
&\quad = \frac{1}{2}\begin{pmatrix} \sin A & 0 \\ 0 & \sin A \end{pmatrix}\begin{pmatrix} (\sin A)^{-1} & (\sin A)^{-1}\mathrm{e}^{-\mathrm{i}A} \\ (\sin A)\,\mathrm{e}^{-\mathrm{i}A} & (\sin A)^{-1} \end{pmatrix} \\
&\quad = \frac{1}{2}\begin{pmatrix} 1 & \mathrm{e}^{-\mathrm{i}A} \\ \mathrm{e}^{-\mathrm{i}A} & 1 \end{pmatrix}
\end{aligned}
\tag{D.12}
$$

Therefore the prefactor becomes

$$
\begin{aligned}
&\left[\left(\det\frac{\mathrm{i}}{2}\sin A\mathrm{e}^{-\mathrm{i}A}\right)^{-1}\det\frac{1}{2}\begin{pmatrix} 1 & \mathrm{e}^{-\mathrm{i}A} \\ \mathrm{e}^{-\mathrm{i}A} & 1 \end{pmatrix}\right]^{\frac{1}{2}} \\
&\qquad = \left[\det -\frac{\mathrm{i}}{2}(\sin A)^{-1}\mathrm{e}^{\mathrm{i}A}\left(1-\mathrm{e}^{-2\mathrm{i}A}\right)\right]^{\frac{1}{2}} \\
&\qquad = \left[\det(\sin A)^{-1}\sin A\right]^{\frac{1}{2}} = 1
\end{aligned}
$$

Moreover, the expansion in the exponent is given by

$$
\begin{aligned}
&\left[\frac{\mathrm{i}}{\hbar}\begin{pmatrix} (\sin A)^{-1}\mathrm{e}^{-\mathrm{i}A} & 0 \\ 0 & (\sin A)^{-1} \end{pmatrix}\begin{pmatrix} J^{(\mathrm{eff})} & -J^{(\mathrm{eff})} \\ -J^{(\mathrm{eff})} & J^{(\mathrm{eff})} \end{pmatrix}\begin{pmatrix} (\sin A)^{-1}\mathrm{e}^{\mathrm{i}A} & 0 \\ 0 & (\sin A)^{-1} \end{pmatrix}\right. \\
&\left.+\,1-\mathrm{i}\begin{pmatrix} \cot A & -\frac{1}{\sin A} \\ -\frac{1}{\sin A} & \cot A \end{pmatrix}\right]^{-1} \\
&= \left[1+\frac{\mathrm{i}}{\hbar}\begin{pmatrix} 1-\mathrm{i}\cot A & \mathrm{i}\,(\sin A)^{-1} \\ \mathrm{i}\,(\sin A)^{-1} & 1-\mathrm{i}\cot A \end{pmatrix}^{-1}\begin{pmatrix} (\sin A)^{-1}\mathrm{e}^{-\mathrm{i}A} & 0 \\ 0 & (\sin A)^{-1} \end{pmatrix}\right. \\
&\left.\times\begin{pmatrix} J^{(\mathrm{eff})} & -J^{(\mathrm{eff})} \\ -J^{(\mathrm{eff})} & J^{(\mathrm{eff})} \end{pmatrix}\begin{pmatrix} (\sin A)^{-1}\mathrm{e}^{\mathrm{i}A} & 0 \\ 0 & (\sin A)^{-1} \end{pmatrix}\right]^{-1}\begin{pmatrix} 1-\mathrm{i}\cot A & \mathrm{i}\,(\sin A)^{-1} \\ \mathrm{i}\,(\sin A)^{-1} & 1-\mathrm{i}\cot A \end{pmatrix}^{-1} \\
&\approx \frac{1}{2}\begin{pmatrix} 1 & \mathrm{e}^{-\mathrm{i}A} \\ \mathrm{e}^{-\mathrm{i}A} & 1 \end{pmatrix} - \frac{\mathrm{i}}{4\hbar}\begin{pmatrix} 1 & \mathrm{e}^{-\mathrm{i}A} \\ \mathrm{e}^{-\mathrm{i}A} & 1 \end{pmatrix}\begin{pmatrix} (\sin A)^{-1}\mathrm{e}^{-\mathrm{i}A} & 0 \\ 0 & (\sin A)^{-1} \end{pmatrix} \\
&\times\begin{pmatrix} J^{(\mathrm{eff})} & -J^{(\mathrm{eff})} \\ -J^{(\mathrm{eff})} & J^{(\mathrm{eff})} \end{pmatrix}\begin{pmatrix} (\sin A)^{-1}\mathrm{e}^{\mathrm{i}A} & 0 \\ 0 & (\sin A)^{-1} \end{pmatrix}\begin{pmatrix} 1 & \mathrm{e}^{-\mathrm{i}A} \\ \mathrm{e}^{-\mathrm{i}A} & 1 \end{pmatrix} \\
&= \frac{1}{2}\begin{pmatrix} 1 & \mathrm{e}^{-\mathrm{i}A} \\ \mathrm{e}^{-\mathrm{i}A} & 1 \end{pmatrix} - \frac{\mathrm{i}}{4\hbar}\begin{pmatrix} (\sin A)^{-1}\mathrm{e}^{-\mathrm{i}A} & (\sin A)^{-1}\mathrm{e}^{-\mathrm{i}A} \\ (\sin A)^{-1}\mathrm{e}^{-2\mathrm{i}A} & (\sin A)^{-1} \end{pmatrix} \\
&\times\begin{pmatrix} J^{(\mathrm{eff})} & -J^{(\mathrm{eff})} \\ -J^{(\mathrm{eff})} & J^{(\mathrm{eff})} \end{pmatrix}\begin{pmatrix} (\sin A)^{-1}\mathrm{e}^{\mathrm{i}A} & (\sin A)^{-1} \\ (\sin A)^{-1}\mathrm{e}^{-\mathrm{i}A} & (\sin A)^{-1} \end{pmatrix}
\end{aligned}
$$

$$
\begin{aligned}
=&\frac{1}{2}\begin{pmatrix} 1 & \mathrm{e}^{-\mathrm{i}A} \\ \mathrm{e}^{-\mathrm{i}A} & 1 \end{pmatrix} \\
&-\frac{\mathrm{i}}{4\hbar}\begin{pmatrix} 0 & 0 \\ (\sin A)^{-1}\left[\mathrm{e}^{-2\mathrm{i}A}-1\right]J^{(\mathrm{eff})} & -(\sin A)^{-1}\left[\mathrm{e}^{-2\mathrm{i}A}-1\right]J^{(\mathrm{eff})} \end{pmatrix} \\
&\times\begin{pmatrix} (\sin A)^{-1}\mathrm{e}^{\mathrm{i}A} & (\sin A)^{-1} \\ (\sin A)^{-1}\mathrm{e}^{-\mathrm{i}A} & (\sin A)^{-1} \end{pmatrix} \\
=&\frac{1}{2}\begin{pmatrix} 1 & \mathrm{e}^{-\mathrm{i}A} \\ \mathrm{e}^{-\mathrm{i}A} & 1 \end{pmatrix}-\frac{\mathrm{i}}{4\hbar}\begin{pmatrix} 0 & 0 \\ (\sin A)^{-1}\left[\mathrm{e}^{-2\mathrm{i}A}-1\right]J^{(\mathrm{eff})} & (\sin A)^{-1}\left(\mathrm{e}^{\mathrm{i}A}-\mathrm{e}^{-\mathrm{i}A}\right) \end{pmatrix}\begin{matrix} 0 \\ 0 \end{matrix} \\
=&\frac{1}{2}\begin{pmatrix} 1 & \mathrm{e}^{-\mathrm{i}A} \\ \mathrm{e}^{-\mathrm{i}A} & 1 \end{pmatrix}-\frac{\mathrm{i}}{\hbar}\begin{pmatrix} 0 & 0 \\ \mathrm{e}^{-\mathrm{i}A}J^{(\mathrm{eff})} & 0 \end{pmatrix}
\end{aligned}
\tag{D.13}
$$

Therefore the effective single-particle propagator in coherent state representation is approximately given by

$$
K_{\boldsymbol{\sigma}}\left(\boldsymbol{\phi}^{(f)},\boldsymbol{\phi}^{(f)};t_f\right)=\mathrm{e}^{-\frac{\left|\boldsymbol{\phi}^{(f)}\right|^2}{2}-\frac{\left|\boldsymbol{\phi}^{(i)}\right|^2}{2}+\boldsymbol{\phi}^{(f)*}\mathrm{e}^{-\mathrm{i}A}\left(1-\frac{\mathrm{i}}{\hbar}J^{(\mathrm{eff})}\right)\boldsymbol{\phi}^{(i)}}. \tag{D.14}
$$

### *D.2.2 The propagator for weak hopping in number representation*

Now the stage is open to transform from coherent states to number eigenstates:

$$
\begin{aligned}
&K_{\boldsymbol{\sigma}}\left(\mathbf{n}^{(f)},\mathbf{n}^{(i)};t_f\right)= \\
&\qquad\frac{1}{\pi^{2l}}\int \mathrm{d}^{2l}\phi^{(f)}\int \mathrm{d}^{2l}\phi^{(i)}\left\langle\mathbf{n}^{(f)}|\boldsymbol{\phi}^{(f)}\right\rangle K_{\boldsymbol{\sigma}}\left(\boldsymbol{\phi}^{(f)},\boldsymbol{\phi}^{(i)};t_f\right)\left\langle\boldsymbol{\phi}^{(i)}|\mathbf{n}^{(i)}\right\rangle
\end{aligned}
$$

Using the overlap between a coherent state and a number eigenstate

$$
\langle n|\phi\rangle=\frac{\phi^n}{\sqrt{n!}}\mathrm{e}^{-\frac{|\phi|^2}{2}}, \tag{D.15}
$$

redefining $J_{jj}^{(\mathrm{eff})}=\mathrm{i}\hbar$ and transforming to radial coordinates gives for the integral over $\phi_j^{(f)}$

$$
\int_0^\infty \mathrm{d}r\int_0^{2\pi}\mathrm{d}\varphi\frac{r^{n_j^{(f)}+1}\mathrm{e}^{\mathrm{i}n_j^{(f)}\varphi}}{\pi\sqrt{n_j^{(f)}!}}\mathrm{e}^{-r^2-\frac{\mathrm{i}}{\hbar}r\mathrm{e}^{-\mathrm{i}\varphi}\mathrm{e}^{-\mathrm{i}A_j}J_{j\alpha}^{(\mathrm{eff})}\phi_\alpha^{(i)}}
$$

One may then substitute $\mathrm{e}^{-\mathrm{i}\varphi} = z$ wich replaces the integral over $\varphi$ by an integral over the unit circle (however counter clock wise) in the complex plain. The integration can then be done using Residue calculus and yields

$$\frac{2\mathrm{e}^{-\mathrm{i}n_j^{(f)}A_j}\left(-\frac{\mathrm{i}}{\hbar}J_{j\alpha}^{(\mathrm{eff})}\phi_\alpha^{(i)}\right)^{n_j^{(f)}}}{\left(n_j^{(f)}!\right)^{\frac{3}{2}}}\int_0^\infty \mathrm{d}r r^{2n_j^{(f)}+1}\mathrm{e}^{-r^2} = \frac{\mathrm{e}^{-\mathrm{i}n_j^{(f)}A_j}\left(-\frac{\mathrm{i}}{\hbar}J_{j\alpha}^{(\mathrm{eff})}\phi_\alpha^{(i)}\right)^{n_j^{(f)}}}{\sqrt{n_j^{(f)}!}}.$$

By using the multinomial theorem and again using radial coordinates for the integration over the initial coherent states one gets

$$\begin{aligned}
&K_{\boldsymbol{\sigma}}\left(\mathbf{n}^{(f)},\mathbf{n}^{(i)};t_f\right)\\
&=\int_0^\infty \mathrm{d}^l r\int_0^{2\pi}\mathrm{d}^l\varphi\prod_{j=1}^l\frac{r_j^{n_j^{(i)}+1}\mathrm{e}^{-\mathrm{i}n_j^{(i)}\varphi_j}\mathrm{e}^{-\mathrm{i}n_j^{(f)}A_j}}{\pi\sqrt{n_j^{(i)}!\,n_j^{(f)}!}}\left(-\frac{\mathrm{i}}{\hbar}J_{j\alpha}^{(\mathrm{eff})}r_\alpha\mathrm{e}^{\mathrm{i}\varphi_\alpha}\right)^{n_j^{(f)}}\mathrm{e}^{-r_j^2}\\
&=\sum_{\boldsymbol{\kappa}^{(1)}:\sum_{\alpha=1}^l\kappa_\alpha^{(1)}=n_1^{(f)}}\cdots\sum_{\boldsymbol{\kappa}^{(l)}:\sum_{\alpha=1}^l\kappa_\alpha^{(l)}=n_l^{(f)}}\prod_{j=1}^l\frac{\mathrm{e}^{-\mathrm{i}n_j^{(f)}A_j}}{\pi\sqrt{n_j^{(i)}!\,n_j^{(f)}!}}\left[\prod_{k=1}^l\left(-\frac{\mathrm{i}}{\hbar}J_{jk}^{(\mathrm{eff})}\right)^{\kappa_k^{(j)}}\right]\\
&\qquad\times\binom{n_j^{(f)}}{\boldsymbol{\kappa}^{(j)}}\int_0^\infty\mathrm{d}r_j\int_0^{2\pi}\mathrm{d}\varphi_j r_j^{n_j^{(i)}+\sum_{\alpha=1}^l\kappa_j^{(\alpha)}+1}\mathrm{e}^{\mathrm{i}\left(\sum_{\alpha=1}^l\kappa_j^{(\alpha)}-n_j^{(i)}\right)\varphi_j}\mathrm{e}^{-r_j^2}\\
&=\sum_{\boldsymbol{\kappa}^{(1)}:\sum_{\alpha=1}^l\kappa_\alpha^{(1)}=n_1^{(f)}}\cdots\sum_{\boldsymbol{\kappa}^{(l)}:\sum_{\alpha=1}^l\kappa_\alpha^{(l)}=n_l^{(f)}}\prod_{j=1}^l\frac{\mathrm{e}^{-\mathrm{i}n_j^{(f)}A_j}}{\sqrt{n_j^{(i)}!\,n_j^{(f)}!}}\left[\prod_{k=1}^l\left(-\frac{\mathrm{i}}{\hbar}J_{jk}^{(\mathrm{eff})}\right)^{\kappa_k^{(j)}}\right]\\
&\qquad\times 2\binom{n_j^{(f)}}{\boldsymbol{\kappa}^{(j)}}\int_0^\infty\mathrm{d}r_j r_j^{2n_j^{(i)}+1}\mathrm{e}^{-r_j^2}\delta_{\sum_{\alpha=1}^l\kappa_j^{(\alpha)},n_j^{(i)}}\\
&=\sum_{\boldsymbol{\kappa}^{(1)}:\sum_{\alpha=1}^l\kappa_\alpha^{(1)}=n_1^{(f)}}\cdots\sum_{\boldsymbol{\kappa}^{(l)}:\sum_{\alpha=1}^l\kappa_\alpha^{(l)}=n_l^{(f)}}\prod_{j=1}^l\binom{n_j^{(f)}}{\boldsymbol{\kappa}^{(j)}}\sqrt{\frac{n_j^{(i)}!}{n_j^{(f)}!}}\mathrm{e}^{-\mathrm{i}n_j^{(f)}A_j}\\
&\qquad\times\delta_{\sum_{\alpha=1}^l\kappa_j^{(\alpha)},n_j^{(i)}}\prod_{k=1}^l\left(-\frac{\mathrm{i}}{\hbar}J_{jk}^{(\mathrm{eff})}\right)^{\kappa_k^{(j)}}.
\end{aligned}$$

APPENDIX E

# Derivation of the propagator for open systems

First of all one needs to derive a propagator, which allows even for an exact treatment of the leads, while the scattering region is taken into account semiclassically. One can show (see Appendix E) that such a propagator is given by

$$\hat{K}\left(\boldsymbol{\phi}^{(f)},\boldsymbol{\phi}^{(i)};t,t_i\right) = {}_{\Lambda}\!\left\langle \boldsymbol{\phi}^{(f)}\right| \hat{K}(t_f,t_i) \left|\boldsymbol{\phi}^{(i)}\right\rangle_{\Lambda} =$$
$$\hat{\mathcal{T}}\exp\left\{-\frac{\mathrm{i}}{\hbar}\int_{t_i}^{t}\mathrm{d}s\left[\hat{H}^{(\Xi)}(s)-\frac{\mathrm{i}}{\hbar}\int_{t_i}^{s}\mathrm{d}r\hat{\mathbf{a}}^{\dagger}C^{\dagger}(s)U(s,r)C(r)\hat{\mathbf{a}}\right.\right.$$
$$\left.\left.+\boldsymbol{\phi}^{(f)^*}U(t_f,s)C(s)\hat{\mathbf{a}}+\hat{\mathbf{a}}^{\dagger}C^{\dagger}(s)U(s,t_i)\boldsymbol{\phi}^{(i)}\right]\right\}K^{(\Lambda)}\left(\boldsymbol{\phi}^{(f)},\boldsymbol{\phi}^{(i)};t,t_i\right). \tag{E.1}$$

In this case, the leads are projected to coherent states, which here are defined such that the overlap between two coherent states is given by

$$\left\langle\phi\,\middle|\,\phi'\right\rangle = \exp\left[-\frac{|\phi|^2}{2}-\frac{|\phi'|^2}{2}+\phi^*\phi'\right].$$

In (E.1), $U(t,s)$ is the classical free propagator within the field, and

$$K^{(\Lambda)}\left(\boldsymbol{\phi}^{(f)},\boldsymbol{\phi}^{(i)};t,t_i\right)=\exp\left[-\frac{\left|\boldsymbol{\phi}^{(f)}\right|^2}{2}-\frac{\left|\boldsymbol{\phi}^{(i)}\right|^2}{2}+\boldsymbol{\phi}^{(f)^*}U(t,t_i)\boldsymbol{\phi}^{(i)}\right] \tag{E.2}$$

is the exact quantum mechanical propagator within the leads in coherent state representation.

This leads to the intuitive path integral representation in quadratures,

$$\begin{aligned}K\left(\mathbf{q}^{(f)},\mathbf{q}^{(i)};\boldsymbol{\phi}^{(f)},\boldsymbol{\phi}^{(i)};s,t_i\right)=&\ {}_{\Xi}\left\langle\mathbf{q}^{(f)}\right|\hat{K}\left(\boldsymbol{\phi}^{(f)},\boldsymbol{\phi}^{(i)};s,t_i\right)\left|\mathbf{q}^{(i)}\right\rangle_{\Xi}=\\ K^{(\Lambda)}\left(\boldsymbol{\phi}^{(f)},\boldsymbol{\phi}^{(i)};s,t_i\right)&\lim_{M\to\infty}\int\left(\prod_{m=1}^{M-1}\frac{\mathrm{d}^Lq^{(m)}\mathrm{d}^Lp^{(m)}}{(4\pi b^2)^L}\right)\int\frac{\mathrm{d}^Lp^{(M)}}{(4\pi b^2)^L}\\ \exp\Bigg\{\frac{\mathrm{i}\tau}{4b^2\hbar}\sum_{m=1}^{M}\Bigg[&2\hbar\mathbf{p}^{(m)}\frac{\left(\mathbf{q}^{(m)}-\mathbf{q}^{(m-1)}\right)}{\tau}-H^{(\Xi)}\left(\boldsymbol{\psi}^{(m)};t_m\right)\\ &-2b\boldsymbol{\phi}^{(f)^*}U(t,t_m)C(t_m)\boldsymbol{\psi}^{(m)}-2b\boldsymbol{\psi}^{(m)^*}C^{\dagger}(t_m)U(t_m,t_i)\boldsymbol{\phi}^{(i)}\\ &+\frac{\mathrm{i}\tau}{\hbar}\sum_{l=1}^{m-1}\boldsymbol{\psi}^{(m)^*}C^{\dagger}(t_m)U(t_m,t_l)C(t_l)\boldsymbol{\psi}^{(l)}\Bigg]\Bigg\}\end{aligned} \tag{E.3}$$

with $\mathbf{q}^{(0)}=\mathbf{q}^{(i)}$, $\mathbf{q}^{(M)}=\mathbf{q}^{(f)}$, $\tau=(s-t_i)/M$, $t_m=t_i+m\tau$ and $\boldsymbol{\psi}^{(m)}=\mathbf{q}^{(m-1)}+\mathrm{i}\mathbf{p}^{(m)}$. Here the final time in the propagator has been changed to be $s$ instead of $t$, since the differential equation has to be solved at any time and not just at time $t$. Hence, when taking the time derivative, one must not take the derivative of $U(t,t_m)$.

The easiest way to show that (E.3) is really the correct path integral representation in quadrature representation is to show that it solves the defining equation

$$\mathrm{i}\hbar\frac{\partial}{\partial t}\hat{K}\left(t,t_i\right)=\hat{H}\left(r\right)\hat{K}\left(t,t_i\right),$$

which in quadrature representation reads

$$\begin{aligned} \mathrm{i}\hbar\frac{\partial K\left(\mathbf{q}^{(f)},\mathbf{q}^{(i)};\boldsymbol{\phi}^{(f)},\boldsymbol{\phi}^{(i)};s,t_i\right)}{\partial s} = \\ \int\frac{\mathrm{d}^{2L_\Lambda}\mu}{\pi^{L_\Lambda}}\int\mathrm{d}^L q\,{}_\Lambda\!\left\langle\boldsymbol{\phi}^{(f)}\right|{}_\Xi\!\left\langle\mathbf{q}^{(f)}\right|\hat{H}(t)\left|\mathbf{q}\right\rangle_\Xi\left|\boldsymbol{\mu}\right\rangle_\Lambda \\ \times{}_\Lambda\!\left\langle\boldsymbol{\mu}\right|{}_\Xi\!\left\langle\mathbf{q}\right|\hat{K}\left(s,t_i\right)\left|\mathbf{q}^{(i)}\right\rangle_\Xi\left|\boldsymbol{\phi}^{(i)}\right\rangle_\Lambda. \end{aligned} \tag{E.4}$$

By taking the derivative of (E.3) with respect to $s$ while taking into account that the first term in the exponential does not depend on time at all, as well as replacing

$$\frac{\exp\left\{\frac{\mathrm{i}}{2b^2}\mathbf{p}^{(k)}\left(\mathbf{q}^{(k)}-\mathbf{q}^{(k-1)}\right)\right\}}{\left(4\pi b^2\right)^2}$$

by

$$\langle\mathbf{q}^{(k)}|\mathbf{p}^{(k)}\rangle\langle\mathbf{p}^{(k)}|\mathbf{q}^{(k-1)}\rangle$$

and utilizing

$$\int\mathrm{d}^L q\,|\mathbf{q}\rangle\,\langle\mathbf{q}| = \hat{1} = \int\mathrm{d}^L p\,|\mathbf{p}\rangle\,\langle\mathbf{p}|\,,$$

where $\hat{1}$ is the unity operator, one can easily verify that (E.3) satisfies (E.4).

## E.1 Splitting off the leads

The aim of this section is, to derive the propagator for the full system, given by the solution of

$$\mathrm{i}\hbar\frac{\partial\hat{K}(t,t_i)}{\partial t} = \hat{H}(t)\hat{K}(t,t_i),$$

which allows for an exact treatment of the leads by projecting them to coherent states. For the non-interacting system, the semiclassical approxi-

mation to the propagator is exact and reads

$$K^{(\Lambda)}\left(\boldsymbol{\phi}^{(f)},\boldsymbol{\phi}^{(i)};t,t_i\right) = \exp\left(-\frac{\left|\boldsymbol{\phi}^{(f)}\right|^2}{2}-\frac{\left|\boldsymbol{\phi}^{(f)}\right|^2}{2}+\boldsymbol{\phi}^{(f)*}U(t,t_i)\boldsymbol{\phi}^{(i)}\right), \tag{E.5}$$

where $\boldsymbol{\phi}^{(f)}$ and $\boldsymbol{\phi}^{(i)}$ are complex vectors representing the coherent states in the leads. Note that here the coherent states are defined such that

$${}_\Lambda\left\langle\boldsymbol{\phi}^{(f)}\,\middle|\,\boldsymbol{\phi}^{(i)}\right\rangle_\Lambda = \exp\left(-\frac{\left|\boldsymbol{\phi}^{(f)}\right|^2}{2}-\frac{\left|\boldsymbol{\phi}^{(i)}\right|^2}{2}+\boldsymbol{\phi}^{(f)*}\cdot\boldsymbol{\phi}^{(i)}\right).$$

With the ansatz

$$\hat{K}(t,t_i)=\hat{K}^{(\Lambda)}(t,t_i)\hat{K}^{(\Xi)}(t,t_i), \tag{E.6}$$

the differential equation for the effective propagator of the scattering system including the coupling to the leads is given by

$$\mathrm{i}\hbar\frac{\partial\hat{K}^{(\Xi)}(t,t_i)}{\partial t}=\hat{H}^{(\Xi)}(t)\hat{K}^{(\Xi)}(t,t_i)+\hat{K}^{(\Lambda)\,\dagger}(t,t_i)\hat{C}(t)\hat{K}^{(\Lambda)}(t,t_i)\hat{K}^{(\Xi)}(t,t_i). \tag{E.7}$$

$\hat{K}^{(\Lambda)}$ may be replaced by a complex number, by projecting the leads onto coherent states, which will define

$$\hat{K}^{(\Xi)}(\boldsymbol{\phi}^{(f)},\boldsymbol{\phi}^{(i)};t,t_i)={}_\Lambda\left\langle\boldsymbol{\phi}^{(f)}\right|\hat{K}^{(\Xi)}(t,t_i)\left|\boldsymbol{\phi}^{(i)}\right\rangle_\Lambda.$$

To this end one has to plug (E.5) into (E.7), project the result within the leads onto coherent states and insert unity operators in terms of coherent states between every pair of neighboring operators acting on the leads. Since the Hamiltonian of the scattering system $\hat{H}^{(\Xi)}(t)$ does not act on the leads, the only term, which has to be examined more closely, is the coupling term:

$$\begin{aligned}&{}_\Lambda\left\langle\boldsymbol{\phi}^{(f)}\right|\hat{K}^{(\Lambda)\,\dagger}(t,t_i)\hat{C}(t)\hat{K}^{(\Lambda)}(t,t_i)\hat{K}^{(\Xi)}(t,t_i)\left|\boldsymbol{\phi}^{(i)}\right\rangle_\Lambda=\\&\int\frac{\mathrm{d}^{2L_\Lambda}\eta}{\pi^{L_\Lambda}}\int\frac{\mathrm{d}^{2L_\Lambda}\mu}{\pi^{L_\Lambda}}\int\frac{\mathrm{d}^{2L_\Lambda}\nu}{\pi^{L_\Lambda}}\mathrm{e}^{-\frac{|\boldsymbol{\mu}|^2}{2}-\frac{|\boldsymbol{\eta}|^2}{2}+\boldsymbol{\eta}^*\cdot\boldsymbol{\mu}}\left[\boldsymbol{\eta}^*C(t)\hat{\mathbf{a}}+\hat{\mathbf{a}}^\dagger C^\dagger(t)\boldsymbol{\mu}\right]\\&\qquad\times K^{(\Lambda)*}\left(\boldsymbol{\eta},\boldsymbol{\phi}^{(f)};t,t_i\right)K^{(\Lambda)}\left(\boldsymbol{\mu},\boldsymbol{\nu};t,t_i\right)\hat{K}^{(\Xi)}\left(\boldsymbol{\nu},\boldsymbol{\phi}^{(i)};t,t_i\right).\end{aligned}$$

Performing the integrals yields

$$
\begin{aligned}
&{}_{\Lambda}\Big\langle \boldsymbol{\phi}^{(f)} \Big|\, \hat{K}^{(\Lambda)\,\dagger}(t,t_i)\hat{C}(t)\hat{K}^{(\Lambda)}(t,t_i)\hat{K}^{(\Xi)}(t,t_i)\,\Big|\boldsymbol{\phi}^{(i)}\Big\rangle_{\Lambda} \\
&\quad = \int \frac{\mathrm{d}^{2L_\Lambda}\boldsymbol{\nu}}{\pi^{L_\Lambda}} \Big[\boldsymbol{\phi}^{(f)*}U^\dagger(t,t_i)C(t)\hat{\mathbf{a}} + \hat{\mathbf{a}}^\dagger C^\dagger(t)U(t,t_i)\boldsymbol{\nu}\Big] \\
&\qquad\qquad \times \exp\left(-\frac{|\boldsymbol{\nu}|^2}{2} - \frac{\left|\boldsymbol{\phi}^{(f)}\right|^2}{2} + \boldsymbol{\phi}^{(f)*}\cdot\boldsymbol{\mu}\right)\hat{K}^{(\Xi)}\Big(\boldsymbol{\nu},\boldsymbol{\phi}^{(i)};t,t_i\Big) \\
&\quad = \int \frac{\mathrm{d}^{2L_\Lambda}\boldsymbol{\nu}}{\pi^{L_\Lambda}} \Big[\boldsymbol{\phi}^{(f)*}U^\dagger(t,t_i)C(t)\hat{\mathbf{a}} + \hat{\mathbf{a}}^\dagger C^\dagger(t)U(t,t_i)\boldsymbol{\nu}\Big] \\
&\qquad\qquad \times {}_{\Lambda}\Big\langle \boldsymbol{\phi}^{(f)}\,\Big|\,\boldsymbol{\nu}\Big\rangle_{\Lambda}\hat{K}^{(\Xi)}\Big(\boldsymbol{\nu},\boldsymbol{\phi}^{(i)};t,t_i\Big)
\end{aligned}
$$

With this the equation for the effective propagator of the scattering system with the leads projected to coherent states finally reads

$$
\begin{aligned}
\mathrm{i}\hbar\frac{\partial\hat{K}^{(\Xi)}\Big(\boldsymbol{\phi}^{(f)},\boldsymbol{\phi}^{(i)};t,t_i\Big)}{\partial t} &= \hat{H}^{(\Xi)}(t)\hat{K}^{(\Xi)}\Big(\boldsymbol{\phi}^{(f)},\boldsymbol{\phi}^{(i)};t,t_i\Big) \\
&+ \int \frac{\mathrm{d}^{2L_\Lambda}\boldsymbol{\mu}}{\pi^{L_\Lambda}} \Big[\boldsymbol{\phi}^{(f)*}U^\dagger(t,t_i)C(t)\hat{\mathbf{a}} + \hat{\mathbf{a}}^\dagger C^\dagger(t)U(t,t_i)\boldsymbol{\mu}\Big] \\
&\qquad \times {}_{\Lambda}\Big\langle \boldsymbol{\phi}^{(f)}\,\Big|\,\boldsymbol{\mu}\Big\rangle_{\Lambda}\hat{K}^{(\Xi)}\Big(\boldsymbol{\mu},\boldsymbol{\phi}^{(i)};t,t_i\Big).
\end{aligned}
\tag{E.8}
$$

## E.2 The full propagator

Computing the first terms of the Dyson series suggests that the solution of (E.8) reads

$$
\begin{aligned}
&\hat{K}^{(\Xi)}\Big(\boldsymbol{\phi}^{(f)},\boldsymbol{\phi}^{(i)};t,t_i\Big) = \\
&\quad \hat{\mathcal{T}}\exp\left\{-\frac{\mathrm{i}}{\hbar}\int_{t_i}^{t}\mathrm{d}s\left[\hat{H}^{(\Xi)}(s) - \frac{\mathrm{i}}{\hbar}\int_{t_i}^{s}\mathrm{d}r\hat{\mathbf{a}}^\dagger C^\dagger(s)U(s,r)C(r)\hat{\mathbf{a}}\right.\right. \\
&\qquad \left.\left. + \boldsymbol{\phi}^{(f)*}U^\dagger(s,t_i)C(s)\hat{\mathbf{a}} + \hat{\mathbf{a}}^\dagger C^\dagger(s)U(s,t_i)\boldsymbol{\phi}^{(i)}\right]\right\}\,{}_{\Lambda}\Big\langle \boldsymbol{\phi}^{(f)}\,\Big|\,\boldsymbol{\phi}^{(i)}\Big\rangle_{\Lambda}.
\end{aligned}
\tag{E.9}
$$

The first term in the exponential corresponds to the usual propagation within the (isolated) scattering region. The second and third term account

for losses due to particles leaving into the leads and never returning during the rest of the propagation and gains due to particles entering through the leads and staying in the scattering region, respectively. Finally the last term accounts for particles having entered one lead at time $r$ but entering the scattering region again at time $t$. Showing that (E.9) indeed solves (E.8) may be done by utilizing the Dyson equation induced by (E.9),

$$\begin{aligned}\hat{K}^{(\Xi)}\left(\boldsymbol{\phi}^{(f)},\boldsymbol{\phi}^{(i)};t,t_i\right) = \\ {}_{\Lambda}\left\langle\boldsymbol{\phi}^{(f)}\,\middle|\,\boldsymbol{\phi}^{(i)}\right\rangle_{\Lambda}\Bigg\{\hat{\mathcal{K}}\left(\boldsymbol{\phi}^{(f)},\boldsymbol{\phi}^{(i)};t,t_i\right) \\ -\hat{\mathcal{T}}\frac{1}{\hbar^2}\int_{t_i}^{t}\mathrm{d}s\int_{t_i}^{s}\mathrm{d}r\hat{\mathcal{K}}\left(\boldsymbol{\phi}^{(f)},\boldsymbol{\phi}^{(i)};t,s\right)\hat{\mathbf{a}}^{\dagger}C^{\dagger}(s)U(s,r)C(r)\hat{\mathbf{a}} \\ \times\hat{K}^{(\Xi)}\left(\boldsymbol{\phi}^{(f)},\boldsymbol{\phi}^{(i)};s,t_i\right)\Bigg\},\end{aligned} \tag{E.10}$$

where

$$\begin{aligned}\hat{\mathcal{K}}\left(\boldsymbol{\phi}^{(f)},\boldsymbol{\phi}^{(i)};t,t_i\right) = \hat{\mathcal{T}}\exp\Bigg\{-\frac{\mathrm{i}}{\hbar}\int_{t_i}^{t}\mathrm{d}s\Big[\hat{H}^{(\Xi)}(s)+\boldsymbol{\phi}^{(f)*}U^{\dagger}(s,t_i)C(s)\hat{\mathbf{a}}+ \\ \hat{\mathbf{a}}^{\dagger}C^{\dagger}(s)U(s,t_i)\boldsymbol{\phi}^{(i)}\Big]\Bigg\}.\end{aligned}$$

Taking the time-derivative of (E.10) then shows that (E.9) is the solution of

$$\begin{aligned}\mathrm{i}\hbar\frac{\partial\hat{K}^{(\Xi)}\left(\boldsymbol{\phi}^{(f)},\boldsymbol{\phi}^{(i)};t,t_i\right)}{\partial t} = \\ \left[\hat{H}^{(\Xi)}(t)+\boldsymbol{\phi}^{(f)*}U^{\dagger}(t,t_i)C(t)\hat{\mathbf{a}}+\hat{\mathbf{a}}^{\dagger}C^{\dagger}(t)U(t,t_i)\boldsymbol{\phi}^{(i)}\right]\hat{K}^{(\Xi)}\left(\boldsymbol{\phi}^{(f)},\boldsymbol{\phi}^{(i)};t,t_i\right) \\ -\frac{\mathrm{i}}{\hbar}\int_{t_i}^{t}\mathrm{d}s\hat{\mathbf{a}}^{\dagger}C^{\dagger}(t)U(t,s)\hat{K}^{(\Xi)}\left(\boldsymbol{\phi}^{(f)},\boldsymbol{\phi}^{(i)};t,s\right)C(s)\hat{\mathbf{a}}\frac{\hat{K}^{(\Xi)}\left(\boldsymbol{\phi}^{(f)},\boldsymbol{\phi}^{(i)};s,t_i\right)}{{}_{\Lambda}\left\langle\boldsymbol{\phi}^{(f)}\,\middle|\,\boldsymbol{\phi}^{(i)}\right\rangle_{\Lambda}}.\end{aligned} \tag{E.11}$$

Thus showing that (E.9) solves (E.8) boils down to showing that (E.8) corresponds to (E.11), which can be done for instance by expanding (E.9) in powers of $\hat{\mathbf{a}}$ and $\hat{\mathbf{a}}^{\dagger}$ by means of a Dyson series.

Thus, the propagator of the complete system with the leads projected to coherent states one finally is indeed given by (E.1).

## E.3 Getting real actions and stationary phase approximation

Starting from the path-integral representation (E.3) and projecting the leads to quadratures as well, using the overlap

$$\langle \boldsymbol{\phi} | \mathbf{Q} \rangle = \frac{1}{\sqrt{b\sqrt{2\pi}}} \exp\left[ -\frac{|\boldsymbol{\phi}|^2}{2} - \left( \frac{\mathbf{Q}}{2b} - \boldsymbol{\phi}^* \right)^2 + \frac{(\boldsymbol{\phi}^*)^2}{2} \right]. \tag{E.12}$$

Therefore, the propagator with the leads also given in quadrature representation reads

$$\begin{aligned}
&K\left(\mathbf{q}^{(f)}, \mathbf{q}^{(i)}; \mathbf{Q}^{(2)}, \mathbf{Q}^{(1)}; t, t_i\right) = \\
&\int \frac{\mathrm{d}^{2L_\Lambda}\phi^{(f)}}{\pi^{L_\Lambda}} \int \frac{\mathrm{d}^{2L_\Lambda}\phi^{(i)}}{\pi^{L_\Lambda}} \frac{\exp\left( -\left|\boldsymbol{\phi}^{(f)}\right|^2 - \left|\boldsymbol{\phi}^{(i)}\right|^2 + \boldsymbol{\phi}^{(f)*} U\left(t, t_i\right) \boldsymbol{\phi}^{(i)} \right)}{\left(\sqrt{2\pi} b\right)^{L_\Lambda}} \\
&\exp\left[ -\left( \frac{\mathbf{Q}^{(2)}}{2b} - \boldsymbol{\phi}^{(f)} \right)^2 + \frac{\boldsymbol{\phi}^{(f)2}}{2} - \left( \frac{\mathbf{Q}^{(1)}}{2b} - \boldsymbol{\phi}^{(i)} d \right)^2 + \frac{\boldsymbol{\phi}^{(i)} d^2}{2} \right] \\
&\lim_{N\to\infty} \int \mathrm{d}^L q^{(1)} \cdots \int \mathrm{d}^L q^{(N-1)} \int \frac{\mathrm{d}^L p^{(1)}}{\left(4\pi b^2\right)^L} \cdots \int \frac{\mathrm{d}^L p^{(N)}}{\left(4\pi b^2\right)^L} \\
&\exp\left\{ \frac{\mathrm{i}\tau}{4b^2\hbar} \sum_{k=1}^{N} \left[ 2\hbar \mathbf{p}^{(k)} \frac{\left(\mathbf{q}^{(k)} - \mathbf{q}^{(k-1)}\right)}{\tau} - H^{(\Xi)}\left(\boldsymbol{\psi}^{(k)}; t_k\right) \right.\right. \\
&-2b\boldsymbol{\phi}^{(f)} dU(t, t_k) C(t_k) \boldsymbol{\psi}^{(k)} - 2b \boldsymbol{\psi}^{(k)\dagger} C^\dagger(t_k) U(t_k, t_i) \boldsymbol{\phi}^{(i)} \\
&\left.\left. + \frac{\mathrm{i}\tau}{\hbar} \sum_{l=1}^{k-1} \boldsymbol{\psi}^{(k)\dagger} C^\dagger(t_i + k\tau) U(t_k, t_l) C(t_i + l\tau) \boldsymbol{\psi}^{(l)} \right] \right\}
\end{aligned} \tag{E.13}$$

yields after performing the integrations

$$
\begin{aligned}
&K\left(\mathbf{q}^{(f)},\mathbf{q}^{(i)};\mathbf{Q}^{(2)},\mathbf{Q}^{(1)};t,t_i\right)= \\
&\frac{\exp\left\{-\frac{\mathrm{i}}{4b^2}\begin{pmatrix}\mathbf{Q}^{(1)}\\ \mathbf{Q}^{(2)}\end{pmatrix}\begin{pmatrix}U^{(i)}U^{(r)} & -U^{(i)}\\ -U^{(i)\mathrm{T}} & U^{(r)}U^{(i)}\end{pmatrix}\begin{pmatrix}\mathbf{Q}^{(1)}\\ \mathbf{Q}^{(2)}\end{pmatrix}\right\}}{\det\sqrt{2\pi b^2\left(1-U^{\mathrm{T}}\left(t,t_i\right)U\left(t,t_i\right)\right)}} \\
&\times\lim_{N\to\infty}\int \mathrm{d}^L q^{(1)}\cdots\int \mathrm{d}^L q^{(N-1)}\int\frac{\mathrm{d}^L p^{(1)}}{\left(4\pi b^2\right)^L}\cdots\int\frac{\mathrm{d}^L p^{(N)}}{\left(4\pi b^2\right)^L} \\
&\exp\left\{\frac{\mathrm{i}\tau}{4b^2\hbar}\sum_{k=1}^{N}\left[2\hbar\mathbf{p}^{(k)}\frac{\left(\mathbf{q}^{(k)}-\mathbf{q}^{(k-1)}\right)}{\tau}-H^{(\Xi)}\left(\boldsymbol{\psi}^{(k)};t_k\right)\right.\right. \\
&\quad+2\mathbf{Q}^{(2)}U^{(i)\mathrm{T}}\Im\left[U^{\dagger}(t_k,t_i)C(t_k)\boldsymbol{\psi}^{(k)}\right]-2\mathbf{Q}^{(1)}U^{(i)}\Im\left[U(t,t_k)C(t_k)\boldsymbol{\psi}^{(k)}\right] \\
&\quad\left.\left.+\frac{2\tau}{\hbar}\Im\left[\boldsymbol{\psi}^{(k)*}C^{\dagger}(t_k)U^{\dagger}(t,t_k)\right]U^{(i)\mathrm{T}}\sum_{l=1}^{k-1}\Im\left[U^{\dagger}(t_l,t_i)C(t_l)\boldsymbol{\psi}^{(l)}\right]\right]\right\},
\end{aligned}
\tag{E.14}
$$

where $U^{(r)}=\Re\left[U(t,t_i)\right]$ and $U^{(i)}=\Im\left[U(t,t_i)\right]$. The second line is again the free propagator of the isolated leads. Note that terms which will vanish in the limit $N\to\infty$ are already neglected.

Evaluatig the path integral in stationary phase approximation yields

the equations of motion

$$
\begin{aligned}
0 = \frac{2\hbar}{\tau}\left(\mathbf{p}^{(k)} - \mathbf{p}^{(k+1)}\right) - \frac{\partial H^{(\Xi)}\left(\boldsymbol{\psi}^{(k)}; t_k\right)}{\partial \mathbf{q}^{(k-1)}} \\
+ 2\Im\left[C^{\mathrm{T}}(t_k)U^{*}(t_k,t_i)\right]U^{(i)}\mathbf{Q}^{(2)} \\
- 2\Im\left[C^{\mathrm{T}}(t_k)U^{\mathrm{T}}(t_f,t_k)\right]{U^{(i)}}^{\mathrm{T}}\mathbf{Q}^{(1)} \\
+ \frac{\tau}{\hbar}\Re\left[C^{\mathrm{T}}(t_k)U^{*}(t_k,t_i)U^{(i)}\sum_{l=1}^{N}U(t_f,t_l)C(t_l)\boldsymbol{\psi}^{(l)}\right] \\
- \frac{\tau}{\hbar}\Re\left[C^{\dagger}(t_k)U^{\dagger}(t_f,t_k){U^{(i)}}^{\mathrm{T}}\sum_{l=1}^{k-1}U^{\dagger}(t_l,t_i)C(t_l)\boldsymbol{\psi}^{(l)}\right] \\
- \frac{\tau}{\hbar}\Re\left[C^{\mathrm{T}}(t_k)U^{*}(t_k,t_i)U^{(i)}\sum_{l=k+1}^{N}U^{*}(t_f,t_l)C^{*}(t_l)\boldsymbol{\psi}^{(l)}\right]
\end{aligned}
\tag{E.15}
$$

$$
\begin{aligned}
0 = \frac{2\hbar}{\tau}\left(\mathbf{q}^{(k)} - \mathbf{q}^{(k-1)}\right) - \frac{\partial H^{(\Xi)}\left(\boldsymbol{\psi}^{(k)}; t_k\right)}{\partial \mathbf{p}^{(k-1)}} \\
+ 2\Im\left[\mathrm{i}C^{\mathrm{T}}(t_k)U^{*}(t_k,t_i)\right]U^{(i)}\mathbf{Q}^{(2)} \\
- 2\Im\left[\mathrm{i}C^{\mathrm{T}}(t_k)U^{\mathrm{T}}(t_f,t_k)\right]{U^{(i)}}^{\mathrm{T}}\mathbf{Q}^{(1)} \\
+ \frac{\tau}{\hbar}\Re\left[\mathrm{i}C^{\mathrm{T}}(t_k)U^{*}(t_k,t_i)U^{(i)}\sum_{l=1}^{N}U(t_f,t_l)C(t_l)\boldsymbol{\psi}^{(l)}\right] \\
+ \frac{\tau}{\hbar}\Re\left[\mathrm{i}C^{\dagger}(t_k)U^{\dagger}(t_f,t_k){U^{(i)}}^{\mathrm{T}}\sum_{l=1}^{k-1}U^{\dagger}(t_l,t_i)C(t_l)\boldsymbol{\psi}^{(l)}\right] \\
- \frac{\tau}{\hbar}\Re\left[\mathrm{i}C^{\mathrm{T}}(t_k)U^{*}(t_k,t_i)U^{(i)}\sum_{l=k+1}^{N}U^{*}(t_f,t_l)C^{*}(t_l)\boldsymbol{\psi}^{(l)}\right]
\end{aligned}
\tag{E.16}
$$

Recognizing that $\mathrm{i}\Im(\mathrm{i}a)+\Im(a) = \mathrm{i}\Re(a)+\Im(a) = \mathrm{i}a^{*}$, $\mathrm{i}\Re(\mathrm{i}a)+\Re(a) = -\mathrm{i}\Im(a)+\Re(a) = a^{*}$, $\mathrm{i}\Im(\mathrm{i}a)-\Im(a) = \mathrm{i}a$ and $\mathrm{i}\Re(\mathrm{i}a)-\Re(a) = -a$, as well as defining $\boldsymbol{\psi}^{(k)} = \left(\mathbf{q}^{(k)} + \mathrm{i}\mathbf{p}^{(k)}\right)/(2b)$, the equations of motion can after

taking the limit $N \to \infty$ be written as

$$\begin{aligned} \mathrm{i}\hbar\dot{\boldsymbol{\psi}}(s) = & \\ \frac{\partial H^{(\Xi)}\left(\boldsymbol{\psi}(s);s\right)}{\partial \boldsymbol{\psi}^*(s)} + \frac{\mathrm{i}}{\hbar} C^\dagger(s) U(s,t_i) U^{(i)} \int_{t_i}^{t_f} \mathrm{d}r \Im\left[U(t_f,r) C(r) \boldsymbol{\psi}(r)\right] & \\ -\frac{\mathrm{i}}{2b} C^\dagger(s) U(s,t_i) U^{(i)} \mathbf{Q}^{(2)} + \frac{\mathrm{i}}{2b} C^\dagger(s) U^\dagger(t_f,s) {U^{(i)}}^{\mathrm{T}} \mathbf{Q}^{(1)} & \\ -\frac{\mathrm{i}}{\hbar} C^\dagger(s) \int_{t_i}^{s} \mathrm{d}r U(s,r) C(r) \boldsymbol{\psi}(r). & \end{aligned} \tag{E.17}$$

APPENDIX F

# Loop contributions

In this appendix, the derivation of the loop contributions will be briefly reviewed following mostly references [32, 33, 37, 250, 252, 253] and adopted to the van-Vleck propagator in Fock space. It will also be illustrated, how the effective Planck's constant $1/N$ enters these contributions.

These contributions arise from trajectories, which at some time come close to themselves or their time reverse. The region in phase space, where this happens is called encounter region, while the remaining parts of the

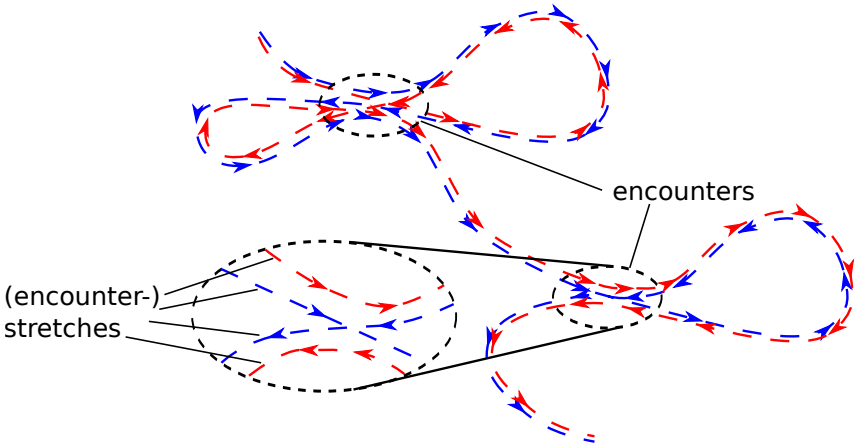


Figure F.1: A trajectory pair consisting of one two- and one three-encounter. The encounter regions are marked by dashed circles. The remaining parts of the trajectory pair are called "links".

trajectories are called links (see also Fig. F.1). Their partner trajectories follow them or their time reverse outside the encounter regions. In such a region, a trajectory and its partner trajectory connect different links. These encounter contributions are also called loop contributions, since if a link starts and ends at the same encounter, the trajectory looks like a loop. However, note that the loops are never closed in phase space, since a trajectory can not cross itself in phase space. For later reference, the parts of the trajectory lying inside the encounter region will be denoted as (encounter-) stretches. Later on it will be discussed in more detail, how to define the borders of an encounter region.

Before starting, there are two comments, which should be noted. First, the trajectories may differ in several such encounter regions, and second, due to the abstract way of presentation, without further discussing the nature of the time reversal operation, the derivations presented here are valid for all symmetry classes GUE, GOE and GSE.

The discussion will start with two-leg-loops, since one-leg-loops can be considered as two-leg-loops, for which the encounter region is shifted to the start or end of the trajectory.

## F.1 Two-leg-loops

### *F.1.1 Phase-space geometry*

First of all consider the trajectory $\gamma$ and label its links in the order of traversal, such that the stretch, in which $\gamma$ starts is the first one, while the one where it ends is the $(O+1)$-th stretch, where $O+1$ is the total number of links.

For this trajectory, define the phase space coordinates

$$\tilde{\mathbf{x}} = (\mathbf{J}, \boldsymbol{\theta}) \tag{F.1}$$

with $J_j = |\psi_j|^2$, $\theta_j = \arg(\psi_j)$.

The next step would be placing a Poincaré surface of section (PSS) $\mathcal{P}$ orthogonal to $\gamma$ at an arbitrary phase space point $\tilde{\mathbf{x}}_{\alpha,1}$ of the trajectory within each encounter region separating the links [32, 33]. Here, $\alpha$ labels the encounter, while the subscript 1 indicates that it is placed along the first traversal of the encounter region.

However, here not only the total energy but also the number of particles is conserved, which leads to the integrability of the 2-site Bose-Hubbard

model and the fact that the trajectory $\gamma$ lives on a $2L-2$-dimensional manifold within the phase space, rather than a $2L-1$-dimensional one. Therefore, $\mathcal{P}$ would be a $2L-3$-dimensional manifold, which means that there are not as many stable as unstable directions. In the derivation of the loop contributions, however, it is important that the number of stable and unstable manifolds are the same.

Thus, one also has to take advantage of the gauge invariance of $\boldsymbol{\psi}$, *i.e.* the fact that, if $\boldsymbol{\psi}(t)$ is a solution of the equations of motion, then $\widetilde{\boldsymbol{\psi}} = \mathrm{e}^{\mathrm{i}\phi}\boldsymbol{\psi}$ is also a solution. This implies that the only information of the phases of the trajectory one needs, are the differences between the phases. Thus, the reduced phase space coordinates can be defined by

$$\mathbf{x} = \left(\frac{J_1}{N}, \ldots, \frac{J_L}{N}, \theta_2 - \theta_1, \ldots, \theta_L - \theta_1\right), \tag{F.2}$$

which then can be used to define the reduced Poincaré surface of section (RPSS) $\mathcal{P}_r$, which in turn is then $2L-4$ dimensional with $L-2$ stable and unstable directions. Note that the amplitudes of $\boldsymbol{\psi}$ have also been devided by the total number of particles, in order to have the effective Planck's constant $\hbar_{\mathrm{eff}} = 1/N$ appearing explicitly in the expression of the action difference later on.

It should be noted that the idea to use constants of motion in order to further reduce the dimensionality of a Poincaré surface of section is not a new one [300]. Furthermore, the definition of the phase space variables in terms of phase differences rather than absolute phases corresponds to an additional projection of the Poincaré surface of section, such as has been frequently used in order to visualize them [300–311].

Within each encounter $\alpha$, such a RPSS is then placed at an arbitrary phase space point $\mathbf{x}_{\alpha,1}$ of $\gamma$ perpendicular to the trajectory and will be denoted as $\mathcal{P}_r^{(\alpha)}$. The time, at which the trajectory pierces through the $\alpha$-th RPSS for the first time will be denoted as $t_{\alpha,1}$. The trajectory then pierces again through $\mathcal{P}_r^{(\alpha)}$ at times $t_{\alpha,j}$ at the phase space point $\mathbf{x}_{\alpha,j}$, where the sequential index $j$ runs from 2 to $o_\alpha$, which is the number of traversals of the $\alpha$-th encounter. An encounter will be denoted according to the number of its traversal as $o_\alpha$-encounter.

Next, depending on whether $\mathbf{x}_{\alpha,j}$ or $\mathcal{T}\mathbf{x}_{\alpha,j}$ is close to $\mathbf{x}_{\alpha,1}$, where $\mathcal{T}$ denotes the classical time reversal operation, the (small) phase space differences $\mathbf{x}_{\alpha,j} - \mathbf{x}_{\alpha,1}$ or $\mathcal{T}\mathbf{x}_{\alpha,j} - \mathbf{x}_{\alpha,1}$ is decomposed into stable and unstable

directions,

$$(\mathcal{T})\mathbf{x}_{\alpha,j} - \mathbf{x}_{\alpha,1} = \sum_{l=1}^{L-2} \left( \tilde{s}_l^{(\alpha,j)} \mathbf{e}_l^s + \tilde{u}_l^{(\alpha,j)} \mathbf{e}_l^u \right), \tag{F.3}$$

where $(\mathcal{T})\mathbf{x}_{\alpha,1}$ is either $\mathbf{x}$, if the stretches are traversed in the same direction, or $\mathcal{T}\mathbf{x}$ else. The vectors $\mathbf{e}_l^s$ and $\mathbf{e}_l^u$ are the unit vectors along the stable and unstable directions and satisfy

$$\mathbf{e}_l^u \wedge \mathbf{e}_l^s = \mathbf{e}_l^u \cdot \begin{pmatrix} 0 & 1 \\ -1 & 0 \end{pmatrix} \mathbf{e}_l^s = 1 \tag{F.4}$$

Now the encounter regions can be defined more precisely. As already stated, each RPSS has to be placed within the corresponding encounter region. Furthermore, the phase space differences (F.3) have to be small, *i.e.* the stable and unstable coordinates have to satisfy,

$$\left| \tilde{s}_l^{(\alpha,j)} \right|, \left| \tilde{u}_l^{(\alpha,j)} \right| < c. \tag{F.5}$$

Here $c$ is an arbitrary constant, which is small enough to allow linearization of the motion, but still large compared to the effective Planck's constant $1/N$. The borders of the encounter region are then defined such that the phase space separations of all stretches are smaller than this classical constant.

Due to exponential behavior of stable and unstable coordinates, the time the trajectory needs from entering the $\alpha$-th encounter region to piercing through $\mathcal{P}_r^{(\alpha)}$ for the first time is approximately given by

$$t_s^{(\alpha)} \sim \frac{1}{\lambda} \min_{l,j} \left( \ln \frac{c}{\left| \tilde{s}_l^{(\alpha,j)} \right|} \right), \tag{F.6}$$

with $\lambda$ being the largest Lyapunov exponent. Likewise the time, the trajectory spends inside the encounter after traversing $\mathbf{x}_{\alpha,1}$ is estimated by

$$t_u^{(\alpha)} \sim \frac{1}{\lambda} \min_{l,j} \left( \ln \frac{c}{\left| \tilde{u}_l^{(\alpha,j)} \right|} \right). \tag{F.7}$$

Note that in Eqns. (F.6) and (F.7) as well as in the following, the minimum is taken with respect to both the dimensional and the sequential indexes $l \in \{1, \ldots, L-2\}$ and $j \in \{2, \ldots, o_\alpha\}$.

The total time the trajectory needs in order to traverse the $\alpha$-th encounter, which is also called the encounter time, is given by the sum of these two times,

$$t_{\text{enc}}^{(\alpha)} = t_s^{(\alpha)} + t_u^{(\alpha)}. \tag{F.8}$$

### *F.1.2 Partner trajectory*

Let's now turn towards the partner trajectory $\gamma'$, which pierces through $\mathcal{P}_r^{(\alpha)}$ at time $t_{\alpha,j}$ in the reduced phase space point $\mathbf{x}'_{\alpha,j}$. Its $j$-th stretch switches within the encounter from following the (time reverse of the) $k$-th to the (time reverse of the) $k'$-th stretch of $\gamma$.

The differences between the piercing points of the partner trajectory can be decomposed again into stable and unstable coordinates $\tilde{s}_k^{(\alpha,j)\prime}$, $\tilde{u}_k^{(\alpha,j)\prime}$ according to (F.3). Since the stable (unstable) coordinates deviate exponentially when evolving the trajectory backward (forward) in time, the stable and unstable coordinates have to satisfy the relations

$$\tilde{\mathbf{s}}^{(\alpha,j)\prime} = \tilde{\mathbf{s}}^{(\alpha,k)} \tag{F.9}$$

$$\tilde{\mathbf{u}}^{(\alpha,j)\prime} = \tilde{\mathbf{u}}^{(\alpha,k')}. \tag{F.10}$$

### *F.1.3 Existence*

The proof of the existence of the loops for the mean field dynamics follows exactly the same lines as for first quantized systems in Ref. [35], except that the phase space points have to be replaced by the reduced ones, (F.2). The proof starts with periodic orbits, for which the existence is shown by linearizing the motion along each loop of $\gamma'$ around $\gamma$.

The linearized motion relates the difference $\mathbf{x}'_{\alpha,j} - \mathbf{x}_{\alpha,k(j)}$ with $\mathbf{x}'_{\alpha,j-1} - \mathbf{x}_{\alpha,k'(j-1)}$, if the $j$-th link of $\gamma'$ follows $\gamma$, while it establishes a connection between $\mathbf{x}'_{\alpha,j} - \mathcal{T}\mathbf{x}_{\alpha,k(j)}$ and $\mathbf{x}'_{\alpha,j-1} - \mathcal{T}\mathbf{x}_{\alpha,k'(j-1)}$, if the $j$-th link of $\gamma'$ follows $\mathcal{T}\gamma$. Here, $k(j)$ denotes the stretch of $\gamma$, along which the $j$-th stretch of $\gamma'$ enters the encounter, while $k'(j)$ is the one along which it exits.

This yields a set of $O$ linear equations, which uniquely define the $O$ phase space coordinates of the partner trajectory $\gamma'$ as functions of the phase space coordinates of $\gamma$. The solution to these equations is given by Eqns. (F.9,F.10) [33].

Finally, note that it turns out that the links have to be non-vanishing, which will be of importance later on.

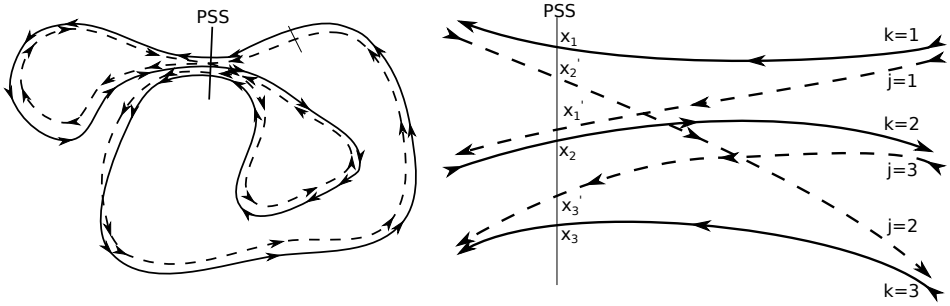


Figure F.2: Periodic orbit with a three-encounter. In this example, the first stretch of the partner trajectory $\gamma'$ connects the first with second one of $\gamma$, the second stretch of $\gamma'$ switches from the first to the third one of $\gamma$ and the third stretch of $\gamma'$ enters along the time reverse of the second one of $\gamma$ and exits along its third one.

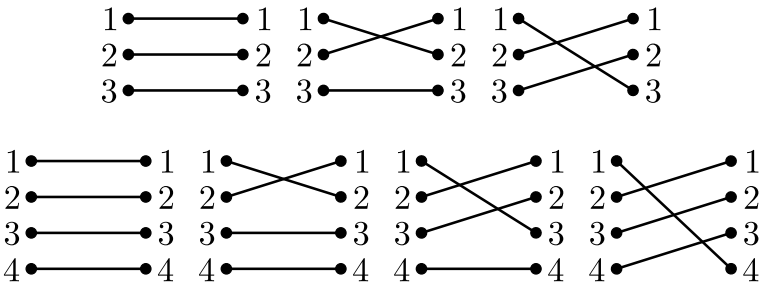

Figure F.3: Creation of a three- (top) and four-encounter (bottom) by reconnecting the initially parallel stretches.

In order to translate the loop contributions to non-periodic orbits, the set of trajectories is assumed to arise from cutting a periodic one into several pieces and using the same argumentation as sketched above.

### *F.1.4 Action difference*

Apart from the encounter regions the links of the trajectory pairs closely follow each other yielding a vanishing (in the limit $\hbar_{\text{eff}} \to 0$) action difference. The only non-vanishing action differences occur in the encounter regions. The total action difference is thus the sum over the action differences of each encounter. Therefore, in this section, it is sufficient to only consider the case of one single $o$-encounter.

In order to compute the action difference of such an encounter, it is best to start from the diagonal case, where the $j$-th stretch of $\gamma'$ just follows the $j$-th stretch of $\gamma$ and successively reconnecting entrances and exits of $\gamma$ by $\gamma'$. Examples of how to generate a 3 and 4-encounter by these reconnections is shown in Fig. F.3 By transforming from the phase space coordinates $\tilde{s}_k^{(j)}, \tilde{u}_k^{(j)}$ to $s_k^{(j)}, u_k^{(j)}$, which are the stable and unstable coordinates after the $j$-th reconnection, the action difference can be written as a sum over action differences of two-encounters [33],

$$\Delta R^{(o)} = \sum_{j=1}^{o-1} \Delta R_j^{(2)}, \tag{F.11}$$

where $\Delta R_j^{(2)}$ is the action difference of the 2-encounter corresponding to the $j$-th reconnection. Note that this coordinate transformation is linear and volume preserving [33].

Therefore, it is enough to consider the action difference $\Delta R^{(2)}$ of a two-encounter. Since the energies are the same for both trajectories, the action difference between the first stretch of $\gamma$ to $\mathbf{x}_1$ and $\gamma'$ to $\mathbf{x}_1'$ is given by the contour integral

$$\Delta R_1 = \hbar \int_{\mathbf{x}_1'}^{\mathbf{x}_1} \mathrm{d}\mathbf{J} \cdot \boldsymbol{\theta}.$$

When choosing the contour of the integration to lie in the RPSS, the unstable directions can be chosen such that the contour coincides with one of the stable directions.

Repeating the same reasoning for the remaining parts of the encounter, gives the action difference as a contour integral over a closed loop, $\Delta R^{(2)} = \hbar \oint \mathrm{d}\mathbf{J} \cdot \boldsymbol{\theta}$ along a parallelogram $\mathbf{x}_1' \to \mathbf{x}_1 \to (\mathcal{T})\mathbf{x}_2' \to (\mathcal{T})\mathbf{x}_2 \to \mathbf{x}_1'$, spanned by $\mathbf{x}_1' - \mathbf{x}_1 = u\mathbf{e}^u$ and $\mathcal{T}\mathbf{x}_2' - \mathbf{x}_1 = s\mathbf{e}^s$. Note that here the stable and unstable directions are chosen such that only one stable and unstable component of the expansion (F.3) is non-zero. Thus, due to normalization, Eq. (F.4), the action difference of a 2-encounter is given by $\Delta R^{(2)} = \hbar N u\mathbf{e}^u \wedge s\mathbf{e}^s = \hbar N s u$, which can be formulated independent of the choice of the stable and unstable directions as $\Delta R^{(2)} = \hbar N \mathbf{s} \cdot \mathbf{u}$. The additional factor given by the total number of particles arises due to the definition of the reduced phase space coordinates (F.2).

Finally, the action difference of an $o$-encounter is given by

$$\Delta R^{(o)} = \hbar N \sum_{j,k} s_k^{(j)} u_k^{(j)}.$$

Note that the action difference is independent of the position of the RPSS [32]. Furthermore, it can be shown that the Maslov indices of the involved trajectories are equal [38].

### *F.1.5 Density of encounters*

As already indicated in section F.1.3, the above considerations also include a whole series of encounters. Therefore, it is convenient to define a vector $\mathbf{v}$ whose components $v_o$ are the number of $o$-encounters. The total number of encounters can thus be written as $N_{\mathrm{enc}} = \sum_o v_o$. Moreover, $O = \sum_o o v_o$ is the total number of encounter stretches.

Note that in the case of several encounters, there is one RPSS $\mathcal{P}_r^{(\alpha)}$ for each encounter $\alpha = 1, \ldots, N_{\mathrm{enc}}$, which is traversed by $\gamma$ at times $t_{\alpha,j}$, $j = 1, \ldots, o_\alpha$ and the $\alpha$-th encounter is characterized by $(L-2)(o_\alpha - 1)$ stable and unstable coordinates $s_l^{(\alpha,j)}, u_l^{(\alpha,j)}$, $l = 1, \ldots, L-2$, $j = 2, \ldots, o_\alpha$.

In the following, the derivation of the density $w_T^{(2ll)}(\mathbf{s}, \mathbf{u})$ of phase-space separations $\mathbf{s}, \mathbf{u}$ for two-leg-loop trajectories with evolution time $T$ will be adopted to the case at hand. Here,

$$\mathbf{s} = \left(\mathbf{s}^{(1,2)}, \ldots, \mathbf{s}^{(N_{enc}, o_{N_{enc}})}\right)$$

is the vector containing all stable coordinates. Likewise $\mathbf{u}$ is the vector containing all unstable coordinates. To make sure that each encounter is counted exactly once, one has to demand that

$$\int_{-c}^{c} \mathrm{d}^{(L-2)(O-N_{enc})} s \mathrm{d}^{(L-2)(O-N_{enc})} u w_T^{(2ll)}(\mathbf{s}, \mathbf{u}) \times \prod_{\alpha,j} \delta\left(\Delta R_\alpha - \hbar N \mathbf{s}^{(\alpha,j)} \cdot \mathbf{u}^{(\alpha,j)}\right)$$

yields the density of encounters sets in a trajectory $\gamma$ leading to trajectory pairs $(\gamma, \gamma')$ with a given structure and an action difference of the $\alpha$-th encounter given by $\Delta R_\alpha$.

$w_T^{(2ll)}(\mathbf{s}, \mathbf{u})$ should be understood as a quantity averaged over the ensemble of all trajectories $\gamma$ with duration $T$ and weighted by the semiclassical amplitude $|A_\gamma|^2$.

Now assume that every RPSS and all times $t_{\alpha,1}$ are fixed. Due to ergodicity, the probability of piercing through $\mathcal{P}_r^{(\alpha)}$ again in a time interval

$[t_{\alpha,j}, t_{\alpha,j} + \mathrm{d}t_{\alpha,j}]$ with stable and unstable coordinates in the set

$$\bigotimes_{l=1}^{L-2} \left( [\hat{s}_l^{(\alpha,j)}, \hat{s}_l^{(\alpha,j)} + \mathrm{d}\hat{s}_l^{(\alpha,j)}] \otimes [\hat{u}_l^{(\alpha,j)}, \hat{u}_l^{(\alpha,j)} + \mathrm{d}\hat{u}_l^{(\alpha,j)}] \right)$$

is given by $\mathrm{d}^{L-2}\hat{s}^{(\alpha,j)}\mathrm{d}^{L-2}\hat{u}^{(\alpha,j)}\mathrm{d}t_{\alpha,j}/\Omega_N(E_\gamma)$, where

$$\Omega_N(E) = \int \mathrm{d}^{2L}\psi \delta(\theta_1)\, \delta\left( N - \sum_{l=1}^{L} |\psi_l|^2 + \frac{L}{2} \right) \delta\left[ H(\boldsymbol{\psi}^*, \boldsymbol{\psi}) - E \right]$$

is the reduced phase space volume and $E_\gamma$ is the energy of the trajectory $\gamma$. Since the overall transformation $(\hat{\mathbf{s}}, \hat{\mathbf{u}}) \to (\mathbf{s}, \mathbf{u})$ is volume preserving, the same uniform probability holds for $(\mathbf{s}, \mathbf{u})$.

Therefore the number

$$\rho_T(\mathbf{s}, \mathbf{u}, t)\mathrm{d}^{(L-2)(O-N_{enc})}s\mathrm{d}^{(L-2)(O-N_{enc})}u\mathrm{d}^{O-N_{enc}}t$$

of sets of $O-N_{enc}$ piercings through the sections $\mathcal{P}_\alpha$, $\alpha = 1, \ldots, N_{enc}$ occuring in time intervals $[t_{\alpha,j}, t_{\alpha,j} + \mathrm{d}t_{\alpha,j}]$ with stable and unstable coordinates in the set

$$\bigotimes_{k=1}^{L-2} \left( [s_k^{(\alpha,j)}, s_k^{(\alpha,j)} + \mathrm{d}s_k^{(\alpha,j)}] \otimes [u_k^{(\alpha,j)}, u_k^{(\alpha,j)} + \mathrm{d}u_k^{(\alpha,j)}] \right)$$

can be determined. However, one has to keep in mind that the links shall not vanish. Therefore, a suitable characteristic function $\Theta_T(\mathbf{s}, \mathbf{u}, t)$ has to be employed, which is equal to 1 for non-vanishing links, and 0 otherwise. Thus

$$\rho_T(\mathbf{s}, \mathbf{u}, t) = \frac{\Theta_T(\mathbf{s}, \mathbf{u}, t)}{\Omega^{O-N_{enc}}}.$$

Finally, the density of phase space separations is given by integrating over the piercing times $t_{\alpha,j}$, $j = 2, \ldots, o_\alpha$, as well as over the positions of the reduced Poincaré sections. However, this integration counts each encounter for a time $t_{enc}^{(\alpha)}$, such that $w_T^{(2ll)}(\mathbf{s}, \mathbf{u})$ has to be devided by this time,

$$w_T^{(2ll)}(\mathbf{s}, \mathbf{u}) = \frac{1}{\Omega_N^{O-N_{enc}} \prod_\alpha t_{enc}^{(\alpha)}} \int \mathrm{d}^O t \Theta(\mathbf{s}, \mathbf{u}, t). \tag{F.12}$$

By substituting $\tilde{t}_j = t_j + t_{j-1}$, the characteristic function $\Theta(\mathbf{s}, \mathbf{u}, t)$ yields the integration limits $0 < \tilde{t}_1 < \ldots < \tilde{t}_O < T - \sum_\alpha o_\alpha t_{enc}^\alpha$ and $w_T^{2ll}(\mathbf{s}, \mathbf{u})$ is

given by

$$w_T^{2ll}(\mathbf{s},\mathbf{u}) = \frac{1}{\Omega_N^{O-N_{enc}} \prod_\alpha t_{enc}^\alpha} \int_0^{T-\sum_\alpha o_\alpha t_{enc}^{(\alpha)}} \mathrm{d}t_O \int_0^{t_O} \mathrm{d}t_{O-1} \cdots \int_0^{t_2} \mathrm{d}t_1 = \frac{(T-\sum_\alpha o_\alpha t_{enc}^{(\alpha)})^O}{O!\,\Omega_N^{O-N_{enc}} \prod_\alpha t_{enc}^{(\alpha)}}. \tag{F.13}$$

Note that the last step, where the time integrals have been performed, can only be done, if the contribution of the trajectory pair does not depend on the propagation times explicitly.

With this, the average number $P_T^{\mathbf{v}}(\Delta R)\mathrm{d}\Delta R$ of partners differing from $\gamma$ in $v_l$ $l$-encounters, with an action difference in the interval $[\Delta R, \Delta R + \mathrm{d}\Delta R]$ can be determined. In order to take into account all possibilities, one has to sum over all structures related to $\mathbf{v}$ and integrate over all phase-space separations $\mathbf{s}, \mathbf{u}$ leading to the same overall action difference $\Delta R = \hbar N \mathbf{s}\cdot\mathbf{u}$. One obtains

$$P_{T,2ll}^{\mathbf{v}}(\Delta R)\mathrm{d}\Delta R = \mathrm{d}\Delta R \mathcal{N}(\mathbf{v}) \int \mathrm{d}^{(L-2)(O-N_{enc})}s \mathrm{d}^{(L-2)(O-N_{enc})}u \, \delta(\Delta R - \hbar N \mathbf{s}\cdot\mathbf{u}) w_T^{(2ll)}(\mathbf{s},\mathbf{u}),$$

where $\mathcal{N}(\mathbf{v})$ is the number of structures related to $\mathbf{v}$.

For a given trajectory $\gamma$, the sum over partner trajectories can finally on disorder average be replaced according to

$$\sum_{\gamma'} \ldots \to \sum_{\mathbf{v}} \int \mathrm{d}\Delta R P_{T,2ll}^{\mathbf{v}}(\Delta R) \ldots$$

This replacement is possible, since the difference in the semiclassical amplitudes $\mathcal{A}_\gamma$ and $\mathcal{A}_{\gamma'}$ of the partner trajectories can be neglected.

## F.2 One-leg-loops

For the discussion of one-leg-loops we will mainly Refs. [250, 252, 253].

Since a one-leg-loop, which ends in an encounter gives the same contribution as one which starts in an encounter, it is sufficient to consider only

the starting point to lie within an encounter region. The fact that both cases give the same contribution can be seen very easily, by noticing that they are related by just exchanging $\mathbf{s}$ and $\mathbf{u}$, which appear symmetrically in the expressions for the action difference and the density of encounters.

In order to evaluate these contributions, consider a RPSS within the first encounter at time

$$t' < \frac{1}{\lambda} \min_{l,j} \left( \ln \frac{c}{\left| s_l^{(1,j)} \right|} \right),$$

such that the encounter time is given by $t_{enc}^{(}1) = t' + t_u$. In order to include every contribution, one has to integrate over all possible $t'$. Thus the density of encounters has to be modified to be given by

$$w_T^{(1ll)}(\mathbf{s},\mathbf{u}) = \frac{1}{\Omega^{O-N_{enc}} \prod_\alpha t_{enc}^{(\alpha)}} \int_0^{T-\sum_\alpha o_\alpha t_{enc}^{(\alpha)}} \mathrm{d}t_O \int_0^{t_O} \mathrm{d}t_{O-1} \cdots \int_0^{t_3} \mathrm{d}t_2 \int_0^{\frac{1}{\lambda}\min_j \left( \ln \frac{c}{|\mathbf{s_j}|} \right)} \mathrm{d}t'. \tag{F.14}$$

Note that this does *not* include the case that both end points are very close to each other and therefore lie in the same encounter, *i.e.* coherent backscattering contributions.

Apart from the changed density of encounters, which also brings along different dependencies on the stable and unstable coordinates, the further evaluation of one-leg-loops is the same as the one for two-leg-loops. Usually, it is reasonable to make a change of variables

$$t'' = t' + \frac{1}{\lambda} \min_j \left( \ln \frac{c}{|u_j|}, \qquad u_j = \frac{c}{\sigma_j}, \qquad s_j = c x_j \sigma_j \right),$$

with integration domains

$$-1 < x_j < 1, \qquad 1 < \sigma_j < \mathrm{e}^{\lambda t''}, \qquad 0 < t'' < \frac{1}{\lambda} \min_j \left( \ln \frac{1}{|x_j|} \right),$$

in order to evaluate the resulting integrations over stable and unstable coordinates.

When summing over all possible encounter structures with a one-leg-loop, one also has to account for the fact that each encounter stretch can

be chosen to contain the starting point of the trajectory. Therefore, an additional sum over the number $o_1$ of stretches of the first encounter has to be inserted, where each term has to be weighted by the number $v_{o_1}$ of such encounters. However, this sum is also included in the total number of encounter structures, $\mathcal{N}(\mathbf{v})$. In order to compensate this double counting, one also has to divide by $O$, such that finally the number of partners for a one-leg-loop is given by

$$P^{\mathbf{v}}_{T,1ll}(\Delta R)\mathrm{d}\Delta R = \mathrm{d}\Delta R \frac{\mathcal{N}(\mathbf{v})}{O} \sum_{o_1} o_1 v_{o_1} \int \mathrm{d}^{(L-2)(O-N_{enc})} s \mathrm{d}^{(L-2)(O-N_{enc})} u$$
$$\delta(\Delta R - \hbar N \mathbf{s}\cdot\mathbf{u}) w_T^{(1ll)}(\mathbf{s},\mathbf{u}).$$

APPENDIX G

# Hubbard-Stratonovich transformation

For the derivation of the van-Vleck propagator we will use a Hubbard-Stratonovich transformation in intermediate steps. Therefore we would like to introduce it very briefly.

The Hubbard-Stratonovich transformation is based on Gaussian or Fresnel integrals and it is used to decouple fourth-order terms in an exponential. Suppose we have an exponential $\mathrm{e}^{\alpha yxyx}$ where $y$ and $x$ do not neccessarily commute (later we will need the case that $y$ is a creation and $x$ an annihilation operator). This exponential can be written as

$$\mathrm{e}^{-\alpha yxyx} = \frac{\int \mathrm{d}\sigma \mathrm{e}^{\beta\sigma^2 + 2\beta\sqrt{\frac{\alpha}{\beta}}\sigma yx}}{\int \mathrm{d}\sigma \mathrm{e}^{\beta\sigma^2}},$$

which can be checked by shifting $\sigma \to \sigma - \sqrt{\alpha/\beta}yx$ in the numerator:

$$\int \mathrm{d}\sigma \mathrm{e}^{\beta\sigma^2 + 2\beta\sqrt{\frac{\alpha}{\beta}}\sigma yx} = \int \mathrm{d}\sigma \mathrm{e}^{\beta\left(\sigma + \sqrt{\frac{\alpha}{\beta}}yx\right)^2 - \alpha yxyx} = \mathrm{e}^{-\alpha yxyx} \int \mathrm{d}\sigma \mathrm{e}^{\beta\sigma^2}.$$

Now lets have a look at what happens in higher dimensions. First we consider the case that the exponent on the left hand side is of the form

$y_\alpha x_\alpha A_{\alpha\beta} y_\beta x_\beta$, where a sum over multiply occuring greek indices is implicit. Then the transformation is

$$\mathrm{e}^{-\alpha y_\eta x_\eta A_{\eta\mu} y_\mu x_\mu} = \frac{\int \mathrm{d}\sigma \mathrm{e}^{\beta\sigma A^{-1}\sigma + 2\beta\sqrt{\frac{\alpha}{\beta}}\sigma_\eta y_\eta x_\eta}}{\int \mathrm{d}\sigma \mathrm{e}^{\beta\sigma A^{-1}\sigma}},$$

where now $\sigma$ is a vector and $A^{-1}$ is the inverse of $A$, or more generally $A^{-1}$ is defined by $\left(A^{-1}\right)_{j\alpha} A_{\alpha k} = \delta_{jk}$, where $\delta_{jk}$ is the Kronecker delta. In this case the shift $\sigma_j \to \sigma_j - \sqrt{\alpha/\beta} A_{j,\eta} y_\eta x_\eta$ shows the identity of the left and the right hand side.

However this not yet includes the most general case of a fourth order term, which would be $x_\alpha x_\beta A_{\alpha\beta\gamma\delta} x_\gamma x_\delta$. Here we will only consider the case that $A^*_{klmn} = A_{mnkl}$ and $A_{klmn} = A_{lkmn} = A_{klnm}$. In this case the integration no longer runs over (real or complex) numbers but over (hermitian) matrices and one possible form of the Hubbard Stratonovich transformation in this case is

$$\mathrm{e}^{-\alpha y_\gamma x_\eta A_{\gamma\delta\eta\mu} y_\delta x_\mu} = \frac{\int \mathrm{d}\sigma \mathrm{e}^{\beta\sigma_{\delta\gamma}\left(A^{-1}\right)_{\gamma\eta\delta\mu}\sigma_{\eta\mu} + 2\beta\sqrt{\frac{\alpha}{\beta}}\sigma_{\gamma\delta} y_\gamma x_\delta}}{\int \mathrm{d}\sigma \mathrm{e}^{\beta\sigma_{\delta\gamma}\left(A^{-1}\right)_{\gamma\eta\delta\mu}\sigma_{\eta\mu}}},$$

where $\left(A^{-1}\right)_{klmn}$ is chosen such that

$$\left(A^{-1}\right)_{k\alpha l\beta} A_{\alpha m\beta n} = A_{\alpha k\beta l} \left(A^{-1}\right)_{\alpha m\beta n} = \delta_{km}\delta_{ln}.$$

To prove this case one has to shift $\sigma_{kl} \to \sigma_{kl} - \sqrt{\alpha/\beta} A_{k\gamma l\delta} y_\gamma x_\delta$.

# Bibliography

# Bibliography


[1] J. Franck and G. Hertz, Verh. Deut. Phys. Ges. **16**, 457 (1914).

[2] N. Bohr, Phil. Mag. S. 6 **26**, 1 (1913).

[3] G. Tanner and K. Richter, Scholarpedia **8**, 9818 (2013).

[4] E. Schrödinger, Phys. Rev. **28**, 1049 (1926).

[5] C. Davisson, Bell System Tech. J. **7**, 90 (1928).

[6] M. Brack and R. Bhaduri, *Semiclassical Physics*, 1st ed. (Westview Press, 1997).

[7] J. H. Van Vleck, Proc. Natl. Acad. Sci. **14**, 178 (1928).

[8] W. Pauli, *Selected topics in field quantization*, 1st ed. (MIT Press, 2000).

[9] R. P. Feynman, Rev. Mod. Phys. **20**, 367 (1948).

[10] R. S. Whitney, Phys. Rev. B **75**, 235404 (2007).

[11] M. C. Gutzwiller, J. Math. Phys. **8**, 1979 (1967).

[12] L. S. Schulman, *Techniques and applications of path integration* (Wiley, New York, 1996).

[13] H. Kleinert, *Path integrals in quantum mechanics, statistics, and polymer physics*, 3rd ed. (World Scientific, New Jersey, 2004).

[14] F. Haake, *Quantum signatures of chaos*, 3rd ed. (Springer, Berlin, 2010).

[15] M. C. Gutzwiller, *Chaos in Classical and Quantum Mechanics* (Springer, 1990).

[16] M. C. Gutzwiller, J. Math. Phys. **12**, 343 (1971).

[17] H. Weyl, Nachr. Ges. Wiss. Gött. math.-phys. Kl. **2**, 110 (1911).

[18] M. V. Berry, Proc. Roy. Soc. London. A. **400**, 229 (1985).

[19] H. U. Baranger, R. A. Jalabert, and A. D. Stone, Phys. Rev. Lett. **70**, 3876 (1993).

[20] H. U. Baranger, R. A. Jalabert, and A. D. Stone, Chaos **3**, 665 (1993).

[21] K. Richter and M. Sieber, Phys. Rev. Lett. **89**, 206801 (2002).

[22] S. Hikami, A. I. Larkin, and Y. Nagaoka, Prog. Theor. Phys. **63**, 707 (1980).

[23] O. Zaitsev, D. Frustaglia, and K. Richter, Phys. Rev. B **72**, 155325 (2005).

[24] P. Jacquod and R. S. Whitney, Phys. Rev. B **73**, 195115 (2006).

[25] R. A. Jalabert and H. M. Pastawski, Phys. Rev. Lett. **86**, 2490 (2001).

[26] A. Goussev, R. A. Jalabert, H. M. Pastawski, and D. A. Wisniacki, Scholarpedia **7**, 11687 (2012).

[27] O. Bohigas, M. J. Giannoni, and C. Schmit, Phys. Rev. Lett. **52**, 1 (1984).

[28] M. Sieber and K. Richter, Physica Scripta **T90**, 128 (2001).

[29] M. Turek, D. Spehner, S. Müller, and K. Richter, Phys. Rev. E **71**, 016210 (2005).

[30] S. Heusler, S. Müller, P. Braun, and F. Haake, J. Phys. A: Math. Gen. **37**, L31 (2004).

[31] S. Müller, S. Heusler, P. Braun, F. Haake, and A. Altland, Phys. Rev. Lett. **93**, 014103 (2004).

[32] S. Müller, S. Heusler, P. Braun, F. Haake, and A. Altland, Phys. Rev. E **72**, 046207 (2005).

[33] S. Müller, *Periodic-Orbit Approach to Universality in Quantum Chaos*, Ph.D. thesis, Universität Duisburg-Essen (2005).

[34] S. Heusler, S. Müller, P. Braun, and F. Haake, Phys. Rev. Lett. **96**, 066804 (2006).

[35] P. Braun, S. Heusler, S. Müller, and F. Haake, J. Phys. A: Math. Gen. **39**, L159 (2006).

[36] T. Nagao, P. Braun, S. Müller, K. Saito, S. Heusler, and F. Haake, J. Phys. A: Math. Theor. **40**, 47 (2007).

[37] S. Müller, S. Heusler, P. Braun, and F. Haake, New J. Phys. **9**, 12 (2007).

[38] M. Turek, *Semiclassics beyond the diagonal approximation*, Ph.D. thesis, Universität Regensburg (2004).

[39] S. Müller, S. Heusler, A. Altland, P. Braun, and F. Haake, N. J. Phys. **11**, 103025 (2009).

[40] J. Kuipers, D. Waltner, C. Petitjean, G. Berkolaiko, and K. Richter, Phys. Rev. Lett. **104**, 027001 (2010).

[41] J. Kuipers, T. Engl, G. Berkolaiko, C. Petitjean, D. Waltner, and K. Richter, Phys. Rev. B **83**, 195316 (2011).

[42] P. A. Lee and A. D. Stone, Phys. Rev. Lett. **55**, 1622 (1985).

[43] R. A. Jalabert, H. U. Baranger, and A. D. Stone, Phys. Rev. Lett. **65**, 2442 (1990).

[44] P. W. Brouwer and S. Rahav, Phys. Rev. B **74**, 075322 (2006).

[45] A. Goussev, D. Waltner, K. Richter, and R. A. Jalabert, N. J. Phys. **10**, 093010 (2008).

[46] B. Gutkin, D. Waltner, M. Gutiérrez, J. Kuipers, and K. Richter, Phys. Rev. E **81**, 036222 (2010).

[47] R. S. Whitney and P. Jacquod, Phys. Rev. Lett. **103**, 247002 (2009).

[48] P. Jacquod and R. S. Whitney, Europhys. Lett. **91**, 67009 (2010).

[49] T. Engl, J. Kuipers, and K. Richter, Phys. Rev. B **83**, 205414 (2011).

[50] T. Hartmann, J. Michl, C. Petitjean, T. Wellens, J.-D. Urbina, K. Richter, and P. Schlagheck, Ann. Phys. **327**, 1998 (2012).

[51] G. Berkolaiko and J. Kuipers, N. J. Phys. **13**, 063020 (2011).

[52] J. Kuipers and K. Richter, J. Phys. A: Math. Theor. **46**, 055101 (2013).

[53] G. Berkolaiko and J. Kuipers, J. Math. Phys. **54**, 112103 (2013).

[54] G. Berkolaiko and J. Kuipers, J. Math. Phys. **54**, 123505 (2013).

[55] J. Kuipers, Q. Hummel, and K. Richter, Phys. Rev. Lett. **112**, 070406 (2014).

[56] E. Abrahams, *50 Years of Anderson Localization* (World Scientific Publishing Company, 2010).

[57] P. Wölfle and D. Vollhardt, Int. J. Mod. Phys. B **24**, 1526 (2010).

[58] P. W. Brouwer and A. Altland, Phys. Rev. B **78**, 075304 (2008).

[59] Q. Hummel, J. D. Urbina, and K. Richter, J. Phys. A: Math. Theor. **47**, 015101 (2014).

[60] W. Nolting, *Quantenmechanik 2: Methoden und Anwendungen* , 5th ed., Springer-Lehrbuch (2004).

[61] S. Weinberg, *The Quantum Theory of Fields, Volume 1: Foundations*, paperback ed., repr. ed. (Cambridge University Press, 2007).

[62] W. Nolting, *Quantenmechanik 1: Grundlagen*, 6th ed., Springer-Lehrbuch (2004).

[63] R. D. Mattuck, *A guide to Feynman diagrams in the many-body problem*, 2nd ed. (Dover, New York, 1992).

[64] J. W. Negele and H. Orland, *Quantum Many-particle Systems* (Westview Press, 1998).

[65] M. Stone, K.-S. Park, and A. Garg, J. Math. Phys. **41**, 8025 (2000).

[66] M. Baranger, M. A. M. de Aguiar, F. Keck, H. J. Korsch, and B. Schellhaaß, J. Phys. A: Math. Gen. **34**, 7227 (2001).

[67] M. Novaes and M. A. M. de Aguiar, Phys. Rev. A **72**, 032105 (2005).

[68] A. D. Ribeiro, M. A. M. de Aguiar, and A. F. R. d. T. Piza, J. Phys. A: Math. Gen. **39**, 3085 (2006).

[69] C. Braun and A. Garg, J. Math. Phys. **48**, 032104 (2007).

[70] M. F. Herman and E. Kluk, Chem. Phys. **91**, 27 (1984).

[71] L. Simon and W. T. Strunz, Phys. Rev. A **89**, 052112 (2014).

[72] E. M. Graefe and H. J. Korsch, Phys. Rev. A **76**, 032116 (2007).

[73] L. Simon and W. T. Strunz, Phys. Rev. A **86**, 053625 (2012).

[74] B. Juliá-Díaz, T. Zibold, M. K. Oberthaler, M. Melé-Messeguer, J. Martorell, and A. Polls, Phys. Rev. A **86**, 023615 (2012).

[75] S. Mossmann and C. Jung, Phys. Rev. A **74**, 033601 (2006).

[76] M. Novaes, J. Math. Phys. **46**, 102102 (2005).

[77] M. A. M. d. Aguiar, M. Baranger, L. Jaubert, F. Parisio, and A. D. Ribeiro, J. Phys. A: Math. Gen. **38**, 4645 (2005).

[78] J. Bolte and S. Keppeler, Phys. Rev. Lett. **81**, 1987 (1998).

[79] R. G. Littlejohn and W. G. Flynn, Phys. Rev. A **45**, 7697 (1992).

[80] J. Bolte and R. Glaser, Ann. H. Poincaré **6**, 625 (2005).

[81] M. Pletyukhov, C. Amann, M. Mehta, and M. Brack, Phys. Rev. Lett. **89**, 116601 (2002).

[82] M. Pletyukhov and O. Zaitsev, J. Phys. A: Math. Gen. **36**, 5181 (2003).

[83] M. Brack, C. Amann, M. Pletyukhov, and O. Zaitsev, Int. J. Mod. Phys. E **13**, 19 (2004).

[84] A. D. Ribeiro, M. A. M. de Aguiar, and A. F. R. de Toledo Piza, J. Math. Phys. **48**, 112103 (2007).

[85] H.-D. Meyer and W. H. Miller, J. Chem. Phys. **71**, 2156 (1979).

[86] W. H. Miller and K. A. White, J. Chem. Phys. **84**, 5059 (1986).

[87] J. Kempe, Contemp. Phys. **44**, 307 (2003).

[88] S. Godoy and S. Fujita, J. Chem. Phys **97**, 5148 (1992).

[89] Y. Aharonov, L. Davidovich, and N. Zagury, Phys. Rev. A **48**, 1687 (1993).

[90] E. Farhi and S. Gutmann, Phys. Rev. A **58**, 915 (1998).

[91] H. B. Perets, Y. Lahini, F. Pozzi, M. Sorel, R. Morandotti, and Y. Silberberg, Phys. Rev. Lett. **100**, 170506 (2008).

[92] V. M. Kendon, Phil. Trans. R. Soc. A **364**, 3407 (2006).

[93] E. Gerjuoy, Phys. Rev. A **67**, 052308 (2003).

[94] R. P. Feynman and A. R. Hibbs, *Quantum mechanics and path integrals* (McGraw-Hill Companies, 1965).

[95] A. Schreiber, K. N. Cassemiro, V. Potoček, A. Gábris, P. J. Mosley, E. Andersson, I. Jex, and C. Silberhorn, Phys. Rev. Lett. **104**, 050502 (2010).

[96] A. Schreiber, A. Gábris, P. P. Rohde, K. Laiho, M. Štefaňák, V. Potoček, C. Hamilton, I. Jex, and C. Silberhorn, Science **336**, 55 (2012).

[97] A. Schreiber, K. N. Cassemiro, V. Potoček, A. Gábris, I. Jex, and C. Silberhorn, Phys. Rev. Lett. **106**, 180403 (2011).

[98] C. K. Hong, Z. Y. Ou, and L. Mandel, Phys. Rev. Lett. **59**, 2044 (1987).

[99] A. Rai, G. S. Agarwal, and J. H. H. Perk, Phys. Rev. A **78**, 042304 (2008).

[100] J. O. Owens, M. A. Broome, D. N. Biggerstaff, M. E. Goggin, A. Fedrizzi, T. Linjordet, M. Ams, G. D. Marshall, J. Twamley, M. J. Withford, and A. G. White, N. J. Phys. **13**, 075003 (2011).

[101] O. Mülken and A. Blumen, Phys. Rep. **502**, 37 (2011).

[102] D. N. Christodoulides, F. Lederer, and Y. Silberberg, Nature **424**, 817 (2003).

[103] A. Rai and D. G. Angelakis, Phys. Rev. A **85**, 052330 (2012).

[104] B. C. Travaglione and G. J. Milburn, Phys. Rev. A **65**, 032310 (2002).

[105] W. Dür, R. Raussendorf, V. M. Kendon, and H.-J. Briegel, Phys. Rev. A **66**, 052319 (2002).

[106] M. Karski, L. Frster, J.-M. Choi, A. Steffen, W. Alt, D. Meschede, and A. Widera, Science **325**, 174 (2009).

[107] H. Schmitz, R. Matjeschk, C. Schneider, J. Glueckert, M. Enderlein, T. Huber, and T. Schaetz, Phys. Rev. Lett. **103**, 090504 (2009).

[108] F. Zähringer, G. Kirchmair, R. Gerritsma, E. Solano, R. Blatt, and C. F. Roos, Phys. Rev. Lett. **104**, 100503 (2010).

[109] R. Grimm, M. Weidemüller, and Y. B. Ovchinnikov, Advances In Atomic, Molecular, and Optical Physics **42** (2000).

[110] O. Dutta, M. Gajda, P. Hauke, M. Lewenstein, D.-S. Lühmann, B. A. Malomed, T. Sowiński, and J. Zakrzewski, arXiv:1406.0181 (2014).

[111] M. Lewenstein, A. Sanpera Trigueros, and V. Ahufinger, *Ultracold atoms in optical lattices : simulating quantum many-body systems*, 1st ed. (Oxford Univ. Press, Oxford, 2012); M. Lewenstein, A. Sanpera, V. Ahufinger, B. Damski, A. Sen(De), and U. Sen, Adv. Phys. **56**, 243 (2007).

[112] H. Feshbach, Ann. Phys. **5**, 357 (1958).

[113] H. Feshbach, Ann. Phys. **19**, 287 (1962).

[114] U. Fano, Phys. Rev. **124**, 1866 (1961).

[115] See C. Chin, R. Grimm, P. Julienne, and E. Tiesinga, Rev. Mod. Phys. **82**, 1225 (2010) for a recent review of Feshbach resonances in ultra-cold atoms.

[116] S. Inouye, R. A. M., J. Stenger, H.-J. Miesner, M. S.-K. D., and W. Ketterle, Nature **392**, 151 (1998).

[117] P. Courteille, R. S. Freeland, D. J. Heinzen, F. A. van Abeelen, and B. J. Verhaar, Phys. Rev. Lett. **81**, 69 (1998).

[118] N. F. Mott and R. Peierls, Proc. Phys. Soc. A **49**, 72 (1937).

[119] N. F. Mott, Proc. Phys. Soc. A **62**, 416 (1949).

[120] M. Greiner, O. Mandel, T. Esslinger, T. W. Hansch, and I. Bloch, Nature **415**, 39 (2002).

[121] D. Jaksch, C. Bruder, J. I. Cirac, C. W. Gardiner, and P. Zoller, Phys. Rev. Lett. **81**, 3108 (1998).

[122] Y. Kurosaki, Y. Shimizu, K. Miyagawa, K. Kanoda, and G. Saito, Phys. Rev. Lett. **95**, 177001 (2005).

[123] P. A. Lee, N. Nagaosa, and X.-G. Wen, Rev. Mod. Phys. **78**, 17 (2006).

[124] P. A. Lee, Rep. Prog. Phys. **71**, 012501 (2008).

[125] D. Jaksch and P. Zoller, Ann. Phys. **315**, 52 (2005).

[126] T. Stöferle, H. Moritz, C. Schori, M. Köhl, and T. Esslinger, Phys. Rev. Lett. **92**, 130403 (2004).

[127] S. Peil, J. V. Porto, B. L. Tolra, J. M. Obrecht, B. E. King, M. Subbotin, S. L. Rolston, and W. D. Phillips, Phys. Rev. A **67**, 051603 (2003).

[128] W. S. Bakr, J. I. Gillen, A. Peng, S. Fölling, and M. Greiner, Nature **462**, 74 (2009).

[129] J. Sherson, C. Weitenberg, M. Endres, M. Cheneau, I. Bloch, and S. Kuhr, Nature **467**, 68 (2010).

[130] J. E. Lye, L. Fallani, M. Modugno, D. S. Wiersma, C. Fort, and M. Inguscio, Phys. Rev. Lett. **95**, 070401 (2005).

[131] K. W. Madison, F. Chevy, W. Wohlleben, and J. Dalibard, Phys. Rev. Lett. **84**, 806 (2000).

[132] J. R. Abo-Shaeer, C. Raman, J. M. Vogels, and W. Ketterle, Science **292**, 476 (2001).

[133] V. Schweikhard, I. Coddington, P. Engels, V. P. Mogendorff, and E. A. Cornell, Phys. Rev. Lett. **92**, 040404 (2004).

[134] Zwierlein M. W., Abo-Shaeer J. R., Schirotzek A., Schunck C. H., and Ketterle W., Nature **435**, 1047 (2005).

[135] Y.-J. Lin, R. Compton, K. Jimenez-García, J. Porto, and I. Spielman, Nature **462**, 628 (2009).

[136] L. Tarruell, D. Greif, T. Uehlinger, G. Jotzu, and T. Esslinger, Nature **483**, 302 (2012).

[137] Y.-J. Lin, K. Jimenez-Garcia, and I. B. Spielman, Nature **471**, 83 (2011).

[138] J. D. Sau, R. Sensarma, S. Powell, I. B. Spielman, and S. Das Sarma, Phys. Rev. B **83**, 140510 (2011).

[139] D. L. Campbell, G. Juzeliūnas, and I. B. Spielman, Phys. Rev. A **84**, 025602 (2011).

[140] S. A. Wolf, D. D. Awschalom, R. A. Buhrman, J. M. Daughton, S. von Molnár, M. L. Roukes, A. Y. Chtchelkanova, and D. M. Treger, Science **294**, 1488 (2001).

[141] I. Žutić, J. Fabian, and S. Das Sarma, Rev. Mod. Phys. **76**, 323 (2004).

[142] S. Bader and S. Parkin, Ann. Rev. Cond. Mat. Phys. **1**, 71 (2010).

[143] M. N. Baibich, J. M. Broto, A. Fert, F. N. Van Dau, F. Petroff, P. Etienne, G. Creuzet, A. Friederich, and J. Chazelas, Phys. Rev. Lett. **61**, 2472 (1988).

[144] G. Binasch, P. Grünberg, F. Saurenbach, and W. Zinn, Phys. Rev. B **39**, 4828 (1989).

[145] M. Julliere, Phys. Lett. A **54**, 225 (1975).

[146] D. Ralph and M. Stiles, J. Mag. Mag. Mat. **320**, 1190 (2008).

[147] Y. A. Bychkov and E. I. Rashba, J. Phys. C: Solid State Phys. **17**, 6039 (1984).

[148] G. Dresselhaus, Phys. Rev. **100**, 580 (1955).

[149] M. I. D'yakonov and V. I. Perel, Sov. Phys. JETP Lett. **13**, 467 (1971); M. I. Dyakonov and V. I. Perel, Phys. Lett. A **35**, 459 (1971).

[150] Y. K. Kato, R. C. Myers, A. C. Gossard, and D. D. Awschalom, Science **306**, 1910 (2004).

[151] C. L. Kane and E. J. Mele, Phys. Rev. Lett. **95**, 226801 (2005).

[152] B. A. Bernevig and S.-C. Zhang, Phys. Rev. Lett. **96**, 106802 (2006).

[153] M. König, S. Wiedmann, C. Brüne, A. Roth, H. Buhmann, L. W. Molenkamp, X.-L. Qi, and S.-C. Zhang, Science **318**, 766 (2007).

[154] J. Maciejko, T. L. Hughes, and S.-C. Zhang, Ann. Rev. Cond. Mat. Phys. **2**, 31 (2011).

[155] S. Datta and B. Das, Appl. Phys. Lett. **56**, 665 (1990).

[156] M. Wu, J. Jiang, and M. Weng, Phys. Rep. **493**, 61 (2010).

[157] D. Averin and K. Likharev, Zh. Eksp. Teor. Fiz. **89**, 733 (1986); D. Averin and K. Likharev, Sov. Phys. JETP **63**, 427 (1986).

[158] L. S. Kuz'min and K. K. Likharev, Pis'ma Zh. Eksp. Teor. Fiz. **45**, 389 (1987); L. S. Kuz'min and K. K. Likharev, JETP Lett. **45**, 495 (1987).

[159] T. A. Fulton and G. J. Dolan, Phys. Rev. Lett. **59**, 109 (1987).

[160] K. Mullen, E. Ben-Jacob, R. C. Jaklevic, and Z. Schuss, Phys. Rev. B **37**, 98 (1988); M. Amman, K. Mullen, and E. BenJacob, J. Appl. Phys. **65**, 339 (1989).

[161] K. Likharev, IBM J. Res. Dev. **32**, 144 (1988).

[162] L. I. Glazman and R. I. Shekhter, J. Phys.: Cond. Mat. **1**, 5811 (1989).

[163] H. van Houten, C.W.J. Beenakker, and A.A.M. Staring, in *Single Charge Tunneling: Coulomb Blockade Phenomena in Nanostructures*, NATO Adv. Sci. Inst. Ser. B, Vol. 294, edited by H. Grabert and M. H. Grabert (WILEY-VCH Verlag GmbH, 1992); see also e-print H. van Houten, C. W. J. Beenakker, and A. A. M. Staring, arXiv:cond-mat/0508454 (2005).

[164] I. Giaever and H. R. Zeller, Phys. Rev. Lett. **20**, 1504 (1968); H. R. Zeller and I. Giaever, Phys. Rev. **181**, 789 (1969).

[165] D. V. Averin and Y. V. Nazarov, Phys. Rev. Lett. **65**, 2446 (1990).

[166] D. Averin and Y. V. Nazarov, in *Single Charge Tunneling: Coulomb Blockade Phenomena in Nanostructures*, NATO Adv. Sci. Inst. Ser. B, Vol. 294, edited by H. Grabert and M. H. Devoret (Plenum Press, 1992) p. 217.

[167] S. De Franceschi, S. Sasaki, J. M. Elzerman, W. G. van der Wiel, S. Tarucha, and L. P. Kouwenhoven, Phys. Rev. Lett. **86**, 878 (2001).

[168] M. Pustilnik and L. Glazman, J. Phys.: Cond. Mat. **16**, R513 (2004).

[169] J. Kondo, Prog. Theor. Phys. **32**, 37 (1964).

[170] W. d. Haas, J. d. Boer, and G. v. d. Berg, Physica **1**, 1115 (1934).

[171] L. Kouwenhoven, C. Marcus, P. McEuen, S. Tarucha, R. Westervelt, and N. Wingreen, in *Mesoscopic Electron Transport*, NATO Adv. Sci. Inst. Ser., Vol. 345, edited by L. Sohn, L. Kouwenhoven, and G. Schön (Springer Netherlands, 1997) p. 105; M. A. Kastner, Rev. Mod. Phys. **64**, 849 (1992).

[172] P. Joyez, V. Bouchiat, D. Esteve, C. Urbina, and M. H. Devoret, Phys. Rev. Lett. **79**, 1349 (1997).

[173] Goldhaber-Gordon D., Shtrikman Hadas, Mahalu D., Abusch-Magder David, Meirav U., and Kastner M. A., Nature **391**, 156 (1998).

[174] S. M. Cronenwett, T. H. Oosterkamp, and L. P. Kouwenhoven, Science **281**, 540 (1998).

[175] J. Schmid, J. Weis, K. Eberl, and K. v. Klitzing, Physica B: Cond. Mat. **256–258**, 182 (1998).

[176] S. Tarucha, D. G. Austing, Y. Tokura, W. G. van der Wiel, and L. P. Kouwenhoven, Phys. Rev. Lett. **84**, 2485 (2000).

[177] L. P. Kouwenhoven, D. G. Austing, and S. Tarucha, Rep. Prog. Phys. **64**, 701 (2001).

[178] Sasaki S., De Franceschi S., Elzerman J. M., van der Wiel W. G., Eto M., Tarucha S., and Kouwenhoven L. P., Nature **405**, 764 (2000).

[179] M. Pustilnik, L. Glazman, D. Cobden, and L. Kouwenhoven, in *Interacting Electrons in Nanostructures*, Lecture Notes in Physics, Vol. 579, edited by R. Haug and H. Schoeller (Springer Berlin Heidelberg, 2001) pp. 3–24.

[180] J. Martinek, Y. Utsumi, H. Imamura, J. Barnaś, S. Maekawa, J. König, and G. Schön, Phys. Rev. Lett. **91**, 127203 (2003).

[181] J. Nygard, D. H. Cobden, and P. E. Lindelof, Nature **408**, 342 (2000).

[182] W. Liang, M. Bockrath, and H. Park, Phys. Rev. Lett. **88**, 126801 (2002).

[183] P. Jarillo-Herrero, J. Kong, H. S. van der Zant, C. Dekker, L. P. Kouwenhoven, and S. De Franceschi, Nature **434**, 484 (2005).

[184] L. Borda, G. Zaránd, W. Hofstetter, B. I. Halperin, and J. von Delft, Phys. Rev. Lett. **90**, 026602 (2003).

[185] M.-S. Choi, R. López, and R. Aguado, Phys. Rev. Lett. **95**, 067204 (2005).

[186] J. S. Lim, M.-S. Choi, M. Y. Choi, R. López, and R. Aguado, Phys. Rev. B **74**, 205119 (2006).

[187] J. S. Lim, R. López, G. L. Giorgi, and D. Sánchez, Phys. Rev. B **83**, 155325 (2011).

[188] D. R. Schmid, S. Smirnov, M. Marganska, A. Dirnaichner, P. L. Stiller, M. Grifoni, A. K. Huettel, and C. Strunk, (2013), arXiv:1312.6586 .

[189] M.-S. Choi, D. Sánchez, and R. López, Phys. Rev. Lett. **92**, 056601 (2004).

[190] I. Affleck, Nucl. Phys. B **336**, 517 (1990).

[191] M. Fowler and A. Zawadowski, Solid State Commun. **9**, 471 (1971).

[192] I. Affleck, Acta Phys. Pol. B **26**, 1869 (1995).

[193] J. P. Bergfield, Z.-F. Liu, K. Burke, and C. A. Stafford, Phys. Rev. Lett. **108**, 066801 (2012).

[194] A. Rosch, J. Paaske, J. Kroha, and P. Wölfle, J. Phys. Soc. Jpn. **74**, 118 (2005).

[195] D. Roosen, M. R. Wegewijs, and W. Hofstetter, Phys. Rev. Lett. **100**, 087201 (2008).

[196] H. Schoeller and F. Reininghaus, Phys. Rev. B **80**, 045117 (2009).

[197] M. A. Kastner, Phys. Today **46**, 24 (1993).

[198] R. C. Ashoori, Nature **379**, 413 (1996).

[199] B. Szafran, S. Bednarek, and J. Adamowski, Phys. Rev. B **67**, 045311 (2003).

[200] K. Jauregui, W. Husler, and B. Kramer, Europhys. Lett. **24**, 581 (1993).

[201] S. Bednarek, T. Chwiej, J. Adamowski, and B. Szafran, Phys. Rev. B **67**, 205316 (2003).

[202] W. H. Miller, J. Chem. Phys. **53**, 1949 (1970).

[203] W. H. Miller, Adv. Chem. Phys. **30**, 77 (1975).

[204] E. J. Heller, J. Chem. Phys. **62**, 1544 (1975).

[205] E. J. Heller, J. Chem. Phys. **75**, 2923 (1981).

[206] M. J. Davis and E. J. Heller, J. Chem. Phys. **71**, 3383 (1979).

[207] K. C. Kulander and E. J. Heller, J. Chem. Phys. **69**, 2439 (1978).

[208] R. A. Marcus, Faraday Discuss. Chem. Soc. **55**, 34 (1973).

[209] W. H. Miller and T. F. George, J. Chem. Phys. **56**, 5637 (1972).

[210] W. H. Miller, J. Chem. Phys. **68**, 4431 (1978).

[211] W. H. Miller and C. W. McCurdy, J. Chem. Phys. **69**, 5163 (1978).

[212] C. W. McCurdy, H. D. Meyer, and W. H. Miller, J. Chem. Phys. **70**, 3177 (1979).

[213] H.-D. Meyer and W. H. Miller, J. Chem. Phys. **70**, 3214 (1979).

[214] W. H. Miller, Adv. Chem. Phys. **25**, 69 (2007).

[215] M. Thoss and G. Stock, Phys. Rev. A **59**, 64 (1999).

[216] B. Li and W. H. Miller, J. Chem. Phys. **137**, 154107 (2012).

[217] D. W. H. Swenson, T. Levy, G. Cohen, E. Rabani, and W. H. Miller, J. Chem. Phys. **134**, 164102 (2011).

[218] B. Li, W. H. Miller, T. J. Levy, and E. Rabani, J. Chem. Phys. **140**, 204106 (2014).

[219] B. Li, E. Y. Wilner, M. Thoss, E. Rabani, and W. H. Miller, J. Chem. Phys. **140**, 104110 (2014).

[220] J. D. Urbina, private communications.

[221] R. Shankar, *Principles of quantum mechanics*, 2nd ed. (Springer, New York, 2008).

[222] P. A. M. Dirac, *The principles of quantum mechanics*, 4th ed., The international series of monographs on physics (Clarendon Press, Oxford, 1970).

[223] F. W. Byron and R. W. Fuller, *Mathematics of classical and quantum physics : two volumes bound as one* (Dover, London, 1992).

[224] H. F. Trotter, Proc. Amer. Math. Soc. **10**, 545 (1959).

[225] M. Morse, *The calculus of variations in the large*, 5th ed. (American Mathematical Society, Providence, 1966).

[226] E. W. Montroll, Communications on Pure and Applied Mathematics **5**, 415 (1952).

[227] F. Schwabl, *Advanced Quantum Mechanics* (Springer, 2008).

[228] W. Vogel and D.-G. Welsch, *Quantum Optics*, 3rd ed. (Wiley-VCH, 2006).

[229] I. Gradshteyn and I. Ryzhik, *Table of Integrals Series and Products*, 4th ed. (Academic, 1965).

[230] F. Berezin, *The Method of Second Quantization* (Academic Press, 1966).

[231] J. R. Klauder, Ann. Phys. **11**, 123 (1960).

[232] E. Akkermans and G. Montambaux, *Mesoscopic Physics of Electrons and Photons* (Cambridge University Press, 2011).

[233] S. Datta, *Electronic Transport in Mesoscopic Systems* (Cambridge University Press, 1997).

[234] A. J. Leggett, Rev. Mod. Phys. **73**, 307 (2001).

[235] M. Pletyukhov, J. Math. Phys. **45**, 1859 (2004).

[236] E. A. Kochetov, J. Math. Phys. **36**, 4667 (1995).

[237] H. G. Solari, J. Math. Phys. **28**, 1097 (1987).

[238] V. Vieira and P. Sacramento, Nucl. Phys. B **448**, 331 (1995).

[239] T. Van Voorhis and E. J. Heller, Phys. Rev. A **66**, 050501 (2002).

[240] T. Van Voorhis and E. J. Heller, J. Chem. Phys. **119**, 12153 (2003).

[241] J. Kaidel, P. Winkler, and M. Brack, Phys. Rev. E **70**, 066208 (2004).

[242] J. Kaidel, *Extended semiclassical approximations for systems with mixed phase-space dynamics*, Ph.D. thesis, Universität Regensburg (2004).

[243] K. T. R. Davies, T. E. Huston, and M. Baranger, Chaos **2**, 215 (1992).

[244] M. Brack, Foundations of Physics **31**, 209 (2001).

[245] M. Brack, M. Mehta, and K. Tanaka, J. Phys. A: Math. Gen. **34**, 8199 (2001).

[246] P. Cvitanović, R. Artuso, R. Mainieri, G. Tanner, and G. Vattay, *Chaos: Classical and Quantum* (Niels Bohr Institute, Copenhagen, 2012).

[247] W. H. Press, S. A. Teukolsky, W. T. Vetterling, and B. P. Flannery, *Numerical Recipes*, 3rd ed. (Cambridge University Press, 2007).

[248] J. Zinn-Justin, *Path Integrals in Quantum Mechanics* (Oxford University Press, 2010).

[249] T. Engl, J. Dujardin, A. Argüelles, P. Schlagheck, K. Richter, and J. D. Urbina, Phys. Rev. Lett. **112**, 140403 (2014).

[250] D. Waltner, *Semiclassical Approach to Mesoscopic Systems*, Springer Tracts in Modern Physics, Vol. 245 (Springer-Verlag, Berlin Heidelberg, 2012).

[251] D. Waltner and K. Richter, "Classical Correlations and Quantum Interference in Ballistic Conductors," in *Nonlinear Dynamics of Nanosystems* (Wiley-VCH, 2010).

[252] D. Waltner, M. Gutiérrez, A. Goussev, and K. Richter, Phys. Rev. Lett. **101**, 174101 (2008).

[253] M. Gutierrez, D. Waltner, J. Kuipers, and K. Richter, Phys. Rev. E **79**, 046212 (2009).

[254] J. Kuipers, D. Waltner, M. Gutiérrez, and K. Richter, Nonlinearity **22**, 1945 (2009).

[255] M.-O. Mewes, M. R. Andrews, D. M. Kurn, D. S. Durfee, C. G. Townsend, and W. Ketterle, Phys. Rev. Lett. **78**, 582 (1997).

[256] B. P. Anderson and M. A. Kasevich, Science **282**, 1686 (1998).

[257] E. W. Hagley, L. Deng, M. Kozuma, J. Wen, K. Helmerson, S. L. Rolston, and W. D. Phillips, Science **283**, 1706 (1999).

[258] I. Bloch, T. W. Hänsch, and T. Esslinger, Phys. Rev. Lett. **82**, 3008 (1999).

[259] G. Cennini, G. Ritt, C. Geckeler, and M. Weitz, Phys. Rev. Lett. **91**, 240408 (2003).

[260] N. P. Robins, C. Figl, S. A. Haine, A. K. Morrison, M. Jeppesen, J. J. Hope, and J. D. Close, Phys. Rev. Lett. **96**, 140403 (2006).

[261] W. Guerin, J.-F. Riou, J. P. Gaebler, V. Josse, P. Bouyer, and A. Aspect, Phys. Rev. Lett. **97**, 200402 (2006).

[262] J. Dujardin *et al.*, "in preparation," .

[263] J. Dujardin, A. Saenz, and P. Schlagheck, Appl. Phys. B , 1 (2014).

[264] A. Peres, Phys. Rev. A **30**, 1610 (1984).

[265] N. Chernov, Scholarpedia **3**, 4862 (2008).

[266] S. Trotzky, Y.-A. Chen, A. Flesch, I. McCulloch, U. Schollwöck, J. Eisert, and I. Bloch, Nat. Phys. **8**, 325 (2012).

[267] M. Gring, M. Kuhnert, T. Langen, T. Kitagawa, B. Rauer, M. Schreitl, I. Mazets, D. A. Smith, E. Demler, and J. Schmiedmayer, Science **337**, 1318 (2012).

[268] T. Langen, R. Geiger, M. Kuhnert, B. Rauer, and J. Schmiedmayer, Nat. Phys. **9**, 640 (2013).

[269] T. Geiger, T. Wellens, and A. Buchleitner, Phys. Rev. Lett. **109**, 030601 (2012).

[270] M. Abramowitz and I. Stegun, *Handbook of mathematical functions* (Dover Publications Inc., New York, 1970).

[271] J. D. Bodyfelt, M. Hiller, and T. Kottos, Europhys. Lett. **78**, 50003 (2007).

[272] P. Schlagheck, private communications.

[273] M. L. Mehta, *Random Matrices*, 3rd ed. (Academic Press, 2004).

[274] Wikipedia, "Spin echo," (2014), [Online; accessed 19-August-2014].

[275] E. L. Hahn, Phys. Rev. **80**, 580 (1950).

[276] J. R. Klauder and P. W. Anderson, Phys. Rev. **125**, 912 (1962).

[277] E. Abe, K. M. Itoh, J. Isoya, and S. Yamasaki, Phys. Rev. B **70**, 033204 (2004).

[278] B. Herzog and E. L. Hahn, Phys. Rev. **103**, 148 (1956).

[279] W. M. Witzel, R. de Sousa, and S. Das Sarma, Phys. Rev. B **72**, 161306 (2005).

[280] X. X. Yi, H. Wang, and W. Wang, Eur. Phys. J. D **45**, 355 (2007).

[281] W.-L. Ma, G. Wolfowicz, N. Zhao, S.-S. Li, J. J. L. Morton, and R.-B. Liu, "Uncovering many-body correlations in nanoscale nuclear spin baths by central spin decoherence," (2014), arXiv:1404.2717 .

[282] M. V. Berry and K. E. Mount, Rep. Prog. Phys. **35**, 315 (1972).

[283] H.-J. Stöckmann, *Quantum Chaos: An Introduction* (Cambridge University Press, 1999).

[284] K. Richter, *Semiclassical theory of mesoscopic quantum systems* (Springer, Berlin, 2000).

[285] L. Wilets, E. Henley, M. Kraft, and A. Mackellar, Nucl. Phys. A **282**, 341 (1977).

[286] C. Dorso, S. Duarte, and J. Randrup, Phys. Lett. B **188**, 287 (1987).

[287] D. H. Boal and J. N. Glosli, Phys. Rev. C **38**, 1870 (1988).

[288] V. Latora, M. Belkacem, and A. Bonasera, Phys. Rev. Lett. **73**, 1765 (1994).

[289] C. Gardiner and P. Zoller, *Quantum Noise*, 3rd ed. (Springer, Berlin, 2004).

[290] A. Sinatra, C. Lobo, and Y. Castin, Phys. Rev. Lett. **87**, 210404 (2001).

[291] D. Walls and G. J. Milburn, *Quantum Optics* (Springer, 2010).

[292] A. Polkovnikov, Ann. Phys. **325**, 1790 (2010).

[293] D. A. Wisniacki, Phys. Rev. E **67**, 016205 (2003).

[294] F. M. Cucchietti, H. M. Pastawski, and D. A. Wisniacki, Phys. Rev. E **65**, 045206 (2002).

[295] F. M. Cucchietti, H. M. Pastawski, and R. A. Jalabert, Phys. Rev. B **70**, 035311 (2004).

[296] C. Petitjean and P. Jacquod, Phys. Rev. E **71**, 036223 (2005).

[297] M. Gutiérrez and A. Goussev, Phys. Rev. E **79**, 046211 (2009).

[298] J. Michl *et al.*, private communications.

[299] S. Flach, (2014), arXiv:1405.1122 .

[300] L. Martinet and P. Magnenat, Astron. Astrophys. **96**, 68 (1981).

[301] C. Froeschlé, Astron. Astrophys. **4**, 115 (1970).

[302] C. Froeschlé, Astron. Astrophys. **16**, 172 (1972).

[303] C. Froeschlé and E. Lega, Celest. Mech. Dyn. Astron. **78**, 167 (2000).

[304] S. Udry and D. Pfenniger, Astron. Astrophys. **198**, 135 (1988).

[305] D. Pfenniger, Astron. Astrophys. **150**, 97 (1985).

[306] C. Skokos, G. Contopoulos, and C. Polymilis, Celest. Mech. Dyn. Astron. **65**, 223 (1996).

[307] P. Magnenat, Celest. Mech. Dyn. Astron. **28**, 319 (1982).

[308] M. N. Vrahatis, T. C. Bountis, and M. Kollmann, Int. J. Bif. Chaos **06**, 1425 (1996).

[309] P. A. Patsis and L. Zachilas, Int. J. Bif. Chaos **04**, 1399 (1994).

[310] M. Katsanikas and P. A. Patsis, Int. J. Bif. Chaos **21**, 467 (2011).

[311] M. Richter, S. Lange, A. Bäcker, and R. Ketzmerick, Phys. Rev. E **89**, 022902 (2014).